University of Trento
University of Brescia
University of Padova
University of Trieste
University of Udine
University IUAV of Venezia

EFFECTS OF THE LAPLACE PRESSURE DURING SINTERING OF CYLINDRICAL SPECIMEN

Laura Galuppi

Advisor
Prof. L. Deseri

2010

UNIVERSITY OF TRENTO
Graduate School in Structural Engineering
Modelling, Preservation and Controls of Materials and Structures
XXII Cycle

Ph.D. Program Head: Prof. D. Bigoni

Final Examination: 19 April 2010

Board of Examiners:
Prof. Prof. Mauro Da Lio, Universita' di Trento
Prof.Alain Molinari, Universite' Paul Verlaine-Metz
Prof. Rosario Ceravolo, Politecnico di Torino

Summary

In the last decades, powder technology has become one of the most important technological processes for the production of metallic and ceramics components; free sintering, hot isostatic pressing and hot forging are different ways to realize a key-phase in which the primary mechanical properties of the final material are obtained.

A theory of sintering is necessary in order to be able to predict the final structure of a body undergoing such a kind of process. In this respect, it is crucial to be able to follow the evolution of the mechanical properties of the material (determined by this structure) during sintering and to get the final features of the compound at the end of this process.

In this thesis, the influence of the pressure called (*sintering stress* or *Laplace pressure*) produced by the gas employed during the process and which gets trapped into the pores is analyzed.

This is done for pre-compacted (micro/nano)-powdered axially-symmetric samples undergoing (i) isostatic pressing (also covering the case of free sintering), (ii) "free" forging (i.e. axial compressive load acting at the top and bottom faces of the specimens, with no lateral confinement) and (iii) constrained forging (i.e. transverse compression of the samples in a rigid die). Such cases are among the ones suggested in [43].

The role of the Laplace pressure in all of the mentioned cases is twofold.

First of all, such a pressure influences the evolution of the porosity and, for instance, its residual value for a given time duration of the process. It is worth emphasizing that threshold pressures below which the sintering stress is actually not negligible are determined in this thesis; the duration of the process is indeed heavily affected by such a stress. In turn, such a duration would be underestimated otherwise. Furthermore, industrial processes often entail loading pressures lower than the thresholds mentioned above, especially of "small" grain sizes.

The second aspect is based on a common feature exhibited by the two modes mentioned above: the loading parameter may be tuned in such a way that, at some stage of the sintering process, its value may equate the Laplace pressure, leading to a constant value of the porosity.

Whenever this is the case, for (i) there exists a whole range of the loading parameter for which the process is actually unstable. Henceforth, in order to

have stability of sintering either the loading parameter must be high enough with respect to the Laplace pressure or zero, leading to (stable) free sintering. For (ii), the stability analysis shows that the results obtained by using the different models for the shear and bulk moduli do not agree for a restricted range of external load. This is of course an intrinsic pathology of this specific loading mode. Moreover, it is worth noting that large strains occur in such a mode. Thus, both the stress and the (infinitesimal) strain employed in this analysis should be replaced by appropriate (possibly work-conjugate) choices of the stress and strain measures, although this goes beyond the aim of this work. For (iii), a stability analysis allows us to conclude that such a value represents a critical threshold, below which the sintering process cannot proceed.

In the second part of the present work, the mechanical behavior of sintered specimens are investigated. Such a behavior is strongly influenced by the stress state at the end of the process, which depends on the final value of the interstitial pressure and of the loading mode used during the process.
For the sake of simplicity, only the two "realistic" cases of isostatic pressing (also covering free sintering) and constrained forging are considered. For such components, isostatic pressing may induce isotropy, whereas constrained forging processes may enforce a transverse isotropic behavior in the direction of forging. Although for prestresses isotropic material the explicit constitutive law is given by Man [28], the analog for the case of transversely isotropic material is deduced here, for the first time, through a method, suggested by Weiyi [30], based upon the partial differentiation of the strain energy with respect to both the strain tensor and the residual stress.

Finally, the residual stress tensor for specimens sintered through (i) and (iii) is obtained and the correspondent stress response is deduced. Equivalent material constants (two constant in the case of isotropy, five in the case of transverse isotropy) arising in the presence of prestress may be introduced; such constants take the place of the classical material moduli characterizing the response in the absence of residual stresses. Finally, an experimental procedure to determine the values of such constants is proposed.

Submitted papers

The main results presented in this thesis have been summarized in the following papers:

1) L.Galuppi, L.Deseri, "Effects of the interstitial stress on isostatic pressing and free sintering of cylindrical specimen." Submitted;

2) L.Galuppi, L.Deseri, "Sintering of cylindrical specimens: Part I - Effects of the Laplace pressure during "free" forging" Submitted;

3) L.Galuppi, L.Deseri, "Sintering of cylindrical specimens: Part II - Effects of the lateral confinement and of the Laplace pressure during constrained forging." Submitted.

Grazie a mia madre per avermi messo al mondo,

a mio padre semplice e profondo,

grazie agli amici per la loro comprensione,

ai giorni felici della mia generazione.

grazie alle ragazze a tutte le ragazze.

Grazie alla neve bianca ed abbondante,

a quella nebbia densa ed avvolgente,

grazie al tuono, piogge e temporali,

al sole caldo che guarisce tutti mali,

grazie alle stagioni a tutte le stagioni.

Grazie alle mani che mi hanno aiutato,

a queste gambe che mi hanno portato,

grazie alla voce che canta i miei pensieri,

al cuore capace di nuovi desideri,

grazie all'emozioni, a tutte le emozioni.

Contents

Chapter 1

Introduction

Powder technology is a forming and fabrication technique that, in the last decades, has become one of the most important technological processes for the production of metallic and ceramics components.
At the same time, sintering has become one of the most important industrial processes, given its key role in powder technology and the several different offered possibilities, spanning from metallic materials (titanium and aluminum alloys, iron, brass, bronze, etc.) to ceramics.

This technology has the advantage to allow for the production of near-net-shape components; this is of course very economical, because no extra treatments and machining are required and a very meaningful time reduction to complete the fabrication are observed with respect to the other available technologies. Furthermore, this technology has been tested for a few decades showing a quite good reliability of both the associated processes and of the final products.

Thanks to the above mentioned features, and because of the presence of (rather small but not negligible) residual porosities, allowing for retaining lubricants, metallic sintered materials are widely used in automotive and aerospace to produce journal bearings, (mini) gears, etc.

In the last few years, besides the traditional fields, new (sintered) ceramic components have been employed for non-standard applications. In particular, the biomedical industry highly benefited from such materials. The good tribological and mechanical properties, including fatigue performances (e.g. of porous coated titanium biomedical alloys [52]) are among the main features of several bio-compatible ceramics, such as titanium and zirconium dioxide, alumina, etc. Self-lubricant properties of such materials make them preferable from the point of view of fabricating prosthetic joints, such as for the knees, hips, ankles, elbows, etc.
Such mechanical properties are also complemented by their good resistance to corrosion and to wear.
Furthermore, in more recent years, nano-powdered materials have been employed to reduce the residual porosity, to randomize its spatial distribution and to decrease the overall size of grains after sintering and also the surface roughness.

In recent years, also ferrous alloys are demonstrated to be reliable as conventional wrought steels, provided that they are correctly produced and, if necessary, heat treated (see [24]). This technology allows for obtaining near-net-shape components; the production of the latter obviously involves several different sequences of technological phases. Such sequences may entail cold/hot pressing and/or sintering. The most common technology consists of three principal stages[14, 26, 27, 41].

- **Powder production**
  First of all, the initial powders are produced either through atomization or using electro-chemical methods or in many other ways. Typically, the different species of powders are mixed in order to obtain the required composition of the target alloy. Indeed, one of the greatest advantages of powder technology versus many other processes is the possibility of designing the chemical composition of the desired compound.

  Powders can be elemental, pre-alloyed, or partially alloyed.

  Elemental powders, e. g. iron and copper, are easy to compress to relatively high density; such powders allow for producing pressed compacts with adequate strength for handling during sintering, although they do not permit to form sintered parts with very high strength.

  Pre-alloyed powders are harder and less compressible than the former ones and, hence, they do require higher pressing loads to produce comparable high density products. However, they are capable of producing high strength sintered materials in comparison with elemental powders.

  Partially alloyed powders are a compromise between the two kinds of materials discussed above.

- **Cold powder compaction**
  During this phase the powder is mixed with a lubricant and pressed to produce a weakly cohesive structure (green material), very near to the shape of the object ultimately to be manufactured, whereas the size of the green may be very different for ceramic compounds.

  In cold uniaxial pressing, the powder is injected into a mold or passed through a die. Cold compaction ensures that the as-compacted, or green, component is dimensionally very accurate, as it is molded precisely to the size and the shape of the die. Irregularly shaped particles are required to ensure that the as-pressed component earns high strength from the interlocking and plastic deformation of individual particles with their neighbors.

  In cold isostatic pressing, metal powders are contained in an enclosure, e.g. a rubber membrane or a metallic can, subject to isostatic external pressure. This process allows for obtaining as-pressed components of uniform density.
  Recent studies of modeling of such a process are [33, 34, 44, 45, 48, 46, 47].

- **Sintering**
  Finally, in the (free) sintering phase, "green compact" parts are heated below the melting point of the base material, namely the dominant species in the compound. This is held at the sintering temperature and then gradually cooled off, without any action of external loads. Sintering transforms the compacted mechanical bonds between the powder particles into either chemical or metallurgical bonds, depending upon the nature of the material.
  This "fusing" of particles results in an increase of the density of the component and, hence, the process is sometimes called densification.

  For metallic products, sintering is the step providing the primary metallurgical and mechanical properties; after this phase, usually no thermal treatments or machining are needed. For ceramics, sintering owes the final size of the component as well as its mechanical features.

In alternative, compaction and sintering can be combined, resulting either in hot isostatic pressing or in hot forging.

The former entails encapsulating powders in a metallic container, usually under vacuum (to avoid contamination of the materials by any residual gas). The powder is then heated and subject to isostatic pressure sufficient to plastically deform both the container and the powder itself. The rate of densification of the granular material depends on its yield strength at the temperatures and pressures chosen for the process. At moderate temperatures such yield strength can still be high and high pressures are required to produce densification in a reasonable time, desirable for economical reasons. Typical values of temperatures and pressure may be of the order or $1000 - 1100°C$ and $100\,MPa$ for ferrous alloys.

In the second case, powders are usually heated up to a forging temperature and then forged in a closed (sufficiently rigid) die. This produces a fully dense component with the shape of the die and with appropriate mechanical properties. Hot forging can also be performed after a phase of pre-compaction.
In the sequel, these technological procedures are called "isostatic pressing" and "constrained forging", respectively. Figure 1.1 shows the different possibilities of technological processes to produce sintered components.

From the microscopic point of view, the evolution from powdered material to its compact (green) state and then to sintered material is mainly due to the diffusion of atoms through the microstructure, to the action of pressure and to the temperature. During hot working, the original microstructure can be improved to be free from defects through densification, diffusion and joining. During sintering, the quasi-discrete connection of particles changes to a dense continuum structure [36].

A rational theory of sintering is necessary in order to be able to predict the required structure of a body in order to follow the evolution of its mechanical

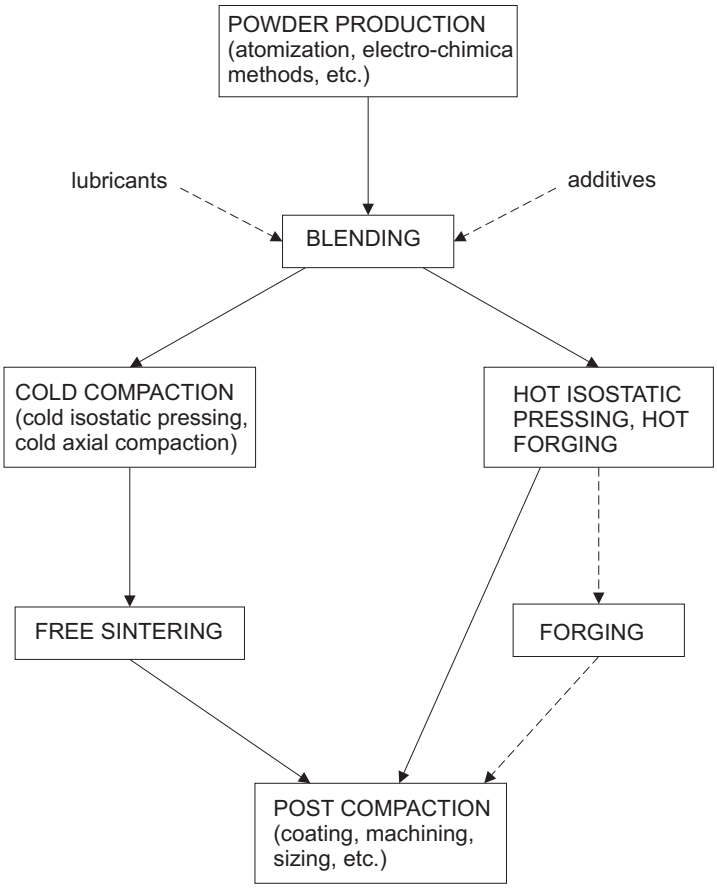

Figure 1.1:

properties (determined by this structure) during sintering and to get the final features of the compound at the and of this process.

A reasonable constitutive law of a material undergoing sintering allows for studying and predicting the effects on the material of the main variables influencing the process, such as the grain size and composition, the duration of sintering, the sintering temperature, the presence of an external load.

Theoretical studies of sintering started in the Forties, and were originally based on ideas of sintering viewed as the collective result of thermally activated adhesion processes producing the growth of contacts between particles and their coalescence. Hence, the approach was based on the investigation of the local kinetics of the process and, subsequently, extended to obtain the behavior of the macroscopic porous body [2, 3, 5].
However, real sintering processes are influenced non only by the properties of the powder particles and by the nature of their interaction but also by macroscopic factors like, for example, inhomogeneity of properties in the volume under investigation, etc. In order to take into account these effects, and to, in practice, implement the theoretical ideas a macroscopic model of sintering was needed.

From the Seventies, a new approach, based on Continuum Mechanics, applied to the description of compaction of porous bodies and upon models of plastic deformation of porous bodies, started to be developed [8, 12, 11, 10]; the so called *Continuum Theory of Sintering* nucleated at that time describes nonlinear-viscous deformation of porous bodies.

Among the earlier models, another interesting approach is to consider sintering as a process of volume and shape deformation caused by the flow of species in the (porous) skeleton of the body. This way of thinking started with Frenkel and, later, developed by by Mackenzie and Shuttleworth, [4]. This was done on the basis of the analysis of two model problems: sintering of two spherical particles and shrinkage of a spherical pore [1]. In this sense, sintering can be treated as a subject entailing rheology. A rheological approach to sintering really started in 1972, through the key-stone book of Skorohod [9], where a complete thermodynamically grounded theory of sintering was performed.
Results obtained in such a framework were intensively developed in the last thirty years; they have been extensively treated by Olevsky in the fundamental review [29].
In more recent years, fundamental contributions are due to Olevsky and Molinari [32, 43].

The present work is a natural extension of [43], dealing with an analysis of the kinetics and the stability of porous axially symmetric bodies undergoing different loading modes. In such a paper, besides an extensive review of the available literature, both about modeling of sintered material (obtained by compacted powders) and about constitutive equations for porous media, the problem is solved for the cases in which the sintering stress is negligible compared with the one due to external loading.
Among other possibilities, the strategy introduced in [43] appears to be the most effective one in order to predict the kinetics of bodies undergoing sintering (even for simple geometry mentioned above). Indeed, Olevsky and Molinari point out that the assumption of homogeneous plane stress through a sample is reasonable even in the case of non-uniform cross-section (see e.g. [13] for tensile tests).
Incidentally, this is equivalent to assuming that specimens undergo constant states of (plane) stresses corresponding to the average of the actual stress fields.
The approach suggested by the assumptions above has the advantage of capturing the essentials of both kinetics and stability, avoiding to search for the solution of complicated (initial) boundary value problems. Nevertheless, in [43], this strategy it has been employed only for the cases of isostatic pressing and "free" forging in which the effect of the Laplace pressure is negligible with respect to the applied stresses. Hence it needs to be extended to the case of moderate stresses in comparison with the interstitial gas pressure.
The effects of the interstitial stress during isostatic pressing (that also cover the case of free sintering), "free" forging (i.e. a transverse compressive force acting at the top and bottom faces of the sample with no lateral confinement) and constrained forging (i.e. an axial compression of the sample in a rigid die), shown in figure 1.2, are analyzed in this thesis. Moreover, the mechanical prop-

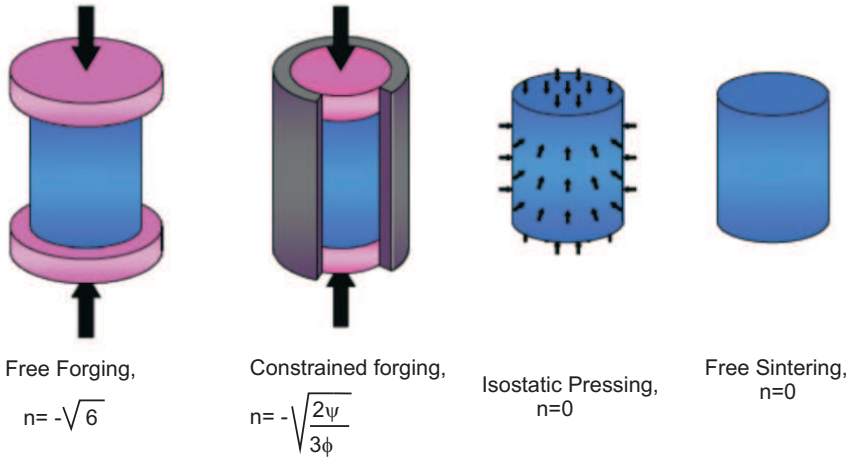

Figure 1.2: Different loading modes: forging, constrained forging, isostatic pressing, free sintering

erties and behavior of the sintered material, strongly influenced by the stress state at the end of sintering, are studied.

The present thesis may be outlined as follows.
In Chapter 2 (see [54]), the case of isostatic pressing, also covering free sintering, is studied. In Section 2.2 a theory of sintering introduced in [29, 43] is essentially summarized.

One of the main quantities influencing sintering is the interstitial stress (Laplace pressure) exerted by the gas permeating the pores. Micromechanics-based approaches are acknowledged to be required for evaluating such a stress and, in particular, two ways to get the result are revisited.
In Section 2.3, the evolution of the porosity is studied for the case of isostatic pressing. Here, and for the first time, it is shown how the effects of the Laplace pressure become very meaningful whenever its magnitude becomes comparable with the stress due to external loads.

In particular, in 2.3.1 the occurrence of equality between such values is explored and it is proved that this circumstance occurs at a definite value of the porosity, which remains constant for some time. For this reason such a value is called *critical porosity*.
Of course the remaining cases, namely when the stress due to external loads is either lower or greater than the Laplace pressure for the whole process are also analyzed.

In 2.3.2, two issues are investigated. First of all, *threshold pressures* on stresses caused by external loads are determined under which the influence of the interstitial pressure cannot be neglected. Such thresholds may strongly be influenced by the strain rate sensitivity of the material and by the average radius of the particles; this feature may have a stronger impact for nano-structured powders. Furthermore, the discrepancy between the values of the

residual porosity evaluated by neglecting or accounting for the Laplace pressure in sintering processes (of a given time-duration) is obtained.

Section 2.3.3 is devoted to analyze free sintering. In particular, since no external stress is applied, it is crucial to examine to what extend different ways to evaluate the Laplace pressure may influence the outcome in terms of evolution of the porosity. Henceforth, a parametric analysis in terms of the given temperature is performed to estimate the sintering time for a target residual porosity.

In Section 2.4, the stability of the process is performed in two steps along the lines traced in [43]. In particular, although not exclusively, the time evolution of the porosity (obtained in Sect. 2.3) is tested against small time perturbations. Whenever this is the only independent perturbed quantity, a lower order analysis does follow (see e.g. Sect. 2.4.1 and [43] for the sake of comparison). This leads to the unrealistic result that the stability of the process may depend upon the choice of the micromechanical model adopted for the evaluation of the shear and the bulk moduli.
Hence a higher order analysis is needed and this is performed in Sect. 2.4.2. Besides the porosity, the stress and the area of the cross section of the sample are perturbed; nevertheless, unlike in [43], the interstitial stress is present and, so, its reference value needs to be perturbed. This more refined analysis shows that an instability arises for the process whenever the applied stress and the Laplace pressure become very close, leading to the possibility of lowering the porosity below its critical value.

Chapter 3 analyzes the case of free forging treated in [55]. This can be outlined as follows.
In Section 3.3, the evolution of the porosity is studied for the case of free forging for the different choices of the models mentioned above. In analogy with in the case of isostatic pressing (see e.g. [54]), in Section 3.3.1 three cases may arise through a comparison between the stress caused by external loading and the Laplace pressure. Whenever such values become equal, a critical porosity is reached. This is precisely the same phenomenon occurring for isostatic pressing; for a prescribed external pressure, such a value of the porosity is different in the two cases because it depends on the specific loading mode.
Moreover, in Sect.2.42, the computation of the axial and radial strain rate during the sintering process is performed.
Like for isostatic pressing, thresholds on stresses caused by external loads under which the influence of the interstitial pressure cannot be neglected, defined as in 2, [54], are determined in 3.4. Such thresholds may strongly be influenced by the strain rate sensitivity of the material and, more importantly, by the grain size of the particles. This feature may have a stronger impact for nanostructured powders, that play an increasingly important role in applications (see e.g. [31, 39, 42, 49]).

In Section 3.5, the stability of the process (namely of the time evolution of the porosity obtained in Sect. 3.3), is performed following the lines traced in [43]. Motivated by the unsatisfactory, and yet self-contradictory, results ob-

tained in 2 and in [54], Sect. 4.1, given by a lower-order stability analysis (obtained by perturbing the porosity alone), a higher order analysis is performed. The porosity, the stress due to the external loading, the cross section of the sample and the reference value of the interstitial stress are then perturbed. This analysis shows that the results obtained by using the different models for the shear and bulk moduli do not agree for a restricted range of external load: whenever the model of Skorohod is employed for evaluating the mentioned moduli, the process turns out to be stable. Hence, there exists a limiting porosity under which the process can not continue; by adopting the other models, the process is instead unstable from the beginning. This is of course an intrinsic pathology of this specific loading mode. Moreover, it is worth noting that large strains occur in such a loading mode. Thus, both the stress and the (infinitesimal) strain employed in this analysis should be replaced by appropriate (possibly work-conjugate) choices of the stress and strain measures, although this goes beyond the aim of this work.

The case of constrained forging, only mentioned in [43] and not treated yet in the literature, is fully examined (both accounting for the effects of the interstitial stress and neglecting them) in Chapter 4 and in [56]. This chapter may be outlined as follows.
In Sect.4.2, the evolution law of the porosity is studied for this case for different choices of the models both for the Laplace pressure and for the shear and bulk moduli. In Section 4.2.1, the same three cases encountered in both isostatic pressing and free forging (see [54] for isostatic pressing and [55] for free forging) may arise by comparison between the stress caused by external loading and the interstitial pressure. In particular, the occurrence of equality between such values is again reached at a critical porosity, different from the value attained in the absence of lateral confinement, which remains constant for some time.
Furthermore, in Sect.4.2.2, the computation of the radial stress (i.e. the pressure acting on the die wall) during the process is performed. In Sect.4.3, the same issues investigated for isostatic pressing and, partially, for free forging are analyzed.
Again, thresholds on stresses caused by external loads are determined under which the influence of the interstitial pressure cannot be neglected. Of course their values are heavily dependent on the lateral confinement. Such thresholds may strongly be influenced by the strain rate sensitivity of the material and the average radius of the particles.
Furthermore, the discrepancy between the values of the residual porosity is evaluated by neglecting or accounting for the Laplace pressure during sintering processes of a given time-duration.
The need of performing stability analyses, in analogy with the previous cases, is evident.
In Section 4.4, the stability of the process (namely of the solution of the problem in terms of time evolution of the porosity, obtained in Sect.4.2) is performed. A higher order analysis will be performed exactly like in the previous cases, since lower order stability is known to produce unreliable results.
The porosity, the stress due to the external loading and the reference value of

the interstitial stress are then perturbed; this analysis shows that the process is stable for the whole time for each given value of the external loading. Whenever the critical porosity is encountered, this represents the lowest threshold under which the (average) longitudinal strain cannot evolve, since and the process can not continue.

It is known that components made of sintered alloys are appreciated to be suitable for applications in the as-sintered state. Sintering is the phase during which the component acquires its required mechanical properties, which are strongly influenced by the stress state at the end of the process. Because of economical reasons thermal annealing is very often ruled out and, hence, the unavoidable residual stresses may then have an influence on the mechanical performances of sintered samples. Such residual stress (often called prestress) depends upon the stress state at the end of the sintering, which is a function of of the final value of the interstitial pressure and of the loading mode used during the process.
For the sake of simplicity, as-sintered axially symmetric specimens are examined, and only the two "realistic" cases of isostatic pressing (also covering free sintering) and constrained forging are considered. For such components, isostatic pressing may induce isotropy, whereas constrained forging processes may enforce a transverse isotropic behavior in the direction of forging.

First of all, it is necessary to consider the constitutive law of a linearly elastic prestressed material. This may be described through the following general constitutive law [28]:

$$\boldsymbol{\sigma} = \overset{\circ}{\boldsymbol{\sigma}} + \mathbf{H}\overset{\circ}{\boldsymbol{\sigma}} + \overset{\circ}{\boldsymbol{\sigma}}\mathbf{H}^T - (tr\mathbf{H})\,\overset{\circ}{\boldsymbol{\sigma}} + \mathfrak{L}[\overset{\circ}{\boldsymbol{\sigma}}, \mathbf{H}], \tag{1.1}$$

where $\boldsymbol{\sigma}$ is the Cauchy stress tensor, $\overset{\circ}{\boldsymbol{\sigma}}$ is the residual stress tensor and $\mathbf{H}$ is the gradient of the displacement field. The sixth-order tensor $\mathfrak{L}$ is the incremental elasticity tensor, which contracts two indexes for each of the arguments and reduces to the forth-order classical elasticity tensor $\mathbb{C}$ whenever $\overset{\circ}{\boldsymbol{\sigma}} = \mathbf{0}$.
Although the representation formula for such a sixth-order tensor in the case of full isotropy is given by Man [28], in Chapter 5 the representation of $\mathfrak{L}$ for linear elastic transversely isotropic material is deduced for the first time in the literature. The method used to get such a result is suggested by Weiyi [30] and it relies upon the partial differentiation of the strain energy density with respect to both the strain tensor and the residual stress.
Chapter 5 may be outlined as follows.
In Section 5.2, the general form of the constitutive equation for linearly elastic prestressed materials are considered. The concept of material-frame indifference, and the definition of isotropic and transversely isotropic material behavior are invoked. In Sections 5.2.3 and 5.2.4, the two mentioned cases are discussed, and the complete list of the necessary scalar and tensor function generators are presented in order to obtain a properly written constitutive equation. This is done both in terms of energy and stress response, in which the isotropy of space and the material symmetries are automatically verified. In Section 5.3, the part of the strain energy due to the presence of the residual stresses is deduced in

the case of transversely isotropic materials. Such an energy is of course a scalar function of the strain tensor and of the residual stress, as well as of the direction of transverse isotropy; indeed, the energy is written as a function of the invariants of such quantities.
In Section 5.4, the stress tensor can be obtained, following the methods of tensor derivation, by differentiating the strain energy with respect to the strain tensor. This allows us to obtain the explicit stress-response for a prestressed linearly elastic transversely isotropic material. In Section 5.5, the same method allows for writing the explicit form of the incremental elasticity (sixth order) tensor $\mathfrak{D}(\overset{\circ}{\boldsymbol{\sigma}}, \boldsymbol{\varepsilon}, n)$. In the last two Sections, 5.6 and 5.7, these results are particularized for incompressible materials and for the case in which the direction of transverse isotropy coincides with z-axis.

In chapter 6, the mechanical response sintered cylindrical specimens (considered in chapters 2 and 4 for the case of isostatic pressing and constrained forging, respectively) are evaluated. The most important assumptions on the mechanical behavior of such specimens are:

- the material presents a behavior depending on the adopted loading mode: specimens sintered through isostatic pressing present a linear elastic isotropic behavior, whereas the ones sintered through constrained forging processes may exhibit (linear elastic) transverse isotropy with respect the to the direction of forging;
- residual stresses may be evaluated through equation (2.1), in which the values of strain rates, of the bulk and shear moduli and of the Laplace pressure are evaluated at the end of the sintering process;
- because the matrix is assumed to be incompressible (during sintering the shrinkage is totally due to the reduction of the porosity) and the porosity does not change after the end of the process, we may also infer that the sintered material is incompressible.

Chapter 6 may be outlined as follows.
In Section 6.2, the general expression for the evolution of the porosity during sintering is highlighted, and the general form of the residual stress as a function of the residual porosity and of the loading mode is presented.
In Section 6.3, the residual stresses in the case of isostatically pressed (and free sintered) material are calculated and the constitutive law for cylindrical specimens sintered through isostatic pressing is deduced. Moreover, the *equivalent shear modulus* (accounting for the residual sintering stresses) is defined and an experimental procedure for its measurement is suggested.
In Section 6.4, the residual stress for specimens sintered through forging in a rigid die is obtained and the correspondent stress response is deduced through the general constitutive law (1.1). This is the exact analog of 6.3 for isostatic pressing. The incremental elasticity tensor for a transversely isotropic material (after enforcing incompressibility and the coincidence of the direction of

transverse isotropy with the z-axis) is obtained in Chapter 5. Five equivalent material constants arising in the presence of prestress may be introduced; such constants take the place of the classical five material moduli characterizing the (linearly elastic) transversely isotropic response in the absence of residual stresses.
Finally, an experimental procedure to determine the mechanical behavior in the presence of transverse isotropy are proposed.

Chapter 2

Effects of the interstitial stress on isostatic pressing and free sintering of cylindrical specimen.

[Submitted]

Abstract
Unlike previous recent contributions [43], the influence of the gas pressure in pores (called *interstitial stress* or *Laplace pressure*) during sintering of pre-compacted metallic (micro/nano)-powdered cylinders is here analyzed. In this paper, the isostatic pressing loading mode, which also covers the case of free sintering, is considered.

The role of the Laplace pressure is twofold.

- First of all, during the sintering process such a pressure influences the evolution of the porosity and, for instance, its residual value at a given time. It is worth emphasizing that threshold pressures are determined below which the sintering stress is actually not negligible; the duration of the process is indeed heavily affected by such a stress whenever the residual porosity is prescribed. In turn, such a duration would be underestimated otherwise. Furthermore, industrial processes often entail loading pressures lower than the thresholds mentioned above, especially of "small" grain sizes.

- In the case of isostatic pressing with non-null external load, the loading parameter may be tuned in such a way that, at some stage of the process, i.e. when a "critical porosity" is reached, its value may equate the Laplace pressure. Henceforth, the porosity would remain constant.

  A stability analysis allows us to conclude that, the equilibrium is unstable at such a value and hence the sintering may keep on going.

  It follows that in order to have stability of sintering either the loading

parameter must be high enough with respect to the Laplace pressure or it must be zero, which would give rise to (stable) free sintering.

Notation

θ= porosity
σ_{ij} = components of the stress tensor
$\dot{\varepsilon}_{ij}$ = components of the strain rate tensor
$\dot{\varepsilon}'_{ij}$ = components of the deviatoric strain rate tensor
$\dot{e}$= first invariant of the strain rate tensor
$\dot{\gamma}$=second invariant of the deviatoric strain rate tensor
p= first invariant of the stress tensor
τ=second invariant of the stress tensor
w= effective equivalent strain rate
$\sigma(w)$= effective equivalent stress
A= time-dependent material constant
m= strain rate sensitivity
ψ= normalized bulk modulus
φ= normalized shear modulus
p_L= Laplace pressure (interstitial stress)
n= loading mode parameter
σ_0= reference stress
$\dot{\varepsilon}_0$= reference strain rate
α= surface tension
r_0= characteristic radius of particles
D= dissipation potential
d=dissipation per unit volume mass
S= cross-sectional area of the specimen
τ_L= dimensionless specific time
$S.E.P.$= specific external pressure
θ^*= critical porosity
θ_r= residual porosity

2.1 Introduction

This work is a natural extension of [43], dealing with an analysis of the kinetics and the stability of porous axially symmetric bodies undergoing sintering under different loading modes. In such a paper, besides an extensive review of the available literature, both about modeling of sintered material obtained by compacted powders and constitutive equations for porous media, the problem is solved for the cases in which the interstitial stress (due to the pressure exerted by the gas in the pores) is negligible compared with the one due to external loading. On the other hand, the strategy introduced in [43] appears to be the most effective one among other possibilities in order to predict the kinetics of bodies undergoing sintering (even for simple geometry mentioned above).

Indeed, Olevsky and Molinari point out that the assumption of homogeneous plane stress through a sample is reasonable even in the case of non-uniform cross-section (see e.g. [13] for tensile tests). Incidentally, this is equivalent to assuming that specimens undergo constant states of (plane) stresses corresponding to the average of the actual stress fields. The approach suggested by the assumptions above has the advantage of capturing the essentials of both kinetics and stability, avoiding to search for the solution of complicated (initial) boundary value problems. Nevertheless, in [43], this strategy it has been employed only for the cases in which the effect of the Laplace pressure is negligible with respect to the applied stresses. Hence it needs to be extended to the case of moderate stresses in comparison with the interstitial gas pressure.

This paper may be outlined as follows.
In Section 2.2 a theory of sintering introduced in [29, 43] is essentially summarized; here the two most used ways to get the interstitial stress are revisited and in 2.2.2 the model for obtaining such a pressure based on the microscopic dissipation is shown to be compatible with the incompressibility of the matrix if and only if the material is nonlinearly viscous.
In Section 2.3, the evolution of the porosity is studied for the case of isostatic pressing. In Section 2.3.1, in order to perform such analysis three cases, which have never been explored before, may arise through a comparison between the stress caused by external loading and the Laplace pressure. In particular, the occurrence of equality between such values is reached at a definite (critical) porosity, which remains constant for some time. In 2.3.2, two issues are investigated. First of all, thresholds on stresses cased by external loads are determined under which the influence of the interstitial pressure cannot be neglected. Such thresholds may strongly be influenced by the strain rate sensitivity of the material and the averaged radius of the particles; this feature may have a stronger impact for nano-structured powders. Furthermore, the discrepancy between the values of the residual porosity is evaluated by neglecting or accounting for the Laplace pressure in sintering processes of a given time-duration. Section 2.3.3 is devoted to analyze free sintering processes. In particular, since no external stress is applied, it is crucial to examine to what extend different ways to evaluate the laplace pressure may influence the outcome in terms of evolution of the porosity. Henceforth, a parametric analysis in terms of the given temperature is performed to estimate the sintering time for a prescribed target residual porosity.
In Section 2.4, the stability of the process, namely of the solution of the problem in terms of time evolution of the porosity obtained in Sect. 2.3, is performed in two steps along the lines traced in [43]. A lower order analysis is performed in Sect. 2.4.1, where perturbations on the porosity alone are considered. This leads to the unrealistic result that the stability of the process may depend upon the choice of the micromechanical model adopted for the evaluation of the shear and the bulk moduli. Hence a higher order analysis is needed. The stress, the cross section of the sample and the reference value of the interstitial stress are then perturbed in Sect. 2.4.2 together with the porosity; this more refined analysis shows that an instability arises for the process whenever the applied

stress and the Laplace pressure become very close, leading to the possibility of lowering the porosity below its critical value.

The analog analysis for different loading modes will be performed in [55, 56].

2.2 Theory of sintering and porosity kinetics

The mechanical response of a porous body with nonlinear-viscous behavior is described by a rheological constitutive relation that inter-relates the components of a stress tensor σ_{ij} and a strain rate tensor $\dot{\varepsilon}_{ij}$[29].

$$\sigma_{ij} = \frac{\sigma(w)}{w}[\varphi\dot{\varepsilon}'_{ij} + \psi\dot{e}\delta_{ij}] + p_l\delta_{ij}, \tag{2.1}$$

where $\dot{\varepsilon}'_{ij}$ denotes the deviatoric strain rate tensor, and w is the effective equivalent strain rate. This is connected with the current porosity and with the invariants of $\dot{\varepsilon}_{ij}$:

$$w = \frac{1}{\sqrt{1-\theta}}\sqrt{\varphi\dot{\gamma}^2 + \psi\dot{e}^2}, \tag{2.2}$$

where

$$\dot{e} = tr\dot{\varepsilon} = \dot{\varepsilon}_{ii}, \tag{2.3}$$

$$\dot{\gamma} = \sqrt{\dot{\varepsilon}'_{ij}\dot{\varepsilon}'_{ij}}, \tag{2.4}$$

i.e. $\dot{\gamma}$ is the second invariant of the deviatoric strain rate tensor.

The quantity p_l represents the interstitial pressure produced by the gas contained in the pores; in the sequel we shall refer to p_l as either the "Laplace pressure" or the "sintering stress" (see [43], [32], [29]).

Equation (2.1) permits to obtain the first invariant of the stress tensor p :

$$p = \frac{1}{3}tr\sigma = \frac{\sigma(w)}{w}\psi\dot{e} + p_l, \tag{2.5}$$

and the second invariant of stress tensor τ:

$$\tau = \sqrt{\sigma'_{ij}\sigma'_{ij}} = \frac{\sigma(w)}{w}\varphi\dot{\gamma}. \tag{2.6}$$

The quantities φ, ψ, p_l and their dependence upon the porosity will be treated in sections 2.1 and 2.2.

Let us consider a cylindrical axisymmetric specimen, subject to an external load. The porosity, θ, is supposed to be constant in the specimen volume and it is defined as the ratio between the pore volume and the total volume (see [43]). Moreover, we will consider the stress tensor,

$$[\sigma_{ij}] = \begin{bmatrix} \sigma_r & 0 & 0 \\ 0 & \sigma_r & 0 \\ 0 & 0 & \sigma_z \end{bmatrix}, \tag{2.7}$$

and the strain rate tensor, averaged on the specimen volume.
If $\dot{\varepsilon}_z$ and $\dot{\varepsilon}_r$ are respectively the axial and radial strain rates, then

$$\dot{e} = \dot{\varepsilon}_z + 2\dot{\varepsilon}_r, \qquad \dot{\gamma} = \sqrt{\frac{2}{3}}|\dot{\varepsilon}_z - \dot{\varepsilon}_r|, \tag{2.8}$$

and $\dot{\gamma}$ is the second invariant of the strain rate tensor

Following Olevsky [43], one can introduce a loading mode parameter n defined by:

$$n = \frac{\tau}{p} = \frac{\varphi\dot{\gamma}}{\psi\dot{e}}. \tag{2.9}$$

The loading mode parameter assumes the following values for the corresponding loading modes:

1. $n = 0$ for isostatic pressing;
2. $n \to \infty$ for pure shear (p = 0);
3. $n = -\sqrt{6}$ for "free" forging;
4. $n = \sqrt{6}$ for drawing;
5. $n = \sqrt{\frac{2}{3}} sgn(\dot{\varepsilon_z})\frac{\varphi}{\psi}$ for constrained forging.

We refer to "free" forging as the loading mode represented in Fig. 2.1.a, a transverse compressive force acting at the top and bottom faces of the sample with no lateral confinement. Henceforth, the case of constrained forging, shown in figure 2.1.b, is nothing but an axial compression of the sample in a rigid die. In the sequel, we shall consider cases 1, 3 and 5 only. From (2.1), (2.8) and (2.9), can be obtained the following relation:

$$\sigma_z = \frac{\sigma(w)}{w}\psi\dot{e}\Big[1 + \sqrt{\frac{2}{3}}n\ sgn(\dot{\varepsilon}_z - \dot{\varepsilon}_r)\Big] + p_l. \tag{2.10}$$

The dependence of effective equivalent stress $\sigma(w)$ on the effective equivalent strain rate w determines the constitutive behavior of a porous material.

Following Ashby [18], a power-law mechanism of deformation is assumed:

$$\frac{\sigma(w)}{\sigma_0} = A\Big(\frac{w}{\dot{\varepsilon}_0}\Big)^m, \tag{2.11}$$

where A and m are material constants (A is the temperature dependent, $0 < m < 1$), σ_0 and ε_0 are the reference stress and the reference strain rate, respectively. Two limiting cases corresponding respectively to the ideal plasticity and

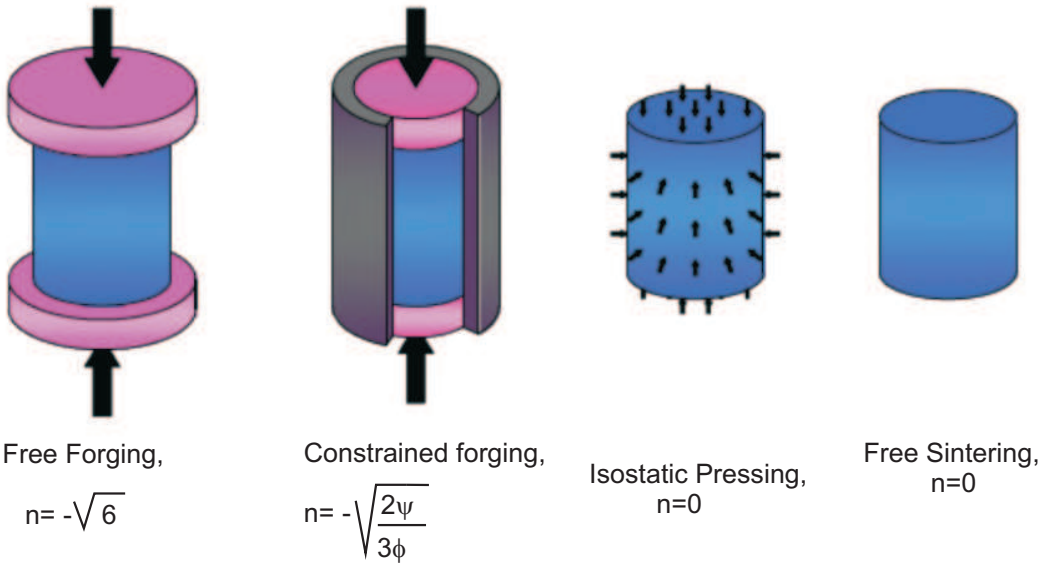

Figure 2.1: Different loading modes: forging, costrained forging, isostatic pressing, free sintering

linear viscosity are given by $m = 0$ and $m = 1$.
Equations (2.11) and (2.2) can be used to obtain the ratio between the effective equivalent stress $\sigma(w)$ and the effective equivalent strain rate w:

$$\frac{\sigma(w)}{w} = \frac{\sigma_0 A}{\dot{\varepsilon}_0^m} w^{m-1} = \frac{\sigma_0 A}{\dot{\varepsilon}_0^m} |\dot{e}|^{m-1} \Big[\frac{\psi}{1-\theta} \Big(\frac{\psi}{\varphi} n^2 + 1 \Big) \Big]^{\frac{m-1}{2}}. \tag{2.12}$$

This paper is meanly denoted to study the influence of the interstitial pressure on the overall stress; for this reason, it is essential to monitor the magnitude $|\sigma_z - p_l|$ for each analyzed loading mode

The expression (2.12) can be related to the constitutive law (2.10) in order to obtain the following relation:

$$|\sigma_z - p_l| = \frac{A\sigma_0}{\dot{\varepsilon}_0^m} |\dot{e}|^m \Big[\frac{\psi}{1-\theta} (\frac{\psi}{\varphi} n^2 + 1) \Big]^{\frac{m-1}{2}} \Big| 1 + \sqrt{\frac{2}{3}} n \; sgn(\dot{\varepsilon}_z - \dot{\varepsilon}_r) \Big|^{\frac{-1}{m}}. \tag{2.13}$$

The evolution law of porosity is given by:

$$\dot{e} = \frac{\dot{\theta}}{1-\theta}. \tag{2.14}$$

Taking into account expression (2.14), relationship (2.13) leads to the following evolution equation for the porosity:

$$\dot{\theta} = sgn(p)\dot{\varepsilon}_0(1-\theta) \Big(\frac{|\sigma_z - p_l|}{A\sigma_0} \Big)^{\frac{1}{m}} \Big[\frac{\psi}{1-\theta} (\frac{\varphi}{\psi} n^2 + 1) \Big]^{\frac{1-m}{2m}} \Big[\psi \Big| 1 + \sqrt{\frac{2}{3}} n sgn(\dot{\varepsilon}_z - \dot{\varepsilon}_r) \Big| \Big]^{\frac{-1}{m}}, \tag{2.15}$$

which accounts for the contribution of the Laplace pressure. The analog of (2.15) by neglecting p_l was obtained by Olevsky and Molinari, [43] eq. 15.

2.2.1 Dependence of shear and bulk moduli on porosity

In literature several studies relative to the determination of the bulk and shear moduli are present.
Here and further, we shall use four different models:

- $\begin{cases} \varphi = (1-\theta)^2 \\ \psi = \frac{2}{3}\frac{(1-\theta)^3}{\theta} \end{cases}$ Skorohod model [9];
- $\begin{cases} \varphi = \frac{(1-\theta)^{\frac{2}{1+m}}}{1+\frac{2}{3}\theta} \\ \psi = \frac{2}{3}\left(\frac{1-\theta^m}{m\theta^m}\right)^{\frac{2}{m+1}} \end{cases}$; Ponte Castaneda-Duva-Crow model [19];
- $\begin{cases} \varphi = \left(\frac{1-\theta}{1+\theta}\right)^{\frac{2}{1+m}} \\ \psi = \frac{2}{3}\left(\frac{1-\theta^m}{m\theta^m}\right)^{\frac{2}{m+1}} \end{cases}$; Mc Meeking-Sofronis model [21];
- $\begin{cases} \varphi = \frac{(1-\theta)^{\frac{2}{1+m}}}{1+\frac{2}{3}\theta} \\ \psi = \frac{m+1}{3}\frac{(1+\theta)(1-\theta)^{\frac{2}{m+1}}}{\theta} \end{cases}$. Cocks model [23].

In figures 2.2 and 2.3 moduli ψ and φ are plotted as functions of the porosity for different values of the parameter m.
The model delivered by Skorohod account for linear-viscous incompressible material with voids only: indeed the moduli ψ e φ are independents from the parameter m.

2.2.2 Dependence of the Laplace pressure on porosity

The effective Laplace pressure p_l is the result of collective action of local capillary stresses in a porous material. A variety of approaches can be found in literature. We shall consider two possible derivations of the expression for the Laplace pressure:

1. *Sintering stress derived by using a stochastic approach*
   This derivation was employed by Skorohod [9], who obtained p_l by calculating the surface free energy per unit mass with respect to the specific volume of the porous material by assuming spherical particles. The achieved result may be stated as follows:

$$p_l = \frac{3\alpha}{r_0}(1-\theta)^2, \tag{2.16}$$

   where α is the surface tension and r_0 is the characteristic radius of particles.

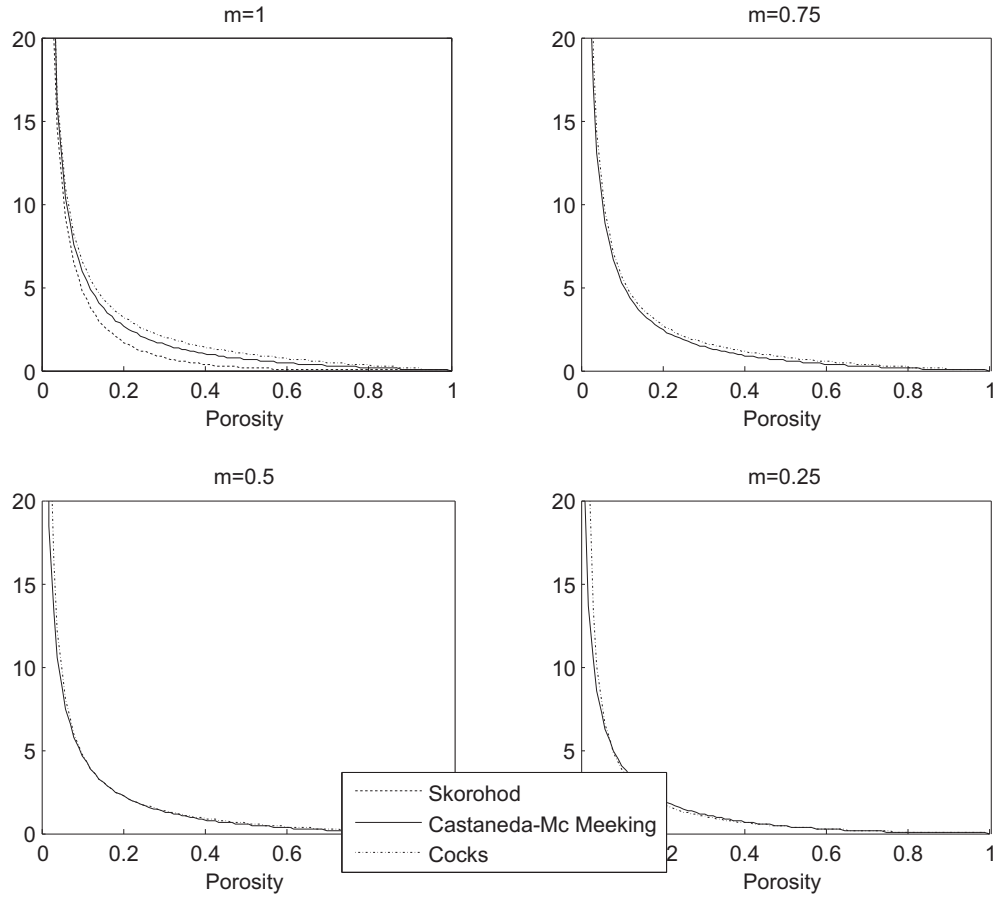

Figure 2.2: Bulk modulus ψ as function of porosity, for different values of the strain rate sensitivity m.

2. *Sintering stress derived by averaging of the dissipation*

   Here we summarize a result shown in [32], where a hollowed sphere is considered as a schematic for a pore (see Figure 2.4). At the surface of such a pore ($r = R_1$), the pressure $p_{l0} = \frac{2\alpha}{r_0}$ is applied and the external boundary ($r = R_2$) is considered to be stress free.
   The porosity is then constant and it is determined by the volume fraction:

$$\theta = \left(\frac{R_1}{R_2}\right)^3. \tag{2.17}$$

   Thus, relation (2.14) gives $\dot{e} = 0$.
   Standard compatibility, written in spherical coordinates, between strain rate and velocity, gives the following relations between the strain rate and the radial velocity $V_r(r)$:

$$\begin{cases} \dot{\varepsilon}_r = \frac{dV_r(r)}{dr}, \\ \dot{\varepsilon}_\Phi = \frac{V_r(r)}{r}. \end{cases} . \tag{2.18}$$

   Using the constitutive law (2.1), the components of the stress tensor turns

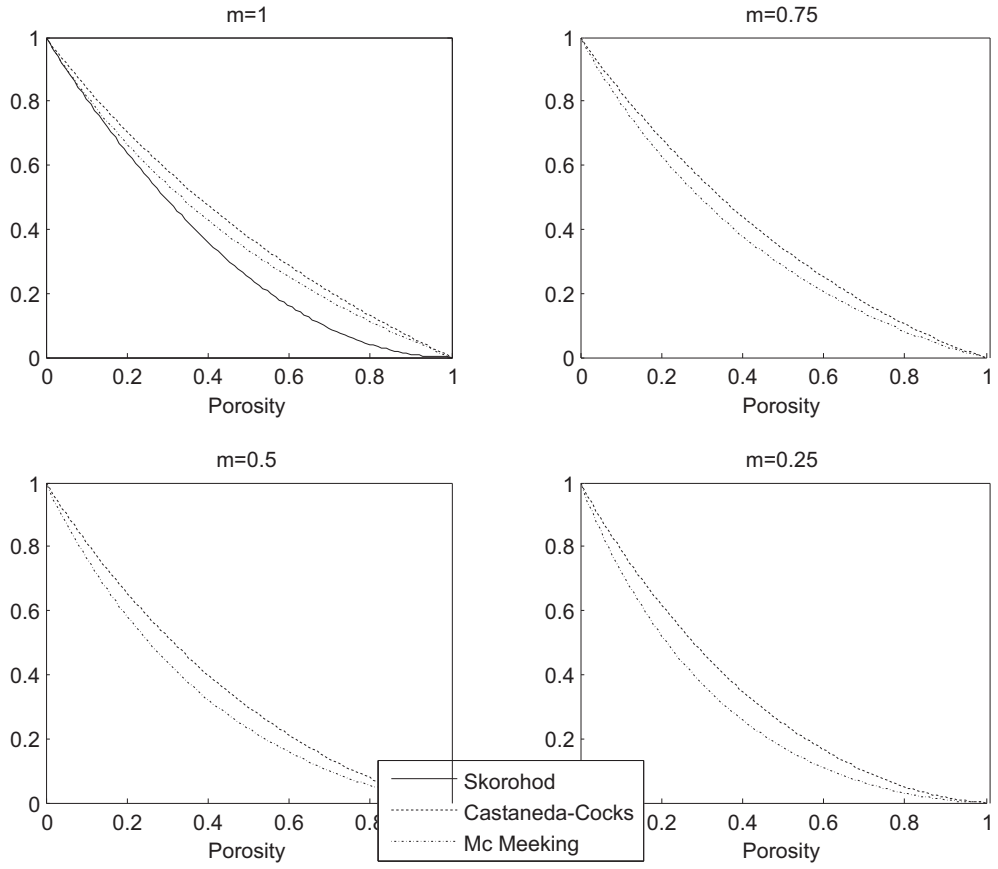

Figure 2.3: Shear modulus φ as function of porosity, for different values of the strain rate sensitivity m.

out to be functions of $V_r(r)$ as follows:

$$\begin{cases} \sigma_r = \frac{2}{3}\frac{\sigma(w)}{w}\varphi\Big[\frac{dV_r(r)}{dr} - \frac{V_r(r)}{r}\Big] + p_l, \\ \sigma_\Phi = -\frac{1}{3}\frac{\sigma(w)}{w}\varphi\Big[\frac{dV_r(r)}{dr} - \frac{V_r(r)}{r}\Big] + p_l. \end{cases} \tag{2.19}$$

Henceforth, to make fully explicit the dependence of σ_r and σ_Φ on the (radial) velocity, equations (2.18) may be inserted in equation (2.4) which, in the present case, takes the form:

$$\dot{\gamma} = \sqrt{\frac{2}{3}}|\dot{\varepsilon}_\Phi - \dot{\varepsilon}_r| = \sqrt{\frac{2}{3}}\Big|\frac{dV_r(r)}{dr} - \frac{V_r(r)}{r}\Big|. \tag{2.20}$$

The latter leads then to the following expression for the rate $\frac{\sigma(w)}{w}$, appearing in equation (2.19):

$$\frac{\sigma(w)}{w} = \frac{A\sigma_0}{\dot{\varepsilon_0}}\Big[\sqrt{\frac{2}{3}}\varphi\Big(\frac{dV_r(r)}{dr} - \frac{V_r(r)}{r}\Big)\Big]^{m-1}. \tag{2.21}$$

On the other hand, the stress balance implies:

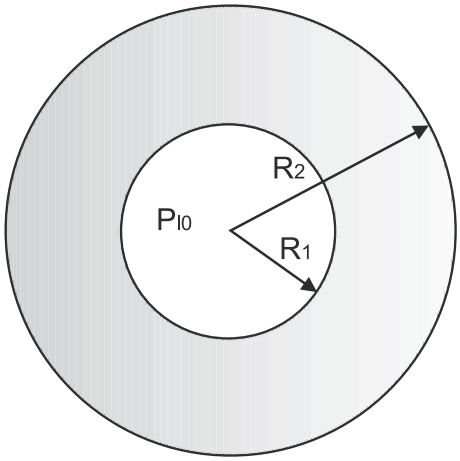

Figure 2.4: A representative element of porous medium

$$\frac{d\sigma_r}{dr} + \frac{2(\sigma_r - \sigma_\Phi)}{r} = 0, \tag{2.22}$$

representing the radial equilibrium.
This may be recast in terms of $V_r(r)$ by means of (2.19) and (2.21), to get:

$$\left\{ \frac{\left[\frac{d^2V_r(r)}{dr^2} - \frac{1}{r}\frac{dV_r(r)}{dr} + \frac{V_r(r)}{r^2}\right]m}{3\left[\frac{dV_r(r)}{dr} - \frac{V_r(r)}{r}\right]} + \frac{1}{r} \right\} \left[\frac{dV_r(r)}{dr} - \frac{V_r(r)}{r}\right]^m = 0. \tag{2.23}$$

It is worth noting that the matrix is incompressible, so that $\dot{e} = 0$. By substituting equation (2.18) into eq. (2.3) we may obtain the following relation:

$$\dot{e} = \frac{dV_r(r)}{dr} + 2\frac{V_r(r)}{r} = 0, \tag{2.24}$$

whose solution is:

$$V_r(r) = \frac{C_3}{r^2}. \tag{2.25}$$

Equations (2.23) may be verified if either the first bracket is zero,i.e.

$$V_r(r) = \left[C_1\frac{m}{3}\left(\frac{1}{r}\right)^{(3/m)} + C_2\right]r, \tag{2.26}$$

or $\frac{dV_r(r)}{dr} = \frac{V_r(r)}{r}$, i.e.

$$V_r(r) = C_4 r, \tag{2.27}$$

which is not admissible by (2.24). Obviously, the only way to satisfy both (2.23) and (2.24) is that

$$m = 1, \tag{2.28}$$

namely the material has linearly-viscous behavior.
By imposing the boundary conditions, we obtain the following expression for V_r:

$$V_r(r) = -\frac{p_{l0} R_1^3 R_2^3}{2\frac{A\sigma_0}{\dot{\varepsilon}_0^m}\varphi(R_2^3 - R_1^3)r^2}, \tag{2.29}$$

which determines the radial and the circumferential strain rates through eq.s (2.18). Furthermore, the second invariant of the strain rate tensor is given by (2.20),i.e.

$$\dot{\gamma} = -\frac{\sqrt{6} p_{l0} R_1^3 R_2^3}{2\frac{A\sigma_0}{\dot{\varepsilon}_0^m}\varphi(R_2^3 - R_1^3)r^2}. \tag{2.30}$$

In this section, we are looking for an expression of p_l based on averaging of the dissipation.
In particular, it is postulated that the dissipation potential has the following form [32]:

$$D = \frac{\frac{A\sigma_0}{\dot{\varepsilon}_0^{(1/m)}}}{m+1}(1-\theta)w^{m+1}. \tag{2.31}$$

- *Dissipation energy per unit volume of matrix*

  In this case, $\theta = 0$, and hence $\dot{e} = 0$ and $\varphi = 1$ (see Figure 2.3). Equation (2.31) permits to determine the dissipation per unit volume of the matrix, which has the form:

  $$d_{matrix} = \frac{\frac{A\sigma_0}{\dot{\varepsilon}_0^{(1/m)}}}{m+1}\dot{\gamma}^{m+1}, \tag{2.32}$$

  since $w = \dot{\gamma}$, because $\dot{\gamma} > 0$ (see eq.(2.4)).
  By averaging this value over the spherical volume, and substituting (2.17) for the porosity, and (2.30), one obtains:

  $$< d >_{matrix} = -\frac{3p_{l0}^2 R_1^3 R_2^3}{4\frac{A\sigma_0}{\dot{\varepsilon}_0}(R_2^3 - R_1^3)^2} = -\frac{3p_{l0}^2\theta}{4\frac{A\sigma_0}{\dot{\varepsilon}_0}(1-\theta)^2}. \tag{2.33}$$

- *Dissipation of the effective porous material*

  The effective porous material is subject to an isostatic stress, so that $\dot{\gamma} = 0$ and

  $$D = \frac{\frac{A\sigma_0}{\dot{\varepsilon}_0^{(1/m)}}}{m+1}(1-\theta)\Big[\sqrt{\frac{\psi}{1-\theta}}|\dot{e}|\Big]^{m+1}. \tag{2.34}$$

  For m=1, relation (2.34), reduces then to:

  $$D = \frac{\frac{A\sigma_0}{\dot{\varepsilon}_0}}{2}\psi\dot{e}^2; \tag{2.35}$$

Because of the free sintering condition, namely $p = 0$, equation (2.5) yields the following relation for $\dot{e}$

$$\dot{e} = -\frac{p_l}{\frac{A\sigma_0}{\dot{\varepsilon}_0}\psi}. \tag{2.36}$$

By substituting (2.36) into equation (2.34), one obtains a very simplified form for the dissipation, that is to say:

$$D = \frac{p_l^2}{2\psi\frac{A\sigma_0}{\dot{\varepsilon}_0}}. \tag{2.37}$$

the dissipation energy of matrix $< d >_{matrix}$ and the one corresponding to the effective porous material D are connected by the Hill's identity, namely:

$$D = (1-\theta) < d >_{matrix} . \tag{2.38}$$

Finally, the form of the Laplace pressure may be evaluated by using equations (2.33), (2.37) and (2.38), that lead to the following expression:

$$p_l = \frac{2\alpha}{r_0}\sqrt{\frac{3}{2}\psi(\theta)\frac{\theta}{1-\theta}}. \tag{2.39}$$

The latter can be particularized to obtain the sintering stress associated to the models cited above; in particular we get:

- $p_l = \frac{2\alpha}{r_0}(1-\theta)$ for the Skorohod model,
- $p_l = \frac{2\alpha}{r0}$ for the Castaneda and Mc Meeking models,
- $p_l = \frac{2\alpha}{r0}\sqrt{1+\theta}$ for the Cocks model.

Figure 2.5 shows the dependence of the Laplace pressure on the porosity θ. The stochastic approach, yielding relation (2.16), gives a parabolic trend of the Laplace pressure. This is increasing when the porosity decreases and it is independent on the value of the parameter m, so that p_l does not depend upon the material behavior.
On the contrary, the motivation leading to (2.28) (i.e. $m = 1$), implies that expression (2.39) (for the four different models) is admissible only for materials with linearly-viscous behavior. Nevertheless, the values of pressure calculated through (2.39) are compatible enough with the ones obtained by (2.16) in the range of interest of porosity for common sintered components.

2.3 Effect of the interstitial stress on sintering processes entailing isostatic-pressing

For the case of isostatic pressing, $\sigma_z = \sigma_r = \sigma$, and the loading mode the parameter n is zero; relation (2.15) reduces to the following expression :

$$\dot{\theta} = -\dot{\varepsilon}_0(1-\theta)^{\frac{3m-1}{2m}}\Big(\frac{|\sigma(\theta) - p_l(\theta)|}{A\sigma_0}\Big)^{\frac{1}{m}}\psi(\theta)^{\frac{-(1+m)}{2m}}. \tag{2.40}$$

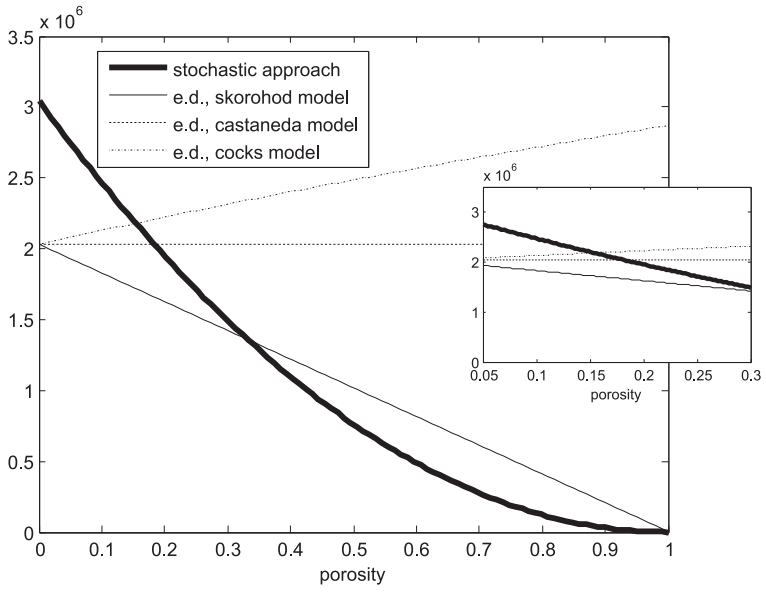

Figure 2.5: the Laplace pressure as function of porosity

Obviously, the shear modulus φ, has no influence on the process. Thus, for this case, Mc Meeking's and Castaneda's models give the same behavior: this is because of the expression of bulk modulus ψ, which is indeed the same for both models.
Because $n = 0$, equation (2.10) allows for recovering the expression of σ, the uniform axial stress

$$\sigma = \frac{\sigma(w)}{w}\psi\dot{e} + p_l = \frac{\sigma(w)}{w}\psi - \dot{\varepsilon}_0[\varphi(1-\theta)]^{\frac{-1+m}{2m}}\Big(\frac{|\sigma(\theta) - p_l(\theta)|}{A\sigma_0}\Big)^{\frac{1}{m}} + p_l. \quad (2.41)$$

To determine the relation between the cross-sectional area of the cylinder and the porosity θ, let us consider a small cylindrical element of height $\Delta h << R$ perpendicular to the specimen axis (see [43]), where R denotes the radius of such a specimen.
The corresponding strain rate components are given by:

$$\dot{\varepsilon_r} = \frac{\dot{R}}{R} \quad , \quad \dot{\varepsilon_z} = \frac{\dot{\Delta h}}{\Delta h}. \quad (2.42)$$

During isostatic pressing we note that $\dot{\varepsilon_z} = \dot{\varepsilon_r}$, then, from (2.42) and (2.14) we obtain the following expression for the rate of change of the porosity:

$$\dot{\theta} = 3(1-\theta)\frac{\dot{R}}{R} = 3(1-\theta)\frac{d(ln(R))}{dt}. \quad (2.43)$$

In order for the latter to hold we must have that

$$\frac{d}{d\theta}ln(R) = \frac{1}{3(1-\theta)}; \quad (2.44)$$

this relationship has a strong implication on the change of the cross-sectional area of the specimen. This is given by $S = \pi R^2$ and hence equation (2.44) yields that the change of the cross-sectional area with the porosity takes the following form:

$$\frac{d}{d\theta}\ln(S) = \frac{2}{3}\frac{1}{1-\theta}. \tag{2.45}$$

The digression on how the cross section does change with porosity on the one hand, and equation (2.41) for the stress on the other hand, would allow for conceiving a fictitious uniaxial compression test driven by a force F_z such that

$$F_z := \sigma S(\theta), \tag{2.46}$$

where now σ play the role of the corresponding uniaxial stress and $S(\theta)$ would change according to the real isostatic state of stress. If S_0 denotes the cross sectional area of the cylinder right before the beginning of such fictitious test, equation (2.46) would yield

$$\sigma = \frac{F_z}{S_0\overline{S}(\theta)} \tag{2.47}$$

where

$$\overline{S}(\theta) = \frac{S(\theta)}{S_0} \tag{2.48}$$

Equation (2.45), together with (2.47), shows that the change of the stress due to external loading, is therefore independent of the adopted model, since the final form of the normal stress turns out to be the following:

$$\sigma = \frac{F_z}{S_0\left(\frac{1-\theta}{1-\theta_0}\right)^{\frac{2}{3}}}, \tag{2.49}$$

where θ_0 denotes the initial porosity.
During the isostatic sintering processes, relative to a fixed fictitious F_z, the stress due to external load σ increases, because of the cross-sectional area diminishes according to the relation in the denominator. On the other hand, the Laplace pressure may vary according to either relation (2.39) and (2.16).
Furthermore, the evolution law (2.40) shows that the rate of change of the porosity $\dot{\theta}$ is proportional to $|\sigma - p_l|$.
It is therefore possible that, for a definite range of external loads, the equality condition $\sigma = p_l$ may be achieved. This range turns out to be very limited, and it corresponds to low values of external loads, which are rarely used in industrial sintering processes.

When the porosity attains the value θ^* for which $\sigma_z = p_l$ an equilibrium situation is reached. Such θ^* may be called *critical porosity*. The stability of such a situation will be studied in section 2.4.

2.3.1 Time-evolution of the porosity during isostatic pressing

Eq. (2.40) may be normalized by using the dimensionless specific time

$$\tau_L = \left[\frac{p_{l0}}{\sigma_0 A}\right]^{\frac{1}{m}} \dot{\varepsilon}_0, \tag{2.50}$$

so that the differential equation (2.40) can be rewritten as follows:

$$\frac{\partial \theta}{\partial \tau_L} = (1-\theta)^{\frac{3m-1}{2m}} |\sigma - p_l|^{\frac{1}{m}} \psi^{\frac{-(1+m)}{2m}} \tag{2.51}$$

The bulk modulus ψ is a known function of the porosity θ; for such a function, here and further, we shall use the expressions given in section 2.1.
Equation (2.51) shows once more that the evolution of the porosity heavily depends on $|\sigma - p_l|$.

We may then distinguish three cases:

- *Case in which $\sigma > p_l$ during the whole process.*
  Neglecting the Laplace pressure is equivalent to consider non-pressurized voids. Henceforth, no pressure could act against stresses caused by external loading. Consequently, the time decay of the porosity would be faster than the real one, although we record that the time evolution of the porosity has a qualitative behavior analog to the one obtained by neglecting the Laplace pressure (see Figure 2.6).
  For further developments, it is useful to introduce a dimensionless pressure parameter defined as follows:

  $$S.E.P. = \frac{F_z}{S_{initial}} \frac{1}{\alpha/r0}, \tag{2.52}$$

  this is called Specific External Pressure (S.E.P.). We recall that α denotes the surface tension.

  Figure 2.6 shows the time evolution of the porosity, obtained by using the Castaneda-Duva-Crow model for $S.E.P. = 10$.
  When the strain rate sensitivity m decreases, the initial part of both graphs become steeper. Indeed, for infinite slope, the material behavior would be perfectly plastic (this would correspond to $m = 0$).

  Moreover, the gap between the two curves is higher for lower values of the strain rate sensitivity m . It turns out that the Laplace pressure has more influence on the sintering process when the material tends towards the plastic behavior. This may be explained by the (Ashby) power-law (eq. (2.11)) relating the equivalent strain rate w and the effective equivalent stress $\sigma(w)$. Indeed, equation (2.11), displayed in Figure 2.7, indicates that for lower values of the parameter m, the strain rate is more sensitive to stress changes and, in particular, it is sensitive to the variation between σ and $\sigma - p_l$.

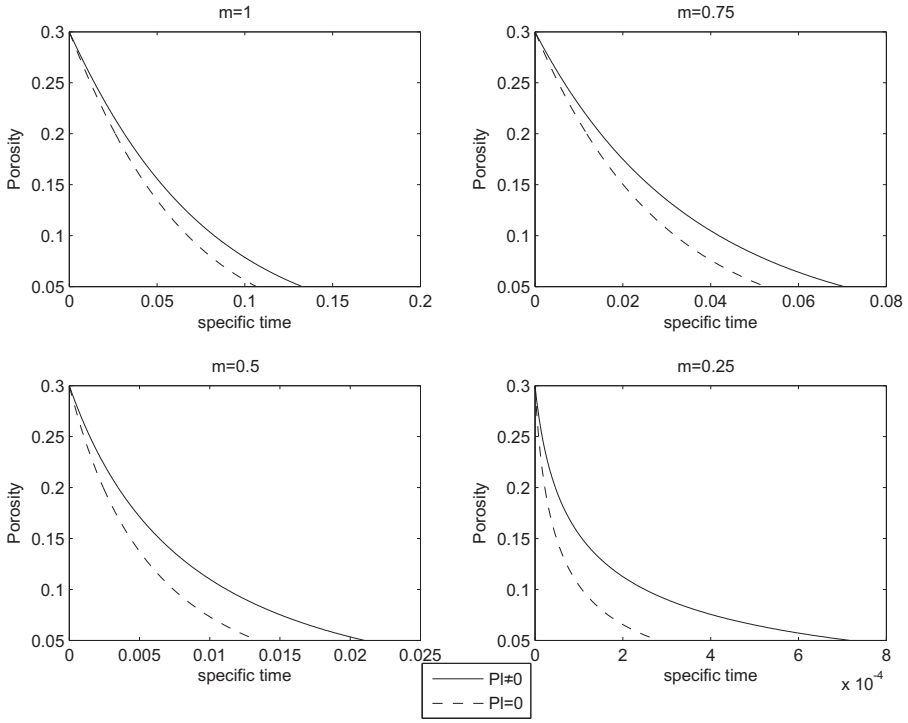

Figure 2.6: ISOSTATIC PRESSING-Evolution of Porosity for S.E.P.=10

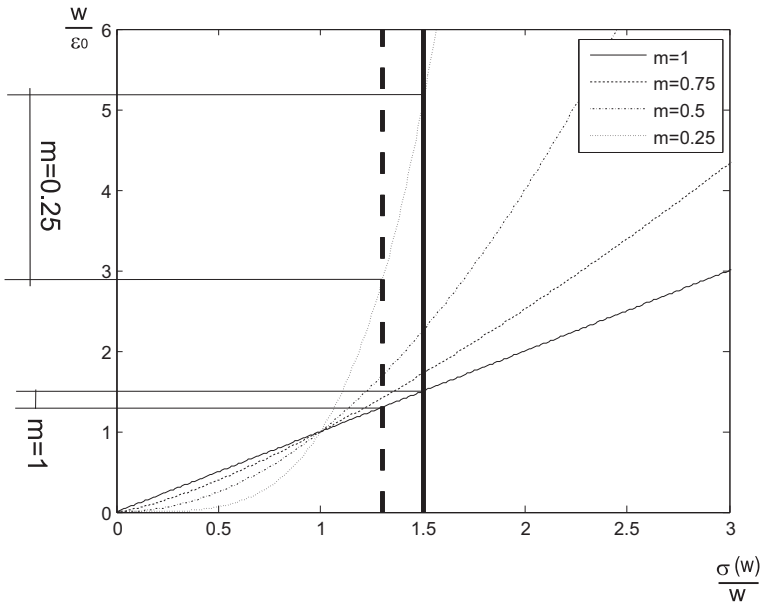

Figure 2.7: (Ashby) power law: sensitivity of the effective equivalent strain rate to the variation between σ and $|\sigma - p_l|$.

- *Case in which $\sigma - p_l$ changes sign during the process .*
  In isostatic pressing, the range of external pressure for which this condition is achieved is very limited. Hence, this case is not interesting from

the industrial point of view.
As we noticed above, in the limiting case for which $\sigma = p_l$, equation (2.51) yields $\dot{\theta} = 0$ and hence $\theta = const.$
The condition $\sigma = p_l$ turns out to be achieved for values of S.E.P. between 1.47 (that corresponds to $\sigma = p_l$ at the beginning of sintering , that is to say $\theta = 30\%$) and 2.21 (that corresponds to $\sigma = p_l$ at the end of the sintering process, namely $\theta = 5\%$). For illustrative purpose, we choose $S.E.P = 1.80$, almost the average the two extremes.

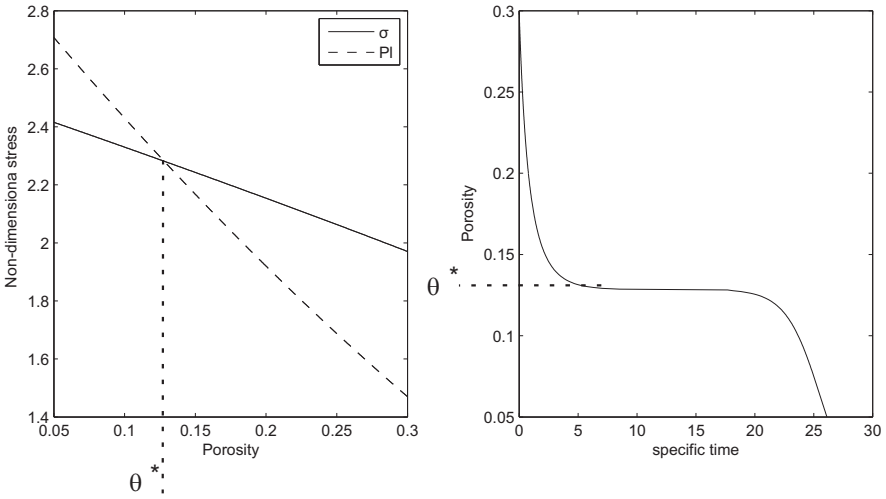

Figure 2.8: ISOSTATIC PRESSING-Evolution of Porosity for S.E.P.=1.80

Figure 2.8 shows the time evolution of the porosity, obtained by using Castaneda-Duva-Crow model, for such S.E.P.. By comparing Figure 2.8.a and 2.8.b, it becomes evident that the constant-porosity corresponds to the condition $\sigma = p_l$.

- *Case in which $\sigma < p_l$ during the whole process.*
  This case may be summarized by analyzing Figure 2.9. Here, the gap between the curves is remarkable. In this case, the "driving sintering force" is basically the Laplace pressure, simply because it is higher than the externally imposed stress.
  Indeed, for "small" and decreasing external loading (i.e. $\sigma > 0$ and small with respect to p_l) the quantity $|\sigma - p_l|$ appearing in equation (2.51) increases, achieving its maximum for $\sigma = 0$ (free sintering).

A comparison among the three different models for the shear and bulk moduli φ ad ϕ and between the two different expression for p_l (see (2.16) e (2.39)) is now performed. Figure 2.10 shows such a comparison for S.E.P.=5 and for

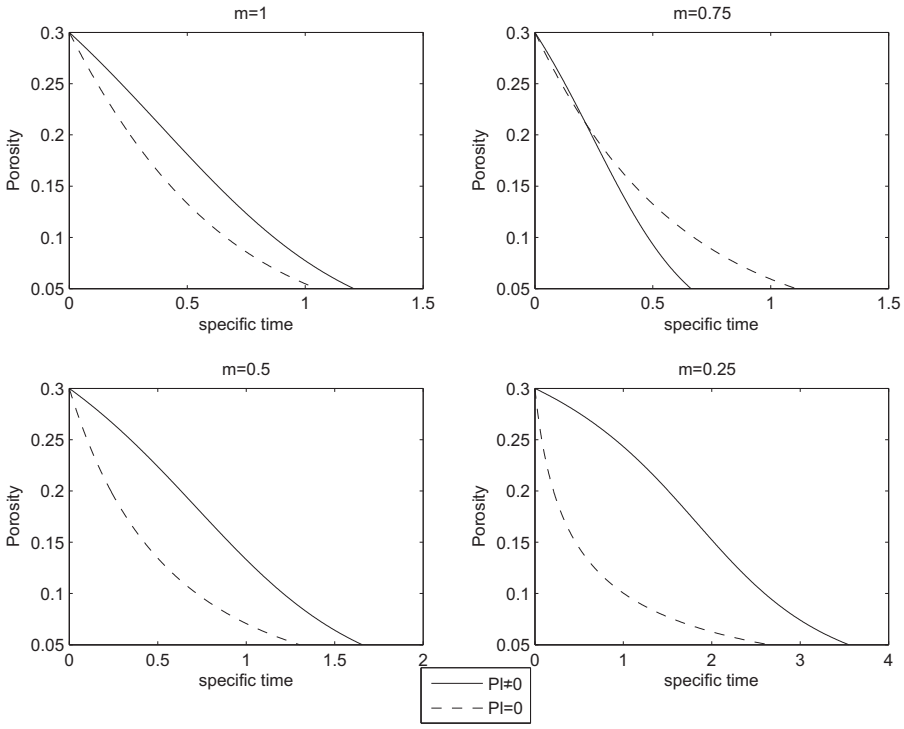

Figure 2.9: ISOSTATIC PRESSING-Evolution of Porosity for S.E.P.=1

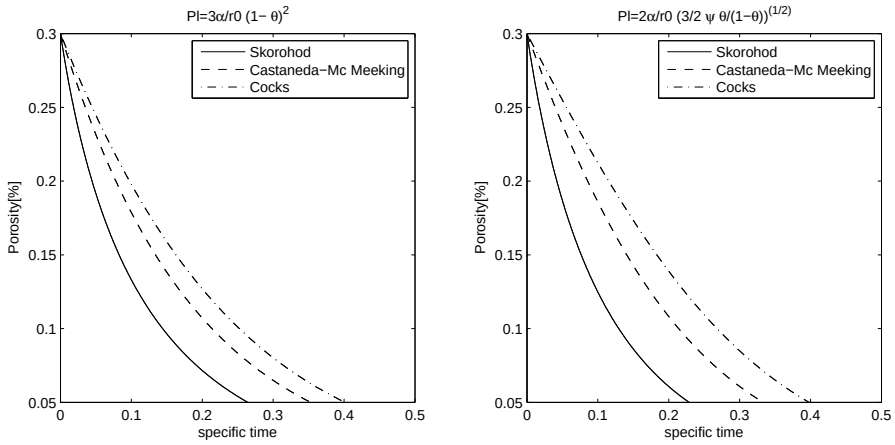

Figure 2.10: ISOSTATIC PRESSING-Evolution of Porosity for S.E.P.=5 ,m=1, for different models

material with linear-viscous behavior (m=1).

Time-evolution diagram shown by figures 2.10.a and 2.10.b are similar, because the value of the Laplace pressure given by equations (2.16) e (2.39) are compatible enough for porosity between 30% and 5% (see Figure 2.5). The differences among curves relative to the different models are due to the corre-

sponding expressions of the bulk modulus ψ.

2.3.2 Influence of the interstitial stress on industrial processes entailing isostatic pressing

A specific metallic alloy (aluminum-zinc-magnesium-copper alloy) is examined in this section. This is motivated by its extended use in industrial sintering processes.
The main features of this material are listed in table 2.1:

Young's modulus	**E**	70,7	GPa
Poisson's ratio	**ν**	0,325	
surface tension	**α**	1,1285	N/m
Activation Energy	**Q**	143 90	kJ
Melting Temperature	**Tm**	659	°C
mean radius of powder particles	**r0**	5/50	µm
sintering pressure	**Pb**	100/350	MPa
sintering temperature	**Ts**	600/610	°C

Table 2.1: Characteristics of the considered aluminum-zinc-magnesium-copper alloy

For aluminum alloys, the average time sintering is thirty minutes and it is usually sintered with external pressure of $100MPa$ [22, 35, 50].
It may be shown that the important parameters that influencing the Laplace pressure, are the powder grain size (indicated here through the radius r_0) and the surface tension α.
Values of powder grain size taken into account are shown in table 2.2.

MICRO-POWDERS	NANO-POWDERS
50 µm	500 nm
10 µm	200 nm
5 µm	100 nm
2 µm	50nm
1 µm	

Table 2.2: Considered values of powder grain size

In the sequel, we shall examine the discrepancies on the estimate of the sintering times evaluated by either neglecting or accounting for the sintering stress p_l. Furthermore, we shall also calculate the residual porosity in both of the cases mentioned above.

Threshold external loading pressures and sintering times

Here, we are interested to compare the sintering times t and t_0 employed to reduce the porosity from 30% to 5% in cases in which the "sintering driving

force" is taken to be either $|\sigma - p_l|$ or $|\sigma|$.

We are also interested into calculating the values of the external pressure p^* for which the discrepancy between the sintering times $D = \frac{t-t_0}{t}$ attains the values 5%, 10% and 15% respectively. Obviously, whenever the external pressure is less than p^*, for the given value of discrepancy, for example $D = 5\%$, an error greater than 5% occurs by neglecting the effect of the Laplace pressure.

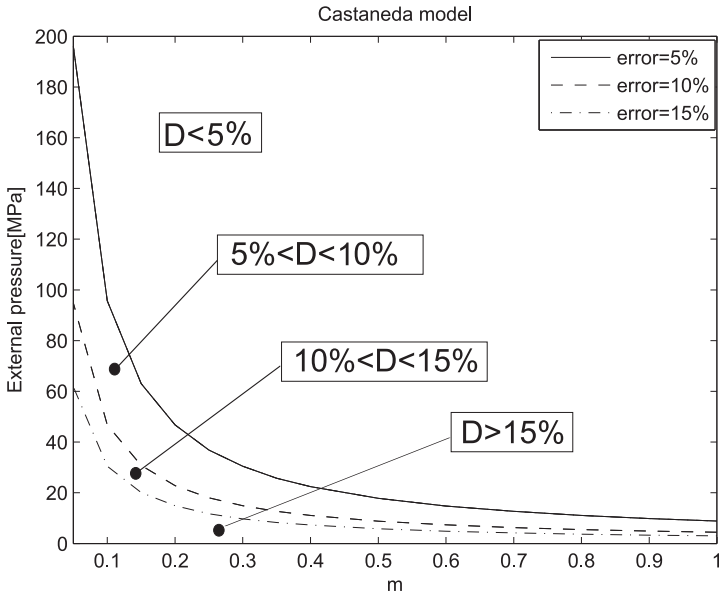

Figure 2.11: Threshold pressure p^*, for $5\mu m$ powder

In Figure 2.11 and 2.12 the threshold pressures for $5\mu m$ and $50nm$ powders (obtained by the model of Castaneda) are shown. It is immediate to note that the effect of the Laplace pressure becomes more relevant for lower values of the powder grain size. Henceforth, in this case the threshold pressures are considerably high.
The comparison between threshold pressures obtained by using the Castaneda and Cocks models show that they do not exhibit meaningful differences.

The result of these sections rely upon the model for the Laplace pressure based on the stochastic approach (equation (2.16), discussed in section 3.2.2). This is due to the fact that equation (2.39), derived instead from averaging of the dissipation, does not allow for evaluating the behavior for different values of strain rate sensitivity the parameter m. However, the values of the threshold pressure obtained by using the latter model of the interstitial stress are in complete agreement with the ones obtained by using the former model. Although this is the case, such threshold values are more sensitive to the different models used to evaluate the shear and bulk moduli φ and ψ.

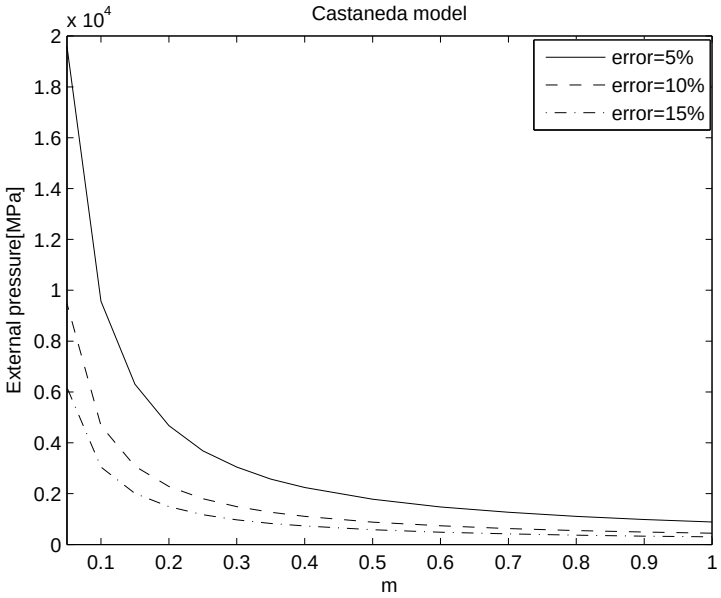

Figure 2.12: Threshold pressure p^*, for $50nm$ powder

Residual porosity

The residual porosity is a fundamental feature of the actual material, because it is the parameter that determines the mechanical properties of a sintered specimen.
A thirty minutes sintering process, with external loading pressure of $100MPa$, is considered. Here, we are interested to compare the residual porosities θ_r and θ_{r0} after thirty minutes, wherever the "sintering driving force" is taken to be either:

- $|\sigma - p_l|$ or
- $|\sigma|$,

respectively.
For the different values of powder grain size listed above, we are able to calculate the value of strain rate sensitivity m that permits to have a sintering reference time of the order of thirty minutes (30'). For the sake of convenience, without loss of generality, in the sequel a time range from twentyone to thirtynine minutes (corresponding to a variation of $\pm 30\%$ of the reference time) is considered.
Figure 2.13 shows the sintering time as a function of m and highlights the values of strain rate sensitivity m that correspond to the real sintering times.

With such values of the parameter m, we may calculate the error

$$e = \frac{\theta_r - \theta_{r0}}{\theta_r}, \tag{2.53}$$

occurring wherever the Laplace pressure p_l is neglected. Figure 2.14 shows values of such an error as a function of the strain rate sensitivity m, for values of the grain size between $100nm$ and $5\mu m$

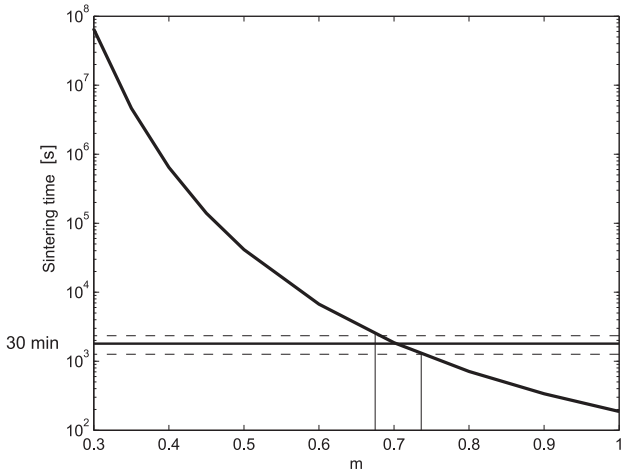

Figure 2.13: Sintering time as a function of the strain rate sensitivity m

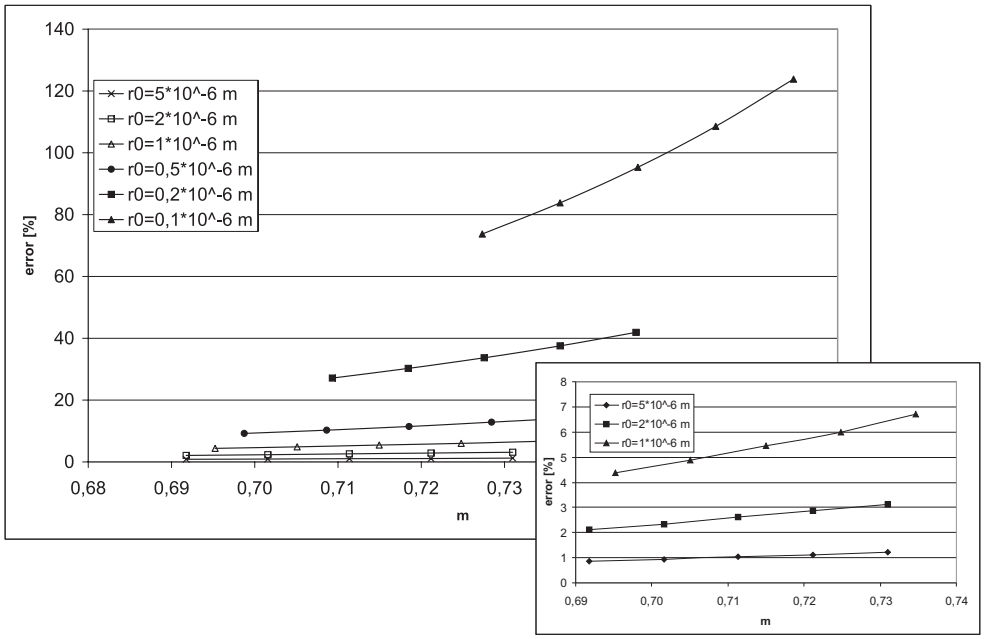

Figure 2.14: Errors $e\%$ on the residual porosity for different values of the grain size r_0

It is immediate to note that, for nano powder (i.e. for grain size less than $1\mu m$) the error becomes much higher than the case of micropowders. In particular, for size of the order of $100nm$, an error of about 150% may occur, while for $50nm$, the error is even 900% (not showed in figure).
It is worth noting that for lower values of grain size, the limiting situation where

$\sigma = p_l$ may be achieved. In Figure 2.15 a range(r_{01}, r_{02}) of critical radiuses may be deduced.
For lower grain sizes, the gap between θ_r and θ_{r0} is higher than the previous cases.

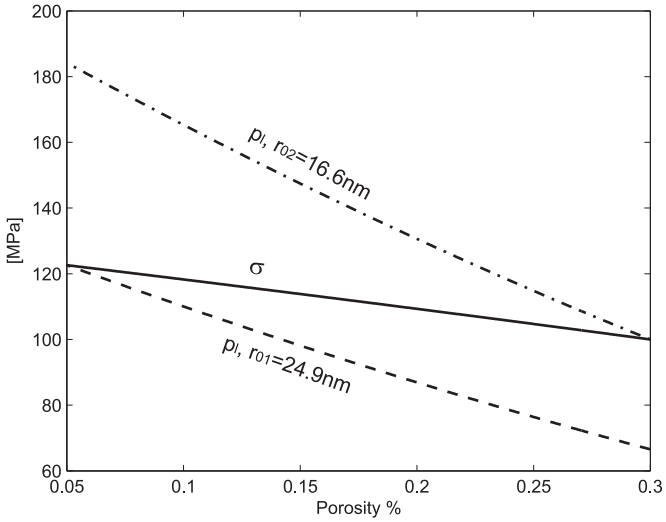

Figure 2.15: Range of critical radius

The second parameter that influences the Laplace pressure is the surface tension α. There are lots of uncertainties on the determination of the value of this the parameter [15]. Hence, because of lack of reliability, the sensitivity of the model to variations in the range of $\alpha(1 \pm 50\%)$ is analyzed.
Figure 2.16 shows the error e as a function of the surface tension α, for different values of powder grain size.
For increasing values of α, the Laplace pressure grows and hence the gap between θ_r and θ_{r0} increases accordingly; this phenomenon turn out to be more relevant for lower powder grain size.

2.3.3 Free sintering

The case of free sintering corresponds to a condition frequently met in industrial processes. In these cases, there is no applied external pressure, so that the shrinkage is due to the sintering stress p_l only.
Here, cylindrical samples of radius R and of height L, subject to free sintering, are considered, i.e. the boundary conditions are the following:

$$\begin{cases} \sigma_r(r = R) = 0, \\ \sigma_z(z = \pm L/2) = 0. \end{cases} \tag{2.54}$$

Substituting the constitutive law (2.1) into (2.54), the first and the second invariant of the strain rate tensor take the form:

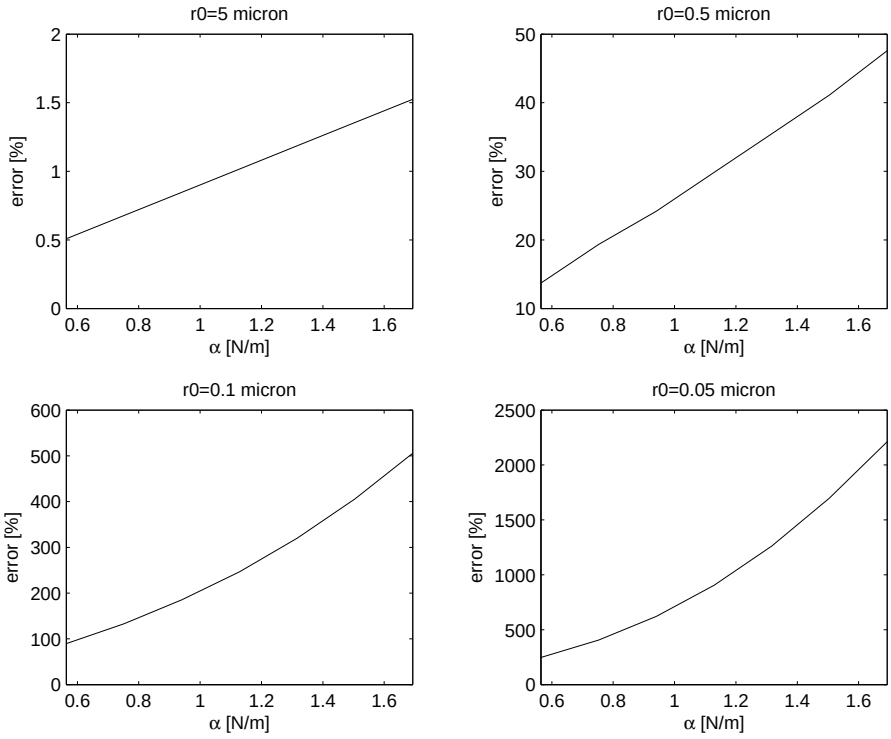

Figure 2.16: Errors $e\%$ on the residual porosity, for different values of the surface tension α

$$\begin{cases} \dot{e} = -\frac{p_l}{\psi}\frac{w}{\sigma(w)}, \\ \dot{\gamma} = 0. \end{cases} \tag{2.55}$$

Following Ashby's power-law (2.7), the first invariant of the strain rate tensor can be written as follows

$$\dot{e} = -\Big(\frac{p_l}{\sigma_0 A}\Big)^{\frac{1}{m}} \dot{\varepsilon_0} \psi^{\frac{-(1+m)}{2m}} (1-\theta)^{\frac{m-1}{2m}}. \tag{2.56}$$

By using relation (2.14), one can obtain the evolution law for the porosity for free sintering, i.e.:

$$\dot{\theta} = -\Big(\frac{p_l}{\sigma_0 A}\Big)^{\frac{1}{m}} \dot{\varepsilon_0} \psi^{\frac{-(1+m)}{2m}} (1-\theta)^{\frac{3m-1}{2m}}. \tag{2.57}$$

The introduction of the dimensionless specific time τ_L, defined by equation (2.50), yields the following normalization of equation (2.57):

$$\frac{\partial \theta}{\partial tau_L} = p_l^{\frac{1}{m}} \psi^{\frac{-(1+m)}{2m}} (1-\theta)^{\frac{3m-1}{2m}}. \tag{2.58}$$

In the case under exam, the stress and strain-rate tensors are purely hydrostatic. Thus, free sintering can be seen as a particular case of isostatic pressing,

with null external loading stress, i.e. equation (2.57) can be obtained from eq.(2.40), by substituting $\sigma = 0$.

Because for free sintering the only force driving the process is the Laplace pressure, it is worth noting that the choice of the approach used to derive its expression (stochastic or dissipation averaging, see section 2.2) has a strong influence on the result. This issue may be studied in the sequel.

1. *Sintering stress by using a stochastic approach ($p_l = \frac{3\alpha}{r_0}(1-\theta)^2$, see section 2.2.2.1)*
   By substituting the expression $p_l = \frac{3\alpha}{r_0}(1-\theta)^2$, equation (2.58)can be

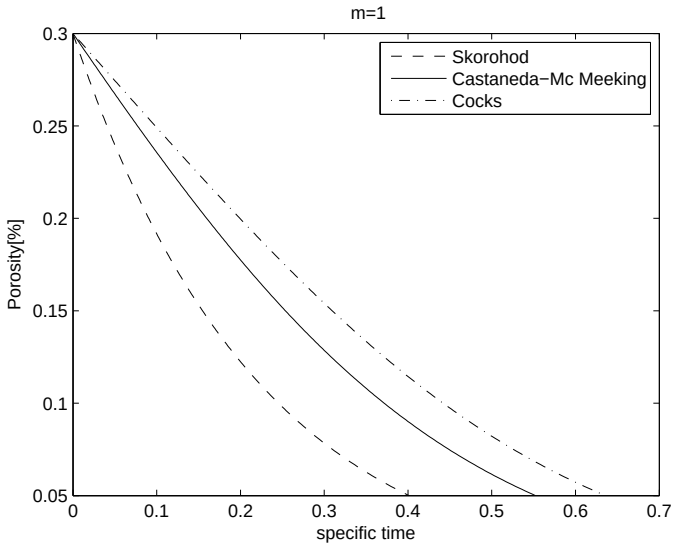

Figure 2.17: Free Sintering-Evolution of Porosity for m=1, $p_l = \frac{3\alpha}{r_0}(1-\theta)^2$

written as follows:

$$\frac{\partial\theta}{\partial\tau_L} = \Big(\frac{3\alpha}{r_0}\Big)^{\frac{1}{m}} \psi^{\frac{-(1+m)}{2m}} (1-\theta)^{3(\frac{m+1}{2m})}. \tag{2.59}$$

In order to compare the evolution of the porosity, for such a case, for the three different models considered in section 2.2.1(Skorohod, Cocks, Castaneda-Duva-Crow and Mc Meeeking; the latter two models coincide for isostatic pressing), Figure 2.17 shows the evolution of the porosity forfor $m = 1$.

It is worth noting that the result obtained for the three considered model are fairly different. This is due to the different expressions of the bulk modulus ψ.
Figure 2.2 (section 2.2.1) shows that the model of Cocks, for m=1, gives

the highest values of ψ in all range of interesting porosities. For such values of ψ, equation (2.57) gives lower values of the rate of change of the porosity $\dot{\theta}$ and it corresponds to higher sintering times.
Because the model of Skorohod introduces the smaller values of ψ, the sintering times obtained by adopting such a model are the shortest.

In Figure 2.18 the different $\dot{\theta}$ are plotted for the models of Castaneda

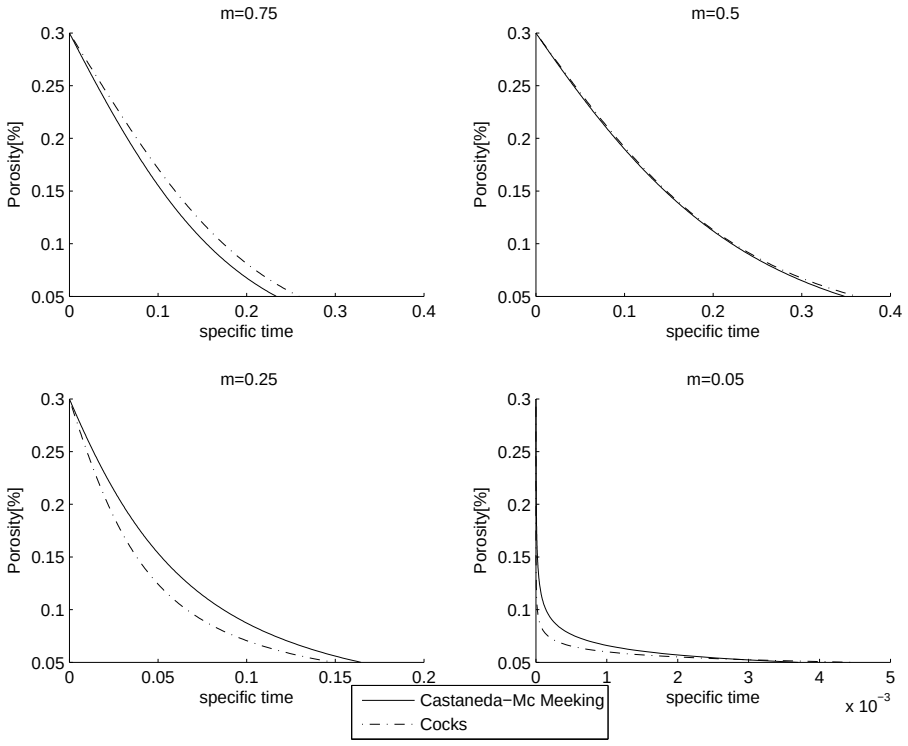

Figure 2.18: Free Sintering-Evolution of Porosity for different values of m , $p_l = \frac{3\alpha}{r_0}(1-\theta)^2$

.

and Mc Meeking, for different values of the parameter m.
Whenever m decreases, Figure 2.2 (section 2.2.1) shows that values of the bulk modulus ψ obtained by using the model of Castaneda increase, whereas the ones coming from the model of Cocks decrease. The same figure shows that, for lower values of m, the model of Castaneda gives values of ψ lower than the ones obtained by using the Cocks expression for the same item. Hence, the employment of the model of Cocks gives sintering times lower than those ones obtained by using the approach of Castaneda. From Figure 2.18, it may also be worth noting that, when m tends to zero (ideal plastic behavior), the time-porosity graph has a steep knee.

2. *Sintering stress from dissipation averaging (i.e.* $p_l = \frac{2\alpha}{r_0}\sqrt{\frac{3}{2}\psi(\theta)\frac{\theta}{1-\theta}}$*, see section 2.2.2.2)*

In this case, expression (2.57), which holds for m=1 only, reduces to

$$\dot{\theta} = -\frac{\dot{\varepsilon_0}}{\sigma_0 A}\frac{2\alpha}{r_0}\sqrt{\frac{3}{2}\frac{\theta(1-\theta)}{\psi}}. \tag{2.60}$$

In the considered range of porosity, the resulting values of the Laplace pressure are lower than the ones obtained by virtue of the expression derived by the stochastic approach (see Figure 2.5) and henceforth the sintering times are higher (see figures 2.19 and 2.17).

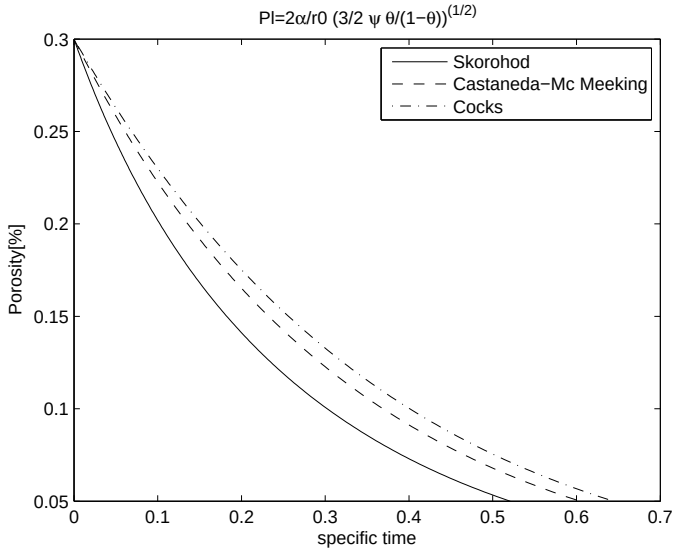

Figure 2.19: Free Sintering-Evolution of Porosity for m=1, $p_l = \frac{2\alpha}{r_0}\sqrt{\frac{3}{2}\psi(\theta)\frac{\theta}{1-\theta}}$

Influence of the temperature on the free sintering time

In this paper, the sintering processes are assumed to be at constant temperature. In fact, pre-heated electric oven are employed in industrial processes, whose thermal capacity may be regarded infinitely large with respect to the one of any specimen under consideration. Henceforth, the temperature remains constant during sintering.
In this section, temperatures are normalized by using the dimensionless specific temperature $T*$, defined as:

$$T^* := \frac{T}{T_{melting}}. \tag{2.61}$$

There are two main phenomena that determine the influence of the temperature on free sintering processes:

1. for lower values of m ($m \to 0$), the material behavior is almost plastic and yet it feels the effects of the temperature more than for higher values of the parameter m (see Figure 2.20).

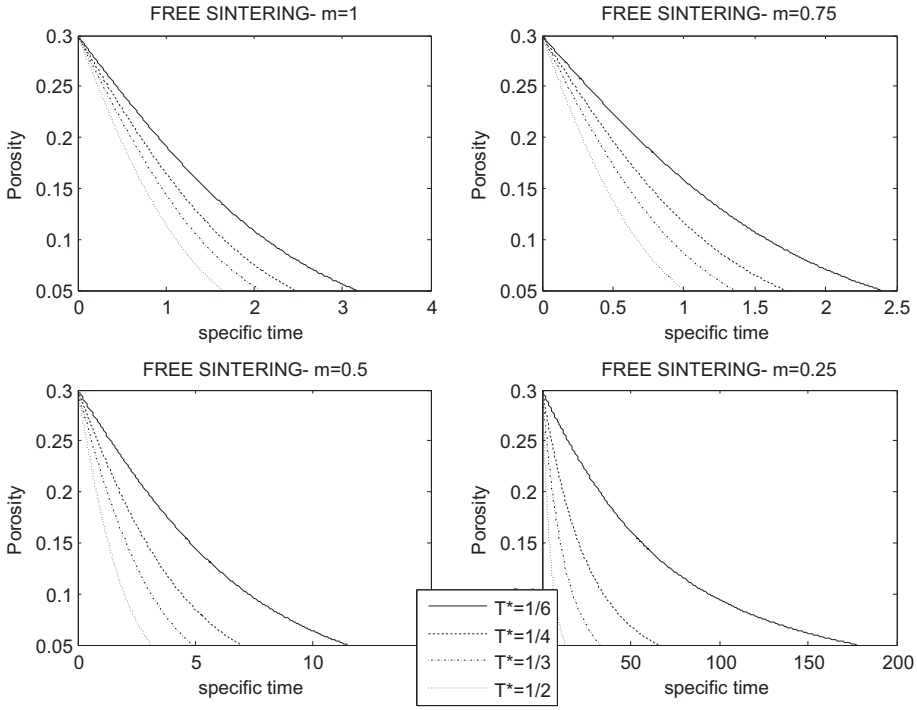

Figure 2.20: Free sintering-Evolution of porosity for different values of the specific temperature.

2. the material behavior is affected by the temperature; thus the values of the parameter m should be a function of the temperature.

The present model takes only into account the first phenomenon, and the implicit dependence on the temperature is given by $A = \tilde{A}(T)$ (see [18]) and the material constant A, appearing in equation (2.57), is raised to $1/m$.
Figure 2.20 shows the evolution of the porosity, evaluated by using the model of Castaneda and for the expression of p_L derived by the stochastic approach, for different values of the strain rate sensitivity m and for different specific temperature T^*. It is evident that, when the temperature increases, the sintering time does decrease. This reduction becomes more important for lower values of the parameter m.

2.4 Stability

2.4.1 Lower order analysis

Here we may denote by $\theta^{(0)}(t)$ the fundamental solution of the evolution law (2.40) associated with an uniform distribution of the initial porosity. Following [43], Sect. 3.1.1, we assume that the perturbed solution has the form

$$\theta(t) = \theta^{(0)}(t) + \delta\theta(t), \tag{2.62}$$

where the magnitude of the perturbation $\delta\theta(t)$ is taken to be much smaller than the one of $\theta^{(0)}(t)$ at all times. In [43], section 3.1.1, a normalized perturbation growth rate with respect to the current rate of change of porosity is considered; this is done in order to have a "first" order information about the stability of the process.
The quantity $\frac{\delta\dot{\theta}}{\delta\theta}$ can be regarded as the perturbation growth rate. It is possible to calculate the quantity $\frac{1}{\dot{\theta}}\frac{\delta\dot{\theta}}{\delta\theta}$ as a function of θ, θ_0, m, p_l and the external pressure. This can be done in the framework of the three different models considered in the previous sections.

Because, during sintering, shrinkage occurs monotonically ($\dot{\theta} \leq 0$), the problem is linearly stable if $\frac{\delta\dot{\theta}}{\delta\theta} < 0$, whereas linearly unstable if $\frac{\delta\dot{\theta}}{\delta\theta} > 0$. The predicted results are plotted in Fig. 2.21, 2.22, 2.23 in terms of the porosity for different values of m, for the three principal cases defined in section 2.3.1.

- *Case in which $\sigma > p_l$ during the whole process.*
  Figure 2.21 shows that the process is always linearly stable, or it is unstable for higher porosities (i.e. values that are very unlikely to occur in real isostatic pressing processes).

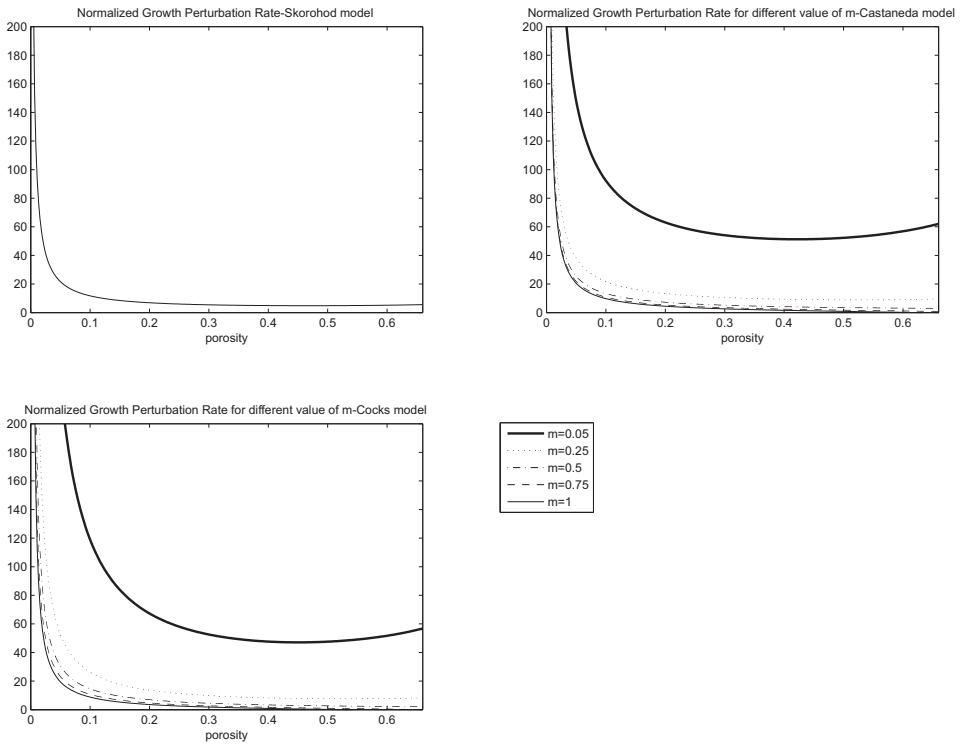

Figure 2.21: Linear stability analysis- Low order, S.E.P.=10

If the Skorohod model is employed, the sintering process turns out to be stable for the meaningful range of porosities considered in this paper (see

Fig. 2.21).
For the model of Castaneda and Mc Meeking, instead, the process is stable for porosities $\theta < 0.6$ whenever m=1, whereas it is always stable for smaller values of the parameter m (see Figure 2.21.b).
Furthermore, for the model of Cocks, the process is stable for porosities $\theta < 0.51$ whenever $m = 1$. By sampling values of m whit negative increments $\Delta m = -0.25$, Figure 2.21.c shows that for $m = 0.75$ such a process is stable if $\theta < 0.64$, and it is always stable in all the other cases.
Thus, it is evident that for lower values of the parameter m, i.e. when the material tends to be more viscoplastic, the process gains stability.

- *Cases in which $\sigma - p_l$ changes sign during the process.*
  The quantity $\frac{1}{\dot{\theta}}\frac{\delta\dot{\theta}}{\delta\theta}$ has an asymptote for $\theta = \theta^*$, which we recall to be the critical porosity occurring whenever $\sigma = p_l$.

  Figure 2.22 shows that, for $\theta > \theta^*$ (i.e. $\sigma > p_l$) the process is stable whatever model for the bulk modulus is chosen.
  For the remaining cases, i.e. whenever $\theta < \theta^*$ (hence $\sigma < p_l$), prediction obtained by means of the different models disagree. In the range $0 < \theta < \theta^*$, although by employing the Skorohod model the process is unstable for higher porosities and stable for lower ones, the achieved results from the other models show exactly the opposite behavior.

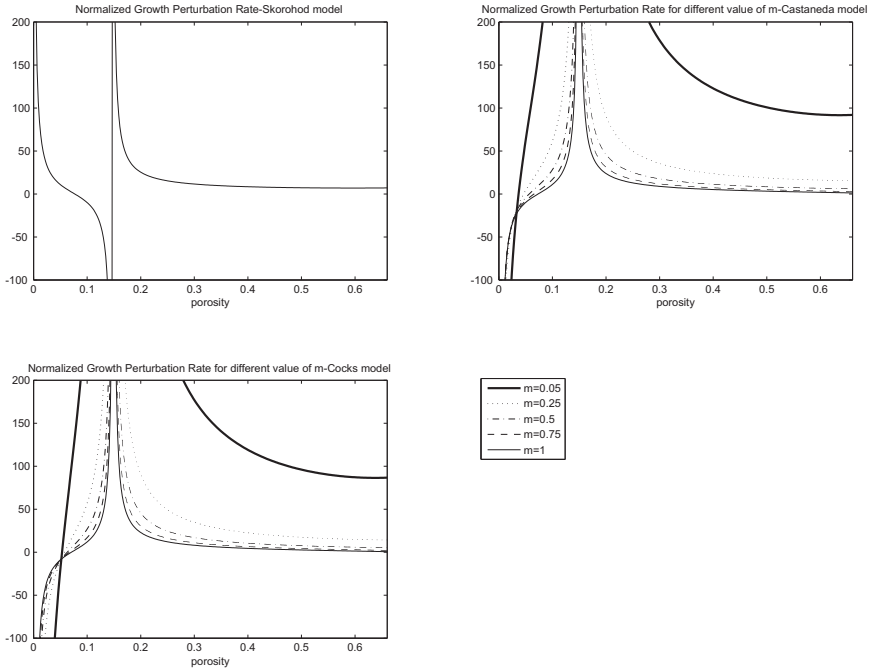

Figure 2.22: Linear stability analysis- Low order, S.E.P.=1.77

- *Cases in which $\sigma < p_l$ during the whole process.*

Like in the previous case, the results coming from the different models totally disagree for $\theta < \theta^*$, as shown in Figure 2.23.
The most interesting case is free sintering. Indeed, by using the model

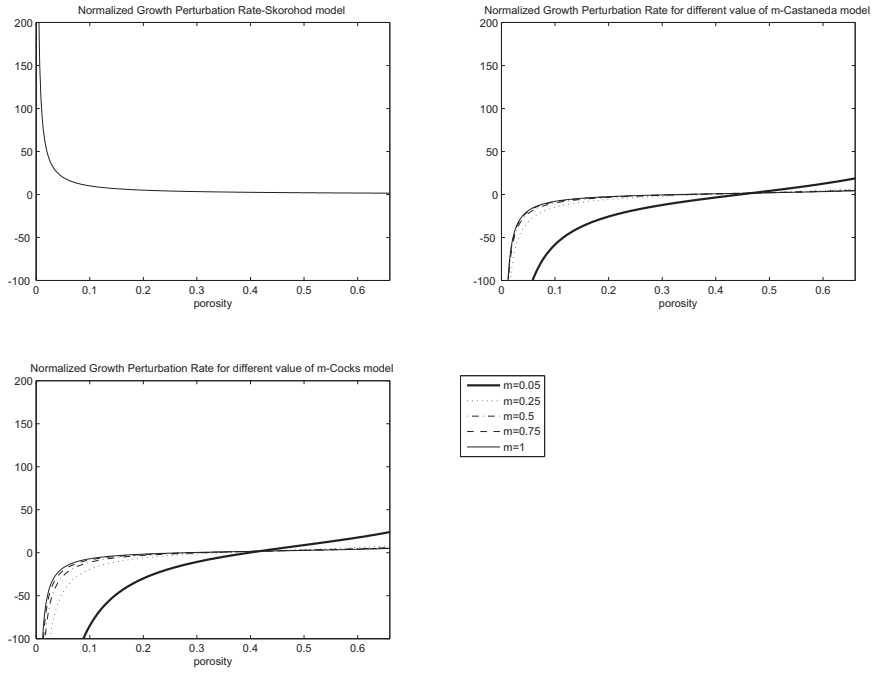

Figure 2.23: Linear stability analysis- Low order, S.E.P.=0 (free sintering)

of Skorohod, such a process is stable. Nevertheless, for the models of Castaneda/Mc Meeking and Cocks, free sintering is unstable for lower porosities. This means that exists a lower bound, under which the process is unstable. Figure 2.23 shows that such a bound varies with the strain rate sensitivity, and the values of this limit porosity are rather high in the explored range and yet unrealistic.
Thereby, the low order analysis can not be considered reliable.

2.4.2 Higher order analysis

The former analysis was meant to explore the consequences of the perturbation of the porosity on the rate of change $\dot{\theta}$, evaluated by equation (2.40).
In the previous section we showed that such approach is not satisfactory, since it leads to contradictory results. Henceforth, a more refined method of producing perturbations is needed. To this end, one may follow the procedure used in [43], Section 3.1.2, owning to account for perturbation of the actual geometry (through the cross sectional area and the porosity itself), of the stress due to

external load and, in our case, of the Laplace pressure.

Two differences may be highlighted between the stability analysis performed in the present work and the one introduced in [43]:

- unlike in [43], here the high order analysis approach is actually required;
- the presence and the perturbation of the sintering stress p_l play here a key role.

A perturbed solution is considered in the following form:

$$\begin{cases} \theta(t) = \theta^0(t) + \delta\theta \exp(\lambda(t-t_0)), \\ \sigma(t) = \sigma^0(t) + \delta\sigma \exp(\lambda(t-t_0)), \\ S(t) = S^0(t) + \delta S \exp(\lambda(t-t_0)), \\ p_{l0}(t) = {p_{l0}}^0(t) + \delta p_{l0} \exp(\lambda(t-t_0)); \end{cases} \tag{2.63}$$

by substituting (2.63) in equations (2.40), (2.45), (2.16) (for the Laplace pressure derived by using stochastic approach) and (2.47), after linearization about the foundamental solution ($\theta^0(t)$, $\sigma^0(t)$, $S^0(t)$, ${p_{l0}}^0(t)$) we have:

$$\begin{bmatrix} 0 & S & \sigma & 0 \\ \frac{\lambda}{\dot\theta} + \frac{\frac{d}{d\theta}G(\theta)}{G(\theta)} & 0 & \frac{1}{S}\left[1 - \frac{\lambda}{\dot\theta G(\theta)}\right] & 0 \\ \frac{1}{\dot\theta}\frac{\partial f(\theta,\sigma,p_{l0})}{\partial\theta} - \frac{\lambda}{\dot\theta} & \frac{1}{\dot\theta}\frac{\partial f(\theta,\sigma,p_{l0})}{\partial\sigma} & 0 & \frac{1}{\dot\theta}\frac{\partial f(\theta,\sigma,p_{l0})}{\partial p_{l0}} \\ \frac{\partial p_l(\theta,p_{l0})}{\partial\theta} & 0 & 0 & \frac{\partial p_l(\theta,p_{l0})}{\partial p_{l0}} \end{bmatrix}_{\theta^0(t),\sigma^0(t),S^0(t),{p_{l0}}^0(t)} \begin{bmatrix} \delta\theta \\ \delta\sigma \\ \delta S \\ \delta p_{l0} \end{bmatrix} = \begin{bmatrix} 0 \\ 0 \\ 0 \\ 0 \end{bmatrix}, \tag{2.64}$$

where

$$\begin{cases} G(\theta) = \frac{2}{3(1-\theta)}, \\ f(\theta,\sigma,p_{l0}) = \dot\varepsilon_0 (1-\theta)^{\frac{3m-1}{2m}} \left(\frac{|\sigma_z - p_l|}{A\sigma_0}\right)^{\frac{1}{m}} \psi^{\frac{-(1+m)}{2m}} \end{cases} \tag{2.65}$$

and the matrix appearing in (2.64)is evaluated at ($\theta^0(t)$, $\sigma^0(t)$, $S^0(t)$, ${p_{l0}}^0(t)$), as specified. Eq. (2.64) has non-trivial solutions if and only if the determinant of the matrix is equal to zero. By imposing this condition, we obtain a characteristic equation with respect to the normalized perturbation growth rate $\frac{\lambda}{\dot\theta}$:

$$\left(\frac{\lambda}{\dot\theta}\right)^2 + B\left(\frac{\lambda}{\dot\theta}\right) + C = 0, \tag{2.66}$$

where $\dot\theta = \dot\theta^0$ and

$$\begin{cases} B = \Big[-G(\theta) + \frac{\left(\frac{\partial f(\theta,\sigma,p_{l0})}{\partial\sigma}\right)\sigma G(\theta) - \frac{\partial f(\theta,\sigma,p_{l0})}{\partial\theta}}{f(\theta,\sigma,p_{l0})} - \frac{2p_{l0}\frac{\partial f(\theta,\sigma,p_{l0})}{\partial p_{l0}}}{f(\theta,\sigma,p_{l0})(1-\theta)} \Big]_{\theta^0(t),\sigma^0(t),S^0(t),{p_{l0}}^0(t)}, \\ C = \Big[\frac{\left(\frac{\partial f(\theta,\sigma,p_{l0})}{\partial\sigma}\right)\sigma\frac{dG(\theta)}{d\theta} + \left(\frac{\partial f(\theta,\sigma,p_{l0})}{\partial\theta}\right)G(\theta)}{f(\theta,\sigma,p_{l0})} + \frac{2p_{l0}\frac{\partial f(\theta,\sigma,p_{l0})}{\partial p_{l0}}}{f(\theta,\sigma,p_{l0})(1-\theta)} \Big]_{\theta^0(t),\sigma^0(t),S^0(t),{p_{l0}}^0(t)}. \end{cases} \tag{2.67}$$

Like in [43], high order stability analysis leads to a second order characteristic equation with respect to the perturbation growth rate.
Roots of equation (2.66) are shown in the following figures for different models and for the three principal cases defined in section 2.3.1.

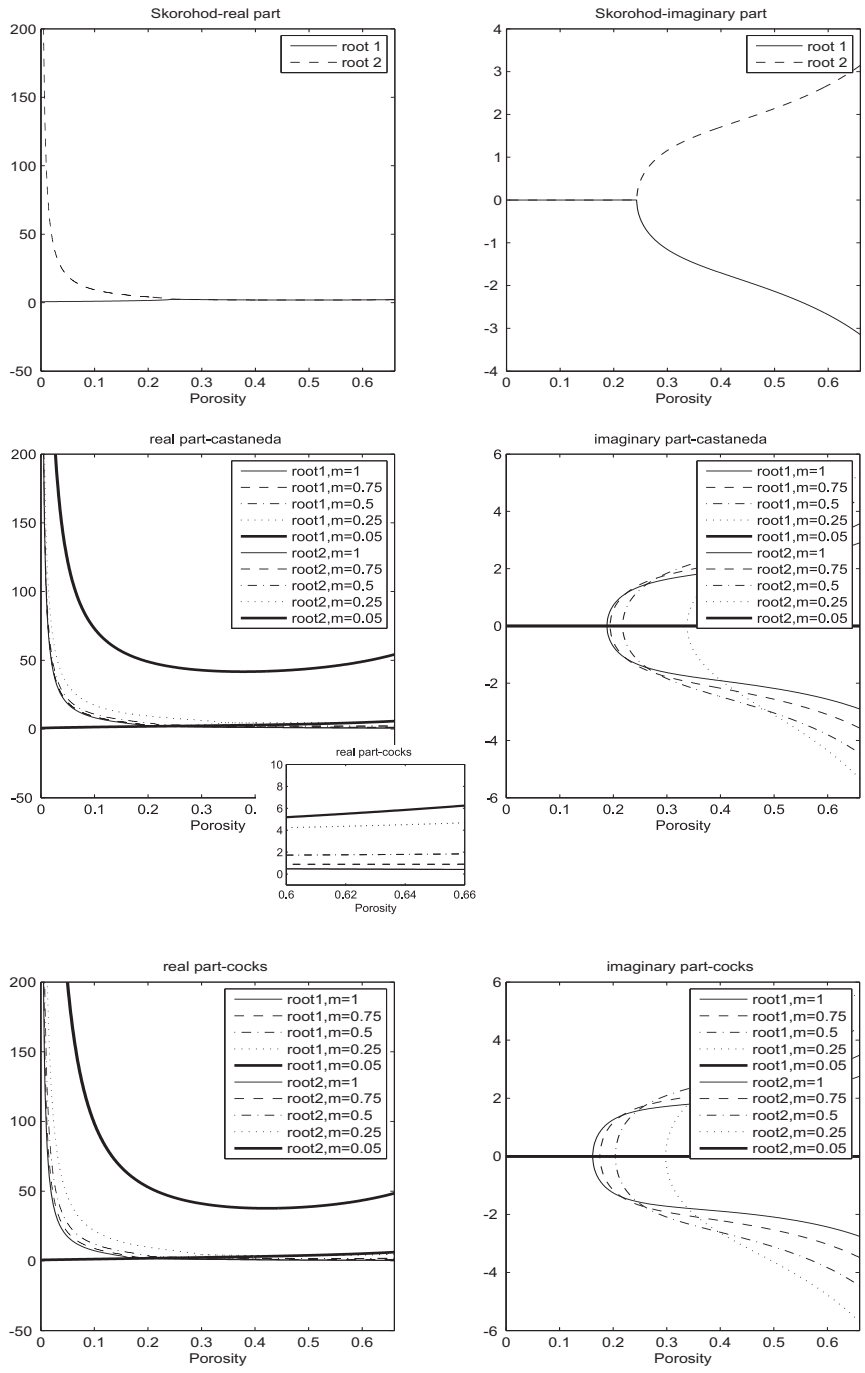

Figure 2.24: High order stability analysis, S.E.P.=10 ($\sigma > p_l$)

- *Case in which $\sigma > p_l$ during the whole process.*

Figure 2.24 summarizes the outcomes of the higher order stability analysis for such case. This figure shows that the process is always linearly stable

for all models. For lower porosities, equation (2.66) has two distinct real roots $\frac{\lambda_1}{\dot{\theta}}, \frac{\lambda_2}{\dot{\theta}}$. The first root is positive and tends to infinity for $\theta \to 0$, and the second (lower) root is also positive. Hence, because $\lambda_1 < 0$, $\lambda_2 < 0$, the problem is linearly stable.

For higher values of the porosity, the roots $\frac{\lambda_1}{\dot{\theta}}$ and $\frac{\lambda_2}{\dot{\theta}}$ become complex, with positive real part. Thus $Re(\lambda_1) < 0$, $Re(\lambda_2) < 0$ and hence the process is asymptotically stable for all range of porosities.

- *Cases in which $\sigma - p_l$ changes sign during the process.*

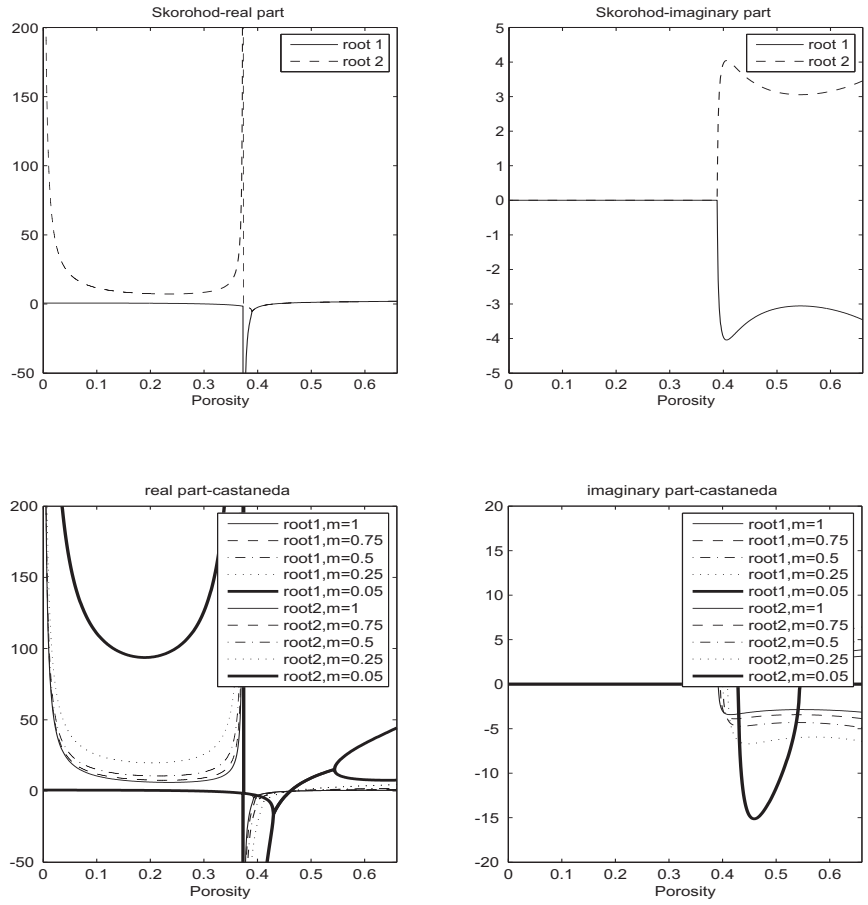

Figure 2.25: High order stability analysis, S.E.P.=1.77 ($\sigma - p_l$ changes sign during the process)

Figure 2.25 and 2.26 show the roots $\frac{\lambda_1}{\dot{\theta}}$ and $\frac{\lambda_2}{\dot{\theta}}$ for the case in which $\sigma - p_l$ changes sign; it is immediate to note that, when $\theta = \theta^*$ (which is achieved for $\sigma = p_l$) such roots have an asymptote, no matter what model is employed.
For higher values of the porosity, these roots are complex with positive

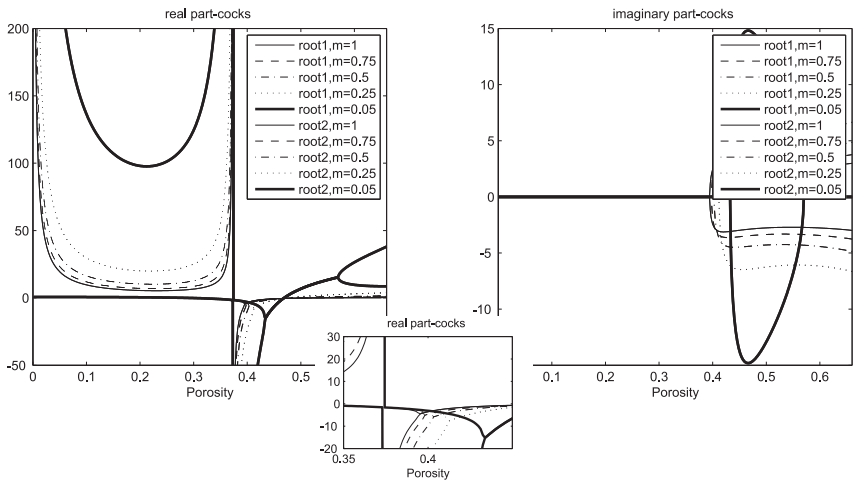

Figure 2.26: High order stability analysis, S.E.P.=1.77 ($\sigma - p_l$ changes sign during the process)

real part; hence the process is asymptotically stable.

Figure 2.27 shows a zoom of Figure 2.25.b for $m = 1$. This figure allows

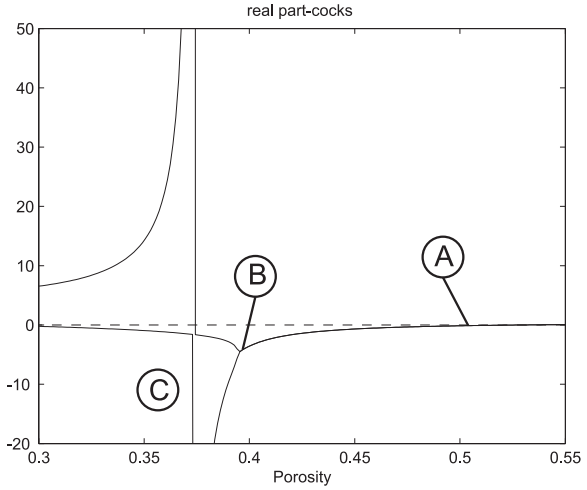

Figure 2.27: High order stability analysis, S.E.P.=1.77, particular

for analyzing the sign of the quantities $\frac{\lambda_1}{\dot{\theta}}$ and $\frac{\lambda_2}{\dot{\theta}}$. Going closer to the asymptote corresponding to $\sigma = p_l$ (denoted by C), first (in the point denoted by A) the real part of both roots becomes negative ($Re(\frac{\lambda_1}{\dot{\theta}}, \frac{\lambda_2}{\dot{\theta}}) < 0$). Then, roots λ_1, λ_2 become real, both greater than zero (in the point denoted by B). This means that, close to the asymptote, the process is unstable; this condition allows sintering to keep on going.
For porosity slightly lower than θ^*, the roots are real and $\lambda_1 < 0$, $\lambda_2 > 0$, and hence the process is linearly unstable. The positive root λ_2 tends to draw away from equilibrium; λ_2 has absolute value very close to zero, and

so this causes a stretch of sintering time.

From Figure 2.25 we see that for lower values of the strain rate sensitivity m, the roots become real for high values of porosity, although this phenomenon does not change the stability. This is because both roots are negative.
For the other model of the Laplace pressure, i.e. the one based on the averaging of dissipation (see equation 2.39), the stability analysis yields analog results.

- *Cases in which $\sigma < p_l$ during the whole process.*

The most interesting case is free sintering; in this process, the initial porosity is usually lower than 30%. For this case, the roots λ_1 and λ_2 are both real and negative and the process is linearly stable. Figure 2.28

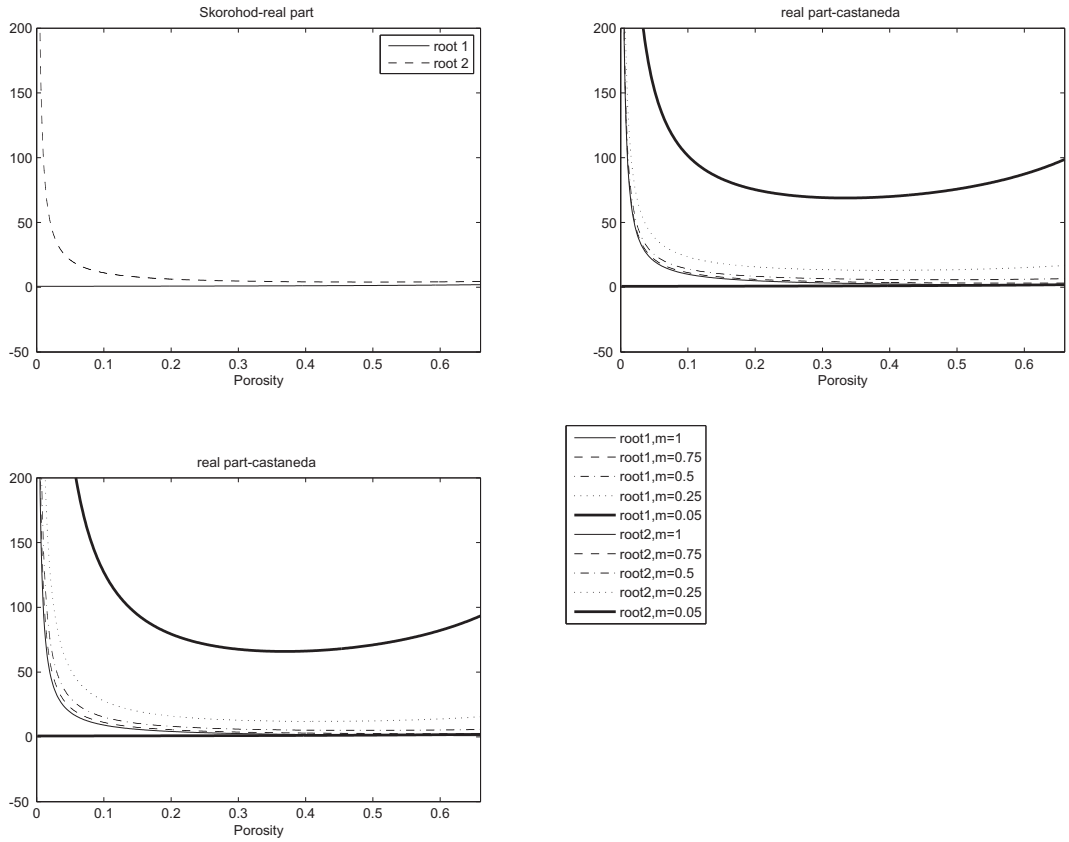

Figure 2.28: High order stability analysis, free sintering, $p_l = \frac{3\alpha}{r0}(1-\theta)^2$

shows the results obtained considering the Laplace pressure evaluated by using the stochastic approach, leading to the following expression for the sintering stress: $p_l = \frac{3\alpha}{r0}(1-\theta)^2$. Results obtained by using the other methodology (that leads to $p_l = \frac{2\alpha}{r0}\sqrt{\frac{2}{3}\psi(\theta)\frac{\theta}{1-\theta}}$) are very similar.

Chapter 3

Sintering of cylindrical specimens: Part I - Effects of the Laplace pressure during "free" forging.

[Submitted]

Abstract

Unlike previous recent contributions, the influence of the gas pressure in pores (called *interstitial stress* or *Laplace pressure*) during sintering of pre-compacted metallic (micro/nano)-powdered cylinders is here analyzed.

The role of the Laplace pressure is twofold.

- First of all, during the sintering process such a pressure influences the evolution of the porosity and, for instance, its residual value at a given time. It is worth emphasizing that threshold pressures are determined below which the sintering stress is actually not negligible; the duration of the process is indeed heavily affected by such a stress whenever the residual porosity is prescribed. In turn, such a duration would be underestimated otherwise. Furthermore, industrial processes often entail loading pressures lower than the thresholds mentioned above, especially for "small" grain sizes.

- The external loading parameter may be tuned in such a way that, at some stage of the process, i.e. when a "critical porosity" is reached, its value may equate the Laplace pressure. Henceforth, the porosity would remain constant for a long time.

  In this paper, the "free" forging loading mode (the case in which a transverse compressive force acts at the top and bottom faces of the sample, with no lateral confinement), is considered. A stability analysis allows us to conclude that, the equilibrium is stable at such a value and hence

the critical porosity θ^* represents a limit threshold under which it is not possible to go.
Moreover, it is worth noting that large strain occur in such a kind of loading mode. Thus, in order to study this problem, both the stress and the (infinitesimal) strain employed in this analysis should be replaced by appropriate (possibly work-conjugate) choice of the stress and strain measures, although this goes beyond the aim of this work.

Notation

θ= porosity
σ_{ij} = components of the stress tensor
$\dot{\varepsilon}_{ij}$ = components of the strain rate tensor
$\dot{\varepsilon}'_{ij}$ = components of the deviatoric strain rate tensor
$\dot{e}$= first invariant of the strain rate tensor
$\dot{\gamma}$=second invariant of the deviatoric strain rate tensor
p= first invariant of the stress tensor
τ=second invariant of the stress tensor
w= effective equivalent strain rate
$\sigma(w)$= effective equivalent stress
A= time-dependent material constant
m= strain rate sensitivity
ψ= normalized bulk modulus
φ= normalized shear modulus
p_L= Laplace pressure (interstitial stress)
n= loading mode parameter
σ_0= reference stress
$\dot{\varepsilon}_0$= reference strain rate
α= surface tension
r_0= characteristic radius of particles
D= dissipation potential
d=dissipation per unit volume mass
S= cross-sectional area of the specimen
τ_E= dimensionless specific time
$S.E.P.$= specific external pressure
θ^*= critical porosity
θ_r= residual porosity

3.1 Introduction

This work deals with the the role of the interstitial stress (due to the pressure exerted by the gas in the pores) during forging of cylindrical specimens. It is intuitive that such a pressure may play an important role for industrial processes involving moderate external loads in comparison with the actual sintering stress. This is not the case in [43], a keystone paper in the subject, dealing with an

analysis of the kinetics and stability of porous axially symmetric bodies undergoing different loading modes. In such a paper, both the issues of (i) modeling of sintered materials obtained by compacted powders and (ii) constitutive equations for porous media are taken from the state of the art of the literature (see e.g. [33, 34, 44, 45] and [19, 21, 20, 23, 36, 51] respectively). Although in [43] the problem is solved by neglecting the Laplace pressure, the introduced strategy appears to be the most effective one among other possibilities to predict the kinetics of bodies undergoing sintering (see e.g. [40]). Indeed, Olevsky and Molinari point out that the assumption of homogeneous plane stress through a sample is reasonable even in the case of non-uniform cross-section (see e.g. [13] for tensile tests). Incidentally, this is equivalent to assuming that specimens undergo constant states of (plane) stresses corresponding to the average of the actual stress fields. The approach suggested by the assumptions above has the advantage of capturing the essentials of both kinetics and stability, avoiding to search for the solution of complicated (initial) boundary value problems. Nevertheless, this strategy needs to be extended to the case of moderate stresses in comparison with the interstitial gas pressure.
This paper may be outlined as follows.
In Section 3.2 a theory of sintering introduced in [29, 43] is essentially revisited; in Sections 3.2.1 and 3.2.2 the different models for the shear and bulk moduli and the interstitial stress respectively are sumarized and discussed.
In Section 3.3, the evolution of the porosity is studied for the case of free forging for the different choices of the models mentioned above. In Section 3.3.1, in order to perform such analysis three cases, analog with the ones analyzed in [54] for the case of isostatic pressing, may arise through a comparison between the stress caused by external loading and the Laplace pressure. In particular, the occurrence of equality between such values is reached at a definite (critical) porosity, which remains constant for some time. Moreover, in Sect.3.3.2, the computation of the axial and radial strain rate during the sintering process is performed. In 3.4, two issues are investigated. First of all, thresholds on stresses cased by external loads are determined under which the influence of the interstitial pressure cannot be neglected. Such thresholds may strongly be influenced by the strain rate sensitivity of the material and, more importantly, by the grain size of the particles. This feature may have a stronger impact for nano-structured powders, that play an increasingly important role in applications (see e.g. [31, 39, 42, 49]).
In Section 3.5, the stability of the process (namely the time evolution of the porosity obtained in Sect. 3.3), is performed following the lines traced in [43]. Motivated by the unsatisfactory, and yet self-contradictory, results obtained in [54], Sect. 4.1, given by a lower-order stability analysis (obtained by perturbing the porosity alone), a higher order analysis is performed. The porosity, the stress due to the external loading, the cross section of the sample and the reference value of the interstitial stress are then perturbed; this analysis shows that the results obtained by using the different models for the shear and bulk moduli do not agree for a restricted range of external load: for Skorohod model, the process is stable, and it exists a limiting porosity, under which the process can not continue; by adopting the other models, the process turn out to be un-

stable from the beginning. Moreover, it is worth noting that large strain occur in such a kind of loading mode. Thus, both the stress and the (infinitesimal) strain employed in this analysis should be replaced by appropriate (possibly work-conjugate) choice of the stress and strain measures, although this goes beyond the aim of this work.
The case of constrained forging (axial load acting at the top and bottom faces of the sample in a rigid die) will be treated in Part II of the present paper.

3.2 Theory of sintering and porosity kinetics

The mechanical response of a porous body with nonlinear-viscous behavior is described by a rheological constitutive relation that inter-relates the components of a stress tensor σ_{ij} and a strain rate tensor $\dot{\varepsilon}_{ij}$ (see [29]) as follows.

$$\sigma_{ij} = \frac{\sigma(w)}{w}[\varphi\dot{\varepsilon}'_{ij} + \psi\dot{e}\delta_{ij}] + p_l\delta_{ij}, \tag{3.1}$$

where $\dot{\varepsilon}'_{ij}$ denotes the deviatoric strain rate tensor, and w is the effective equivalent strain rate. This is connected with the current porosity and with the invariants of $\dot{\varepsilon}_{ij}$:

$$w = \frac{1}{\sqrt{1-\theta}}\sqrt{\varphi\dot{\gamma}^2 + \psi\dot{e}^2}, \tag{3.2}$$

where

$$\dot{e} = \dot{\varepsilon}_{ii}, \tag{3.3}$$

$$\dot{\gamma} = \sqrt{\dot{\varepsilon}'_{ij}\dot{\varepsilon}'_{ij}}, \tag{3.4}$$

i.e. $\dot{\gamma}$ is the second invariant of the deviatoric strain rate tensor and repeated indexes in the same formulae denotes summation over such indexes.

The quantity p_l represents the interstitial pressure produced by the gas contained in the pores; in the sequel we shall refer to p_l as either the "Laplace pressure" or the "sintering stress" (see [29, 32, 43]).

Equation (3.1) permits to obtain the first invariant of the stress tensor p :

$$p = \frac{1}{3}tr\sigma = \frac{\sigma(w)}{w}\psi\dot{e} + p_l, \tag{3.5}$$

and the second invariant of stress tensor τ:

$$\tau = \sqrt{\sigma'_{ij}\sigma'_{ij}} = \frac{\sigma(w)}{w}\varphi\dot{\gamma}. \tag{3.6}$$

The quantities φ, ψ, p_l and their dependence upon the porosity will be treated in sections 2.1 and 2.2.

Let us consider a cylindrical axisymmetric specimen, subject to an external load. The porosity, θ, is assumed to be constant in the specimen volume and it is defined as the ratio between the pore volume and the total volume (see [43]). Moreover, we will consider the stress tensor,

$$[\sigma_{ij}] = \begin{bmatrix} \sigma_r & 0 & 0 \\ 0 & \sigma_r & 0 \\ 0 & 0 & \sigma_z \end{bmatrix}, \tag{3.7}$$

and the strain rate tensor, averaged on the specimen volume.
If $\dot{\varepsilon}_z$ and $\dot{\varepsilon}_r$ are respectively the axial and radial strain rates, then

$$\dot{e} = \dot{\varepsilon}_z + 2\dot{\varepsilon}_r, \qquad \dot{\gamma} = \sqrt{\frac{2}{3}}|\dot{\varepsilon}_z - \dot{\varepsilon}_r|, \tag{3.8}$$

and $\dot{\gamma}$ is the second invariant of the strain rate tensor

Following Olevsky [43], one can introduce a loading mode parameter n defined by:

$$n = \frac{\tau}{p} = \frac{\varphi\dot{\gamma}}{\psi\dot{e}}. \tag{3.9}$$

The loading mode parameter assumes the following values for the corresponding loading modes:

1. $n = 0$ for isostatic pressing;
2. $n \to \infty$ for pure shear (p = 0);
3. $n = -\sqrt{6}$ for "free" forging;
4. $n = \sqrt{6}$ for drawing;
5. $n = \sqrt{\frac{2}{3}} sgn(\dot{\varepsilon_z})\frac{\varphi}{\psi}$ for constrained forging.

We refer to free forging as the loading mode represented in Fig. 3.1.a, a transverse compressive force acting at the top and bottom faces of the sample with no lateral confinement. Henceforth, the case of constrained forging, shown in figure 3.1.b, is nothing but an axial compression of the sample in a rigid die. In the sequel, we shall consider cases 1, 3 and 5 only. From (3.1), (3.8) and (3.9), can be obtained the following relation:

$$\sigma_z = \frac{\sigma(w)}{w}\psi\dot{e}\Big[1 + \sqrt{\frac{2}{3}}n\ sgn(\dot{\varepsilon}_z - \dot{\varepsilon}_r)\Big] + p_l. \tag{3.10}$$

The dependence of effective equivalent stress $\sigma(w)$ on the effective equivalent strain rate w determines the constitutive behavior of a porous material.

Following Ashby [18], a power-law mechanism of deformation is assumed:

$$\frac{\sigma(w)}{\sigma_0} = A\Big(\frac{w}{\dot{\varepsilon}_0}\Big)^m, \tag{3.11}$$

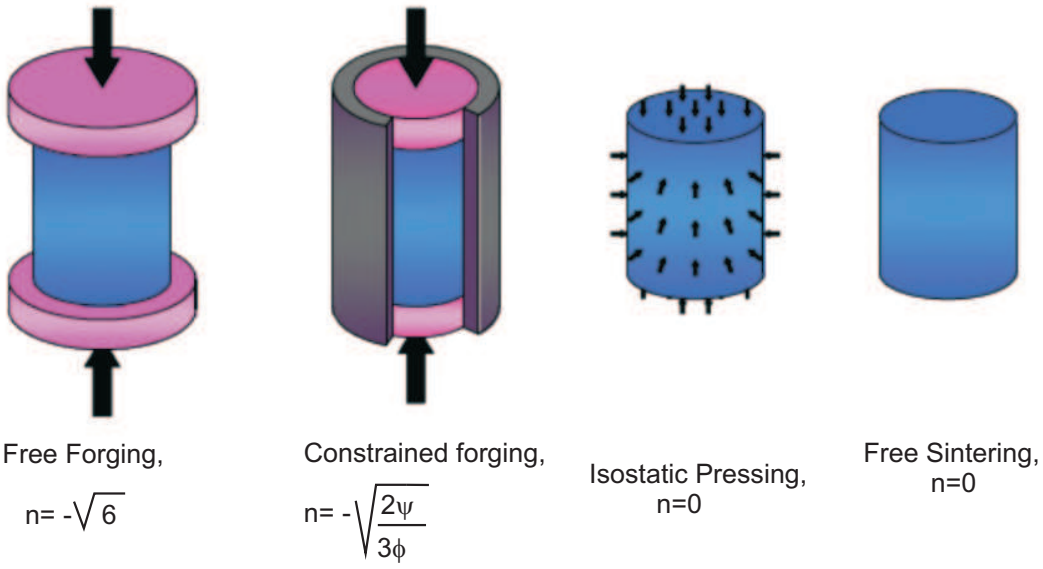

Figure 3.1: Different loading modes: forging, costrained forging, isostatic pressing, free sintering

where A and m are material constants (A is the temperature dependent, $0 < m < 1$), σ_0 and ε_0 are the reference stress and the reference strain rate, respectively. Two limiting cases corresponding respectively to the ideal plasticity and linear viscosity are given by $m = 0$ and $m = 1$ respectively.
Equations (3.11) and (3.2) can be used to obtain the ratio between the effective equivalent stress $\sigma(w)$ and the effective equivalent strain rate w:

$$\frac{\sigma(w)}{w} = \frac{\sigma_0 A}{\dot{\varepsilon}_0^m} w^{m-1} = \frac{\sigma_0 A}{\dot{\varepsilon}_0^m} |\dot{e}|^{m-1} \Big[\frac{\psi}{1-\theta} \Big(\frac{\psi}{\varphi} n^2 + 1 \Big) \Big]^{\frac{m-1}{2}}. \tag{3.12}$$

This paper is meanly denoted to study the influence of the interstitial pressure on the overall stress; for this reason, it is essential to monitor the magnitude $|\sigma_z - p_l|$ for each analyzed loading mode

The expression (3.12) can be related to the constitutive law (3.10) in order to obtain the following relation:

$$|\sigma_z - p_l| = \frac{A\sigma_0}{\dot{\varepsilon}_0^m} |\dot{e}|^m \Big[\frac{\psi}{1-\theta} \Big(\frac{\psi}{\varphi} n^2 + 1 \Big) \Big]^{\frac{m-1}{2}} \Big| 1 + \sqrt{\frac{2}{3}} n \; sgn(\dot{\varepsilon}_z - \dot{\varepsilon}_r) \Big|^{\frac{-1}{m}}. \tag{3.13}$$

The evolution law of porosity is given by:

$$\dot{e} = \frac{\dot{\theta}}{1-\theta}. \tag{3.14}$$

Taking into account expression (3.14), relationship (3.13) leads to the following evolution equation:

$$\dot{\theta} = sgn(p)\dot{\varepsilon}_0(1-\theta)\Big(\frac{|\sigma_z - p_l|}{A\sigma_0}\Big)^{\frac{1}{m}}\Big[\frac{\psi}{1-\theta}(\frac{\varphi}{\psi}n^2+1)\Big]^{\frac{1-m}{2m}}\Big[\psi\Big|1+\sqrt{\frac{2}{3}}nsgn(\dot{\varepsilon}_z-\dot{\varepsilon}_r)\Big|\Big]^{\frac{-1}{m}}, \tag{3.15}$$

which accounts for the contribution of the Laplace pressure. The analog of (3.15) obtained by neglecting p_l was found by Olevsky and Molinari, [43] eq. 15.

3.2.1 Dependence of shear and bulk moduli on porosity

In the literature several studies relative to the determination of the bulk and shear moduli are present.
In the sequel, we shall use four different models:

- $\begin{cases} \varphi = (1-\theta)^2 \\ \psi = \frac{2}{3}\frac{(1-\theta)^3}{\theta} \end{cases}$ Skorohod [9];
- $\begin{cases} \varphi = \frac{(1-\theta)^{\frac{2}{1+m}}}{1+\frac{2}{3}\theta} \\ \psi = \frac{2}{3}(\frac{1-\theta^m}{m\theta^m})^{\frac{2}{m+1}} \end{cases}$; Ponte Castaneda-Duva-Crow [19];
- $\begin{cases} \varphi = \Big(\frac{1-\theta}{1+\theta}\Big)^{\frac{2}{1+m}} \\ \psi = \frac{2}{3}(\frac{1-\theta^m}{m\theta^m})^{\frac{2}{m+1}} \end{cases}$; Mc Meeking-Sofronis [21];
- $\begin{cases} \varphi = \frac{(1-\theta)^{\frac{2}{1+m}}}{1+\frac{2}{3}\theta} \\ \psi = \frac{m+1}{3}\frac{(1+\theta)(1-\theta)^{\frac{2}{m+1}}}{\theta} \end{cases}$. Cocks m[23].

In figures 3.2 and 3.3 moduli ψ and φ are plotted as functions of the porosity for different values of the parameter m.
The model delivered by Skorohod account for linear-viscous incompressible material with voids only: indeed the moduli ψ e φ do not depend upon the strain rate sensitivity m.

3.2.2 Dependence of the Laplace pressure on porosity

The effective Laplace pressure p_l is the result of collective action of local capillary stresses in a porous material. A variety of approaches can be found in literature. We shall consider two possible derivations of the expression for the Laplace pressure:

1. *Sintering stress derived by using a stochastic approach*
   This derivation was employed by Skorohod [9], who obtained p_l by calculating the surface free energy per unit mass with respect to the specific volume of the porous material by assuming spherical particles. The achieved result may be stated as follows:

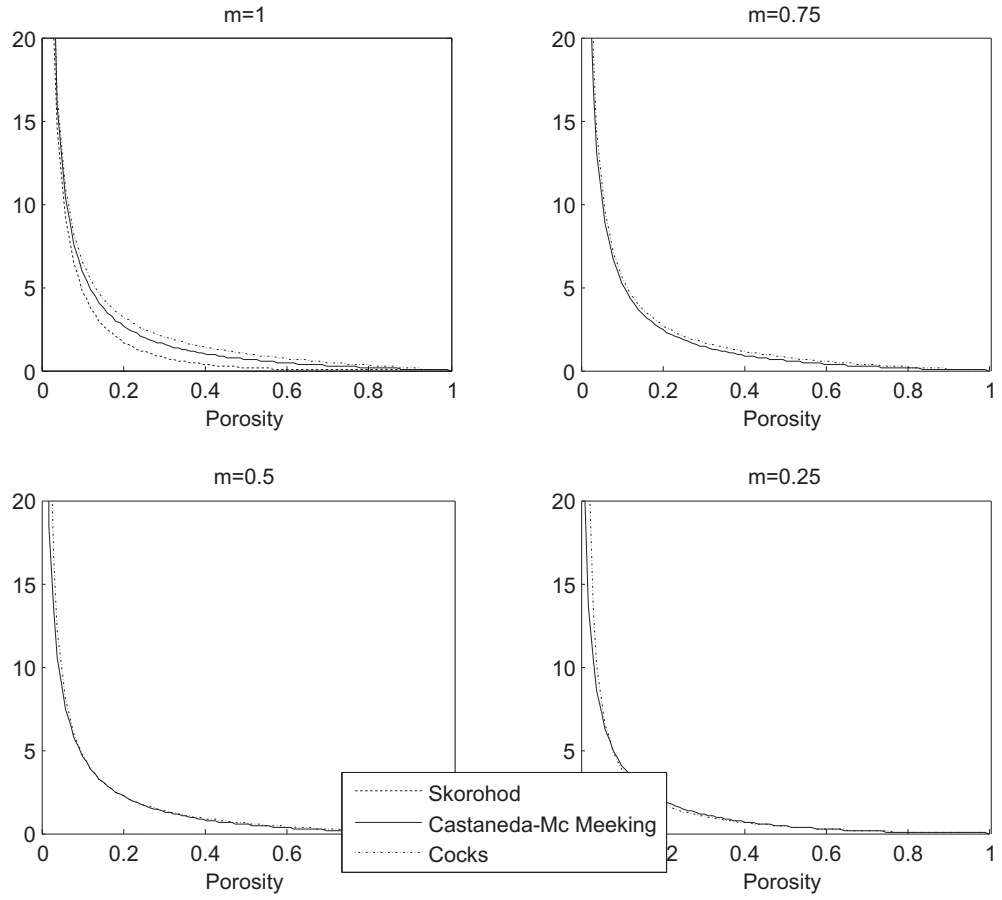

Figure 3.2: Bulk modulus ψ as function of porosity, for different values of the strain rate sensitivity m.

$$p_l = \frac{3\alpha}{r_0}(1-\theta)^2, \tag{3.16}$$

where α is the surface tension and r_0 is the characteristic radius of particles.

2. *Sintering stress derived by averaging of the energy dissipation* [32]
Following Olevsky (see [32]), in [54], Sect. 2.2, a hollowed sphere is considered as a schematic for a pore (see Figure 3.4). At the surface of such a pore ($r = R_1$), the pressure $p_{l0} = \frac{2\alpha}{r_0}$ is applied and the external boundary ($r = R_2$) is considered to be stress free.

   The constitutive law (3.1) allows us to write the equilibrium equation in terms of the derivative of the radial velocity V_r in the following way:

$$\left\{ \frac{\left[\frac{d^2V_r(r)}{dr^2} - \frac{1}{r}\frac{dV_r(r)}{dr} + \frac{V_r(r)}{r^2}\right]m}{3\left[\frac{dV_r(r)}{dr} - \frac{V_r(r)}{r}\right]} + \frac{1}{r} \right\} \left[\frac{dV_r(r)}{dr} - \frac{V_r(r)}{r}\right]^m = 0. \tag{3.17}$$

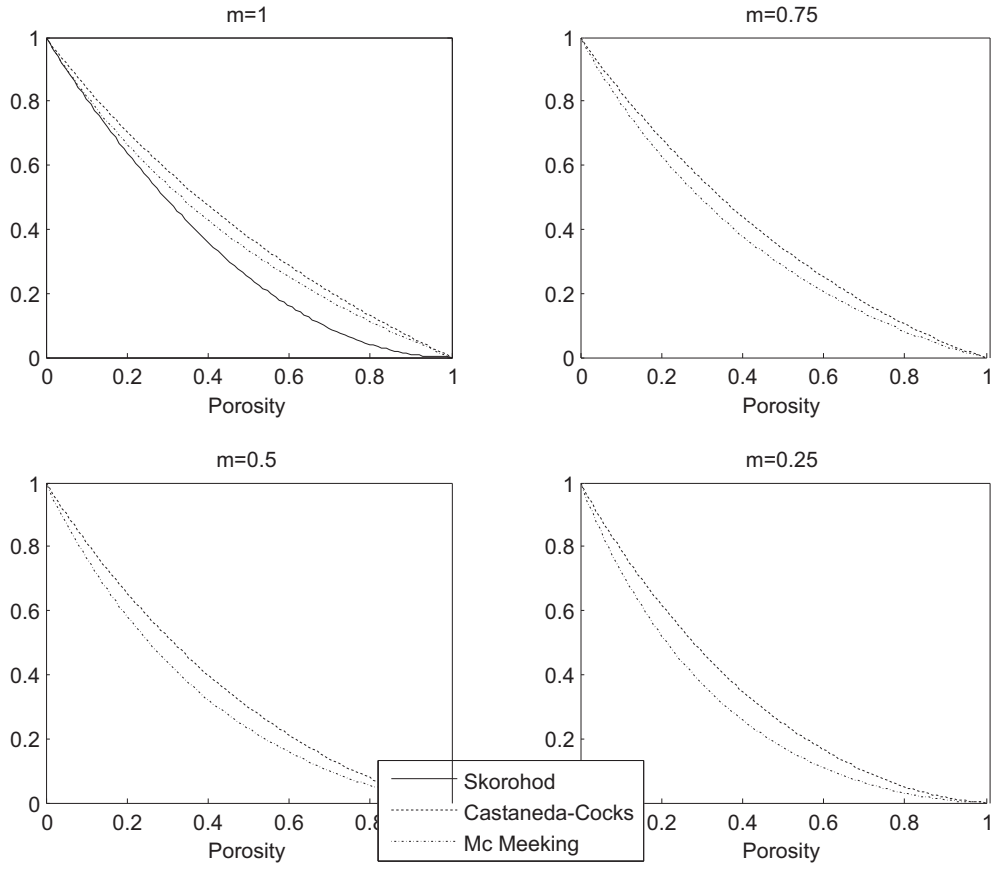

Figure 3.3: Shear modulus φ as function of porosity, for different values of the strain rate sensitivity m.

The obtained differential equation permits to determine the invariants of the strain rate tensor, $\dot{e}$ and $\dot{\gamma}$ as function of the porosity, of p_{l0} and of the shear and bulk moduli.

The assumed incompressibility of the matrix (i.e. $\dot{e} = 0$) expressed in terms of the radial velocity into (3.3) allows us to write a differential equation for V_r:

$$\dot{e} = \frac{dV_r(r)}{dr} + 2\frac{V_r(r)}{r} = 0. \tag{3.18}$$

The only way to satisfy both (3.17) and (3.18) is that (see [54] Sect. 2.2) the following relation holds:

$$m = 1. \tag{3.19}$$

Finally, it is possible to evaluate the dissipation energy for the matrix and for the effective porous material (see [54], Sect. 2.2 equations (33) and (37) respectively):

$$< d >_{matrix} = -\frac{3p_{l0}^2 R_1^3 R_2^3}{4\frac{A\sigma_0}{\dot{\varepsilon}_0}(R_2^3 - R_1^3)^2} = -\frac{3p_{l0}^2\theta}{4\frac{A\sigma_0}{\dot{\varepsilon}_0}(1-\theta)^2}, \tag{3.20}$$

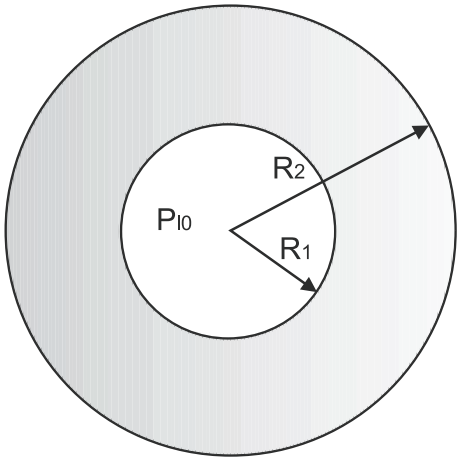

Figure 3.4: A representative element of porous medium

$$D = \frac{p_l^2}{2\psi \frac{A\sigma_0}{\dot{\varepsilon}_0}}. \tag{3.21}$$

The two expressions above are connected by the Hill's identity,

$$D = (1-\theta) < d >_{matrix} . \tag{3.22}$$

This relationship allows us to determine the final form of the Laplace pressure (see [54] for the complete derivation), namely:

$$p_l = \frac{2\alpha}{r_0}\sqrt{\frac{3}{2}\psi(\theta)\frac{\theta}{1-\theta}}. \tag{3.23}$$

Expression (3.23) can be particularized to obtain the sintering stress associated to the model cited above; in particular we get:

- $p_l = \frac{2\alpha}{r_0}(1-\theta)$ (Skorohod);
- $p_l = \frac{2\alpha}{r0}$ (Castaneda and Mc Meeking);
- $p_l = \frac{2\alpha}{r0}\sqrt{1+\theta}$ (Cocks).

Figure 3.5 shows the dependence of the Laplace pressure on the porosity θ. The stochastic approach, yielding relation (3.16), gives a parabolic trend of the Laplace pressure. This is increasing when the porosity decreases and it is independent on the value of the parameter m, so that p_l does not depend upon the material behavior.

On the contrary, the motivation leading to (3.19) (i.e. $m = 1$), implies that expression (3.23) (for the four different models) is admissible only for materials with linearly-viscous behavior. Nevertheless, fig. 3.5 shows that the values of pressure calculated through (3.23) are comparable with the ones obtained by (3.16) in the range of interest of porosity.

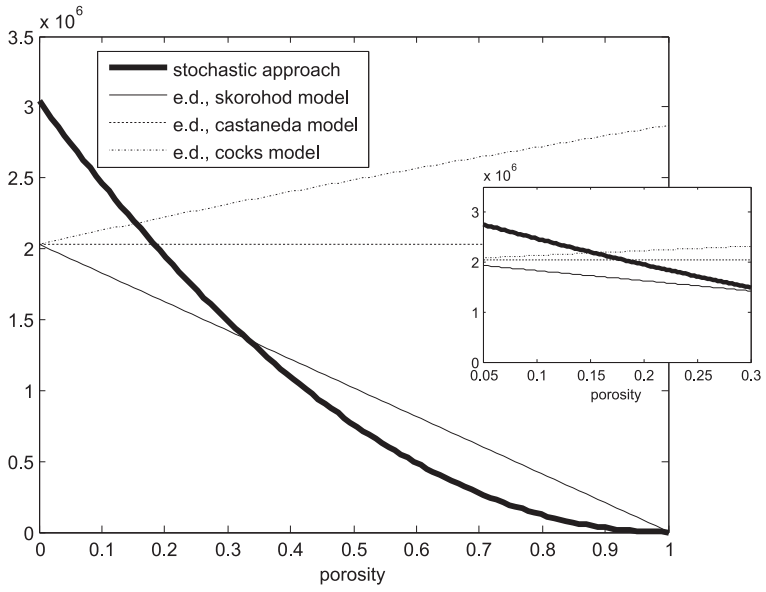

Figure 3.5: the Laplace pressure as function of porosity

3.3 Effect of the Laplace pressure on free forging

For the case of forging, the loading mode parameter is $n = -\sqrt{6}$ and relation (3.15) reduces to:

$$\dot{\theta} = \dot{\varepsilon}_0(1-\theta)\Big(\frac{|\sigma_z - p_l|}{A\sigma_0}\Big)^{\frac{1}{m}}\Big[\frac{\psi}{1-\theta}\Big(\frac{6\psi}{\varphi}+1\Big)\Big]^{\frac{1-m}{2m}}[3\psi]^{\frac{-1}{m}}. \tag{3.24}$$

The axial stress σ_z can be represented by the ratio of the axial force F_z (acting on the top and the bottom face of the cylindrical specimen) and the cross-sectional area S through the relation

$$\sigma = \sigma_z = \frac{F_z}{S} = \frac{F_z}{S_0\bar{S}(\theta)}, \tag{3.25}$$

where the dependence of S on the porosity is given by [43], eq. (27), i.e.

$$\bar{S}(\theta) = \exp\Big\{\int_{\theta_0}^{\theta}\frac{\frac{\varphi}{3} - \frac{|n|\psi}{\sqrt{6}}}{\varphi(1-\theta)}\Big\}. \tag{3.26}$$

Such a relationship can be rewritten by using the four available expressions for the shear and bulk moduli φ and ψ (given in Sect. 3.2.1).

The dependence of σ_z on the porosity is plotted in figure 3.6 for $m = 1$, compared to the one relative to the isostatic pressing case (see [54]). In the following diagram a dimensionless external loading parameter $\frac{\sigma_z}{p_b}$ (called specific stress) is actually considered, where $p_b = \frac{F_z}{S_0}$. The Laplace pressure may vary according to either relation (3.23) and (3.16) (the influence of the parameter m on σ_z will be discussed in section 4.2).

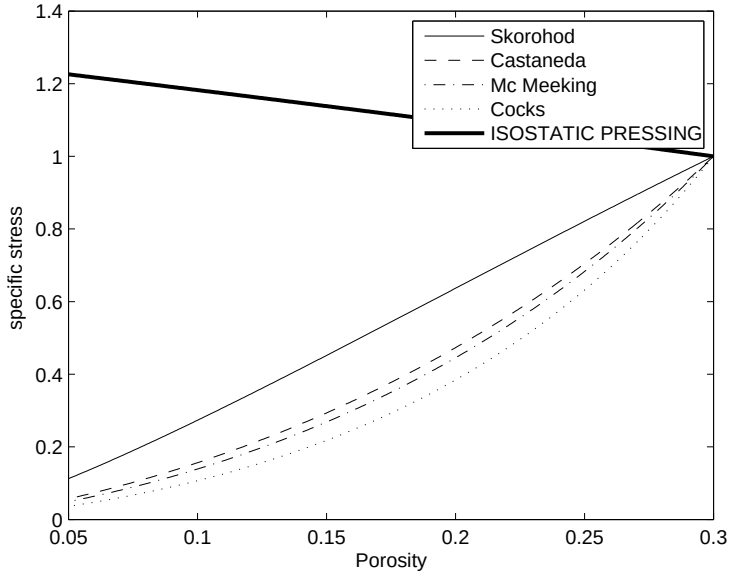

Figure 3.6: Evolution of the specific stress $\frac{\sigma_z}{p_b}$ during the isostatic pressing and the free forging process, for $m = 1$.

During isostatic pressing, the stress due to external loading slightly increases, whereas in free forging there is a strong increasing of the cross-sectional area and, consequently, a strong decreasing of σ_z.
This phenomenon produces a considerable difference between the values of critical porosities θ^* in the two cases mentioned above.

3.3.1 Time-evolution of the porosity in free forging

Eq. (3.24) can be normalized by using the dimensionless specific time τ_E, defined as follows:

$$\tau_E = \Big[\frac{F_z}{S_0\sigma_0 A}\Big]^{\frac{1}{m}}\dot{\varepsilon_0}t. \tag{3.27}$$

Henceforth, the differential equation (3.24) can be recast in the following way:

$$\frac{\partial\theta}{\partial\tau_E} = 3^{\frac{-1}{m}}(1-\theta)^{\frac{3m-1}{2m}}|\sigma_z - p_l|^{\frac{1}{m}}\Big(\frac{6\psi}{\varphi}+1\Big)^{\frac{1-m}{2m}}\psi^{\frac{-(1+m)}{2m}}. \tag{3.28}$$

Of course, such equation can be integrated (since the bulk and the shear moduli ψ and φ are known functions (given in section 2.1) of the porosity θ).

A dimensionless pressure parameter, called Specific External Pressure (S.E.P.) in the sequel, may be introduced as follows:

$$S.E.P. = \frac{F_z}{S_0}\frac{1}{\alpha/r_0}, \tag{3.29}$$

(we recall that α denotes the surface tension and r_0 is the characteristic radius of particles, see [54], Sect. 2.2).
In the sequel, it will turn out that the four considered models of moduli φ and ψ bring to discrepancies in the time-evolution of the porosity. This is basically due to the different evolution of the axial stress σ_z during the sintering process, shown in figure 3.6.

During sintering, the stress σ_z due to external load increases, because of the cross-sectional area diminishes according to (3.26). On the other hand, the evolution law (3.24) shows that the rate of change of the porosity $\dot{\theta}$ is proportional to $|\sigma_z - p_l|$.
It is therefore possible that, for a definite range of external loads, the equality condition $\sigma_z = p_l$ may be achieved.
When the porosity attains the value θ^* for which $\sigma_z = p_l$ an equilibrium situation is reached. Such θ^* may be called *critical porosity*. The stability of the process about such a value will be studied in section 3.5.

Hence, we can distinguish three cases:

- $\sigma > p_l$
- $\sigma < p_l$

  } during the whole sintering process

- $\sigma - p_l$ change sign during the process

For the case of isostatic pressing, this range turns out to be very limited, and it corresponds to low values of external loads, which are rarely used in industrial sintering processes (see [54]). In the case of free forging, the condition $\sigma_z = p_l$ is achieved for a very wide range of external pressure; this range includes values of the external load usually employed in real industrial processes.
In the case of isostatic pressing (see [54]), such a range is very limited. This different behavior is due to the relevant difference between the stress evolution during forging and during isostatic pressing, shown in figure 3.6. In order to compare the cases of isostatic pressing and free forging, we may consider a process during which the porosity is reduced from 30% to 5%. For instance, we may choose the expression of the Laplace pressure obtained by using the stochastic approach and the model of Castaneda for the moduli ψ and φ.

For the case of isostatic pressing, the condition $\sigma = p_l$ is achieved for values of S.E.P. between 1.47 and 2.21 (the former value corresponds to $\sigma = p_l$ at the beginning of sintering, that is to say $\theta = 30\%$, whereas the latter corresponds to $\sigma = p_l$ at the end of the process, that is to say $\theta = 5\%$, see [54], Sect. 3.1).
A wider range of S.E.P. is achieved in the case of free forging. Hence, the lower threshold is still 1.47, although the upper one depends on the values of the

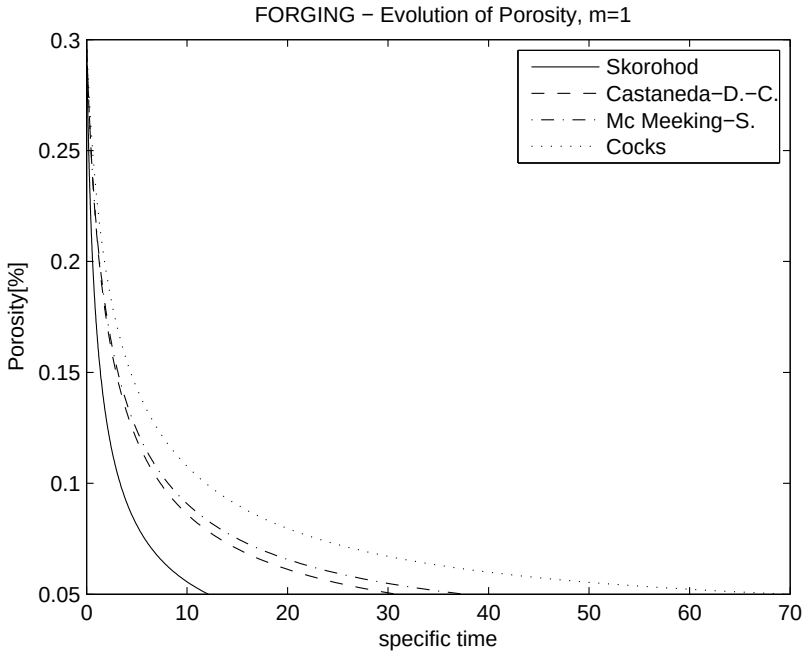

Figure 3.7: FREE FORGING- Evolution of porosity for S.E.P.=100, for different models, $p_l = \frac{3\alpha}{r_0}(1-\theta)^2$

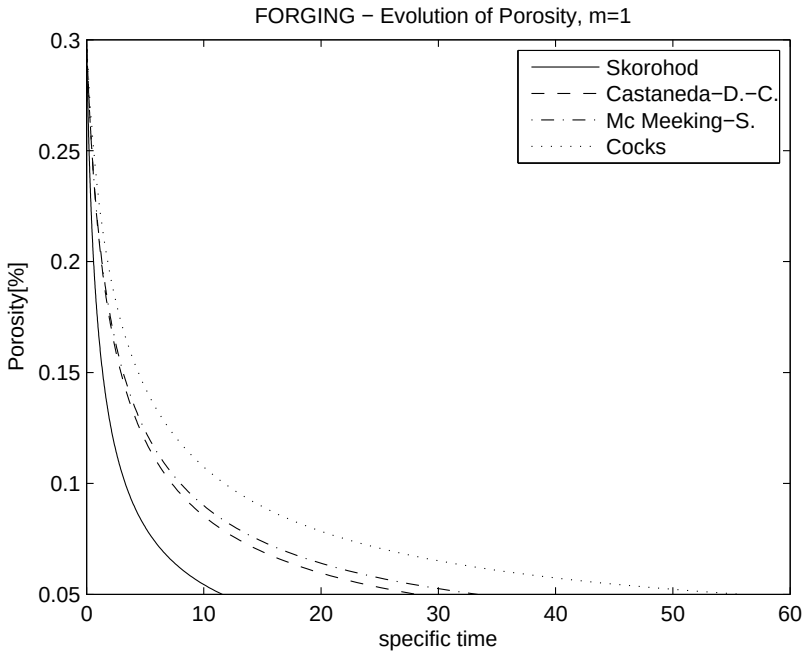

Figure 3.8: FREE FORGING- Evolution of porosity for S.E.P.=100, for different models, $p_l = \frac{2\alpha}{r_0\varphi}\sqrt{\frac{3}{2}\psi(\theta)\frac{\theta}{1-\theta}}$

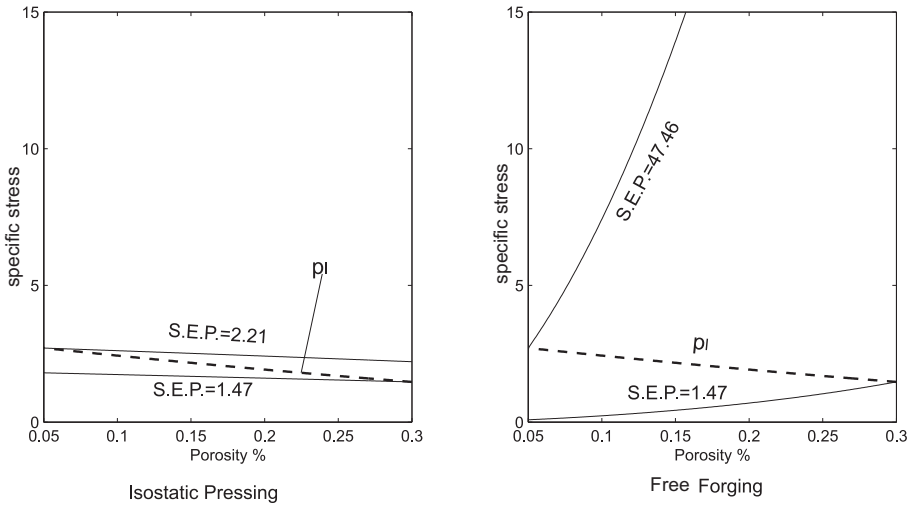

Figure 3.9: FREE FORGING- Range of S.E.P. for which the condition $\sigma = p_l$ is achieved, for isostatic pressing and free forging case (Castaneda model)

strain rate sensitivity m and on the model. For $m = 1$, the upper threshold values achievable by the S.E.P. are one order of magnitude higer than the ones encountered for isostatic pressing, i.e. 24.08, 47.46, 54.74 and 74.92 for Skorohod, Castaneda, Mc Meeking and Cocks model respectively. For lower values of the parameter m, the upper threshold do decrease, although they turn out to be definitely greater than the ones relative to isostatic pressing.
Figure 3.9 shows the range of S.E.P. for isostatic pressing and free forging case (the model of Castaneda is used for the sake of illustration).
It is worth noting that by using the expression of the Laplace pressure obtained by averaging of the energy dissipation, the obtained range of S.E.P. is roughly the same of the other case.

The following graphs summarize the time-evolution of the porosity obtained by using the model of Castaneda and the expression of the Laplace pressure derived by means of stochastic approach ($p_l = \frac{3\alpha}{r_0}(1-\theta)^2$). This is done for the three different cases mentioned above.

- *Case in which $\sigma_z > p_l$ during the whole process.*
  Here the driving force of sintering is the stress σ_z due to external loading, whereas the action of the Laplace pressure p_l is to oppose σ_z. Consequently, the decay of the porosity calculated by neglecting the effect of the Laplace pressure is lower than the real one.
  Figure 3.10 shows the time-evolution of the porosity for S.E.P.=50, for different values of strain rate sensitivity m.

  When m decreases, the initial part of the graph becomes more vertical, i.e. the material tends to behave plastically. The trends of the time-evolution of θ shows that the gap between the curves obtained by considering the

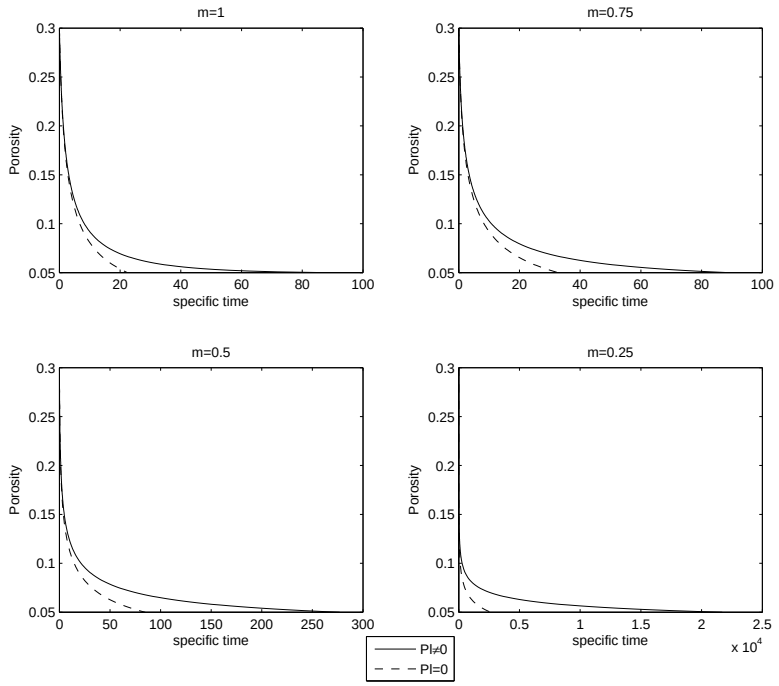

Figure 3.10: FREE FORGING- Evolution of porosity for S.E.P.=50, Castaneda Model

sintering stress and the one evaluated by neglecting p_l increases for lower values of m.

- *Cases in which $\sigma_z - p_l$ change sign during the process.*
  As stated above, in free forging the range of external pressures for which this condition is achieved is very large in comparison to the one exhibited during isostatic pressing. Hence, this case is very interesting by an industrial point of view.
  When the condition $\sigma_z = p_l$ is achieved (this happens at a critical porosity $\theta = \theta^*$) both σ_z and p_l remains constant. The stability analysis of this case will be studied in Section 3.5.

  Figure 3.11 shows that, at the beginning of the process, i.e. for $\theta > \theta^*$, sintering is carried on by the external loading $p_b = \frac{F_z}{S_0}$. The graph of the porosity has a convex shape, analog to the one obtained by neglecting the Laplace pressure (see dashed line). In the second part of the process ($\theta < \theta^*$), sintering is driven by the Laplace pressure p_l; in this region the graph exhibits a change in curvature.
  Figure 3.12 shows that when the strain rate sensitivity m decreases, the sintering time and the critical porosity θ^* do increase. For low values of the parameter m, the material tends to behave plastically and, hence, it exhibit a suddenly drop in porosity at the beginning of the process(see e.g. $m = 0.25$: there θ initially jumps from 30% to 11.5%). When the

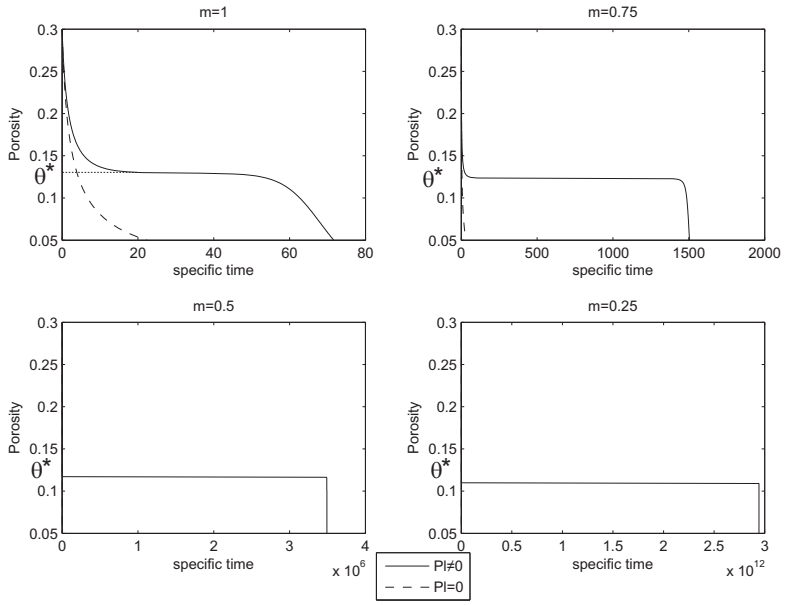

Figure 3.11: FREE FORGING- Evolution of porosity for S.E.P.=10, for different values of m, Castaneda Model

condition $\sigma = p_l$ is achieved, the porosity tends to remain constant for a long time (see, e.g., Figg. 3.11.c and 3.11.d.

By comparing Figures 3.11 and 3.13, both the dual role of σ_z and $\mathbf{p}_l$ are highly noticeable. For low values of τ_E, the role of σ_z is dominant and so agonist to sintering, whereas p_l is anti-agonist: this occurs for $\theta > \theta^*$. For higher τ_e, $\theta < \theta^*$, the two roles of σ_z and $\mathbf{p}_l$ are reversed.
In particular, for much lower value of the load, i.e. S.E.P.=2 (one fifth of the previous case), the critical porosity is actually very close to the initial value. Hence, the sintering stress p_l is the responsible of the shrinkage (to be measured by the reduction of porosity).

- *Case in which $\sigma < p_l$ during the whole sintering process.*
  For low values of external pressure, the "driving force" of sintering process is the Laplace pressure. This case is not interesting, because in industrial free forging process, it is not used.

3.3.2 Strain rate computation

From the definition of the volumetric and shear strain rates (3.8) and of the loading mode parameter n (3.9), one can obtain the following relationship between the strain rates :

$$\dot{e} = \frac{3\dot{\varepsilon}_z}{1 + \sqrt{6} sgn(\dot{\varepsilon}_z - \dot{\varepsilon}_r)\frac{\psi n}{\varphi}}. \tag{3.30}$$

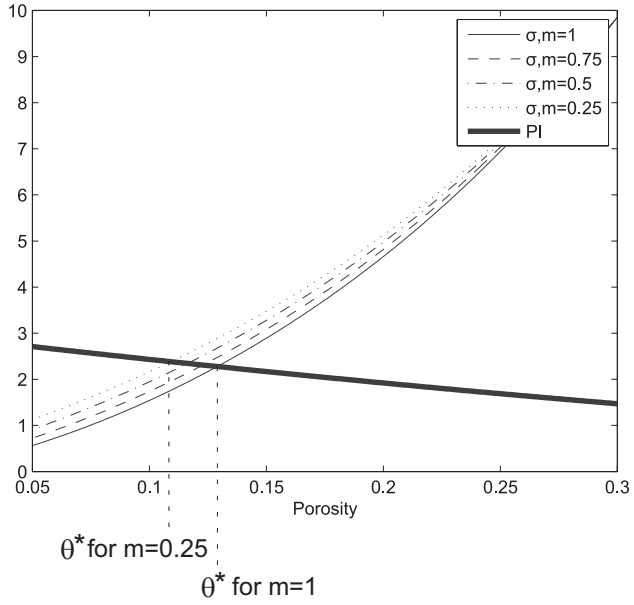

Figure 3.12: FORGING- S.E.P.=10- Evolution of the Laplace pressure and tension due to external load, for different values of m, Castaneda Model

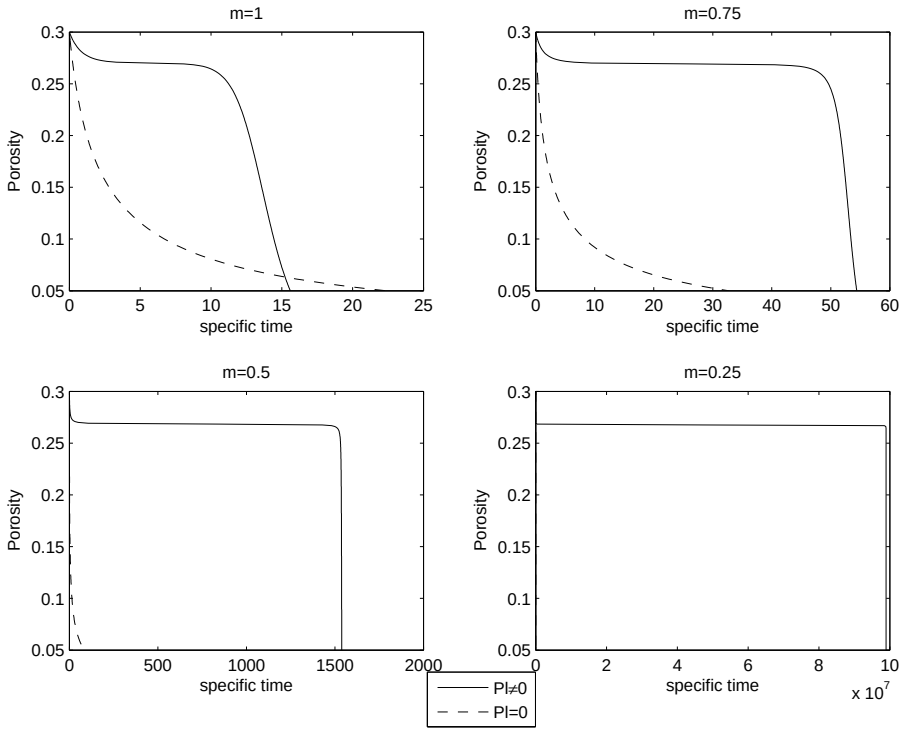

Figure 3.13: FREE FORGING- Evolution of porosity for S.E.P.=2, for different values of m, Castaneda Model

For the case of free forging, we have $n = -\sqrt{6}$, we may evaluate the ratio between the radial and the longitudinal strain rates,in analogy of Poisson's ratio, defined by Olevsky [43]:

$$\nu^* = -\frac{\dot{\varepsilon}_r}{\dot{\varepsilon}_z} = -\frac{\varphi - 3\psi}{\varphi + 6\psi}. \tag{3.31}$$

Equation (3.31) relates ν^* to the porosity alone through the parameter m and the adopted model for the shear and the bulk moduli (φ and ψ). This is shown in figure 3.14.

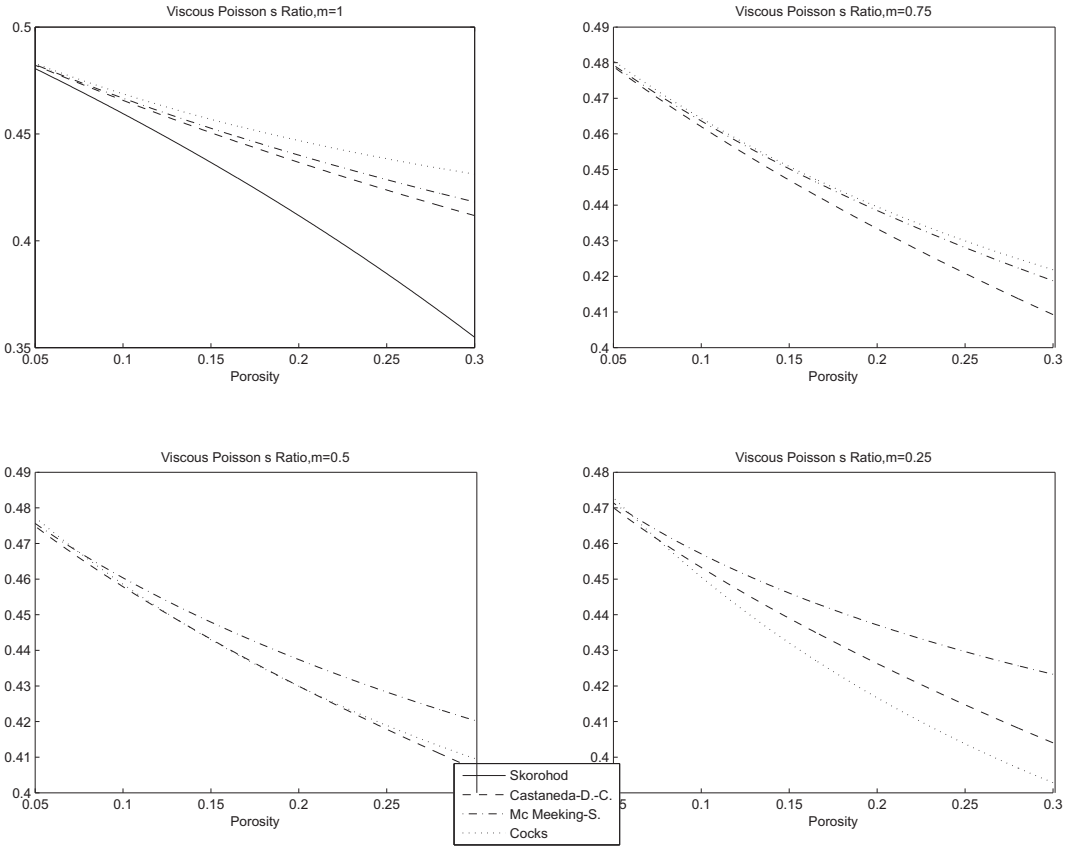

Figure 3.14: Poisson's ratio analogy as function of porosity

The time dependence of the analogy of the Poisson's ratio may now be investigated. A step-by-step analysis allows for evaluating the evolution of the porosity and, hence, the time dependence of ν^*. This turns out to be influenced by the difference between the value of external load and the Laplace pressure, $|\sigma - p_l|$.

From equations (3.31) and (3.14), one can obtain the expressions of axial and radial strain rate $\dot{\varepsilon}_z$ and $\dot{\varepsilon}_r$:

$$\begin{cases} \dot{\varepsilon}_r = \frac{\varphi-3\psi}{\varphi+6\psi}\frac{1}{1+2\frac{\varphi-3\psi}{\varphi+6\psi}}\frac{\dot{\theta}}{1-\theta}; \\ \dot{\varepsilon}_z = \frac{1}{1+2\frac{\varphi-3\psi}{\varphi+6\psi}}\frac{\theta}{1-\theta}. \end{cases} \tag{3.32}$$

By prescribing the value of the external pressure p_b, it is possible to study the behavior of ν^* and of the axial and radial strain rate during sintering, as a function of time and porosity. This will be studied for different values of the strain rate sensitivity m.

The results obtained by using the expression of the Laplace pressure derived by using the stochastic approach mentioned throughout the paper (see Section 3.2.2) are shown in the following figures.

- *Case in which $\sigma_z > p_l$ during the whole process .*

  Figure 3.15 show the evolution of radial and axial strain rate as functions of time and porosity, for different models.

  As expected, the axial strain rate is negative, whereas the radial strain rate is positive. Absolute values of the strain rates decrease during sintering, according to the evolution of the porosity.
  As m diminishes, the strain rates are more relevant at the beginning of the process; the behavior tends to be almost plastic as m decreases since the rates go to zero for fairly low values of the specific time.

- *Cases in which $\sigma_z - p_l$ changes sign.*
  It is well known that, whenever the condition $\sigma_z = p_l$ is achieved, the porosity remains constant at its critical value $\theta = \theta^*$ and, so, there is equilibrium. Therefore, radial and axial strain rates are also zero. Figure 3.16 allows to compare the time-evolution of the porosity to the time-evolution of the axial and radial strain rates.

3.4 Influence of the Laplace pressure on industrial processes entailing free forging

In [54] an aluminium-zinc-magnesium-copper alloy is considered in order to explore the influence of the sintering stress in isostatic pressing. The main characteristics of this material are listed in table 3.1: For aluminum alloys, the average time of sintering is thirty minutes and it is usually sintered with external pressure of $100\mathsf{div}200MPa$ [22, 35, 50].
It may be shown that very important the parameters that influence the Laplace pressure, are the powder grain size (indicated here through the radius r_0) and the surface tension α.

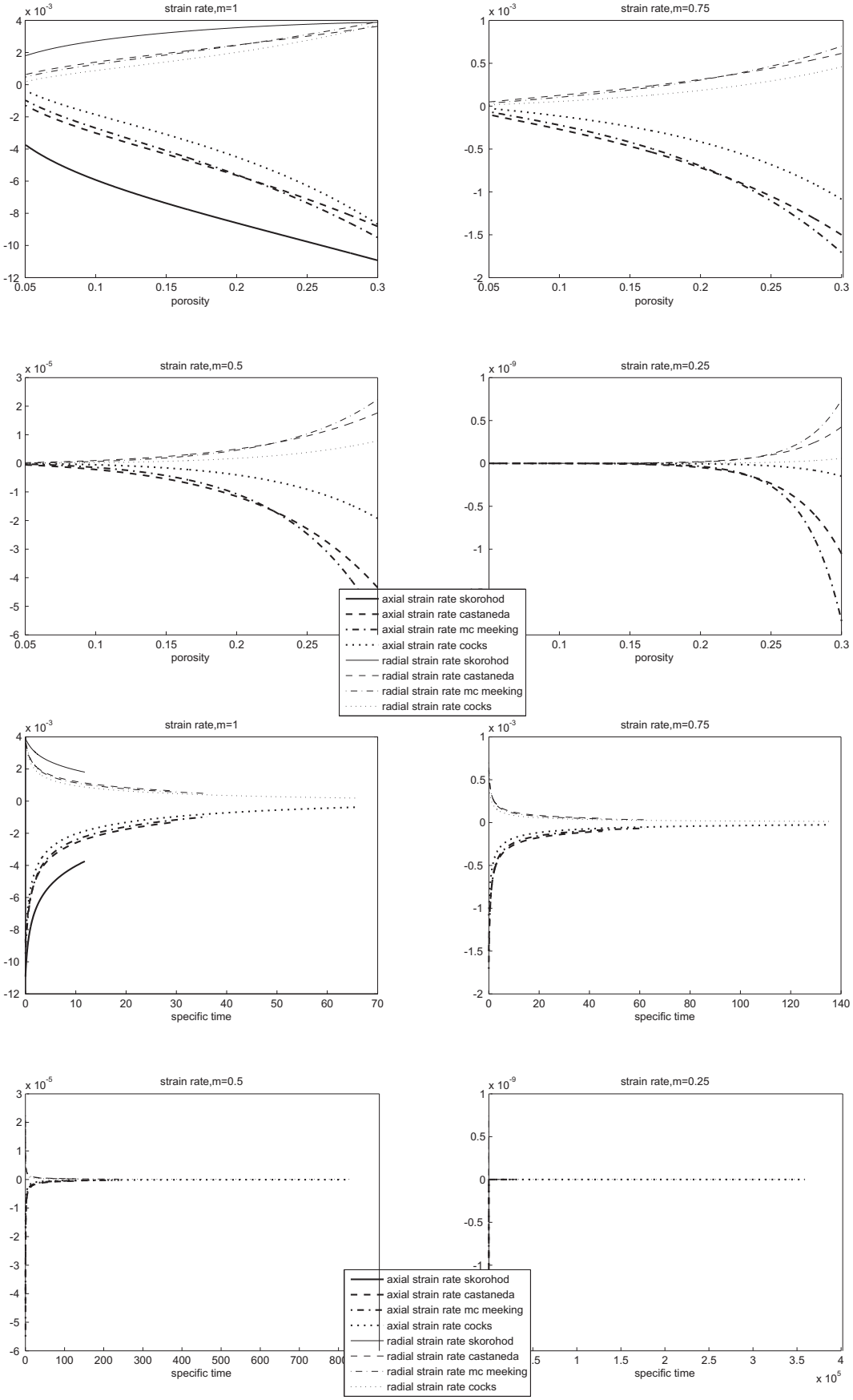

Figure 3.15: Radial and axial strain rates as function of porosity and of specific time for S.E.P.=100, for different values of m

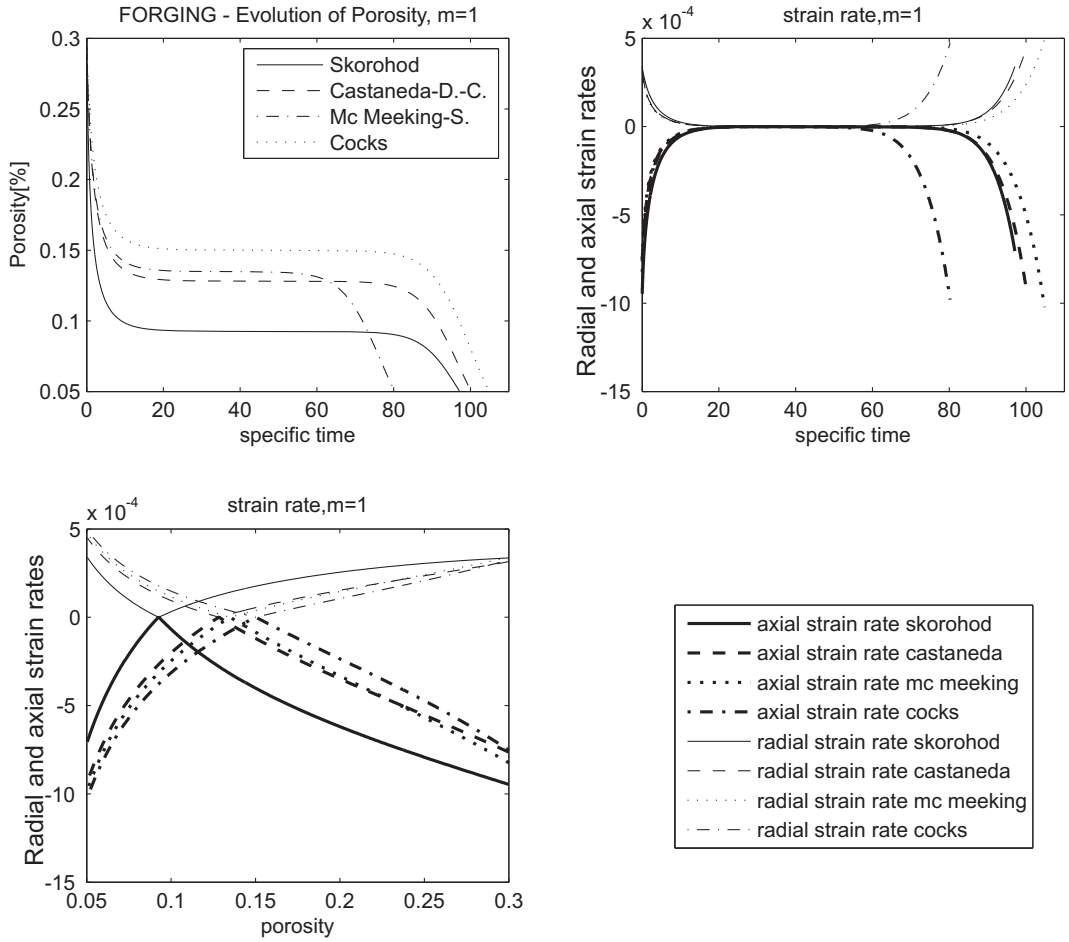

Figure 3.16: Evolution of porosity and strain rates for S.E.P.=10

Young's modulus	**E**	70,7	GPa
Poisson's ratio	**ν**	0,325	
surface tension	**α**	1,1285	N/m
Activation Energy	**Q**	143 90	kJ
Melting Temperature	**Tm**	659	°C
mean radius of powder particles	**r0**	5/50	µm
sintering pressure	**Pb**	100/350	MPa
sintering temperature	**Ts**	600/610	°C

Table 3.1: Characteristics of the considered aluminum-zinc-magnesium-copper alloy

Thus, several values of powder grain size (listed in table 3.2) are there taken into account, and the sensitivity of the model to variations of the order of $\pm 50\%$ of the surface tension α is analyzed.

We consider a process which reduces the porosity from 30% to 5%. Furthermore, we can define:

- t= sintering time accounting for the Laplace pressure;

MICRO-POWDERS	NANO-POWDERS
50 μm	500 nm
10 μm	200 nm
5 μm	100 nm
2 μm	50nm
1 μm	

Table 3.2: Considered values of powder grain size

- t_0= sintering time neglecting p_l.

In order to establish threshold values p^* of the pressure p, we can calculate p^* for which the discrepancy D between t and t_0, where $D = \frac{t-t_0}{t}$, is of the order of 5%, 10% and 15% respectively.
Wherever the external pressure is less than p^*, for the given value of discrepancy, for example $D = 5\%$, by neglecting the effect of the Laplace pressure an error greater than 5% occurs.

In figures 3.17 and 3.18, threshold pressures obtained by using the model of Castaneda are shown, for grain size of $5\mu m$ and $50nm$ respectivelyas a function of the strain rate sensitivity m.

It is worth noting that the values of the threshold pressure p^* obtained in this case are significantly higher than the ones arising in the case of isostatic pressing (see [54]). Therefore, for free forging processes, the contribution of the Laplace pressure has a leading role.

Figure 3.19 shows the comparison among threshold pressures (associated with a 10% error) obtained by using the models of Castaneda, Mc Meeking and Cocks. Unlike for the case of isostatic pressing (see [54]), the achieved results show meaningful differences. This is due to different porosity-stress response for different choices of the models owing to the moduli ψ and φ appearing in (3.1) (see e.g. Figure 3.6).

The results obtained in these sections are relative to the Laplace pressure derived by the stochastic approach. The alternative expression for the sintering stress (obtained by averaging of the energy dissipation) does not allow for evaluating the threshold pressures for different values of strain rate sensitivity (m). However, the threshold pressures obtained by using such an approach denote a stronger dependence on the model used for moduli ψ and φ. Nevertheless, they are completely in agreement with those ones obtained by using the first approach.

There are two main phenomena governing the dependence of p^* on quantity $\sigma - p_l$:

1. The rate of change of the porosity $\dot{\theta}$ is proportional to $|\sigma - p_l|^{\frac{1}{m}}$ (see equation (3.15)); thus, when the parameter m decreases, the influence of $\sigma - p_l$ on the time-evolution of the porosity increases;

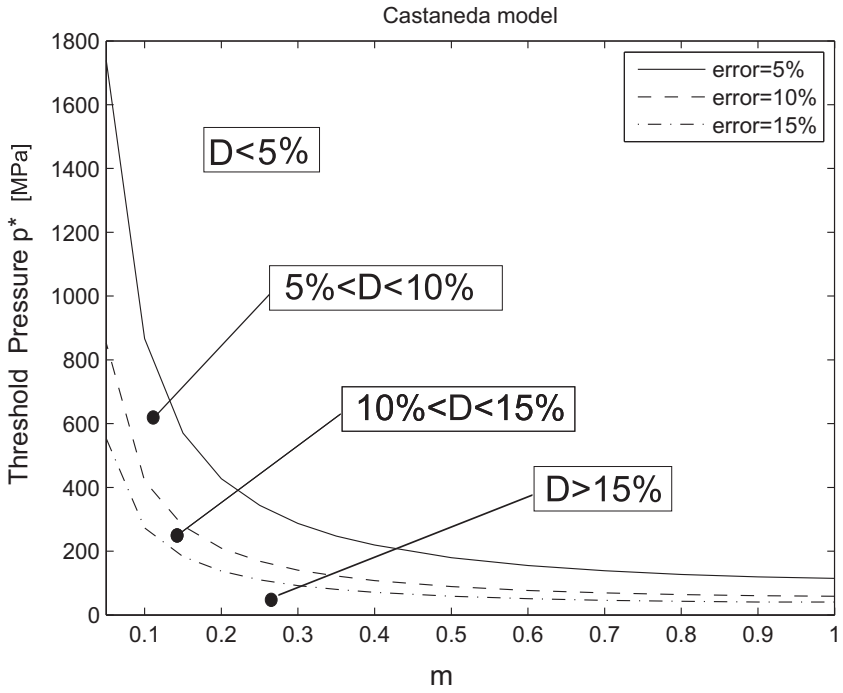

Figure 3.17: Threshold pressure for 5μ powder

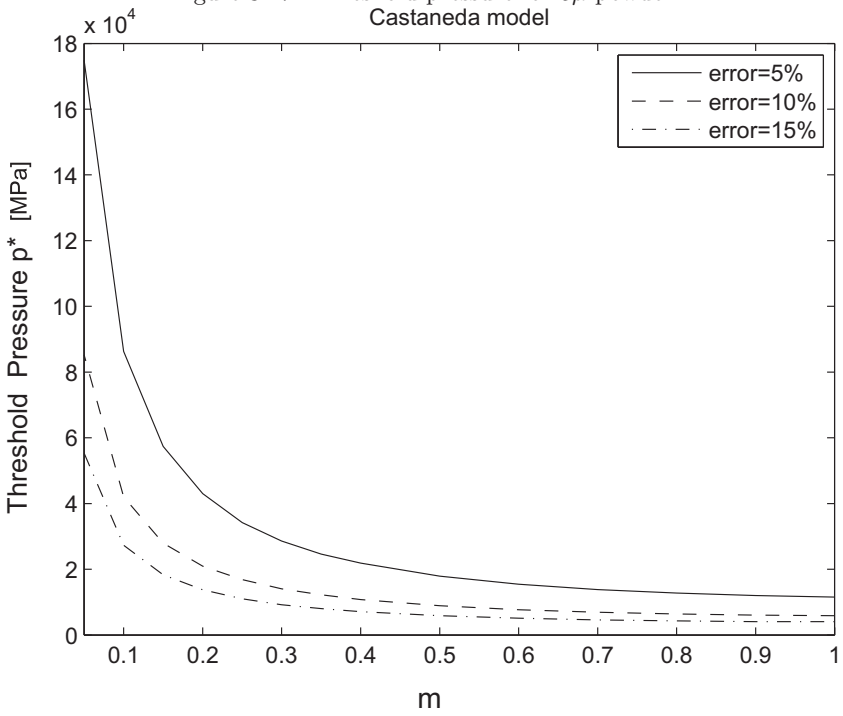

Figure 3.18: Threshold pressure for $50nm$ powder

2. the evolution of the cross-sectional area (and consequently the associated change in stress σ_z due to the external load) is also dependent on the parameter m .

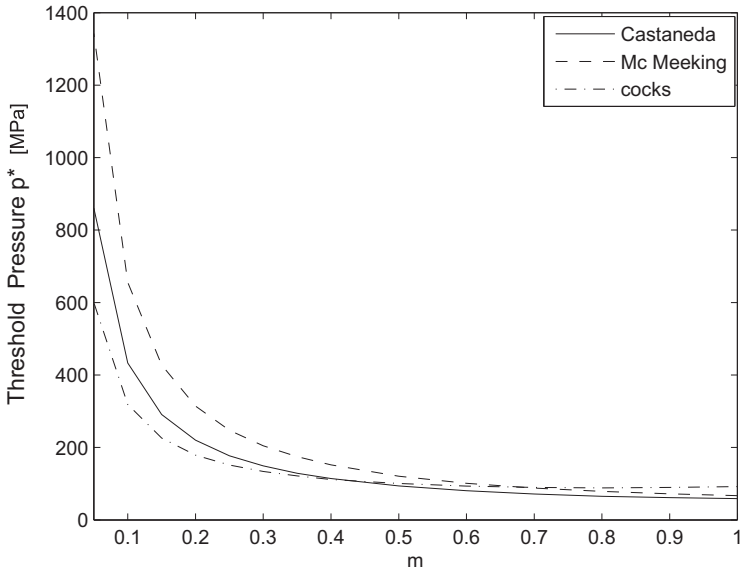

Figure 3.19: Threshold pressure for different models, $p_l = \frac{3\alpha}{r_0}(1-\theta)^2$

As it is shown in figure 3.20, a common feature of all the models employed to calculate the moduli is that as the parameter m decreases during the process, for each given porosity, the stress drop with respect to the initial value decreases monotonically. Because of this phenomenon, when m decreases, the critical porosity θ^* decreases (see e.g. figure 3.12). Therefore, in order not to achieve the condition $\sigma = p_l$, it is sufficient to impose external forces leading to lower external pressures. Henceforth, the resulting threshold pressure is lower than the one obtained for higher values of m. In order to highlight this phenomenon, it is possible to calculate (always by considering processes that reduce the porosity from 30% to 5%) the lowest value of external pressure that allows *not* to achieve the condition $\sigma = p_l$. The results are shown in figure 3.21, for different models.

By comparing figures 3.21 and 3.19, it is evident that the two phenomena are opposing one another.

The second phenomenon can be more or less relevant (it depends on the choice of the model for shear and bulk moduli), dependently by the adopted model for shear and bulk moduli φ and ψ. For Cocks model, the second phenomenon is more relevant (as shown in figure 3.21) and the graph of the threshold pressure has a minimum. However, the first phenomenon is dominant.

Figure 3.22 shows the evolution of the porosity for external pressure $p_b = 100MPa$; such a value of external pressure is widely used in industrial processes for aluminium alloys. It is evident that the condition $\sigma = p_l$ is not achieved, although the time-porosity curve is strongly influenced by the Laplace pressure. Indeed, for higher values of the specific time (see e.g. Equation (3.27)), the trend of the evolution is to reach a plateau. This would correspond to the critical

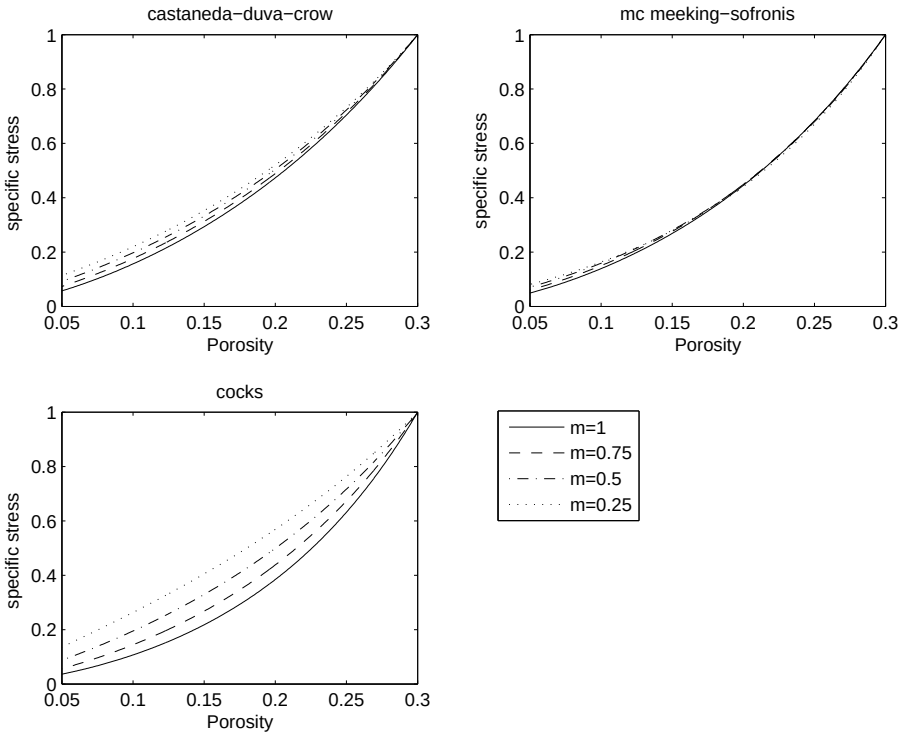

Figure 3.20: σ_z as a function of porosity, for different values of the parameter m

value of the porosity θ^* introduced earlier in this paper.

3.5 Stability analysis

Motivated by the unsatisfactory, and yet self-contradictory, results obtained in [54], Sect. 4.1, given by a lower-order stability analysis (obtained by perturbing the porosity alone), a higher order analysis will be performed. This may be done by following the procedure in [43], Section 3.1.2, owning to account for perturbations of:

- the actual geometry, through:
  - cross sectional area;
  - porosity;
- the stress due to external load;
- the Laplace pressure.

A perturbed solution is considered in the following form:

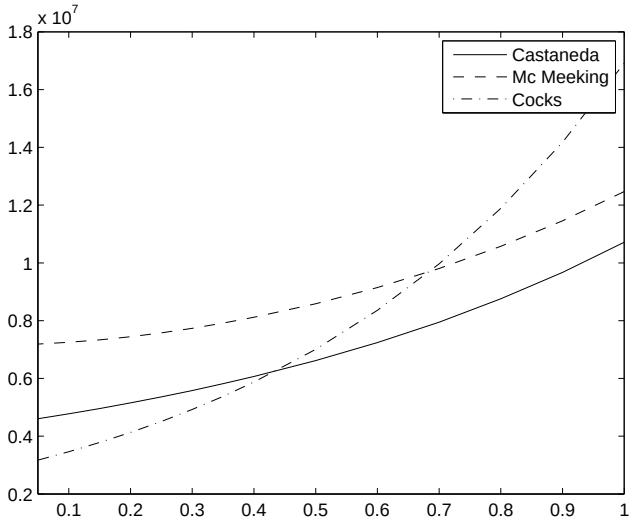

Figure 3.21: Minimal pressure for which the condition $\sigma = p_l$ is not achieved

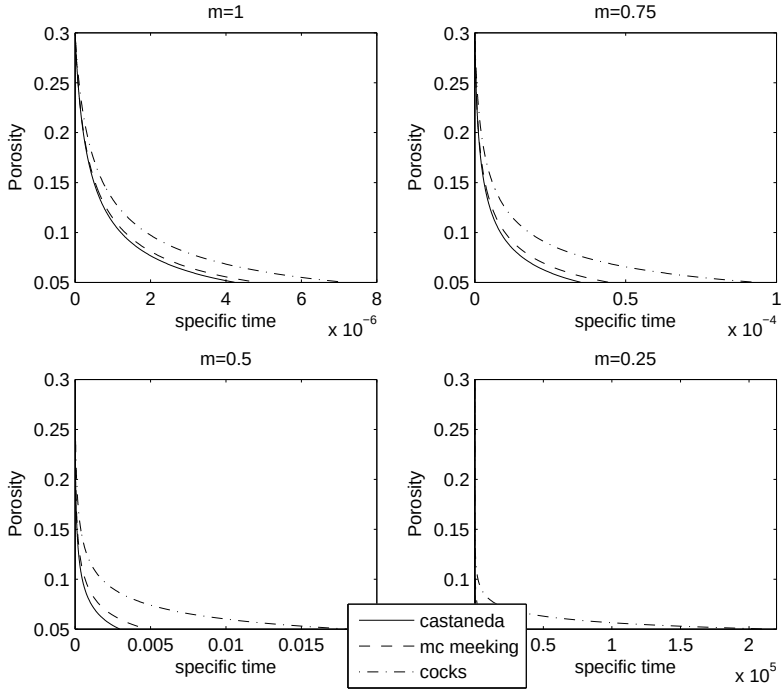

Figure 3.22: Evolution of porosity for external pressure of 100MPa

$$\begin{cases} \theta(t) = \theta^0(t) + \delta\theta \exp(\lambda(t - t_0)), \\ \sigma_z(t) = \sigma_z^0(t) + \delta\sigma \exp(\lambda(t - t_0)), \\ S(t) = S^0(t) + \delta S \exp(\lambda(t - t_0)), \\ p_{l0}(t) = {p_{l0}}^0(t) + \delta p_{l0} \exp(\lambda(t - t_0)). \end{cases} \tag{3.33}$$

By substituting such solutions in equations (3.24), (3.26), (3.25) and (3.16) (for the Laplace pressure derived by using stochastic approach) or (3.23) (for the other formulation of the Laplace pressure), after linearization, we have:

$$\left[\begin{array}{cccc} 0 & S & \sigma & 0 \\ \frac{\lambda}{\dot\theta}+\frac{\frac{d}{d\theta}G(\theta)}{G(\theta)} & 0 & \frac{1}{S}\left[1-\frac{\lambda}{\dot\theta G(\theta)}\right] & 0 \\ \frac{1}{\dot\theta}\frac{\partial f(\theta,\sigma,p_{l0})}{\partial\theta}-\frac{\lambda}{\dot\theta} & \frac{1}{\dot\theta}\frac{\partial f(\theta,\sigma,p_{l0})}{\partial\sigma} & 0 & \frac{1}{\dot\theta}\frac{\partial f(\theta,\sigma,p_{l0})}{\partial p_{l0}} \\ \frac{\partial p_l(\theta,p_{l0})}{\partial\theta} & 0 & 0 & \frac{\partial p_l(\theta,p_{l0})}{\partial p_{l0}} \end{array}\right]_{\theta^0(t),\sigma^0(t),S^0(t),{p_{l0}}^0(t)} \left[\begin{array}{c}\delta\theta\\ \delta\sigma\\ \delta S\\ \delta p_{l0}\end{array}\right]=\left[\begin{array}{c}0\\0\\0\\0\end{array}\right], \tag{3.34}$$

where

$$\begin{cases} G(\theta)=\frac{2\left(\frac{1}{3}\varphi-\psi\right)}{\varphi(1-\theta)}, \\ f(\theta,\sigma,p_{l0})=-3^{-\frac{1}{m}}\dot\varepsilon_0(1-\theta)^{\frac{3m-1}{2m}}\left(\frac{|\sigma_z-p_l|}{A\sigma_0}\right)^{\frac{1}{m}}\psi^{\frac{-(1+m)}{2m}}\left(\frac{6\psi}{\varphi}+1\right)^{\frac{1-m}{2m}}. \end{cases} \tag{3.35}$$

Eq. (3.34) has non-trivial solutions if and only if the determinant of the matrix is equal to zero. The resulting (second order) characteristic equation from such a condition is

$$\left(\frac{\lambda}{\dot\theta}\right)^2+B\left(\frac{\lambda}{\dot\theta}\right)+C=0, \tag{3.36}$$

where

$$\begin{cases} B=\left[-G(\theta)+\frac{\left(\frac{\partial f(\theta,\sigma,p_{l0})}{\partial\sigma}\right)\sigma G(\theta)-\frac{\partial f(\theta,\sigma,p_{l0})}{\partial\theta}}{f(\theta,\sigma,p_{l0})}+\frac{\frac{\partial p_l(\theta,p_{l0})}{\partial\theta}\frac{\partial f(\theta,\sigma,p_{l0})}{\partial p_{l0}}}{f(\theta,\sigma,p_{l0})\frac{\partial p_l(\theta,p_{l0})}{\partial p_{l0}}}\right]_{\theta^0(t),\sigma^0(t),S^0(t),{p_{l0}}^0(t)}; \\ C=\left[\frac{\left(\frac{\partial f(\theta,\sigma,p_{l0})}{\partial\sigma}\right)\sigma\frac{dG(\theta)}{d\theta}+\left(\frac{\partial f(\theta,\sigma,p_{l0})}{\partial\theta}\right)G(\theta)}{f(\theta,\sigma,p_{l0})}-\frac{\frac{\partial p_l(\theta,p_{l0})}{\partial\theta}\frac{\partial f(\theta,\sigma,p_{l0})}{\partial p_{l0}}}{f(\theta,\sigma,p_{l0})\frac{\partial p_l(\theta,p_{l0})}{\partial p_{l0}}}\right]_{\theta^0(t),\sigma^0(t),S^0(t),{p_{l0}}^0(t)}. \end{cases} \tag{3.37}$$

Roots of Eq (3.36) are shown in figures 3.23 for different models (Skorohod, Castaneda, etc.) and for the expression of the Laplace pressure derived by averaging of the energy dissipation.

Like in [54], we analyze processes capable to reduce the porosity from 66% to zero. In this case, the condition $\sigma_z = p_l$ is achieved for a very wide range of external pressures. The values used in real sintering are included in such a range, and hence the case of interest is the one in which the quantity $\sigma_z - p_l$ changes sign during the process.

It is immediate to note that the results obtained by adopting the model of Skorohod are slightly different from the others.
Using such a model, the roots are complex for high porosity, with positive real

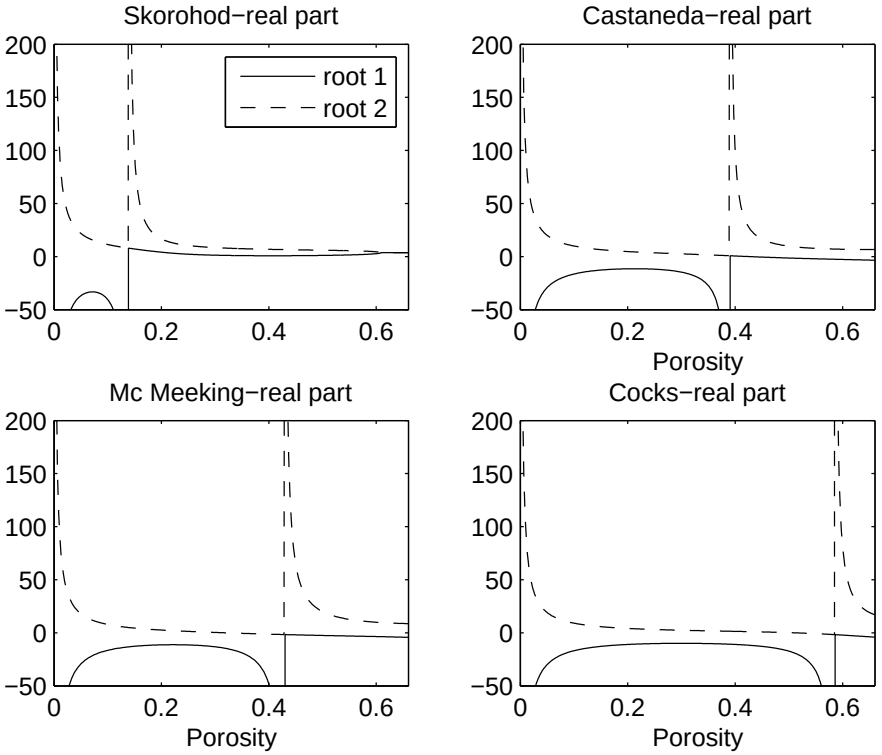

Figure 3.23: High order stability analysis - Forging - S.E.P.=10,$p_l = \frac{2\alpha}{r_0}\sqrt{\frac{3}{2}\psi(\theta)\frac{\theta}{1-\theta}}$

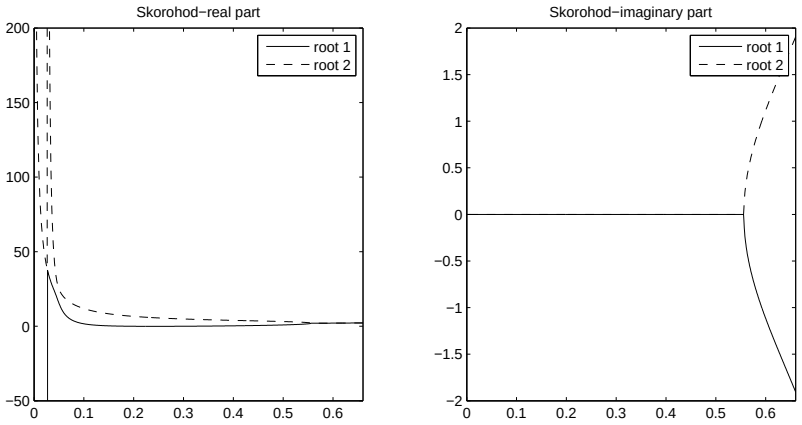

Figure 3.24: High order stability analysis - Forging - S.E.P.=100

part $Re\left[\left(\frac{\lambda}{\dot{\theta}}\right)_{1,2}\right] > 0$, thus the process is linearly stable. Roots are positive until the attainment of the asymptote occurring whenever $\sigma_z = p_l$ and hence the process is stable. Therefore, the sintering process can not go any further.This means that the critical porosity θ^* is a limit threshold under which it is not possible to go.

For higher values of the external pressure, it is possible to have unstable behavior for porosity higher than critical value, that is for $\sigma > p_l$ (see figure 3.24).

For Castaneda, Mc Meeking and Cocks the roots are real and $\frac{\lambda_1}{\theta} > 0$, $\frac{\lambda_2}{\theta} < 0$ for high values of porosity; thus, the process is linearly unstable from the beginning.

Figure 3.25 shows the results obtained by using the expression of the Laplace pressure obtained by using the stochastic approach. These results are very similar to those obtained by using the stochastic approach; indeed the qualitative behavior of the real parts of the roots of (3.36) does not change as m decreases (obviously the value of the critical porosity θ^* are m-dependent).

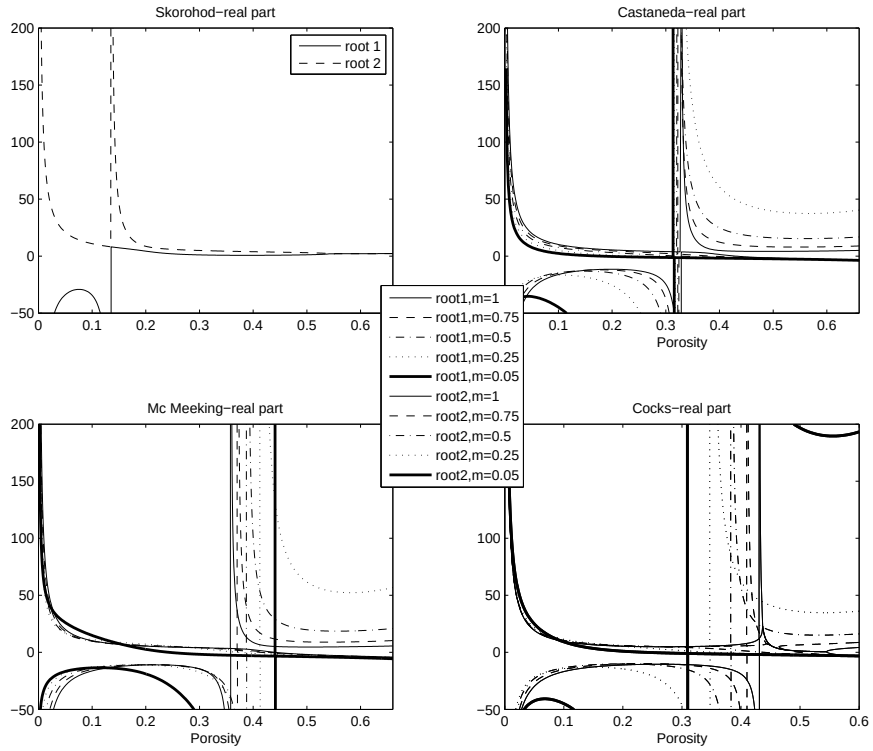

Figure 3.25: High order stability analysis - Forging - S.E.P.=10,$p_l = \frac{3\alpha}{r0}(1-\theta)^2$

This stability analysis shows that the free forging process is unstable.
It is worth noting that large strains occur in such a kind of loading mode. In fact, by considering a process reducing the porosity from 30% to 5%, there is a strong increment of cross-sectional area, as shown in figure 3.26. In order to study this problem, both the stress and the (infinitesimal) strain employed in this analysis should be replaced by appropriate (possibly work-conjugate) choice of the stress and strain measures.

Nevertheless, it appears to be necessary to study a different, and yet analog,

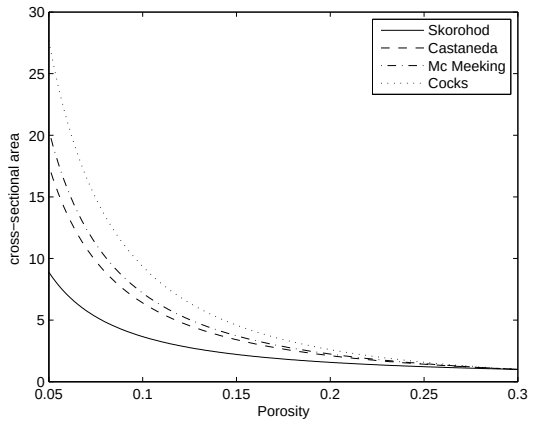

Figure 3.26: FREE FORGING: Evolution of cross-sectional area

case, i.e. forging in a rigid die. This problem will be discussed in the Part II of the present paper.

Chapter 4

Sintering of cylindrical specimens: Part II - Effects of the lateral confinement and of the Laplace pressure during constrained forging.

[Submitted]

Abstract

The role of the gas pressure in pores (called *sintering stress* or *Laplace pressure*) during sintering of pre-compacted metallic and ceramic (micro/nano)-powdered cylinders is analyzed in [54, 55] for isostatic pressing (also including free sintering) and "free" forging respectively. In the present work, the case of constrained forging, i.e. a transverse compressive force acting at the top and bottom faces of the sample in a rigid die, is investigated for the first time. This study analyzes the effects of the lateral confinement, i.e.:

- lowering of the sintering time required to achieve a prescribed porosity with respect to free forging;
- only small strains are involved during the process;
- obviously radial stresses arise.

Moreover, the effects of the interstitial stress are investigated:

- the external loading parameter may be tuned in such a way that the corresponding stress may equate the Laplace pressure whenever a "critical

porosity" is reached. This is exactly the same phenomenon detected in [54] and [55] for isostatic pressing and free forging respectively. Unlike the latter case, the exhibited plateau in the time-porosity response arises for a very small range of external loads which, like in isostatic pressing, does not include values of the external pressure usually employed in real processes;

- whenever such a critical value of the porosity is reached, the sintering time and the residual porosity do increase.

Furthermore, another beneficial effect of the confinement is to always stabilize the process. Whenever the critical porosity is reached, this stabilizing effect does prevent any further shrinking.

Notation

θ= porosity
σ_{ij} = components of the stress tensor
$\dot{\varepsilon}_{ij}$ = components of the strain rate tensor
$\dot{\varepsilon}'_{ij}$ = components of the deviatoric strain rate tensor
$\dot{e}$= first invariant of the strain rate tensor
$\dot{\gamma}$=second invariant of the deviatoric strain rate tensor
p= first invariant of the stress tensor
τ=second invariant of the stress tensor
w= effective equivalent strain rate
$\sigma(w)$= effective equivalent stress
A= time-dependent material constant
m= strain rate sensitivity
ψ= normalized bulk modulus
φ= normalized shear modulus
p_l= Laplace pressure (interstitial stress)
n= loading mode parameter
σ_0= reference stress
$\dot{\varepsilon}_0$= reference strain rate
α= surface tension
r_0= characteristic radius of particles
D= dissipation potential
d=dissipation per unit volume mass
S= cross-sectional area of the specimen
τ_E= dimensionless specific time
$S.E.P.$= specific external pressure
θ^*= critical porosity
θ_r= residual porosity

4.1 Introduction

This work is a natural extension of [55], where the effects of the interstitial stress during sintering in free forging are analyzed and discussed. In the current paper, a study of the kinetics and the stability of porous axially symmetric bodies undergoing constrained forging is investigated for the first time in the literature. This process is one of the most used in industry, since "as-pressed" components, obtained by cold compaction (for modeling of such a process see e.g. [33, 34, 44, 45]), are subsequently heated-up to temperatures significantly below values reached during free sintering and then forged in (rigid) dies.

The approach followed in this paper has been fruitfully introduced in [43] and used in [54, 55]. This entails to assume homogeneous plane stress through a sample, which is equivalent to consider constant states of plane stress (corresponding to the average of the actual stress fields). In [43], where this strategy it has been employed only for the cases in which the effect of the Laplace pressure is negligible with respect to the applied stresses, the case of constrained forging has only been mentioned and not treated yet. In the sequel, such a case is fully examined both accounting for the effects of the interstitial stress and neglecting them. This is a part of a work developed in [54] and [55], devoted to investigate the role of the interstitial stress during isostatic pressing (and obviously free sintering) and free forging of axially symmetric samples, respectively.

This paper may be outlined as follows. In Sect.4.2, the evolution law of the porosity is studied for the case of constrained forging, for different choices of the models both for the Laplace pressure and the shear and bulk moduli. In Section 4.2.1, in order to perform such analysis, three cases, analog to the ones treated in [54] (for isostatic pressing) and in [55] (for free forging), may arise through a comparison between the stress caused by external loading and the interstitial pressure. In particular, the occurrence of equality between such values is reached at a definite (critical) porosity, which remains constant for some time. Moreover, in Sect.4.2.2, the computation of the radial stress (i.e. the pressure acting on the die wall) during the process is performed. In Sect.4.3, two issues are investigated. First of all, thresholds on stresses caused by external loads are determined under which the influence of the interstitial pressure cannot be neglected. Such thresholds may strongly be influenced by the strain rate sensitivity of the material and the average radius of the particles; this feature may have a stronger impact for nano-structured powders, that play a key role in industrial applications (see e.g. [31, 39, 42, 49]). Furthermore, the discrepancy between the values of the residual porosity is evaluated by neglecting or accounting for the Laplace pressure during sintering processes of a given time-duration.
In Section 4.4, the stability of the process (namely of the solution of the problem in terms of time evolution of the porosity, obtained in Sect.4.2) is performed following the lines traced in [43]. Motivated by the unsatisfactory, and yet self-contradictory, results obtained in [54], Sect. 4.1, through a lower-order stability approach, a higher order analysis will be performed. The porosity, the stress due to the external loading and the reference value of the interstitial stress are then perturbed; this analysis shows that the process is stable for the whole processes

for each given value of the external loading. Whenever the critical porosity is encountered, this represents the lowest threshold under which the (average) longitudinal strain cannot evolve, since and the process can not continue.

4.2 Effects of the Laplace pressure on constrained forging

In industrial processes entailing sintering through forging, the specimen is usually laterally confined by a cast. In the sequel we shall consider the case of forging in a rigid die, with axial stress due to external load F_z. Denoting, as usual, by $\dot{\varepsilon_r}$ the rate of change of the average radial strain, the fact that the radial displacement are zero on the cast implies $\varepsilon_r = 0$ and hence $\dot{\varepsilon_r} = 0$. Obviously, in this case, the cross-sectional area remains constant during the process, i.e. $S = S_0$. Thus, the stress σ_z due to the external load remains constant, i.e. $\sigma_z = \frac{F_z}{S_0}$. The Laplace pressure varies according to equation (23) or (16) from Part I [55]. Therefore, the loading mode parameter n, defined in [55] by equation (9), is dependent on the porosity through the shear and bulk moduli ψ and φ:

$$n = \frac{\tau}{p} = -\sqrt{\frac{2}{3}}\frac{\varphi}{\psi}. \tag{4.1}$$

By substituting this value into the general evolution law for the porosity (see [55], Eq. (15)), it reduces to:

$$\dot{\theta} = -\dot{\varepsilon}_0 \Big(\frac{|\sigma_z - p_l|}{A\sigma_0}\Big)^{\frac{1}{m}} (1-\theta)^{\frac{3m-1}{2m}} \Big(\frac{2\varphi}{3} + \psi\Big)^{\frac{-(1+m)}{2m}}. \tag{4.2}$$

4.2.1 Evolution of the porosity during constrained forging

Eq. (4.2) can be expressed by using the dimensionless specific time τ_E defined by eq. (27) Part I [55], obtaining the differential equation

$$\frac{\partial\theta}{\partial\tau_E} = |\sigma_z - p_l|^{\frac{1}{m}} (1-\theta)^{\frac{3m-1}{2m}} \Big(\frac{2\varphi}{3} + \psi\Big)^{\frac{-(1+m)}{2m}}. \tag{4.3}$$

Eq. (4.3) can be integrated because the bulk modulus ψ and the shear modulus φ are known functions of the porosity θ, given in section 2.1.
The Specific External Pressure S.E.P., a dimensionless loading parameter, defined in [55], equation (29), is employed in the sequel.

Considering a process reducing the porosity from 30% to 5% and the expression of the Laplace pressure derived by the stochastic approach, the balance condition $\sigma_z = p_l$ is achieved for values of S.E.P. between 1.47 (which corresponds to the same condition at the beginning of the process, namely $\theta = 30\%$) and 2.71

(that corresponds to $\sigma_z = p_l$ at the end of the sintering process, i.e. $\theta = 5\%$). The range in which the condition $\sigma_z = p_l$ is achieved is very small, and does not include values of the external pressure usually employed in real industrial processes. Thus, only the case in which $\sigma_z > p_l$ for the whole sintering process will be studied.
A straight comparison concerning the balance condition $\sigma_z = p_l$, among the case under exam, the case of isostatic pressing (treated in [54]) and the case of free forging (see [55], Sect. 3.1,) may be done. For isostatic pressing, the balance between the Laplace pressure and the external stress is achieved for values of S.E.P. between 1.47 and 2.21. For free forging, the lower threshold is unchanged, whereas the upper one depends on the values of the strain rate sensitivity m and on the model; for $m = 1$ and for the different choices of the model for φ and ψ, such a threshold varies between 24.08 and 74.92. Using the expression of the Laplace pressure derived by averaging the energy dissipation, the range is roughly the same of the latter case.

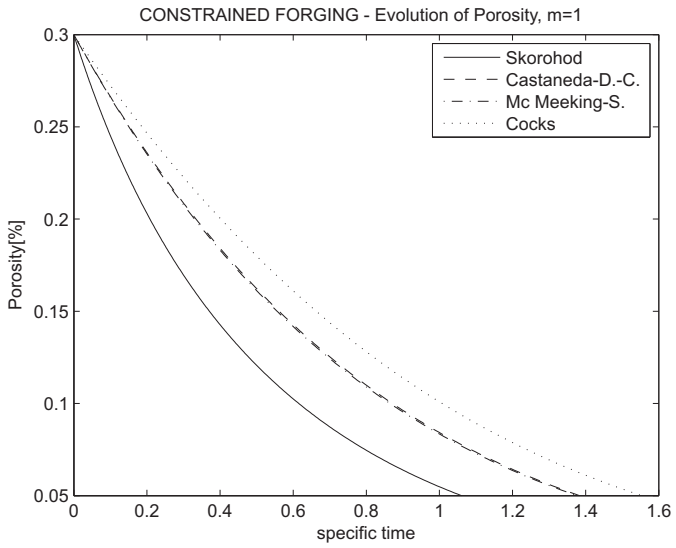

Figure 4.1: CONSTRAINED FORGING- Evolution of porosity for S.E.P.=100, for different models, $p_l = \frac{3\alpha}{r_0}(1-\theta)^2$

Figures 4.1 and 4.2 show the evolution of the porosity as a function of specific time τ_E, obtained by using the four different models for the shear and the bulk moduli, under high external pressure, for instance $S.E.P. = 100$, and for different expressions of the sintering stress. By comparing the figures mentioned above with figures (7) and (8) of [55] (evolution of the porosity for free forging at S.E.P.=100), it is immediate to note that the sintering time in constrained forging is undoubtely shorter than the one encounterede in free forging.
Moreover, the gap among the evolution of the porosity obtained by using different models is much lower in the case former case than in the latter one. Indeed, during free forging, the shear and bulk moduli influence both the time-evolution

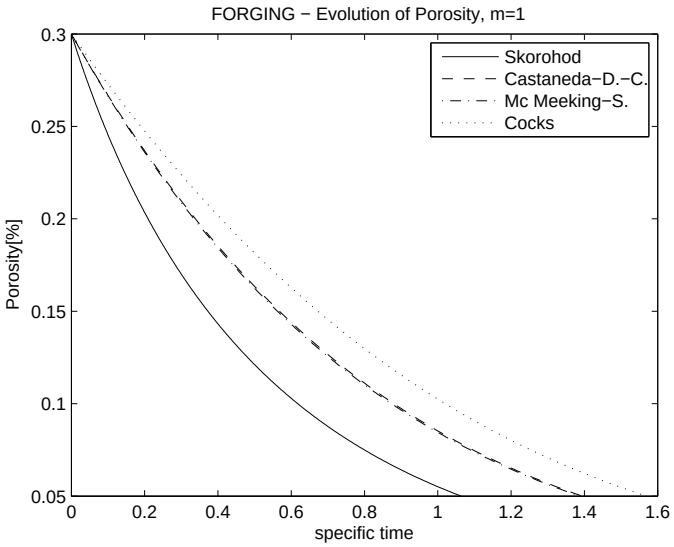

Figure 4.2: CONSTRAINED FORGING- Evolution of porosity for S.E.P.=100, for different models, $p_l = \frac{2\alpha}{r_0\varphi}\sqrt{\frac{3}{2}\psi(\theta)\frac{\theta}{1-\theta}}$

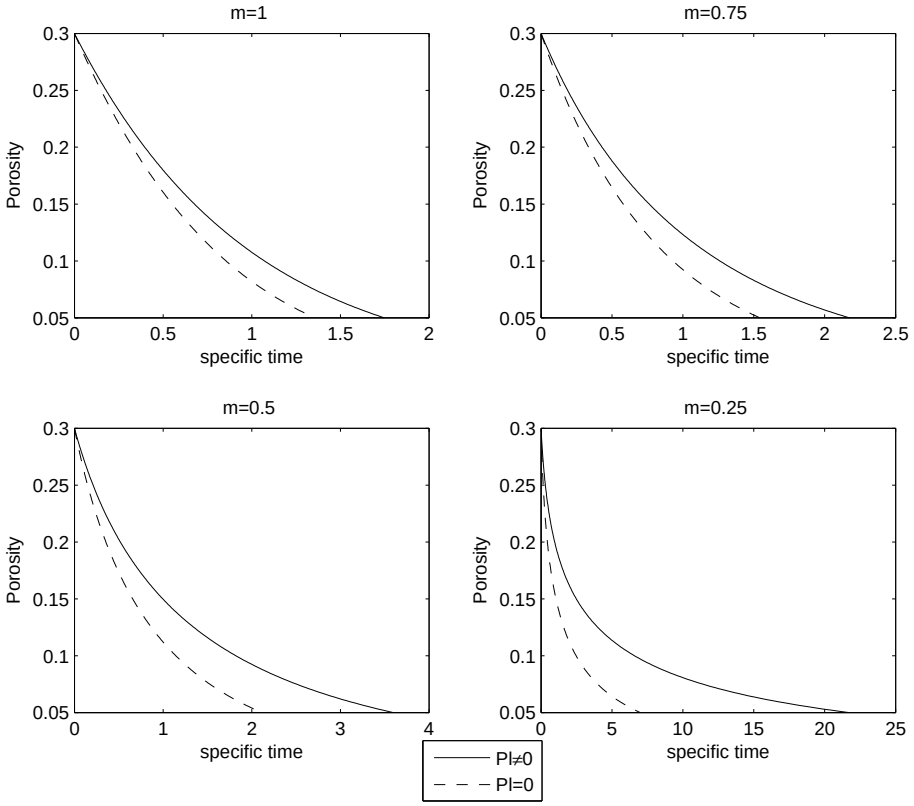

Figure 4.3: CONSTRAINED FORGING- Evolution of porosity for S.E.P.=10

of the porosity (see [55], eq. (24)) and the stress due to the external load. On the contrary, during constrained forging the external loading delivers a constant stress and so φ and ψ influence only equation (4.2).

Figure 4.3 shows the evolution of the porosity as a function of time for different values of the strain rate sensitivity m, for the model of Castaneda. It turns out that the behavior is qualitatively similar to the one obtained in [54], Section 4, for the case of isostatic pressing, and for the case of forging at high pressures. In analogy with the case of isostatic pressing (see [54]), the gap between the curves obtained by considering the contribution of the Laplace pressure and the ones obtained by neglecting it, is greater for low values of the strain rate sensitivity m (see figure 4.3).

4.2.2 Computation of the radial stress

It may be useful to evaluate the pressure acting on the die wall as the process of constrained forging proceeds. Such a pressure is nothing but the radial component of the stress tensor σ_r. This may be calculated from the constitutive law:

$$\sigma_r = \frac{\sigma(w)}{w}[\varphi\dot{\varepsilon}'_r + \psi\dot{e}] + p_l, \tag{4.4}$$

where, in the case of constrained forging, the first and second invariant of the strain rate tensor (defined in [55], equation (8)) assume the following values:

$$\dot{e} = \dot{\varepsilon}_z, \qquad \dot{\gamma} = \sqrt{\frac{2}{3}}|\dot{\varepsilon}_z|. \tag{4.5}$$

Hence, the radial and axial component of the stress tensor can be written as follows, since the axial strain rate $\dot{\varepsilon}_z$ is a negative quantity:

$$\begin{cases} \sigma_r = -\frac{\sigma(w)}{w}|\dot{\varepsilon}_z|[-\frac{\varphi}{3} + \psi] + p_l, \\ \sigma_z = -\frac{\sigma(w)}{w}|\dot{\varepsilon}_z|[\frac{2\varphi}{3} + \psi] + p_l, \end{cases} \tag{4.6}$$

where the equivalent strain rate w, defined in equation (2)of Part I ([55]), can be written as:

$$w = \frac{1}{\sqrt{1-\theta}}|\dot{\varepsilon}_z|\sqrt{\frac{2}{3}\varphi + \psi}. \tag{4.7}$$

Equation (4.7) and the Ashby power-law (see equation (11), [55]) can be used to obtain the ratio between the effective equivalent stress $\sigma(w)$ and the effective equivalent strain rate in the case of constrained forging:

$$\frac{\sigma(w)}{w} = \frac{\sigma_0 A}{\dot{\varepsilon}_0^m} w^{m-1} = \frac{\sigma_0 A}{\dot{\varepsilon}_0^m}|\dot{\varepsilon}_z|^{m-1}\Big[\frac{1}{1-\theta}\Big(\frac{2}{3}\varphi + \psi\Big)\Big]^{\frac{m-1}{2}}. \tag{4.8}$$

Relation (4.8) can be substitute into (4.6) in order to obtain:

$$\begin{cases} \sigma_r = -\frac{\sigma_0 A}{\dot{\varepsilon}_0^m}|\dot{\varepsilon}_z|^m\Big[\frac{1}{1-\theta}\Big(\frac{2}{3}\varphi + \psi\Big)\Big]^{\frac{m-1}{2}}[-\frac{\varphi}{3} + \psi] + p_l, \\ \sigma_z = -\frac{\sigma_0 A}{\dot{\varepsilon}_0^m}|\dot{\varepsilon}_z|^m\Big[\frac{1}{1-\theta}\Big]^{\frac{m-1}{2}}\Big[\frac{2}{3}\varphi + \psi\Big]^{\frac{m+1}{2}} + p_l. \end{cases} \tag{4.9}$$

From (4.9).2 can be simply obtain the following expression of $\dot{\varepsilon}_z$:

$$\dot{\theta} = -\dot{\varepsilon}_0 \Big(\frac{|\sigma_z - p_l|}{A\sigma_0} \Big)^{\frac{1}{m}} (1-\theta)^{\frac{m-1}{2m}} \Big(\frac{2\varphi}{3} + \psi \Big)^{\frac{-(1+m)}{2m}}, \tag{4.10}$$

and hence, by substituting (4.10) into equation (4.9).1, the following relation between the radial and the axial component of the stress tensor can be obtained:

$$\sigma_r = \Big[\frac{\psi - \frac{\varphi}{3}}{\psi + \frac{2}{3}\varphi} \Big] (\sigma_z - p_l) + p_l. \tag{4.11}$$

This equation allows for an easy computational procedure to evaluate the radial stress at each time step based on the step-by-step knowledge of σ_z and p_l; this depends on the the external load (through the axial stress σ_z), the porosity θ, the shear and bulk moduli φ and ψ and the strain rate sensitivity m.

Figure 4.4 and 4.5 shows the evolution of σ_r during the process, as a function

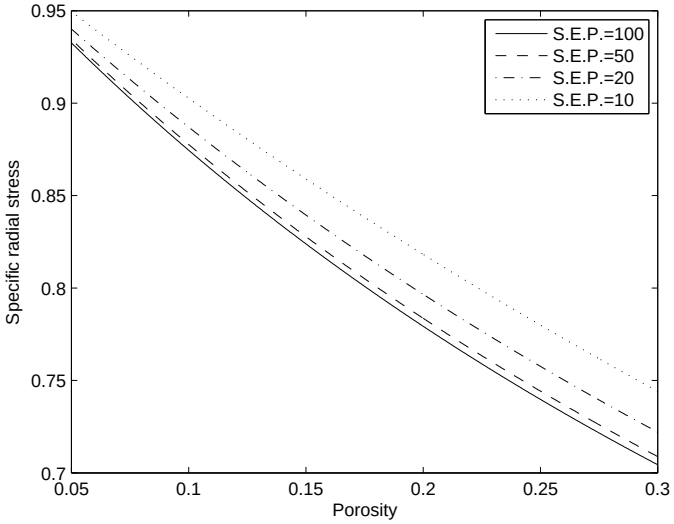

Figure 4.4: Specific radial stress $\frac{\sigma_r}{p_b}$ vs porosity

of porosity and time respectively. In these figures, the dimensionless quantity $\frac{\sigma_r}{p_b} = \frac{\sigma_r}{\sigma_z}$ is plotted for different values of S.E.P., for a process that reduced the porosity form 30% to 5%; the model of Castaneda and the expression of the Laplace pressure derived by using stochastic approach are used for the sake of illustration.

Obviously, in the case in which the critical porosity is reached, $\sigma_z = p_l$, the radial stress remains constant at the value $\sigma_r = p_l = \sigma_z$, as shown in figure 4.6 for $S.E.P. = 2$. For porosity lower than the critical one, σ_r becomes higher then the axial stress.

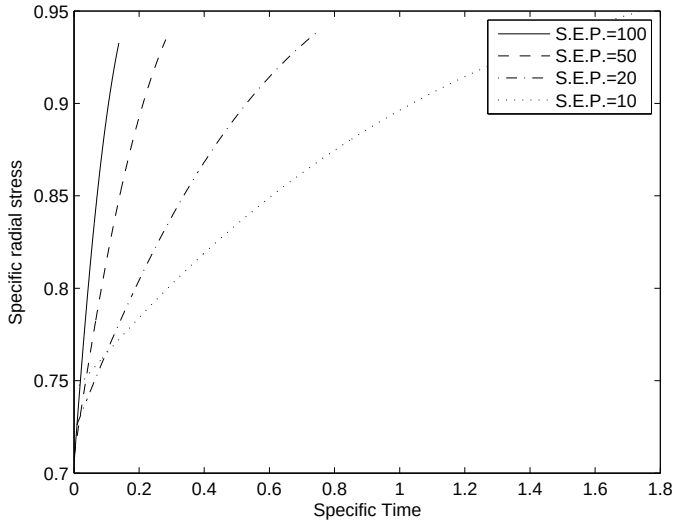

Figure 4.5: Specific radial $\frac{\sigma_r}{p_b}$ stress vs time

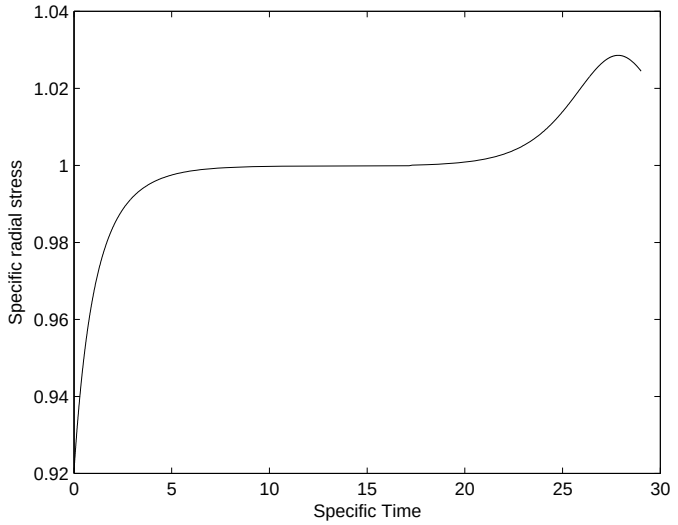

Figure 4.6: Specific radial $\frac{\sigma_r}{p_b}$ stress vs time, S.E.P.=2

4.3 Influence of the Laplace pressure for industrial process entailing constrained forging

Similarly to what was done for isostatic pressing [54] and for free forging cases (see [55], Sect. 4) and in order to study the effect of the Laplace pressure p_l, the aluminium-zinc-magnesium-copper alloy cited in [55], Section 4 is examined. The main features of this material are shown in [55], table 1.

Here, we are able to calculate the threshold pressure p^*, namely the external pressure inducing an error D (defined in [55], Sect.4) of 5%, 10% and 15% respectively between the time needed to reduce the porosity from 30% to 5%, accounting for the effect of the Laplace pressure, and the time obtained by neglecting it. Finally, the error on the residual porosity is calculated for different values of the grain size r_0 and the surface tension α of the material.

4.3.1 Threshold external loading pressures and sintering times

In figures 4.7 and 4.8 the threshold pressures obtained by means of Castaneda model are shown, for $5\mu m$ and $50nm$ powders.

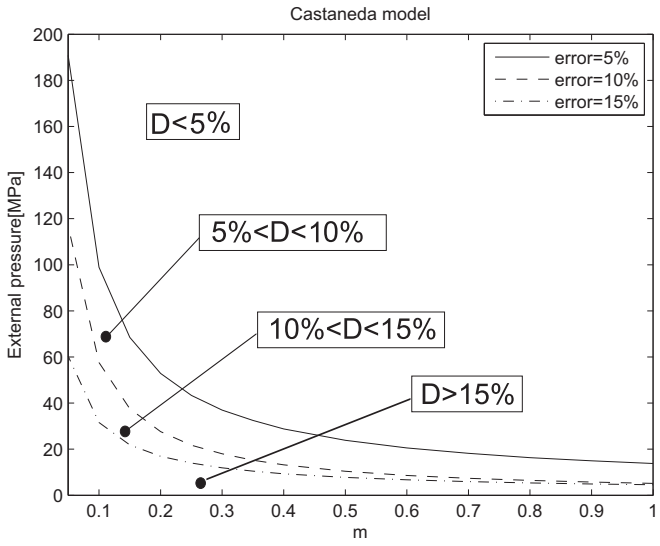

Figure 4.7: Threshold pressure p^* for $5\mu m$ powder

Figure 4.9 shows the comparison between the threshold pressures (giving a 10% error) obtained with the models of Castaneda, Mc Meeking and Cocks; no meaningful differences are shown in the three graphs.

By comparing the obtained results to those ones obtained in the case of free forging (see [55], figure 16) we note that in the current case the different models give very similar threshold pressures, while before the achieved results had meaningful differences. This is because for the case of free forging, choosing different models for the moduli φ and ψ, the stress due to external loading (σ_z) evolves in different ways during the sintering process (see [55], figure 6).
On the other hand, during constrained forging the stress σ_z, instead, remains constant and the difference among the results obtained by using different models is only due to the term involving the Laplace pressure in the evolution law (4.2).

Incidentally, the results obtained in these sections are related to the model of the sintering stress derived through stochastic approach, since the model obtained by averaging the energy dissipation is not sensitive to the strain rate

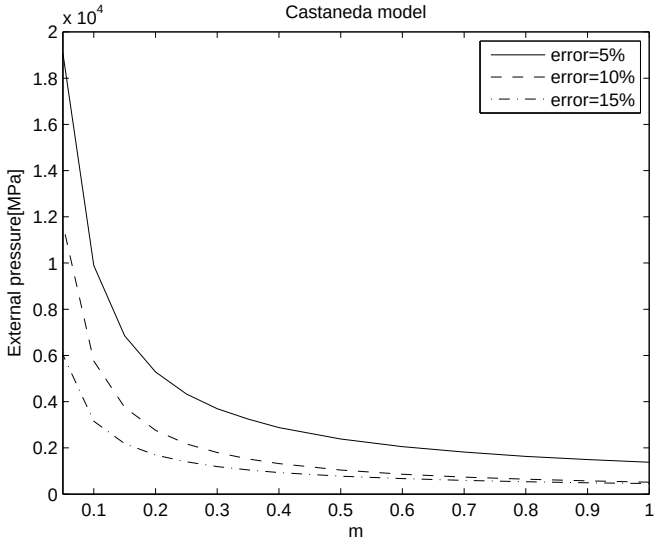

Figure 4.8: Threshold pressure p^* for $50nm$ powder

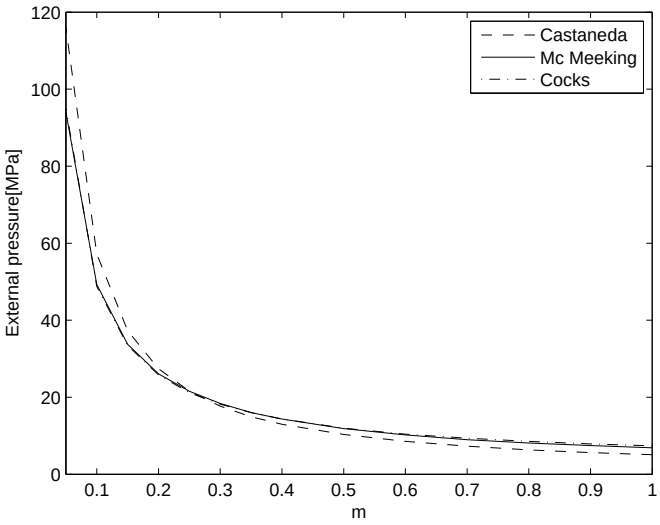

Figure 4.9: Threshold pressure p^* for different models

sensitivity m.

The obtained threshold pressures show that, especially for low values of the parameter m, the effect of the Laplace pressure cannot be neglected.

4.3.2 Residual porosity

The residual porosity is a key property of the actual material; indeed, this obviously determines the mechanical properties of a sintered specimen.
In the sequel, a thirty minutes sintering process, with external loading pressure of $100MPa$, is considered. Here, we are interested to compare the residual porosities θ_r and θ_{r0} after thirty minutes, wherever the "sintering driving force" is taken to be:

- $|\sigma_z - p_l|$,
- $|\sigma_z|$,

respectively. For the different values of powder grain size listed in Section 4 of Part I (see [55]), we are able to calculate the value of strain rate sensitivity m that allow for sintering times of the order of thirty minutes.
Furthermore, a time range from twentyone to thirtynine minutes is considered. Figure 4.10 shows the sintering time as a function of m, and highlights the values of strain rate sensitivity that correspond to the real sintering times. With such

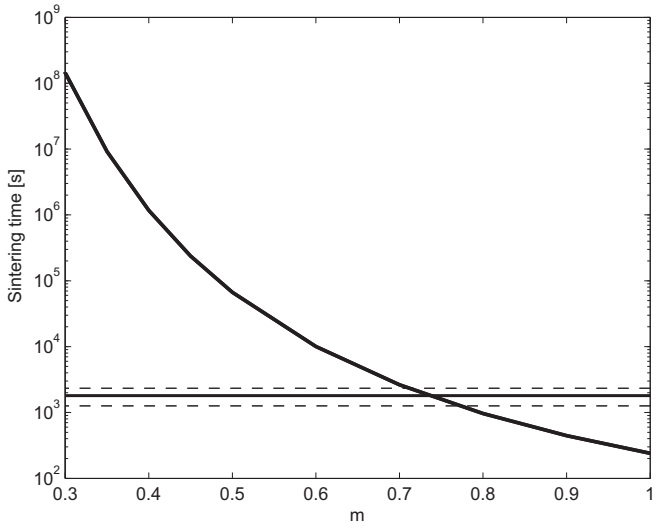

Figure 4.10: Sintering time as a function of the strain rate sensitivity m

values of the parameter m, we are able to evaluate the residual porosity after thirty minutes, by taking into account the effect of the Laplace pressure and the one obtained by neglecting it. Finally, the error occurring wherever the Laplace pressure p_l is neglected, defined as follows

$$e = \frac{\theta_r - \theta_{r0}}{\theta_r}, \tag{4.12}$$

is calculated.

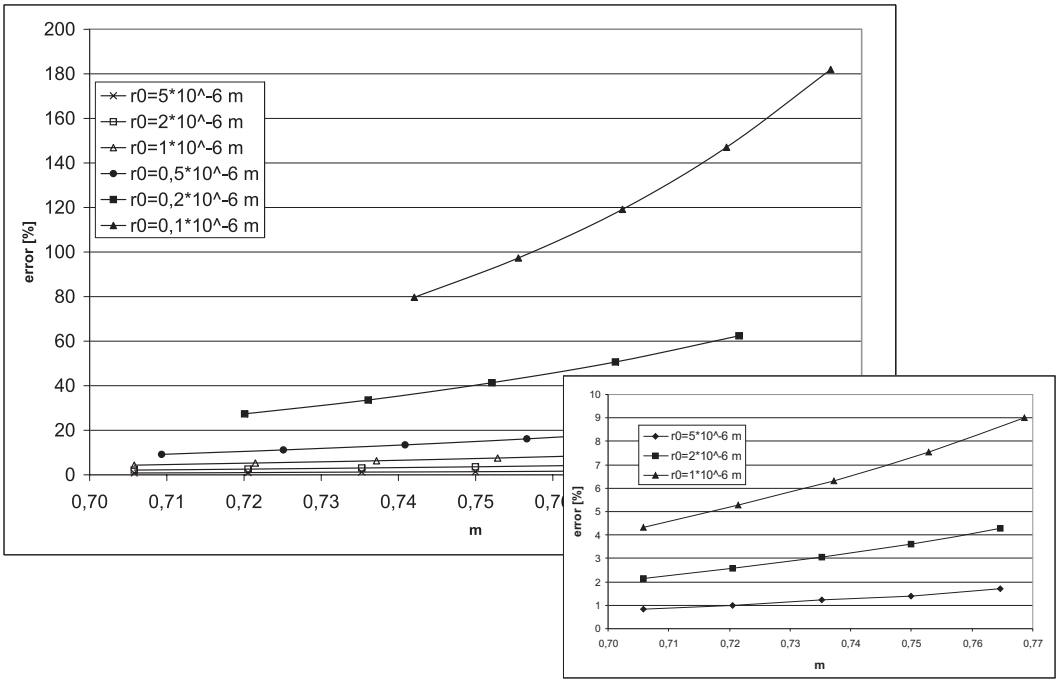

Figure 4.11: Error on the threshold pressures for different grain sizes

Figure 4.11 shows values of this error as a function of the strain rate sensitivity m, for values of powder grain size between $100nm$ and $5\mu m$. We note that, similarly to the case of isostatic pressing, for grain sizes of the order of 5div0.5μm the error is small, yet not negligible, whereas for grain sizes less than $0.5\mu m$ the error becomes really meaningful. For sizes of the order of $100nm$ powders, an error of about 200% may occur, while for $50nm$ powders, the order of magnitude of the error is even 500% (not showed in figure). For even lower powder grain sizes, namely values less than $30nm$, the Laplace pressure becomes greater than the stress due to external loading, and the gap between the real residual porosity θ_r and the porosity calculated by neglecting the Laplace pressure θ_{r0} is higher.

The second parameter influencing the Laplace pressure is the surface tension α; in analogy with the case of isostatic pressing case, the sensitivity of the model to changes of $\pm 50\%$ of the given values of α is analyzed. Figure 4.12 shows the error as a function of the surface tension α, for different values of the grain size.

The results obtained here are analog to the ones obtained for the case of isostatic pressing (see [54], Section 3.2.2).

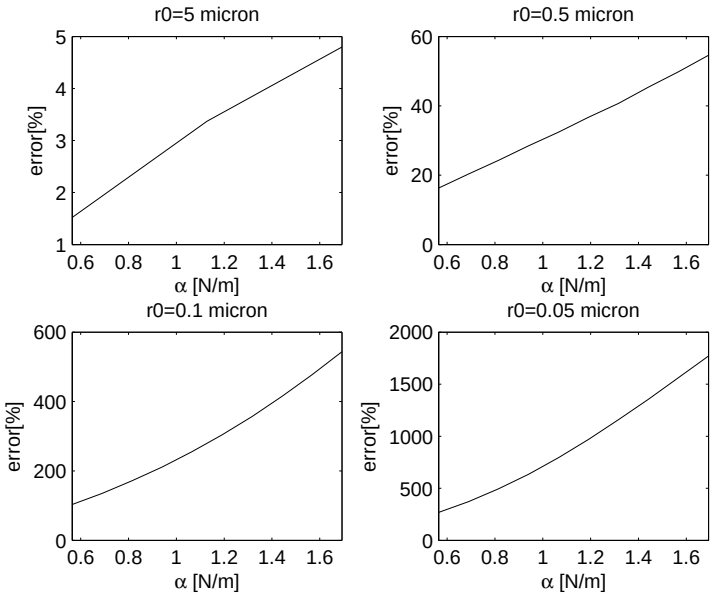

Figure 4.12: Error on the threshold pressure vs changes in α

4.4 Stability analysis

The procedure employed in this section has been introduced in [43] and it has been implemented, for isostatic pressing and free forging, in [54] and in Section 5 of the Part I of the present paper ([55]) respectively.

For constrained forging, the cross-section remains constant, and hence perturbations are not admissible for such a quantity. Therefore, perturbations of the porosity, of the Laplace pressure and of the axial stress may be introduced as follows:

$$\begin{cases} \theta(t) = \theta^0(t) + \delta\theta^0 \exp(\lambda(t-t_0)), \\ \sigma(t) = \sigma^0(t) + \delta\sigma^0 \exp(\lambda(t-t_0)), \\ p_{l0}(t) = p_{l0}^0(t) + \delta p_{l0}^0 \exp(\lambda(t-t_0)). \end{cases} \tag{4.13}$$

By substituting such a perturbation in equations (4.2), (16) for the Laplace pressure derived by using stochastic approach or (23) for the other formulation of the Laplace pressure and (25) of [55], the following system is obtained:

$$\left[\begin{array}{ccc} 0 & S & 0 \\ \frac{1}{\theta}\frac{\partial f(\theta,\sigma,p_{l0})}{\partial\theta} - \frac{\lambda}{\theta} & \frac{1}{\theta}\frac{\partial f(\theta,\sigma,p_{l0})}{\partial\sigma} & \frac{1}{\theta}\frac{\partial f(\theta,\sigma,p_{l0})}{\partial p_{l0}} \\ \frac{\partial p_l(\theta,p_{l0})}{\partial\theta} & 0 & \frac{\partial p_l(\theta,p_{l0})}{\partial p_{l0}} \end{array} \right]_{\theta^0(t),\sigma^0(t),{p_{l0}}^0(t)} \left[\begin{array}{c} \delta\theta \\ \delta\sigma \\ \delta p_{l0} \end{array} \right] = \left[\begin{array}{c} 0 \\ 0 \\ 0 \end{array} \right], \tag{4.14}$$

where

$$f(\theta,\sigma,p_{l0}) = \Big[-\dot{\varepsilon}_0\Big(\frac{|\sigma_z - p_{l0}(1-\theta)^2|}{A\sigma_0}\Big)^{\frac{1}{m}}(1-\theta)^{\frac{3m-1}{2m}}\Big(\frac{2\varphi}{3}+\psi\Big)^{\frac{-(1+m)}{2m}}\Big]_{\theta^0(t),\sigma^0(t),{p_{l0}}^0(t)}. \tag{4.15}$$

Eq. (4.14) has non-trivial solutions if and only if the determinant of the matrix appearing in such a system is equal to zero. From this condition, we obtain a first order equation with respect to the normalized perturbation growth rate $\frac{\lambda}{\dot{\theta}}$:

$$\Big(\frac{\lambda}{\dot{\theta}}\Big) + B = 0, \tag{4.16}$$

where

$$B = \Big[\frac{-\frac{\partial p_l(\theta,p_{l0})}{\partial p_{l0}}\frac{\partial f(\theta,\sigma,p_{l0})}{\partial \theta} + \frac{\partial p_l(\theta,p_{l0})}{\partial \theta}\frac{\partial f(\theta,\sigma,p_{l0})}{\partial p_{l0}}}{f(\theta,\sigma,p_{l0})\frac{\partial p_l(\theta,p_{l0})}{\partial p_{l0}}}\Big]_{\theta^0(t),\sigma^0(t),{p_{l0}}^0(t)}. \tag{4.17}$$

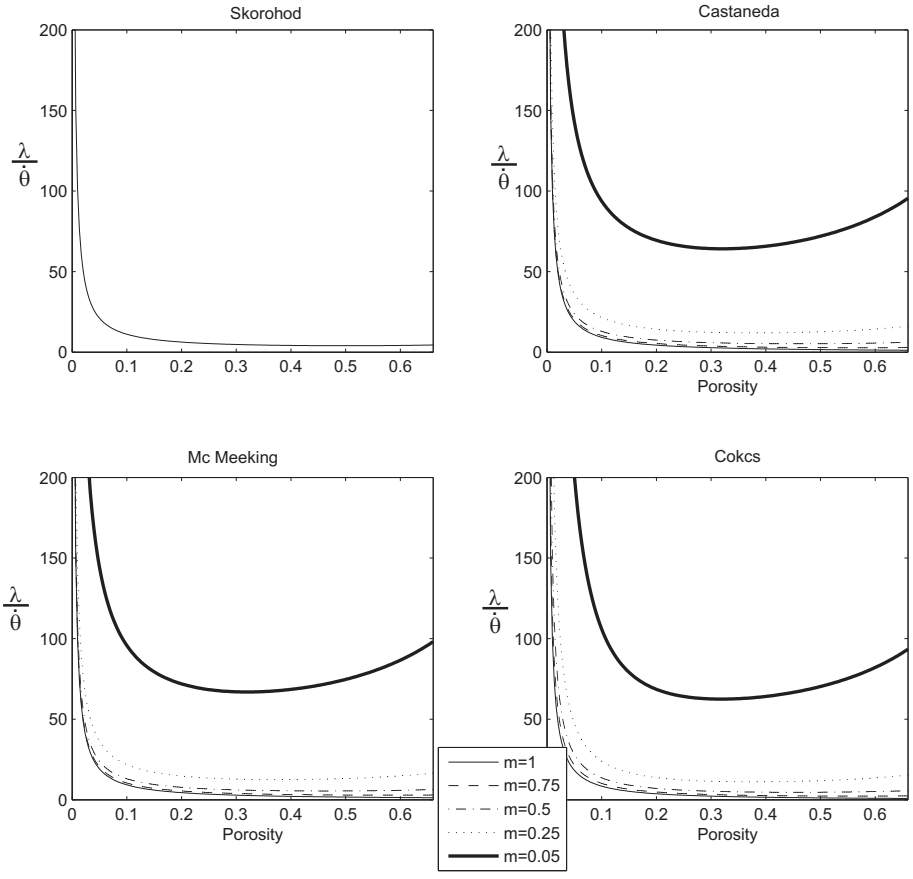

Figure 4.13: High order stability analysis, S.E.P.=10

Figures 4.13 and 4.14 show the behavior of $\frac{\lambda}{\dot{\theta}}$ as a function of the porosity θ for different external loadings (here considered through the Specific External

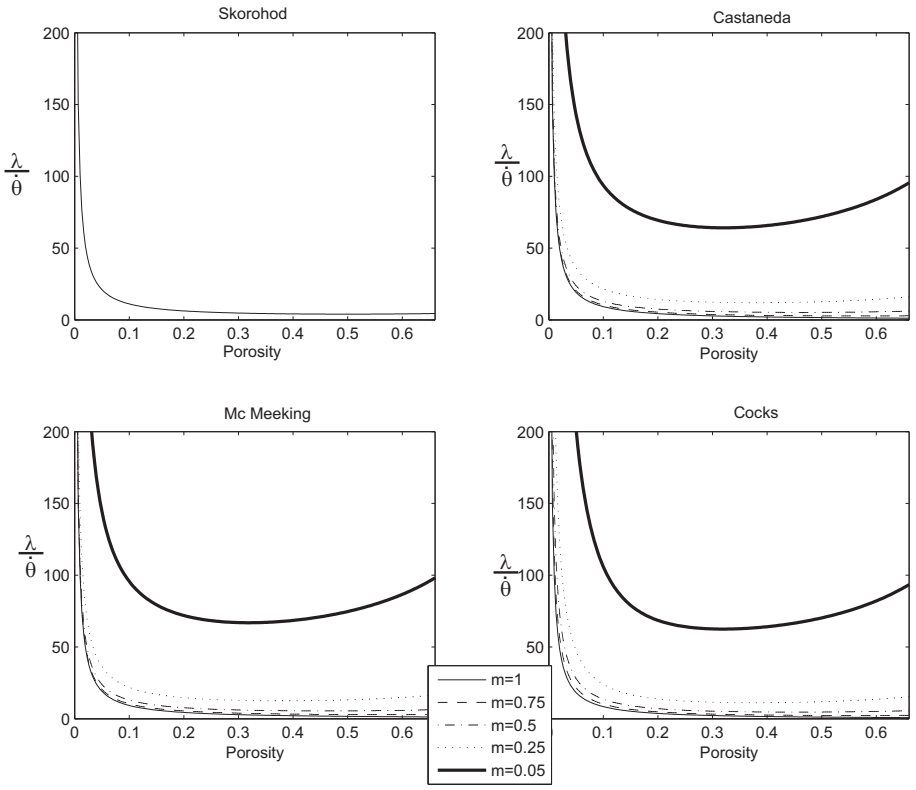

Figure 4.14: High order stability analysis, S.E.P.=2

Pressure, defined by [55], equation (29) S.E.P.=10 and S.E.P.=2.

Figure 4.13 and 4.14 show the obtained results considering the Laplace pressure obtained by using the stochastic approach (i.e. $p_l = \frac{3\alpha}{r0}(1-\theta)^2$). The corresponding values of $\frac{\lambda}{\dot{\theta}}$ obtained by using $p_l = \frac{2\alpha}{r0}\sqrt{\frac{2}{3}\psi(\theta)\frac{\theta}{1-\theta}}$ turn out to be very similar to these ones.

The figures above show that the roots are positive for the whole range of porosity (between 0 and 66%), thus the process is linearly stable.
It is worth noting that, whenever the function $f(\theta, \sigma, p_{l0})$ is zero, which is the case for $\sigma_z = p_l$ (and hence $\theta = \theta^*$), equation (4.15) implies that its derivatives with respect to θ and p_{l0} are also both zero. Therefore, $B = \frac{\lambda}{\dot{\theta}} = \frac{0}{0}$ and so for $\theta = \theta^*$, the root $\frac{\lambda}{\dot{\theta}}$ is not defined. Nevertheless, the right and left limits exist and they do coincide; such a common value turns out to be positive and hence, the process is stable. This means that, for a narrow range of external loads, there exists a limiting porosity.
For instance, this occurs for S.E.P.=2, whereas it does not happen for S.E.P.=10. Incidentally, in Sect. 4.2.1 it has been stated that whenever the porosity vary from 30% to 5%, the range of S.E.P. for which the critical porosity θ^* is encountered go from 1.47 to 2.71. This actually represents the lowest threshold value under which the (averaged) longitudinal strain cannot evolve since $\dot{\varepsilon}_z = 0$.

Figure 4.15 shows the evolution of λ and $\dot{\theta}$ as a function of the porosity θ, for S.E.P.=2, for Castaneda model.

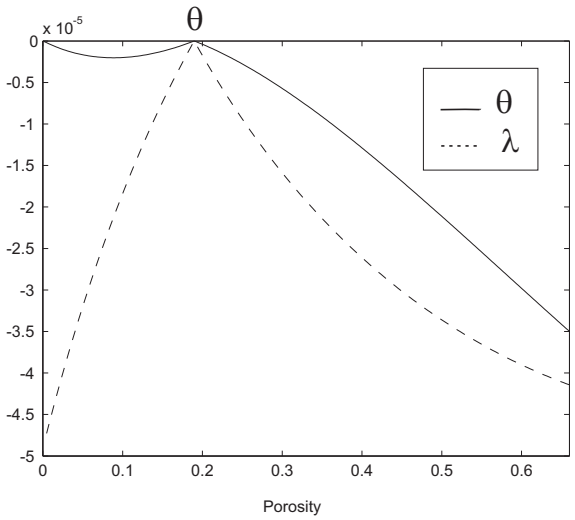

Figure 4.15: Evolution of λ and $\dot{\theta}$ for S.E.P.=2, for Castaneda model.

Chapter 5

Derivation of the general form of the elasticity tensor of a transverse isotropic material with residual stress

5.1 Introduction

It is known that mechanical components made of sintered alloys are appreciated for their suitable for applications in the as-sintered state.
Whenever thermal annealing processes are ruled out of the industrial process because of economical reasons, the unavoidable residual stresses originated by sintering may then have an influence on the mechanical performances of sintered samples.

The residual stress (often called prestress) depends upon the stress state at the end of the sintering, that is a function of of the final value of the interstitial pressure and of the loading mode used during the process.

For the sake of simplicity, as-sintered axially symmetric specimens are examined. For such components, isostatic pressing may induce isotropy, whereas constrained forging processes may enforce a transverse isotropic behavior in the direction of forging.

The mechanical behavior of linearly elastic prestressed materials may be described through the following general constitutive law [28]:

$$\boldsymbol{\sigma} = \overset{\circ}{\boldsymbol{\sigma}} + \mathbf{H}\overset{\circ}{\boldsymbol{\sigma}} + \overset{\circ}{\boldsymbol{\sigma}}\mathbf{H}^T - (tr\mathbf{H})\ \overset{\circ}{\boldsymbol{\sigma}} + \mathfrak{L}[\overset{\circ}{\boldsymbol{\sigma}}, \mathbf{H}], \tag{5.1}$$

where $\boldsymbol{\sigma}$ is the Cauchy stress tensor, $\overset{\circ}{\boldsymbol{\sigma}}$ is the residual stress tensor and $\mathbf{H}$ is the gradient of the displacement vector. By using the classical definition of the symmetric and antisymmetric part of $\mathbf{H}$, i.e.

$$\begin{cases} \boldsymbol{\varepsilon} = \frac{\mathbf{H}+\mathbf{H}^T}{2}, \\ \mathbf{W} = \frac{\mathbf{H}-\mathbf{H}^T}{2}, \end{cases} \tag{5.2}$$

equation (5.1) can be rearranged as follows:

$$\boldsymbol{\sigma} - (\mathbf{W}\overset{\circ}{\boldsymbol{\sigma}} + \overset{\circ}{\boldsymbol{\sigma}}\mathbf{W}^{\mathbf{T}}) = \overset{\circ}{\boldsymbol{\sigma}} + \boldsymbol{\varepsilon}\overset{\circ}{\boldsymbol{\sigma}} + \overset{\circ}{\boldsymbol{\sigma}}\boldsymbol{\varepsilon}^{T} - (tr\boldsymbol{\varepsilon})\ \overset{\circ}{\boldsymbol{\sigma}} + \mathfrak{L}[\overset{\circ}{\boldsymbol{\sigma}}, \mathbf{H}], \tag{5.3}$$

where the quantity $\boldsymbol{\sigma} - (\mathbf{W}\overset{\circ}{\boldsymbol{\sigma}} + \overset{\circ}{\boldsymbol{\sigma}}\mathbf{W}^{\mathbf{T}})$ ultimately represents a corotational term inherited through the presence of the residual stress.

The sixth-order tensor $\mathfrak{L}$ is the incremental elasticity tensor, which contract two indexes for each of the arguments and reduces to the forth-order classical elasticity tensor $\mathbb{C}$ whenever $\overset{\circ}{\boldsymbol{\sigma}} = 0$.

A representation formula for such a sixth-order tensor in the case of full isotropy is given by Man [28]. In the following chapter, the representation of $\mathfrak{L}$ for linear elastic transversely isotropic material is deduced for the first time in the literature. The method used to get such a result is suggested by Weiyi [30] and it relies upon the partial differentiation of the strain energy density with respect to the strain tensor and the residual stress tensor.

5.2 Preliminaries

For a linear isotropic material, in the absence of prestress, it is well known that the relation between the stress and the strain tensor can be expressed through two parameters:

$$\mathbb{C}[\boldsymbol{\varepsilon}] = \lambda(tr\boldsymbol{\varepsilon})\mathbf{I} + 2\mu\boldsymbol{\varepsilon} \Rightarrow \mathbb{C} = \lambda\mathbf{I}\otimes\mathbf{I} + 2\mu\mathbb{I}, \tag{5.4}$$

where λ and μ are the Lame's constants.
In the case of linear transversely isotropic elastic material, the relation depends on five independent parameters (see e.g. Weiyi, [30]):

$$\begin{gathered}\mathbb{C}[\boldsymbol{\varepsilon}] = \lambda(tr\boldsymbol{\varepsilon})\mathbf{I}+2\mu\boldsymbol{\varepsilon}+\alpha_1(n\boldsymbol{\varepsilon}n)n\otimes n+\alpha_2[\mathbf{I}(n\boldsymbol{\varepsilon}n)+tr(\boldsymbol{\varepsilon})n\otimes n]+2\alpha_3[n\cdot\boldsymbol{\varepsilon}\otimes n+n\otimes\boldsymbol{\varepsilon}\cdot n] \Rightarrow \\ \Rightarrow \mathbb{C} = \lambda\mathbf{I}\otimes\mathbf{I} + 2\mu\mathbb{I} + \alpha_1 n\otimes n\otimes n\otimes n + \alpha_2[\mathbf{I}\otimes n\otimes n + n\otimes n\otimes\mathbf{I}]+ \\ \alpha_3[n\otimes e_i\otimes n\otimes e_i + e_i\otimes n\otimes e_i\otimes n + e_i\otimes n\otimes n\otimes e_i + n\otimes e_i\otimes e_i\otimes n]\end{gathered} \tag{5.5}$$

Following Man (see [28]), the incremental elasticity tensor $\mathfrak{L}[\overset{\circ}{\boldsymbol{\sigma}}, \boldsymbol{\varepsilon}]$ (see constitutive law (5.1) can be written as follows:

$$\mathfrak{L}[\overset{\circ}{\boldsymbol{\sigma}}, \boldsymbol{\varepsilon}] = \mathbb{C}[\boldsymbol{\varepsilon}] + \mathfrak{D}[\overset{\circ}{\boldsymbol{\sigma}}, \boldsymbol{\varepsilon}], \tag{5.6}$$

where, for isotropic material,

$$\mathfrak{D}[\overset{\circ}{\boldsymbol{\sigma}}, \boldsymbol{\varepsilon}] = \beta_1(tr\boldsymbol{\varepsilon})(tr\ \overset{\circ}{\boldsymbol{\sigma}})\mathbf{I} + \beta_2(tr\ \overset{\circ}{\boldsymbol{\sigma}})\boldsymbol{\varepsilon} + \beta_3[(tr\boldsymbol{\varepsilon})\ \overset{\circ}{\boldsymbol{\sigma}} + (tr\boldsymbol{\varepsilon}\ \overset{\circ}{\boldsymbol{\sigma}})] + \beta_4[\boldsymbol{\varepsilon}\ \overset{\circ}{\boldsymbol{\sigma}} + \overset{\circ}{\boldsymbol{\sigma}}\ \boldsymbol{\varepsilon}], \tag{5.7}$$

where $\beta_1, ..., \beta_4$ are material constants.
Combining equations (5.1), (5.4), (5.6) and (5.7),the constitutive equation for linear elastic isotropic material with residual stress can be written as follows:

$$\begin{gathered}\boldsymbol{\sigma} - (\mathbf{W}\overset{\circ}{\boldsymbol{\sigma}} + \overset{\circ}{\boldsymbol{\sigma}}\mathbf{W}^{\mathbf{T}}) = \overset{\circ}{\boldsymbol{\sigma}} + \boldsymbol{\varepsilon}\ \overset{\circ}{\boldsymbol{\sigma}} + \overset{\circ}{\boldsymbol{\sigma}}\ \boldsymbol{\varepsilon}^{T} + (tr\boldsymbol{\varepsilon})\ \overset{\circ}{\boldsymbol{\sigma}} + \lambda(tr\boldsymbol{\varepsilon})\mathbf{I} + 2\mu\boldsymbol{\varepsilon} + \\ + \beta_1(tr\boldsymbol{\varepsilon})(tr\ \overset{\circ}{\boldsymbol{\sigma}})\mathbf{I} + \beta_2(tr\ \overset{\circ}{\boldsymbol{\sigma}})\boldsymbol{\varepsilon} + \beta_3[(tr\boldsymbol{\varepsilon})\ \overset{\circ}{\boldsymbol{\sigma}} + (tr\boldsymbol{\varepsilon}\ \overset{\circ}{\boldsymbol{\sigma}})] + \beta_4[\boldsymbol{\varepsilon}\ \overset{\circ}{\boldsymbol{\sigma}} + \overset{\circ}{\boldsymbol{\sigma}}\ \boldsymbol{\varepsilon}].\end{gathered} \tag{5.8}$$

For the linear elastic transversely isotropic material with residual stress, the sixth-order tensor $\mathfrak{D}(\overset{\circ}{\boldsymbol{\sigma}}, \boldsymbol{\varepsilon}, n)$ is deduced, in the sequel, by the method of tensor derivatives [16], that originates from the theory f invariants [7, 17].

5.2.1 Isotropy of space and material frame-indifference on the stress response

In order to obtain the evaluate the stress response of both the isotropic and transversely isotropic sintered materials, it is necessary to focus on the general invariant forms of their constitutive equation.
Following Boehler [17], we consider the most general case of anisotropic material, where the constitutive equation gives the stress, $\boldsymbol{\sigma}$, a symmetric second order tensor, which is a function $\mathbf{F}$ of:

- the structural tensor $\boldsymbol{\xi}$ (taking into account the intrinsic symmetries of the internal structures of the material),

- the mechanical agency $\mathbf{D}$ (i.e. the strain tensor in the case of elastic behavior, the stretching tensor in case of plastic or viscous behavior, the strain tensor and the residual stress tensor in the case of elastic behavior with prestress),

i.e.

$$\boldsymbol{\sigma} = \mathbf{F}(\mathbf{D}, \boldsymbol{\xi}). \tag{5.9}$$

In general, the principal direction of $\mathbf{D}$ do not coincide with the principal directions of $\boldsymbol{\sigma}$.

The principle of isotropy of space states that the constitutive laws governing the internal conditions of a physical system and the interactions between its parts should not depend on whatever external frame of reference is used to describe them. A consequence of this principle is that an arbitrary transformation Q of the orthogonal group $Orth$, applied to both the material and the agency, results in the same orthogonal transformation of the material response $\boldsymbol{\sigma}$. The concept of objectivity (frame-indifference), in science means that qualitative and quantitative descriptions of physical phenomena remain unchanged when the phenomena are observed under a variety of conditions. With reference to figure 5.1, for observer 1 the constitutive equation (5.9) relates the response $\boldsymbol{\sigma}$ to the structural tensor $\boldsymbol{\xi}$ and the mechanical agency D, whereas (as shown in figure 5.1) observer 2 "sees" these tensors rotated of Q, i.e.:

$$\begin{cases} \boldsymbol{\xi}^* = \mathbf{Q}\boldsymbol{\xi}\mathbf{Q}^{\mathbf{T}}, \\ \mathbf{D}^* = \mathbf{Q}\mathbf{D}\mathbf{Q}^{\mathbf{T}}, \\ \boldsymbol{\sigma}^* = \mathbf{Q}\boldsymbol{\sigma}\mathbf{Q}^{\mathbf{T}}, \end{cases} \tag{5.10}$$

and, hence,

$$\boldsymbol{\sigma}^* = \mathbf{F}(\mathbf{D}^*, \boldsymbol{\xi}^*) = \mathbf{F}(\mathbf{Q}\mathbf{D}\mathbf{Q}^{\mathbf{T}}, \mathbf{Q}\boldsymbol{\xi}\mathbf{Q}^{\mathbf{T}}) = \mathbf{Q}\boldsymbol{\sigma}\mathbf{Q}^{\mathbf{T}} = \mathbf{Q}\mathbf{F}(\mathbf{D}, \boldsymbol{\xi})\mathbf{Q}^{\mathbf{T}} \tag{5.11}$$

The tensor-valued function $\mathbf{F}$, subject to the invariance condition (5.11), is called *spatially* isotropic with respect to its arguments $(\mathbf{D}, \boldsymbol{\xi})$.

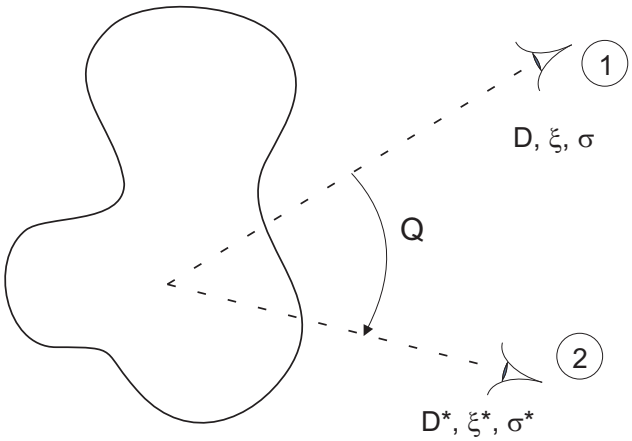

Figure 5.1:

5.2.2 Material symmetries and energy response

A constitutive equation has to be independent on the reference frame (assumption of material frame indifference). However, the dependence of the material behavior on the choice of the reference configuration cannot be ruled out: a change of reference configuration, i.e. a rotation of the structural tensor $\boldsymbol{\xi}$, may influence the response. If, for a particular class of rotations, this change in the response does not occur, then there is a property of material symmetry; this particular class of rotations form the "symmetry group"of the material.

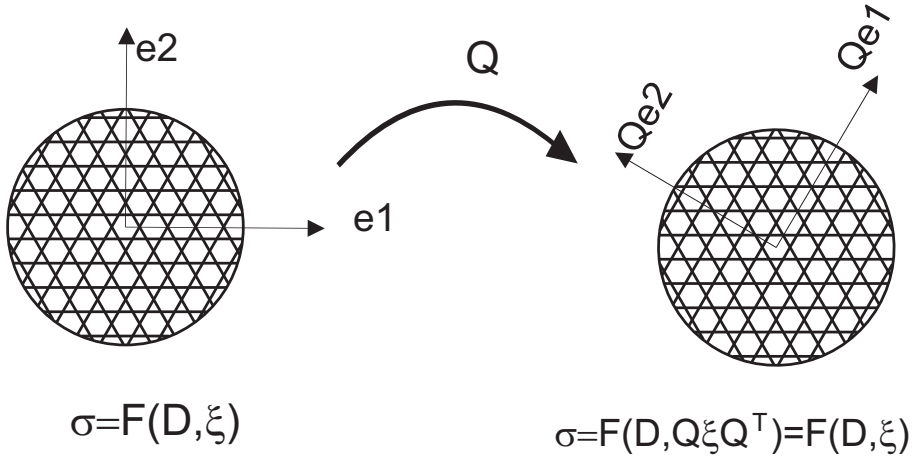

Figure 5.2: Notion of symmetry group

Mathematically,
if $\boldsymbol{\sigma} = \mathbf{F}(\mathbf{D}, \boldsymbol{\xi}) = \mathbf{F}(\mathbf{D}, \mathbf{Q}\boldsymbol{\xi}\mathbf{Q}^{\mathbf{T}}) \Leftrightarrow \mathbf{Q} \ \epsilon \ \mathcal{G}$,
where $\mathcal{G}$ is he symmetry group of the material.

In the sequel, only the interesting cases of isotropy and transverse isotropy are examined. In the present framework, the goal is to properly represent the strain energy as a scalar function of the strain tensor $\boldsymbol{\varepsilon}$ and the residual stress tensor $\overset{\circ}{\boldsymbol{\sigma}}$, i.e. of the invariants of these tensors, consistently with the mentioned material symmetries.
Such symmetries impose definite restrictions on the form of the constitutive relation. In order to obtain a properly written constitutive equation, both in terms of energy $U = f(\mathbf{D}, \boldsymbol{\xi})$ and stress response $\boldsymbol{\sigma} = \mathbf{F}(\mathbf{D}, \boldsymbol{\xi})$ in which such symmetries are automatically verified, one may proceed as follows:

- a basic set of polynomial scalar invariants $(I_1, I_2, ...I_n)$ is necessary in order for the function f to fully reflect the symmetries of material and the frame indifference determine;

- a generating set of tensors $(\mathbf{G_1}, \mathbf{G_2}, ..., \mathbf{G_n})$ such that the tensor function $\mathbf{F}$ can be expressed as a linear combination:

$$\mathbf{F} = \sum_{1...n} \alpha_i \mathbf{G_i}; \tag{5.12}$$

  where α_i are arbitrary polynomial scalar function of the invariants $(I_1, I_2, ...I_n)$, is required to obtain a stress response $\mathbf{F}$ enjoying the symmetries mentioned above.

5.2.3 Isotropic materials

A material is called isotropic if an arbitrary transformation $\mathbf{Q}$ of the orthogonal group $Orth$, applied to the material (but not to the agency), results in the same material response $\boldsymbol{\sigma}$, i.e.

$$\boldsymbol{\sigma} = \mathbf{F}(\mathbf{D}, \boldsymbol{\xi}) = \mathbf{F}(\mathbf{D}, \mathbf{Q}\boldsymbol{\xi}\mathbf{Q}^{\mathbf{T}}) \ \ \forall \ \ \mathbf{Q} \ \ \epsilon \ \ Orth, \mathbf{D} \ \ \epsilon \ \ \ Sym. \tag{5.13}$$

Thus, $\mathcal{G}_I \equiv Orth$.
It is easy to see that this conditions leads to $\boldsymbol{\xi} = \lambda\mathbf{I}$, and hence the constitutive equation (5.9) can be reduces to $\boldsymbol{\sigma} = \mathbf{F}(\mathbf{D}, \boldsymbol{\xi}) = \mathbf{F}(\mathbf{D})$ [17].
This behavior is shown in figure 5.3.
By applying the principle of isotropy of space, it is easy to obtain that, for an arbitrary rotation $R \epsilon Orth$,

$$\mathbf{R}\boldsymbol{\sigma}\mathbf{R}^{\mathbf{T}} = \mathbf{R}\mathbf{F}(\mathbf{D}, \boldsymbol{\xi})\mathbf{R}^{\mathbf{T}} = \mathbf{F}(\mathbf{R}\mathbf{D}\mathbf{R}^{\mathbf{T}}, \mathbf{R}\boldsymbol{\xi}\mathbf{R}^{\mathbf{T}}) \tag{5.14}$$

for the principle of isotropy of space. Moreover, for isotropic material, we have

$$\mathbf{F}(\mathbf{R}\mathbf{D}\mathbf{R}^{\mathbf{T}}, \mathbf{R}\boldsymbol{\xi}\mathbf{R}^{\mathbf{T}}) = \mathbf{F}(\mathbf{R}\mathbf{D}\mathbf{R}^{\mathbf{T}}, \mathbf{R}\mathbf{Q}\boldsymbol{\xi}\mathbf{Q}^{\mathbf{T}}\mathbf{R}^{\mathbf{T}}) \tag{5.15}$$

By choosing RQ=I, we can obtain

$$\mathbf{R}\boldsymbol{\sigma}\mathbf{R}^{\mathbf{T}} = \mathbf{F}(\mathbf{R}\mathbf{D}\mathbf{R}^{\mathbf{T}}, \boldsymbol{\xi}) \tag{5.16}$$

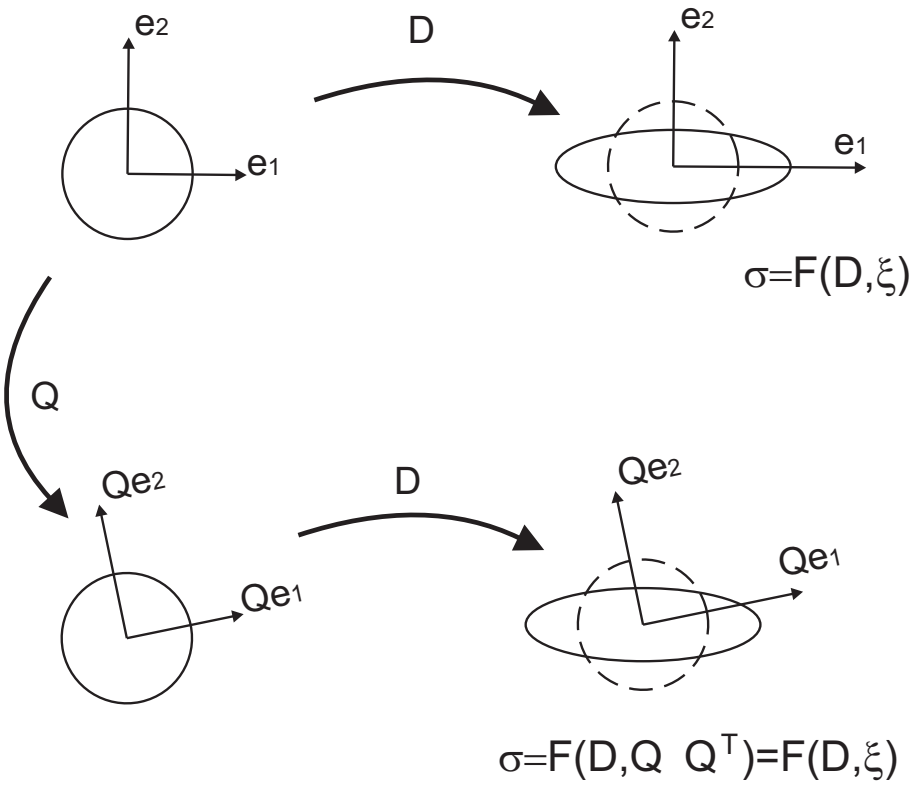

Figure 5.3: Behavior of an isotropic body

which means that the constitutive function $\mathbf{F}$, and hence the material response, is isotropic with respect to the agent $\mathbf{D}$.

For such a case, Boehler [17], grounding on a method developed by Rivlin and Ericksen [6], indicates:

- the set of invariants necessary to obtain the correct irreducible representation for an isotropic scalar-valued function f of a tensor $\mathbf{A}$: $tr(\mathbf{A}), tr(\mathbf{A^2}), tr(\mathbf{A^3})$
- the minimal set of tensor generators for the representation of a tensor-valued function $\mathbf{F}$: $\mathbf{I}, \mathbf{A}, \mathbf{A^2}$

In the case in which f and $\mathbf{F}$ are functions of two generic tensors $\mathbf{A}$ and $\mathbf{B}$, we have, in analogy with the previous case,

- invariants: $tr(\mathbf{A}), tr(\mathbf{A^2}), tr(\mathbf{A^3}), tr(\mathbf{B}), tr(\mathbf{B^2}), tr(\mathbf{B^3}), tr(\mathbf{AB}), tr(\mathbf{A^2B}), tr(\mathbf{AB^2}), tr(\mathbf{A^2B^2})$
- tensor generators: $\mathbf{I}, \mathbf{A}, \mathbf{A^2}, \mathbf{B}, \mathbf{B^2}, \mathbf{AB}+\mathbf{BA}, \mathbf{A^2B}+\mathbf{BA^2}, \mathbf{AB^2}+\mathbf{B^2A}$

It is worth noting, through the structural tensor $\boldsymbol{\xi}$, that the constitutive law (5.7) has the latter conformation, where $\overset{\circ}{\boldsymbol{\sigma}}$ and $\boldsymbol{\varepsilon}$ replace $\mathbf{A}$ and $\mathbf{B}$, although no quadratic terms in neither tensors are present; indeed while $\mathbf{D}$ must be linear in $\boldsymbol{\varepsilon}$, it also turns out to be linear in $\overset{\circ}{\boldsymbol{\sigma}}$ (see [28]).

5.2.4 Transversely isotropic materials

A material is called transversely isotropic, with privileged direction n, if an arbitrary transformation $\mathbf{Q} \quad \epsilon \quad Orth$, applied to the material (through the structural tensor $\boldsymbol{\xi}$) but not to the agency $\mathbf{D}$, results in the same response if and only if $\mathbf{Q}$ represents either a rotation about the axis n or a reflection (with respect to the direction n).
The following schematic, 5.4, shows how a rotation about the axis of transverse isotropy e_1 leaves the stress response unchanged.
The response is

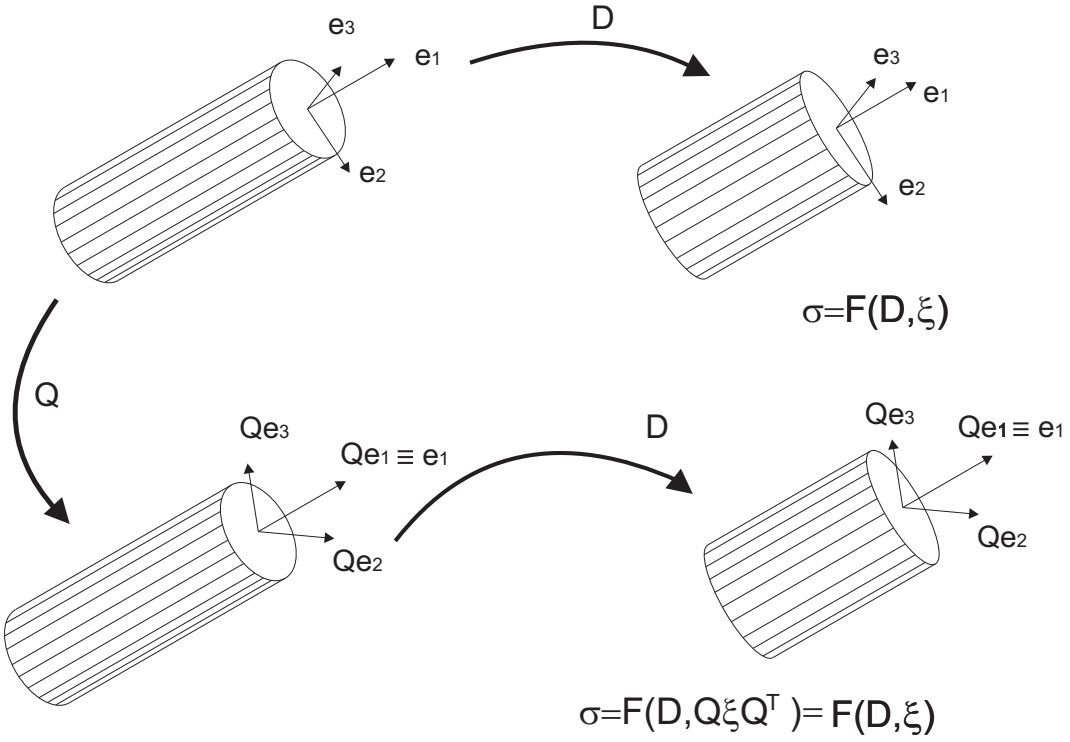

Figure 5.4: Behavior of a transversely isotropic body

$$\boldsymbol{\sigma} = \mathbf{F}(\mathbf{D}, \boldsymbol{\xi}) = \mathbf{F}(\mathbf{D}, \mathbf{Q}\boldsymbol{\xi}\mathbf{Q}^{\mathbf{T}}) \quad \forall \quad \mathbf{Q} \quad \epsilon \quad \mathcal{G}_{T.I.}, \quad \mathbf{D} \quad \epsilon \quad Sym \tag{5.17}$$

where the symmetry group $\mathcal{G}_{T.I.}$ is given by all the rotation about the axis n, the reflection with respect to all the planes containing n, and the identity tensor. In analogy with the isotropic case, it is easy to demonstrate that the constitutive function $\mathbf{F}$, and hence the material response, is transversely isotropic with respect to the agent $\mathbf{D}$.

It is easy to show that, for a general tensor function $\mathbf{F}$, the condition (5.17) implies that $\boldsymbol{\xi} = \mathbf{Q}\boldsymbol{\xi}\mathbf{Q}^{\mathbf{T}}$, i.e. the symmetry group is the invariance group of the structural tensor $\boldsymbol{\xi}$.
If we consider the tensor $\mathbf{N} := n \otimes n$; we may show that the invariance group

of this tensor is the symmetry group $\mathcal{G}_{T.I.}$,

$$\mathbf{Q} \ \epsilon \ \mathcal{G}_{T.I.} \quad \Leftrightarrow \quad \mathbf{QNQ^T} = \mathbf{N}. \tag{5.18}$$

Hence, $\mathbf{N}$ is the structural tensor for transversely isotropic material.

The functional bases for general orthotropic and transversely isotropic scalar and tensor-valued function have been established in [17], employing a generalization of the method developed by Rivlin and Ericksen.
The set of invariants necessary to obtain the irreducible representation for an isotropic scalar and tensor function of a tensor $\mathbf{A}$ is:
- invariants: $tr(\mathbf{A}), tr(\mathbf{A^2}), tr(\mathbf{A^3}, tr(\mathbf{NA}), tr(\mathbf{NA^2}), tr(\mathbf{NA^3})$
- tensor generators:$\mathbf{I}, \mathbf{A}, \mathbf{A^2}, \mathbf{AN} + \mathbf{NA}, \mathbf{A^2N} + \mathbf{NA^2}$

For the case in which the scalar and tensor are functions of two generic tensors $\mathbf{A}$ and $\mathbf{B}$, the set of arguments becomes:
- invariants: $tr(\mathbf{A}), tr(\mathbf{A^2}), tr(\mathbf{A^3}), tr(\mathbf{B}), tr(\mathbf{B^2}), tr(\mathbf{B^3}), tr(\mathbf{AB})$, $tr(\mathbf{A^2B}), tr(\mathbf{AB^2}), tr(\mathbf{A^2B^2}), tr(\mathbf{NA}), tr(\mathbf{NA^2}), tr(\mathbf{NB}), tr(\mathbf{NB^2}), tr(\mathbf{NAB})$, $tr(\mathbf{NA^2B}), tr(\mathbf{NAB^2}), tr(\mathbf{NA^2B^2})$
- tensor generators: $\mathbf{I}, \mathbf{A}, \mathbf{A^2}, \mathbf{B}, \mathbf{B^2}, \mathbf{AB} + \mathbf{BA}, \mathbf{A^2B} + \mathbf{BA^2}, \mathbf{AB^2} + \mathbf{B^2A}$, $\mathbf{AN} + \mathbf{NA}, \mathbf{A^2N} + \mathbf{NA^2}, \mathbf{BN} + \mathbf{NB}, \mathbf{B^2N} + \mathbf{NB^2}, \mathbf{NAB} + \mathbf{BAN}$, $\mathbf{NBA} + \mathbf{ABN}, \mathbf{NA^2B} + \mathbf{BA^2N}, \mathbf{NBA^2} + \mathbf{A^2BN}, \mathbf{NAB^2} + \mathbf{B^2AN}$, $\mathbf{NB^2A} + \mathbf{AB^2N}$

Note that the invariants of the type $tr(\mathbf{NA})$ can be written as $n \cdot \mathbf{A}n$.

5.3 Strain Energy for transversely isotropic material

For such materials, the part of the strain energy U due to the presence of the residual stress $\overset{\circ}{\boldsymbol{\sigma}}$, here and further is indicated by U_R. This can be expressed as a scalar function of the strain tensor $\boldsymbol{\varepsilon}$, the residual stress tensor $\overset{\circ}{\boldsymbol{\sigma}}$ and the structural tensor $\mathbf{N} = n \otimes n$ (through the vector n, denoting the direction of transverse isotropy), i.e.

$$U_R = U_R(\boldsymbol{\varepsilon}, \overset{\circ}{\boldsymbol{\sigma}}, n). \tag{5.19}$$

Such an energy can thus be written as a function of the invariants of $\boldsymbol{\varepsilon}$, $\overset{\circ}{\boldsymbol{\sigma}}$ for the case of transverse isotropy with axes n. The complete list of the polynomial invariants is (see [7, 17]),

$$
\begin{aligned}
J_1 &= tr(\boldsymbol{\varepsilon}) \\
J_2 &= tr(\boldsymbol{\varepsilon}^2) \\
J_3 &= tr(\boldsymbol{\varepsilon}^3) \\
J_4 &= n \cdot \boldsymbol{\varepsilon} n \\
J_5 &= n \cdot \boldsymbol{\varepsilon}^2 n \\
J_6 &= tr(\overset{\circ}{\boldsymbol{\sigma}}) \\
J_7 &= tr(\overset{\circ}{\boldsymbol{\sigma}}^2) \\
J_8 &= tr(\overset{\circ}{\boldsymbol{\sigma}}^3) \\
J_9 &= n \cdot \overset{\circ}{\boldsymbol{\sigma}}\, n \\
J_{10} &= n \cdot \overset{\circ}{\boldsymbol{\sigma}}^2\, n \\
J_{11} &= tr(\boldsymbol{\varepsilon}\, \overset{\circ}{\boldsymbol{\sigma}}) \\
J_{12} &= tr(\boldsymbol{\varepsilon}^2\, \overset{\circ}{\boldsymbol{\sigma}}) \\
J_{13} &= tr(\boldsymbol{\varepsilon}\, \overset{\circ}{\boldsymbol{\sigma}}^2) \\
J_{14} &= tr(\boldsymbol{\varepsilon}^2\, \overset{\circ}{\boldsymbol{\sigma}}^2) \\
J_{15} &= n \cdot (\boldsymbol{\varepsilon}\, \overset{\circ}{\boldsymbol{\sigma}}) n \\
J_{16} &= n \cdot (\boldsymbol{\varepsilon}^2\, \overset{\circ}{\boldsymbol{\sigma}}) n \\
J_{17} &= n \cdot (\boldsymbol{\varepsilon}\, \overset{\circ}{\boldsymbol{\sigma}}^2) n \\
J_{18} &= n \cdot (\boldsymbol{\varepsilon}^2\, \overset{\circ}{\boldsymbol{\sigma}}^2) n
\end{aligned}
\tag{5.20}
$$

For a linear elastic material, for which the strain energy U_R ($\boldsymbol{\varepsilon}$,$\overset{\circ}{\boldsymbol{\sigma}}$,n) is at most function of the squaree strain, and a first order function of the residual stress, the interesting invariants are

$$
\begin{aligned}
J_1 &= tr(\boldsymbol{\varepsilon}) \\
J_2 &= tr(\boldsymbol{\varepsilon}^2) \\
J_4 &= n \cdot \boldsymbol{\varepsilon} n \\
J_5 &= n \cdot \boldsymbol{\varepsilon}^2 n \\
J_6 &= tr(\overset{\circ}{\boldsymbol{\sigma}}) \\
J_9 &= n \cdot \overset{\circ}{\boldsymbol{\sigma}}\, n \\
J_{11} &= tr(\boldsymbol{\varepsilon}\, \overset{\circ}{\boldsymbol{\sigma}}) \\
J_{12} &= tr(\boldsymbol{\varepsilon}^2\, \overset{\circ}{\boldsymbol{\sigma}}) \\
J_{15} &= n \cdot (\boldsymbol{\varepsilon}\, \overset{\circ}{\boldsymbol{\sigma}}) n \\
J_{16} &= n \cdot (\boldsymbol{\varepsilon}^2\, \overset{\circ}{\boldsymbol{\sigma}}) n
\end{aligned}
\tag{5.21}
$$

only.
The function U_R, representing the part of the strain energy due to the presence of residual stresses, can be expressed as a linear combination of all the terms including the first order powers in $\overset{\circ}{\boldsymbol{\sigma}}$ and the second order powers in $\boldsymbol{\varepsilon}$. Hence, such terms are obtained by combining the invariants (5.21). Finally, U_R may be written in the following way:

$$U_R(\boldsymbol{\varepsilon}, \overset{\circ}{\boldsymbol{\sigma}}, n) = \hat{U_R}(J_i) = \beta_1 J_1^2 J_6 + \beta_2 J_1^2 J_9 + \beta_3 J_1 J_4 J_6 + \beta_4 J_1 J_4 J_9 + \beta_5 J_1 J_{11} + \beta_6 J_1 J_{15} + \beta_7 J_4^2 J_6 + \beta_8 J_4^2 J_9 + \beta_9 J_4 J_{11} + \beta_{10} J_4 J_{15} + \beta_{11} J_2 J_6 + \beta_{12} J_2 J_9 + \beta_{13} J_5 J_6 + \beta_{14} J_5 J_9 + \beta_{15} J_{12} + \beta_{16} J_{16} \quad (5.22)$$

where the coefficients $\beta_1, ..., \beta_{16}$ denote the material constants, independent on $\boldsymbol{\varepsilon}$, $\overset{\circ}{\boldsymbol{\sigma}}$ and n.

5.4 Derivation of the Stress tensor

It is worth noting that the stress can be obtained by deriving the strain energy U_R with respect to the strain tensor $\boldsymbol{\varepsilon}$, thus

$$\boldsymbol{\sigma}_R(\boldsymbol{\varepsilon}, \overset{\circ}{\boldsymbol{\sigma}}, n) = \frac{\partial U_R(\boldsymbol{\varepsilon}, \overset{\circ}{\boldsymbol{\sigma}}, n)}{\partial \boldsymbol{\varepsilon}} = \frac{\partial \hat{U_R}(J_i)}{\partial \boldsymbol{\varepsilon}} =$$
$$= \beta_1[J_1^2\frac{\partial J_6}{\partial \boldsymbol{\varepsilon}} + 2J_1J_6\frac{\partial J_1}{\partial \varepsilon}] + \beta_2[J_1^2\frac{\partial J_9}{\partial \boldsymbol{\varepsilon}} + 2J_1J_9\frac{\partial J_1}{\partial \boldsymbol{\varepsilon}}] + \beta_3[J_1J_4\frac{\partial J_6}{\partial \boldsymbol{\varepsilon}} + J_1J_6\frac{\partial J_4}{\partial \boldsymbol{\varepsilon}} + J_4J_6\frac{\partial J_1}{\partial \boldsymbol{\varepsilon}}] +$$
$$\beta_4[J_1J_4\frac{\partial J_9}{\partial \boldsymbol{\varepsilon}} + J_1J_9\frac{\partial J_4}{\partial \boldsymbol{\varepsilon}} + J_4J_9\frac{\partial J_1}{\partial \boldsymbol{\varepsilon}}] + \beta_5[J_1\frac{\partial J_{11}}{\partial \boldsymbol{\varepsilon}} + J_{11}\frac{\partial J_1}{\partial \boldsymbol{\varepsilon}}] + \beta_6[J_1\frac{\partial J_{15}}{\partial \boldsymbol{\varepsilon}} + J_{15}\frac{\partial J_1}{\partial \boldsymbol{\varepsilon}}] +$$
$$\beta_7[J_4^2\frac{\partial J_6}{\partial \boldsymbol{\varepsilon}} + 2J_4J_6\frac{\partial J_4}{\partial \boldsymbol{\varepsilon}}] + \beta_8[J_4^2\frac{\partial J_9}{\partial \boldsymbol{\varepsilon}} + 2J_4J_9\frac{\partial J_1}{\partial \boldsymbol{\varepsilon}}] + \beta_9[J_4\frac{\partial J_{11}}{\partial \boldsymbol{\varepsilon}} + J_{11}\frac{\partial J_4}{\partial \boldsymbol{\varepsilon}}] +$$
$$\beta_{10}[J_4\frac{\partial J_{15}}{\partial \boldsymbol{\varepsilon}} + J_{15}\frac{\partial J_4}{\partial \boldsymbol{\varepsilon}}] + \beta_{11}[J_2\frac{\partial J_6}{\partial \boldsymbol{\varepsilon}} + J_6\frac{\partial J_2}{\partial \boldsymbol{\varepsilon}}] + \beta_{12}[J_2\frac{\partial J_9}{\partial \boldsymbol{\varepsilon}} + J_9\frac{\partial J_2}{\partial \boldsymbol{\varepsilon}}] + \beta_{13}[J_5\frac{\partial J_6}{\partial \boldsymbol{\varepsilon}} + J_6\frac{\partial J_5}{\partial \boldsymbol{\varepsilon}}] +$$
$$\beta_{14}[J_5\frac{\partial J_9}{\partial \boldsymbol{\varepsilon}} + J_9\frac{\partial J_5}{\partial \boldsymbol{\varepsilon}}] + \beta_{15}\frac{\partial J_{12}}{\partial \boldsymbol{\varepsilon}} + \beta_{16}\frac{\partial J_{16}}{\partial \boldsymbol{\varepsilon}} \quad (5.23)$$

It is immediate to note that the invariants J_6 and J_9 are independent on $\boldsymbol{\varepsilon}$, i.e. $\frac{\partial J_6}{\partial \boldsymbol{\varepsilon}} = 0$ and $\frac{\partial J_9}{\partial \boldsymbol{\varepsilon}} = 0$. Thus, expression (5.23) can be reduced to be:

$$\boldsymbol{\sigma}_R(\boldsymbol{\varepsilon}, \overset{\circ}{\boldsymbol{\sigma}}, n) = \frac{\partial U_R(\boldsymbol{\varepsilon}, \overset{\circ}{\boldsymbol{\sigma}}, n)}{\partial \boldsymbol{\varepsilon}} = \frac{\partial \hat{U_R}(J_i)}{\partial \boldsymbol{\varepsilon}} =$$
$$= 2\beta_1 J_1J_6\frac{\partial J_1}{\partial \boldsymbol{\varepsilon}} + 2\beta_2 J_1J_9\frac{\partial J_1}{\partial \boldsymbol{\varepsilon}} + \beta_3[J_1J_6\frac{\partial J_4}{\partial \boldsymbol{\varepsilon}} + J_4J_6\frac{\partial J_1}{\partial \boldsymbol{\varepsilon}}] + \beta_4[J_1J_9\frac{\partial J_4}{\partial \boldsymbol{\varepsilon}} + J_4J_9\frac{\partial J_1}{\partial \boldsymbol{\varepsilon}}] +$$
$$\beta_5[J_1\frac{\partial J_{11}}{\partial \boldsymbol{\varepsilon}} + J_{11}\frac{\partial J_1}{\partial \boldsymbol{\varepsilon}}] + \beta_6[J_1\frac{\partial J_{15}}{\partial \boldsymbol{\varepsilon}} + J_{15}\frac{\partial J_1}{\partial \boldsymbol{\varepsilon}}] + 2\beta_7 J_4J_6\frac{\partial J_4}{\partial \boldsymbol{\varepsilon}} + 2\beta_8 J_4J_9\frac{\partial J_1}{\partial \boldsymbol{\varepsilon}} +$$
$$\beta_9[J_4\frac{\partial J_{11}}{\partial \boldsymbol{\varepsilon}} + J_{11}\frac{\partial J_4}{\partial \boldsymbol{\varepsilon}}] + \beta_{10}[J_4\frac{\partial J_{15}}{\partial \boldsymbol{\varepsilon}} + J_{15}\frac{\partial J_4}{\partial \boldsymbol{\varepsilon}}] + \beta_{11}J_6\frac{\partial J_2}{\partial \boldsymbol{\varepsilon}} + \beta_{12}J_9\frac{\partial J_2}{\partial \boldsymbol{\varepsilon}} + \beta_{13}J_6\frac{\partial J_5}{\partial \boldsymbol{\varepsilon}} +$$
$$\beta_{14}J_9\frac{\partial J_5}{\partial \boldsymbol{\varepsilon}} + \beta_{15}\frac{\partial J_{12}}{\partial \boldsymbol{\varepsilon}} + \beta_{16}\frac{\partial J_{16}}{\partial \boldsymbol{\varepsilon}} \quad (5.24)$$

The quantities

$$\mathbf{B}_i := \frac{\partial J_i(\boldsymbol{\varepsilon})}{\partial \boldsymbol{\varepsilon}} \quad (5.25)$$

can be calculated through the definition of the derivation of a scalar function of a second order tensor.
In the case under exam, $\boldsymbol{\varepsilon} \epsilon Sym$, and hence $\mathbf{A} \epsilon Sym$. For the sake of brevity,

from now on, we shall use the following notation for the inner product:

$$uv := u \cdot v = u_i v_i. \tag{5.26}$$

Since J_i is a real valued function of the second order tensor $\boldsymbol{\varepsilon}$, the derivative of J_i with respect to $\boldsymbol{\varepsilon}$ is the second order tensor B_i defined as:

$$\mathbf{B}_i \cdot \mathbf{A} = \frac{\partial J_i(\varepsilon)}{\partial \boldsymbol{\varepsilon}} \cdot \mathbf{A} := \lim_{\tau \to 0} \frac{dJ_i(\boldsymbol{\varepsilon} + \tau \mathbf{A})}{d\tau} \tag{5.27}$$

where $\mathbf{B} \cdot \mathbf{A} = \mathbf{B}_{ij}\mathbf{A}_{ij}$.
For example, for $i = 5$ we get:

$$\mathbf{B}_5 \cdot \mathbf{A} = \frac{\partial J_5(\varepsilon)}{\partial \boldsymbol{\varepsilon}} \cdot \mathbf{A} = \lim_{\tau \to 0} \frac{d[J_5(\boldsymbol{\varepsilon} + \tau \mathbf{A})]}{d\tau} = \lim_{\tau \to 0} \frac{d[n(\boldsymbol{\varepsilon} + \tau \mathbf{A})(\boldsymbol{\varepsilon} + \tau \mathbf{A})n]}{d\tau} =$$

$$\lim_{\tau \to 0} \frac{d[n\boldsymbol{\varepsilon}^2 n + \tau n \mathbf{A}\boldsymbol{\varepsilon} n + \tau n \boldsymbol{\varepsilon}\mathbf{A} n + \tau^2 n \mathbf{A}^2 n)}{d\tau} = \lim_{\tau \to 0}[n\mathbf{A}\boldsymbol{\varepsilon} n + n\boldsymbol{\varepsilon}\mathbf{A} n + 2\tau n \mathbf{A}^2 n] =$$

$$nA\boldsymbol{\varepsilon} n + n\boldsymbol{\varepsilon}\mathbf{A} n = (n\boldsymbol{\varepsilon} \otimes n)\mathbf{A} + (n \otimes \boldsymbol{\varepsilon} n)\mathbf{A}$$

$$\Rightarrow \mathbf{B}_5 := \frac{\partial J_5(\varepsilon)}{\partial \boldsymbol{\varepsilon}} = (n\boldsymbol{\varepsilon} \otimes n) + (n \otimes \boldsymbol{\varepsilon} n) = \boldsymbol{\varepsilon}(n \otimes n) + (n \otimes n)\boldsymbol{\varepsilon} \tag{5.28}$$

The derivatives of the invariants (5.21) with respect to the strain tensor $\boldsymbol{\varepsilon}$ turn out to be as follows:

$$\frac{\partial J_1}{\partial \boldsymbol{\varepsilon}} = \frac{\partial [tr(\boldsymbol{\varepsilon})]}{\partial \boldsymbol{\varepsilon}} = \mathbf{I} \tag{5.29a}$$

$$\frac{\partial J_2}{\partial \boldsymbol{\varepsilon}} = \frac{\partial [tr(\boldsymbol{\varepsilon}^2)]}{\partial \boldsymbol{\varepsilon}} 2\boldsymbol{\varepsilon} \tag{5.29b}$$

$$\frac{\partial J_4}{\partial \boldsymbol{\varepsilon}} = \frac{\partial [n\boldsymbol{\varepsilon} n]}{\partial \boldsymbol{\varepsilon}} = n \otimes n \tag{5.29c}$$

$$\frac{\partial J_5}{\partial \boldsymbol{\varepsilon}} = \frac{\partial [n\boldsymbol{\varepsilon}^2 n]}{\partial \boldsymbol{\varepsilon}} = n\boldsymbol{\varepsilon} \otimes n + n \otimes \boldsymbol{\varepsilon} n = \boldsymbol{\varepsilon}(n \otimes n) + (n \otimes n)\boldsymbol{\varepsilon} \tag{5.29d}$$

(since $\boldsymbol{\varepsilon} \in Sym$)

$$\frac{\partial J_{11}}{\partial \boldsymbol{\varepsilon}} = \frac{\partial [tr(\boldsymbol{\varepsilon} \overset{\circ}{\boldsymbol{\sigma}})]}{\partial \boldsymbol{\varepsilon}} = \overset{\circ}{\boldsymbol{\sigma}} \tag{5.29e}$$

$$\frac{\partial J_{12}}{\partial \boldsymbol{\varepsilon}} = \frac{\partial [tr(\boldsymbol{\varepsilon}^2 \overset{\circ}{\boldsymbol{\sigma}})]}{\partial \boldsymbol{\varepsilon}} = \boldsymbol{\varepsilon} \overset{\circ}{\boldsymbol{\sigma}} + \overset{\circ}{\boldsymbol{\sigma}} \boldsymbol{\varepsilon} \tag{5.29f}$$

$$\frac{\partial J_{15}}{\partial \boldsymbol{\varepsilon}} = \frac{\partial [(n\boldsymbol{\varepsilon} \overset{\circ}{\boldsymbol{\sigma}} n + n \overset{\circ}{\boldsymbol{\sigma}} \boldsymbol{\varepsilon} n)]}{\partial \boldsymbol{\varepsilon}} = n \overset{\circ}{\boldsymbol{\sigma}} \otimes n + n \otimes \overset{\circ}{\boldsymbol{\sigma}} n = \overset{\circ}{\boldsymbol{\sigma}} (n \otimes n) + (n \otimes n) \overset{\circ}{\boldsymbol{\sigma}} \tag{5.29g}$$

(since $\overset{\circ}{\boldsymbol{\sigma}} \in Sym$)

$$\frac{\partial J_{16}}{\partial \boldsymbol{\varepsilon}} = \frac{\partial [(n\boldsymbol{\varepsilon}^2 \overset{\circ}{\boldsymbol{\sigma}} n + n \overset{\circ}{\boldsymbol{\sigma}} \boldsymbol{\varepsilon}^2 n + n\boldsymbol{\varepsilon} \overset{\circ}{\boldsymbol{\sigma}} \boldsymbol{\varepsilon} n)]}{\partial \boldsymbol{\varepsilon}}$$

$$= \overset{\circ}{\boldsymbol{\sigma}} \boldsymbol{\varepsilon}(n \otimes n) + \overset{\circ}{\boldsymbol{\sigma}} (n \otimes n)\boldsymbol{\varepsilon} + \boldsymbol{\varepsilon} \overset{\circ}{\boldsymbol{\sigma}} (n \otimes n) + \boldsymbol{\varepsilon}(n \otimes n) \overset{\circ}{\boldsymbol{\sigma}} + (n \otimes n) \overset{\circ}{\boldsymbol{\sigma}} \boldsymbol{\varepsilon} + (n \otimes n)\boldsymbol{\varepsilon} \overset{\circ}{\boldsymbol{\sigma}} \tag{5.29h}$$

By substituting equations (5.29) into the expression of the stress tensor (5.24), we can obtain the following relation:

$$\begin{aligned}
&\boldsymbol{\sigma}_R(\boldsymbol{\varepsilon},\overset{\circ}{\boldsymbol{\sigma}},n)=\frac{\partial\hat{U_R}(J_i)}{\partial\boldsymbol{\varepsilon}}=\\
&=2\beta_1 tr(\boldsymbol{\varepsilon})tr(\overset{\circ}{\boldsymbol{\sigma}})\mathbf{I}+2\beta_2 tr(\boldsymbol{\varepsilon})(n\,\overset{\circ}{\boldsymbol{\sigma}}\,n)\mathbf{I}+\beta_3 tr(\overset{\circ}{\boldsymbol{\sigma}})[tr(\boldsymbol{\varepsilon})(n\otimes n)+(n\boldsymbol{\varepsilon}n)\mathbf{I}]+\\
&\beta_4(n\,\overset{\circ}{\boldsymbol{\sigma}}\,n)[tr(\boldsymbol{\varepsilon})(n\otimes n)+(n\boldsymbol{\varepsilon}n)\mathbf{I}]+\beta_5[tr(\boldsymbol{\varepsilon})\,\overset{\circ}{\boldsymbol{\sigma}}+tr(\boldsymbol{\varepsilon}\,\overset{\circ}{\boldsymbol{\sigma}})\mathbf{I}]+\\
&\beta_6\{tr(\boldsymbol{\varepsilon})[\overset{\circ}{\boldsymbol{\sigma}}\,(n\otimes n)+(n\otimes n)\,\overset{\circ}{\boldsymbol{\sigma}}]+(n\boldsymbol{\varepsilon}\,\overset{\circ}{\boldsymbol{\sigma}}\,n+n\,\overset{\circ}{\boldsymbol{\sigma}}\,\boldsymbol{\varepsilon}n)\mathbf{I}\}+2\beta_7(n\boldsymbol{\varepsilon}n)tr(\overset{\circ}{\boldsymbol{\sigma}}\,(n\otimes n)+\\
&2\beta_8(n\boldsymbol{\varepsilon}n)(n\,\overset{\circ}{\boldsymbol{\sigma}}\,n)(n\otimes n)+\beta_9[(n\boldsymbol{\varepsilon}n)\,\overset{\circ}{\boldsymbol{\sigma}}+tr(\boldsymbol{\varepsilon}\,\overset{\circ}{\boldsymbol{\sigma}})(n\otimes n)]+\beta_{10}\{(n\boldsymbol{\varepsilon}n)[\overset{\circ}{\boldsymbol{\sigma}}\,(n\otimes n)+\\
&(n\otimes n)\,\overset{\circ}{\boldsymbol{\sigma}}]+(n\boldsymbol{\varepsilon}\,\overset{\circ}{\boldsymbol{\sigma}}\,n+n\,\overset{\circ}{\boldsymbol{\sigma}}\,\boldsymbol{\varepsilon}n)(n\otimes n)\}+2\beta_{11}tr(\overset{\circ}{\boldsymbol{\sigma}})\boldsymbol{\varepsilon}+2\beta_{12}(n\,\overset{\circ}{\boldsymbol{\sigma}}\,n)\boldsymbol{\varepsilon}+\\
&\beta_{13}tr(\overset{\circ}{\boldsymbol{\sigma}})[\boldsymbol{\varepsilon}(n\otimes n)+(n\otimes n)\boldsymbol{\varepsilon}]+\beta_{14}(n\,\overset{\circ}{\boldsymbol{\sigma}}\,n)[\boldsymbol{\varepsilon}(n\otimes n)+(n\otimes n)\boldsymbol{\varepsilon}]++\beta_{15}(\boldsymbol{\varepsilon}\,\overset{\circ}{\boldsymbol{\sigma}}+\overset{\circ}{\boldsymbol{\sigma}}\,\boldsymbol{\varepsilon})+\\
&\beta_{16}[\overset{\circ}{\boldsymbol{\sigma}}\,\boldsymbol{\varepsilon}(n\otimes n)+\overset{\circ}{\boldsymbol{\sigma}}\,(n\otimes n)\boldsymbol{\varepsilon}+\boldsymbol{\varepsilon}\,\overset{\circ}{\boldsymbol{\sigma}}\,(n\otimes n)+\boldsymbol{\varepsilon}(n\otimes n)\,\overset{\circ}{\boldsymbol{\sigma}}+(n\otimes n)\,\overset{\circ}{\boldsymbol{\sigma}}\,\boldsymbol{\varepsilon}+(n\otimes n)\boldsymbol{\varepsilon}\,\overset{\circ}{\boldsymbol{\sigma}}]
\end{aligned}\tag{5.30}$$

In order to simplify equation (5.30), we can define two second order tensor:

$$\begin{cases}\boldsymbol{\varepsilon}^*:=\boldsymbol{\varepsilon}(n\otimes n)+(n\otimes n)\boldsymbol{\varepsilon},\\ \overset{\circ}{\boldsymbol{\sigma}}{}^*:=\overset{\circ}{\boldsymbol{\sigma}}\,(n\otimes n)+(n\otimes n)\,\overset{\circ}{\boldsymbol{\sigma}}\,.\end{cases}\tag{5.31}$$

It is simple to show that $\boldsymbol{\varepsilon}^*$ and $\overset{\circ}{\boldsymbol{\sigma}}{}^*$ are symmetric tensors:

$$\begin{aligned}
\boldsymbol{\varepsilon}^{*T}&=[\boldsymbol{\varepsilon}(n\otimes n)+(n\otimes n)\boldsymbol{\varepsilon}]^T=(n\otimes n)^T\boldsymbol{\varepsilon}^T+\boldsymbol{\varepsilon}^T(n\otimes n)^T=(n\otimes n)\boldsymbol{\varepsilon}+\boldsymbol{\varepsilon}(n\otimes n)=\boldsymbol{\varepsilon}^*;\\
\overset{\circ}{\boldsymbol{\sigma}}{}^{*T}&=[\overset{\circ}{\boldsymbol{\sigma}}\,(n\otimes n)+(n\otimes n)\,\overset{\circ}{\boldsymbol{\sigma}}]^T=(n\otimes n)^T\,\overset{\circ}{\boldsymbol{\sigma}}{}^T+\overset{\circ}{\boldsymbol{\sigma}}{}^T\,(n\otimes n)^T=\\
&(n\otimes n)\,\overset{\circ}{\boldsymbol{\sigma}}+\overset{\circ}{\boldsymbol{\sigma}}\,(n\otimes n)=\overset{\circ}{\boldsymbol{\sigma}}{}^*\,.
\end{aligned}\tag{5.32}$$

Equation (5.30) can be rewritten as:

$$\begin{aligned}
&\boldsymbol{\sigma}_R(\boldsymbol{\varepsilon},\overset{\circ}{\boldsymbol{\sigma}},n)=\frac{\partial\hat{U_R}(J_i)}{\partial\boldsymbol{\varepsilon}}=\\
&=2\beta_1 tr(\boldsymbol{\varepsilon})tr(\overset{\circ}{\boldsymbol{\sigma}})\mathbf{I}+2\beta_2 tr(\boldsymbol{\varepsilon})(n\,\overset{\circ}{\boldsymbol{\sigma}}\,n)\mathbf{I}+\beta_3 tr(\overset{\circ}{\boldsymbol{\sigma}})[tr(\boldsymbol{\varepsilon})n\otimes n+(n\boldsymbol{\varepsilon}n)\mathbf{I}]+\\
&\beta_4(n\,\overset{\circ}{\boldsymbol{\sigma}}\,n)[tr(\boldsymbol{\varepsilon})n\otimes n+(n\boldsymbol{\varepsilon}n)\mathbf{I}]+\beta_5[tr(\boldsymbol{\varepsilon})\,\overset{\circ}{\boldsymbol{\sigma}}+tr(\boldsymbol{\varepsilon}\,\overset{\circ}{\boldsymbol{\sigma}})\mathbf{I}]+\\
&\beta_6\{tr(\boldsymbol{\varepsilon})\,\overset{\circ}{\boldsymbol{\sigma}}{}^*+(n\boldsymbol{\varepsilon}\,\overset{\circ}{\boldsymbol{\sigma}}\,n+n\,\overset{\circ}{\boldsymbol{\sigma}}\,\boldsymbol{\varepsilon}n)\mathbf{I}\}+2\beta_7(n\boldsymbol{\varepsilon}n)tr(\overset{\circ}{\boldsymbol{\sigma}}\,(n\otimes n)+\\
&2\beta_8(n\boldsymbol{\varepsilon}n)(n\,\overset{\circ}{\boldsymbol{\sigma}}\,n)(n\otimes n)+\beta_9[(n\boldsymbol{\varepsilon}n)\,\overset{\circ}{\boldsymbol{\sigma}}+tr(\boldsymbol{\varepsilon}\,\overset{\circ}{\boldsymbol{\sigma}})(n\otimes n)]+\\
&\beta_{10}[(n\boldsymbol{\varepsilon}n)\,\overset{\circ}{\boldsymbol{\sigma}}{}^*+(n\boldsymbol{\varepsilon}\,\overset{\circ}{\boldsymbol{\sigma}}\,n+n\,\overset{\circ}{\boldsymbol{\sigma}}\,\boldsymbol{\varepsilon}n)(n\otimes n)+2\beta_{11}tr(\overset{\circ}{\boldsymbol{\sigma}})\boldsymbol{\varepsilon}+\\
&2\beta_{12}(n\,\overset{\circ}{\boldsymbol{\sigma}}\,n)\boldsymbol{\varepsilon}+\beta_{13}tr(\overset{\circ}{\boldsymbol{\sigma}})\boldsymbol{\varepsilon}^*+\beta_{14}(n\,\overset{\circ}{\boldsymbol{\sigma}}\,n)\boldsymbol{\varepsilon}^*+\\
&+\beta_{15}(\boldsymbol{\varepsilon}\,\overset{\circ}{\boldsymbol{\sigma}}+\overset{\circ}{\boldsymbol{\sigma}}\,\boldsymbol{\varepsilon})+\beta_{16}[\overset{\circ}{\boldsymbol{\sigma}}\,\boldsymbol{\varepsilon}^*+\boldsymbol{\varepsilon}\,\overset{\circ}{\boldsymbol{\sigma}}{}^*+(n\otimes n)(\overset{\circ}{\boldsymbol{\sigma}}\,\boldsymbol{\varepsilon}+\boldsymbol{\varepsilon}\,\overset{\circ}{\boldsymbol{\sigma}})]
\end{aligned}\tag{5.33}$$

It is important to note that:

- the tensor $[\boldsymbol{\varepsilon}\ \mathring{\boldsymbol{\sigma}} + \mathring{\boldsymbol{\sigma}}\ \boldsymbol{\varepsilon}]$ is symmetric because

$$[\mathring{\boldsymbol{\sigma}}\ \boldsymbol{\varepsilon}]^T = \boldsymbol{\varepsilon}^T\ \mathring{\boldsymbol{\sigma}}^T = \boldsymbol{\varepsilon}\ \mathring{\boldsymbol{\sigma}} \tag{5.34}$$

- the tensor $[\mathring{\boldsymbol{\sigma}}\ \boldsymbol{\varepsilon}(n\otimes n)+\ \mathring{\boldsymbol{\sigma}}\ (n\otimes n)\boldsymbol{\varepsilon}+\boldsymbol{\varepsilon}\ \mathring{\boldsymbol{\sigma}}\ (n\otimes n)+\boldsymbol{\varepsilon}(n\otimes n)\ \mathring{\boldsymbol{\sigma}}\ +(n\otimes n)\ \mathring{\boldsymbol{\sigma}}\ \boldsymbol{\varepsilon} + (n\otimes n)\ \mathring{\boldsymbol{\sigma}}\ \boldsymbol{\varepsilon}]$ is symmetric because:

$$\begin{aligned} &- \quad \mathring{\boldsymbol{\sigma}}\ \boldsymbol{\varepsilon}(n\otimes n) = [(n\otimes n)\boldsymbol{\varepsilon}\ \mathring{\boldsymbol{\sigma}}]^T, \\ &- \quad \mathring{\boldsymbol{\sigma}}\ (n\otimes n)\boldsymbol{\varepsilon} = [\boldsymbol{\varepsilon}(n\otimes n)\ \mathring{\boldsymbol{\sigma}}]^T, \\ &- \quad \boldsymbol{\varepsilon}\ \mathring{\boldsymbol{\sigma}}\ (n\otimes n) = [(n\otimes n)\ \mathring{\boldsymbol{\sigma}}\ \boldsymbol{\varepsilon}]^T. \end{aligned} \tag{5.35}$$

Hence, it is possible to verify that, since the strain tensor and the residual stress are symmetric, the stress tensor turns out to be symmetric as expected. In other words, $\boldsymbol{\sigma}$ can be written as linear combination of symmetric tensors:

$$\begin{aligned} &\boldsymbol{\sigma}_R(\boldsymbol{\varepsilon}, \mathring{\boldsymbol{\sigma}}, n) = \frac{\partial \hat{U_R}(J_i)}{\partial \boldsymbol{\varepsilon}} = \\ &= \{2\beta_1 tr(\boldsymbol{\varepsilon})tr(\mathring{\boldsymbol{\sigma}})+2\beta_2 tr(\boldsymbol{\varepsilon})(n\ \mathring{\boldsymbol{\sigma}}\ n)+\beta_3 tr(\mathring{\boldsymbol{\sigma}})(n\varepsilon n)+\beta_4(n\ \mathring{\boldsymbol{\sigma}}\ n)(n\varepsilon n)+\beta_5 tr(\boldsymbol{\varepsilon}\ \mathring{\boldsymbol{\sigma}})+ \\ &\beta_6(n\boldsymbol{\varepsilon}\ \mathring{\boldsymbol{\sigma}}\ n + n\ \mathring{\boldsymbol{\sigma}}\ \varepsilon n)\}\mathbf{I} + \{\beta_3 tr(\mathring{\boldsymbol{\sigma}})tr(\boldsymbol{\varepsilon}) + \beta_4(n\ \mathring{\boldsymbol{\sigma}}\ n)tr(\boldsymbol{\varepsilon}) + 2\beta_7(n\varepsilon n)tr(\mathring{\boldsymbol{\sigma}})+ \\ &2\beta_8(n\varepsilon n)(n\ \mathring{\boldsymbol{\sigma}}\ n) + \beta_9 tr(\boldsymbol{\varepsilon}\ \mathring{\boldsymbol{\sigma}}) + \beta_{10}(n\boldsymbol{\varepsilon}\ \mathring{\boldsymbol{\sigma}}\ n + n\ \mathring{\boldsymbol{\sigma}}\ \varepsilon n)\}(n\otimes n)+ \\ &\{\beta_5 tr(\boldsymbol{\varepsilon}) + \beta_9(n\varepsilon n)\}\ \mathring{\boldsymbol{\sigma}}\ +\{2\beta_{11}tr(\mathring{\boldsymbol{\sigma}}) + 2\beta_{12}(n\ \mathring{\boldsymbol{\sigma}}\ n)\}\boldsymbol{\varepsilon}+ \\ &\{\beta_6 tr(\boldsymbol{\varepsilon}) + \beta_{10}(n\varepsilon n)\}\ \mathring{\boldsymbol{\sigma}}^*\ +\{\beta_{13}tr(\mathring{\boldsymbol{\sigma}}) + \beta_{14}(n\ \mathring{\boldsymbol{\sigma}}\ n)\}\boldsymbol{\varepsilon}^* + +\beta_{15}(\boldsymbol{\varepsilon}\ \mathring{\boldsymbol{\sigma}} + \mathring{\boldsymbol{\sigma}}\ \boldsymbol{\varepsilon})+ \\ &\beta_{16}[\mathring{\boldsymbol{\sigma}}\ \boldsymbol{\varepsilon}(n\otimes n)+\ \mathring{\boldsymbol{\sigma}}\ (n\otimes n)\boldsymbol{\varepsilon}+\boldsymbol{\varepsilon}\ \mathring{\boldsymbol{\sigma}}\ (n\otimes n)+\boldsymbol{\varepsilon}(n\otimes n)\ \mathring{\boldsymbol{\sigma}}\ +(n\otimes n)\ \mathring{\boldsymbol{\sigma}}\ \boldsymbol{\varepsilon}+(n\otimes n)\boldsymbol{\varepsilon}\ \mathring{\boldsymbol{\sigma}}] \end{aligned} \tag{5.36}$$

Equation (5.36) give the stress-strain relation for linear elastic transversely isotropic material with residual stress. The complete constitutive equation for such a material can be simply obtained by substituting equations (5.36), (5.5) into equation (5.6) and, finally, in equation (5.1) for small strains, i.e.

$$\begin{aligned} &\boldsymbol{\sigma} - (\mathbf{W}\mathring{\boldsymbol{\sigma}} + \mathring{\boldsymbol{\sigma}}\mathbf{W}^{\mathbf{T}} = \mathring{\boldsymbol{\sigma}} + \boldsymbol{\varepsilon}\ \mathring{\boldsymbol{\sigma}} + \mathring{\boldsymbol{\sigma}}\ \boldsymbol{\varepsilon}^T - (tr\boldsymbol{\varepsilon})\ \mathring{\boldsymbol{\sigma}} + \mathfrak{L}[\mathring{\boldsymbol{\sigma}}, \boldsymbol{\varepsilon}] = \\ &\mathring{\boldsymbol{\sigma}} + \boldsymbol{\varepsilon}\ \mathring{\boldsymbol{\sigma}} + \mathring{\boldsymbol{\sigma}}\ \boldsymbol{\varepsilon}^T - (tr\boldsymbol{\varepsilon})\ \mathring{\boldsymbol{\sigma}} + \mathbb{C}[\boldsymbol{\varepsilon}] + \mathfrak{D}[\mathring{\boldsymbol{\sigma}}, \boldsymbol{\varepsilon}] = \mathring{\boldsymbol{\sigma}} + \boldsymbol{\varepsilon}\ \mathring{\boldsymbol{\sigma}} + \mathring{\boldsymbol{\sigma}}\ \boldsymbol{\varepsilon}^T - (tr\boldsymbol{\varepsilon})\ \mathring{\boldsymbol{\sigma}} + \\ &\lambda(tr\boldsymbol{\varepsilon})\mathbf{I}+2\mu\boldsymbol{\varepsilon}+\alpha_1(n\varepsilon n)n\otimes n+\alpha_2[\mathbf{I}(n\varepsilon n)+tr(\boldsymbol{\varepsilon})n\otimes n]+2\alpha_3[n\cdot\boldsymbol{\varepsilon}\otimes n+n\otimes\boldsymbol{\varepsilon}\cdot n]+ \\ &+ \{2\beta_1 tr(\boldsymbol{\varepsilon})tr(\mathring{\boldsymbol{\sigma}}) + 2\beta_2 tr(\boldsymbol{\varepsilon})(n\ \mathring{\boldsymbol{\sigma}}\ n) + \beta_3 tr(\mathring{\boldsymbol{\sigma}})(n\varepsilon n) + \beta_4(n\ \mathring{\boldsymbol{\sigma}}\ n)(n\varepsilon n)+ \\ &\beta_5 tr(\boldsymbol{\varepsilon}\ \mathring{\boldsymbol{\sigma}}) + \beta_6(n\boldsymbol{\varepsilon}\ \mathring{\boldsymbol{\sigma}}\ n + n\ \mathring{\boldsymbol{\sigma}}\ \varepsilon n)\}\mathbf{I} + \{\beta_3 tr(\mathring{\boldsymbol{\sigma}})tr(\boldsymbol{\varepsilon}) + \beta_4(n\ \mathring{\boldsymbol{\sigma}}\ n)tr(\boldsymbol{\varepsilon})+ \\ &2\beta_7(n\varepsilon n)tr(\mathring{\boldsymbol{\sigma}})+2\beta_8(n\varepsilon n)(n\ \mathring{\boldsymbol{\sigma}}\ n)+\beta_9 tr(\boldsymbol{\varepsilon}\ \mathring{\boldsymbol{\sigma}})+\beta_{10}(n\boldsymbol{\varepsilon}\ \mathring{\boldsymbol{\sigma}}\ n+n\ \mathring{\boldsymbol{\sigma}}\ \varepsilon n)\}(n\otimes n)+ \\ &\{\beta_5 tr(\boldsymbol{\varepsilon})+\beta_9(n\varepsilon n)\}\ \mathring{\boldsymbol{\sigma}}\ +\{2\beta_{11}tr(\mathring{\boldsymbol{\sigma}})+2\beta_{12}(n\ \mathring{\boldsymbol{\sigma}}\ n)\}\boldsymbol{\varepsilon}+\{\beta_6 tr(\boldsymbol{\varepsilon})+\beta_{10}(n\varepsilon n)\}\ \mathring{\boldsymbol{\sigma}}^*\ + \\ &\{\beta_{13}tr(\mathring{\boldsymbol{\sigma}}) + \beta_{14}(n\ \mathring{\boldsymbol{\sigma}}\ n)\}\boldsymbol{\varepsilon}^* + +\beta_{15}(\boldsymbol{\varepsilon}\ \mathring{\boldsymbol{\sigma}} + \mathring{\boldsymbol{\sigma}}\ \boldsymbol{\varepsilon})+ \\ &\beta_{16}[\mathring{\boldsymbol{\sigma}}\ \boldsymbol{\varepsilon}(n\otimes n)+\ \mathring{\boldsymbol{\sigma}}\ (n\otimes n)\boldsymbol{\varepsilon}+\boldsymbol{\varepsilon}\ \mathring{\boldsymbol{\sigma}}\ (n\otimes n)+\boldsymbol{\varepsilon}(n\otimes n)\ \mathring{\boldsymbol{\sigma}}\ +(n\otimes n)\ \mathring{\boldsymbol{\sigma}}\ \boldsymbol{\varepsilon}+(n\otimes n)\boldsymbol{\varepsilon}\ \mathring{\boldsymbol{\sigma}}] \end{aligned} \tag{5.37}$$

5.5 Derivation of the incremental elasticity tensor

The elasticity tensor $\mathfrak{L}(\boldsymbol{\varepsilon}, \overset{\circ}{\boldsymbol{\sigma}})$ can be written as follows:

$$\mathfrak{L}[\boldsymbol{\varepsilon}, \overset{\circ}{\boldsymbol{\sigma}}] = \mathbb{C}[\boldsymbol{\varepsilon}] + \mathfrak{D}[\boldsymbol{\varepsilon}, \overset{\circ}{\boldsymbol{\sigma}}], \tag{5.38}$$

where the sixth order tensor $\mathfrak{D}$, depending on $\boldsymbol{\varepsilon}$, $\overset{\circ}{\boldsymbol{\sigma}}$ and n is the second derivative of the part of the stress tensor due to the residual stress $\boldsymbol{\sigma}_R$ with respect to the strain tensor and the residual stress tensor:

$$\mathfrak{D}(\boldsymbol{\varepsilon}, \overset{\circ}{\boldsymbol{\sigma}}, n) = \frac{\partial^2 \boldsymbol{\sigma}_R(\boldsymbol{\varepsilon}, \overset{\circ}{\boldsymbol{\sigma}}, n)}{\partial \boldsymbol{\varepsilon} \partial \overset{\circ}{\boldsymbol{\sigma}}} = \frac{\partial^3 U_R(\boldsymbol{\varepsilon}, \overset{\circ}{\boldsymbol{\sigma}}, n)}{\partial \boldsymbol{\varepsilon}^2 \partial \overset{\circ}{\boldsymbol{\sigma}}}. \tag{5.39}$$

First of all, it is necessary to calculate the second derivative of the strain energy function U with respect to $\boldsymbol{\varepsilon}$:

$$\frac{\partial^2 U_R(\boldsymbol{\varepsilon}, \overset{\circ}{\boldsymbol{\sigma}}, n)}{\partial \boldsymbol{\varepsilon}^2} = \frac{\partial \boldsymbol{\sigma}_R(\boldsymbol{\varepsilon}, \overset{\circ}{\boldsymbol{\sigma}}, n)}{\partial \boldsymbol{\varepsilon}} \tag{5.40}$$

The derivatives of the different terms of $\boldsymbol{\sigma}_R(\boldsymbol{\varepsilon}, \overset{\circ}{\boldsymbol{\sigma}}, n)$ can be calculated according to the definition of derivative of a tensor function with respect to a second-order tensor.
Since $\mathbf{B}$ is a second-order tensor valued function of $\boldsymbol{\varepsilon}$, the derivative of $\mathbf{B}$ with respect to $\boldsymbol{\varepsilon}$ is the forth-order tensor $\mathbb{D}$ defined as follows:

$$\mathbb{D} : \mathbf{A} = \frac{\partial \mathbf{B}(\boldsymbol{\varepsilon})}{\partial \boldsymbol{\varepsilon}} : \mathbf{A} := \lim_{\tau \to 0} \frac{d\mathbf{B}(\boldsymbol{\varepsilon} + \tau \mathbf{A})}{d\tau} \tag{5.41}$$

where $[\mathbb{D} : \mathbf{A}]_{ij} = \mathbb{D}_{ijkl}\mathbf{A}_{kl}, \quad \mathbf{A} \ \epsilon \ Sym.$
For example,

$$\begin{gathered}
\mathbb{D}_3 : \mathbf{A} = \frac{\partial J_1(\boldsymbol{\varepsilon}) J_6(\boldsymbol{\varepsilon}) \frac{\partial J_4(\boldsymbol{\varepsilon})}{\partial \boldsymbol{\varepsilon}}}{\partial \boldsymbol{\varepsilon}} : \mathbf{A} = \lim_{\tau \to 0} \frac{d}{d\tau} [J_1(\boldsymbol{\varepsilon}+\tau\mathbf{A}) J_6(\boldsymbol{\varepsilon}+\tau\mathbf{A}) \frac{\partial J_4}{\partial \boldsymbol{\varepsilon}}(\boldsymbol{\varepsilon}+\tau\mathbf{A})] = \\
= \lim_{\tau \to 0} \frac{d}{d\tau} [tr(\boldsymbol{\varepsilon} + \tau\mathbf{A}) tr(\overset{\circ}{\boldsymbol{\sigma}})(n \otimes n)] = tr(\overset{\circ}{\boldsymbol{\sigma}}) \lim_{\tau \to 0} \frac{d}{d\tau} [((\boldsymbol{\varepsilon} + \tau\mathbf{A}) \bullet \mathbf{I})(n \otimes n)] = \\
= tr(\overset{\circ}{\boldsymbol{\sigma}}) \lim_{\tau \to 0} [(\mathbf{A} \cdot \mathbf{I})(n \otimes n)] = tr(\overset{\circ}{\boldsymbol{\sigma}}) [(\mathbf{A} \bullet \mathbf{I})(n \otimes n)] = tr(\overset{\circ}{\boldsymbol{\sigma}}) [(n \otimes n) \otimes \mathbf{I})] \mathbf{A} = \mathbb{D}_3 : \mathbf{A} \\
\Rightarrow \mathbb{D}_3 = tr(\overset{\circ}{\boldsymbol{\sigma}}) [(n \otimes n) \otimes \mathbf{I}]
\end{gathered} \tag{5.42}$$

$$\begin{gathered}
\mathbb{D}_4 : \mathbf{A} = \frac{\partial J_4(\boldsymbol{\varepsilon}) J_6(\boldsymbol{\varepsilon}) \frac{\partial J_1(\boldsymbol{\varepsilon})}{\partial \boldsymbol{\varepsilon}}}{\partial \boldsymbol{\varepsilon}} : \mathbf{A} = \lim_{\tau \to 0} \frac{d}{d\tau} [J_4(\boldsymbol{\varepsilon}+\tau\mathbf{A}) J_6(\boldsymbol{\varepsilon}+\tau\mathbf{A}) \frac{\partial J_1}{\partial \boldsymbol{\varepsilon}}(\boldsymbol{\varepsilon}+\tau\mathbf{A})] = \\
\lim_{\tau \to 0} \frac{d}{d\tau} [(n(\boldsymbol{\varepsilon} + \tau\mathbf{A})n) tr(\overset{\circ}{\boldsymbol{\sigma}}) \mathbf{I}] = tr(\overset{\circ}{\boldsymbol{\sigma}}) \lim_{\tau \to 0} \frac{d}{d\tau} [(n(\boldsymbol{\varepsilon} + \tau\mathbf{A})n) \mathbf{I}] = \\
tr(\overset{\circ}{\boldsymbol{\sigma}}) \lim_{\tau \to 0} [(n\mathbf{A}n) \mathbf{I}] = tr(\overset{\circ}{\boldsymbol{\sigma}}) [(n\mathbf{A}n) \mathbf{I}] = \mathbb{D}_4 : \mathbf{A}
\end{gathered} \tag{5.43}$$

where

$$\begin{cases} [\mathbf{D}_4 : \mathbf{A}]_{hk} = \mathbf{D}_{4hkst}\mathbf{A}_{st}. \\ tr(\overset{\circ}{\boldsymbol{\sigma}})[(n\mathbf{A}n)\mathbf{I}]_{hk} = tr(\overset{\circ}{\boldsymbol{\sigma}})n_i\mathbf{A}_{ij}n_j\delta hk \end{cases} \tag{5.44}$$

Hence,

$$\mathbb{D}_{4hkst}\mathbf{A}_{st} = tr(\overset{\circ}{\boldsymbol{\sigma}})n_i\mathbf{A}_{ij}n_j\delta_{hk}\delta si\delta_{tj} = tr(\overset{\circ}{\boldsymbol{\sigma}})n_sn_t\delta_{hk}\mathbf{A}_{st}$$
$$\Rightarrow \mathbb{D}_4 = tr(\overset{\circ}{\boldsymbol{\sigma}})[\mathbf{I}\otimes(n\otimes n)] \tag{5.45}$$

The derivatives of all the terms appearing in (5.24) may be summarized as follows:

$$\frac{\partial}{\partial\boldsymbol{\varepsilon}}[J_1J_6\frac{\partial J_1}{\partial\boldsymbol{\varepsilon}}] = \frac{\partial}{\partial\boldsymbol{\varepsilon}}[tr(\boldsymbol{\varepsilon})tr(\overset{\circ}{\boldsymbol{\sigma}})\mathbf{I}] = tr(\overset{\circ}{\boldsymbol{\sigma}})\frac{\partial}{\partial\boldsymbol{\varepsilon}}[(\boldsymbol{\varepsilon}\cdot\mathbf{I})\mathbf{I}] = tr(\overset{\circ}{\boldsymbol{\sigma}})\mathbf{I}\otimes\mathbf{I} \tag{5.46a}$$

$$\frac{\partial}{\partial\boldsymbol{\varepsilon}}[J_1J_9\frac{\partial J_1}{\partial\boldsymbol{\varepsilon}}] = \frac{\partial}{\partial\boldsymbol{\varepsilon}}[tr(\boldsymbol{\varepsilon})(n\ \overset{\circ}{\boldsymbol{\sigma}}\ n)\mathbf{I}] = (n\ \overset{\circ}{\boldsymbol{\sigma}}\ n)\frac{\partial}{\partial\boldsymbol{\varepsilon}}[(\boldsymbol{\varepsilon}\cdot\mathbf{I})\mathbf{I}] = (n\ \overset{\circ}{\boldsymbol{\sigma}}\ n)\mathbf{I}\otimes\mathbf{I} \tag{5.46b}$$

$$\frac{\partial}{\partial\boldsymbol{\varepsilon}}[J_1J_6\frac{\partial J_4}{\partial\boldsymbol{\varepsilon}}] = \frac{\partial}{\partial\boldsymbol{\varepsilon}}[tr(\boldsymbol{\varepsilon})tr(\overset{\circ}{\boldsymbol{\sigma}})(n\otimes n)] = tr(\overset{\circ}{\boldsymbol{\sigma}})\frac{\partial}{\partial\boldsymbol{\varepsilon}}[(\boldsymbol{\varepsilon}\cdot\mathbf{I})(n\otimes n)] = tr(\overset{\circ}{\boldsymbol{\sigma}})(n\otimes n)\otimes\mathbf{I} \tag{5.46c}$$

$$\frac{\partial}{\partial\boldsymbol{\varepsilon}}[J_4J_6\frac{\partial J_1}{\partial\boldsymbol{\varepsilon}}] = \frac{\partial}{\partial\boldsymbol{\varepsilon}}[(n\boldsymbol{\varepsilon}n)tr(\overset{\circ}{\boldsymbol{\sigma}})\mathbf{I}] = tr(\overset{\circ}{\boldsymbol{\sigma}})\frac{\partial}{\partial\boldsymbol{\varepsilon}}[(n\boldsymbol{\varepsilon}n)\mathbf{I}] = tr(\overset{\circ}{\boldsymbol{\sigma}})\mathbf{I}\otimes(n\otimes n) \tag{5.46d}$$

$$\frac{\partial}{\partial\boldsymbol{\varepsilon}}[J_1J_9\frac{\partial J_4}{\partial\boldsymbol{\varepsilon}}] = \frac{\partial}{\partial\boldsymbol{\varepsilon}}[tr(\boldsymbol{\varepsilon})(n\ \overset{\circ}{\boldsymbol{\sigma}}\ n)(n\otimes n)] = (n\ \overset{\circ}{\boldsymbol{\sigma}}\ n)\frac{\partial}{\partial\boldsymbol{\varepsilon}}[(\boldsymbol{\varepsilon}\cdot\mathbf{I})(n\otimes n)] =$$
$$(n\ \overset{\circ}{\boldsymbol{\sigma}}\ n)(n\otimes n)\otimes\mathbf{I} \tag{5.46e}$$

$$\frac{\partial}{\partial\boldsymbol{\varepsilon}}[J_4J_9\frac{\partial J_1}{\partial\boldsymbol{\varepsilon}}] = \frac{\partial}{\partial\boldsymbol{\varepsilon}}[(n\boldsymbol{\varepsilon}n)(n\ \overset{\circ}{\boldsymbol{\sigma}}\ n)\mathbf{I}] = (n\ \overset{\circ}{\boldsymbol{\sigma}}\ n)\frac{\partial}{\partial\boldsymbol{\varepsilon}}[(n\boldsymbol{\varepsilon}n)\mathbf{I}] = (n\ \overset{\circ}{\boldsymbol{\sigma}}\ n)\mathbf{I}\otimes(n\otimes n) \tag{5.46f}$$

$$\frac{\partial}{\partial\boldsymbol{\varepsilon}}[J_1\frac{\partial J_{11}}{\partial\boldsymbol{\varepsilon}}] = \frac{\partial}{\partial\boldsymbol{\varepsilon}}[tr(\boldsymbol{\varepsilon})\ \overset{\circ}{\boldsymbol{\sigma}}] = \frac{\partial}{\partial\boldsymbol{\varepsilon}}[(\boldsymbol{\varepsilon}\cdot\mathbf{I})\ \overset{\circ}{\boldsymbol{\sigma}}] = \overset{\circ}{\boldsymbol{\sigma}}\otimes\mathbf{I} \tag{5.46g}$$

$$\frac{\partial}{\partial\boldsymbol{\varepsilon}}[J_{11}\frac{\partial J_1}{\partial\boldsymbol{\varepsilon}}] = \frac{\partial}{\partial\boldsymbol{\varepsilon}}[tr(\boldsymbol{\varepsilon}\ \overset{\circ}{\boldsymbol{\sigma}})\mathbf{I}] = \frac{\partial}{\partial\boldsymbol{\varepsilon}}[(\boldsymbol{\varepsilon}\cdot\ \overset{\circ}{\boldsymbol{\sigma}})\mathbf{I}] = \mathbf{I}\otimes\ \overset{\circ}{\boldsymbol{\sigma}} \tag{5.46h}$$

$$\frac{\partial}{\partial\boldsymbol{\varepsilon}}[J_1\frac{\partial J_{15}}{\partial\boldsymbol{\varepsilon}}] = \frac{\partial}{\partial\boldsymbol{\varepsilon}}[tr(\boldsymbol{\varepsilon})\ \overset{\circ}{\boldsymbol{\sigma}}^*] = \frac{\partial}{\partial\boldsymbol{\varepsilon}}[(\boldsymbol{\varepsilon}\cdot\mathbf{I})\ \overset{\circ}{\boldsymbol{\sigma}}^*] = \overset{\circ}{\boldsymbol{\sigma}}^*\otimes\mathbf{I} \tag{5.46i}$$

$$\frac{\partial}{\partial\boldsymbol{\varepsilon}}[J_{15}\frac{\partial J_1}{\partial\boldsymbol{\varepsilon}}] = \frac{\partial}{\partial\boldsymbol{\varepsilon}}[tr(\boldsymbol{\varepsilon})(n\boldsymbol{\varepsilon}\ \overset{\circ}{\boldsymbol{\sigma}}\ n+n\ \overset{\circ}{\boldsymbol{\sigma}}\ \boldsymbol{\varepsilon}n)\mathbf{I}] = \frac{\partial}{\partial\boldsymbol{\varepsilon}}[(\boldsymbol{\varepsilon}\cdot\mathbf{I})(n\boldsymbol{\varepsilon}\ \overset{\circ}{\boldsymbol{\sigma}}\ n+n\ \overset{\circ}{\boldsymbol{\sigma}}\ \boldsymbol{\varepsilon}n)\mathbf{I}] =$$
$$\mathbf{I}\otimes n\otimes n\ \overset{\circ}{\boldsymbol{\sigma}}+\mathbf{I}\otimes\ \overset{\circ}{\boldsymbol{\sigma}}\ n\otimes n = \mathbf{I}\otimes[(n\otimes n)\ \overset{\circ}{\boldsymbol{\sigma}}+\ \overset{\circ}{\boldsymbol{\sigma}}\ (n\otimes n)] = \mathbf{I}\otimes\ \overset{\circ}{\boldsymbol{\sigma}}^* \tag{5.46j}$$

$$\frac{\partial}{\partial\boldsymbol{\varepsilon}}[J_4J_6\frac{\partial J_4}{\partial\boldsymbol{\varepsilon}}] = \frac{\partial}{\partial\boldsymbol{\varepsilon}}[(n\boldsymbol{\varepsilon}n)tr(\overset{\circ}{\boldsymbol{\sigma}})(n\otimes n)] = tr(\overset{\circ}{\boldsymbol{\sigma}})\frac{\partial}{\partial\boldsymbol{\varepsilon}}[(n\boldsymbol{\varepsilon}n)(n\otimes n)] =$$
$$tr(\overset{\circ}{\boldsymbol{\sigma}})(n\otimes n)\otimes(n\otimes n) \tag{5.46k}$$

$$\frac{\partial}{\partial \boldsymbol{\varepsilon}}[J_4 J_9 \frac{\partial J_4}{\partial \boldsymbol{\varepsilon}}] = \frac{\partial}{\partial \boldsymbol{\varepsilon}}[(n\boldsymbol{\varepsilon}n)(n\ \mathring{\boldsymbol{\sigma}}\ n)(n\otimes n)] = (n\ \mathring{\boldsymbol{\sigma}}\ n)\frac{\partial}{\partial \boldsymbol{\varepsilon}}[(n\boldsymbol{\varepsilon}n)(n\otimes n)] = (n\ \mathring{\boldsymbol{\sigma}}\ n)(n\otimes n)\otimes(n\otimes n) \quad (5.46l)$$

$$\frac{\partial}{\partial \boldsymbol{\varepsilon}}[J_4 \frac{\partial J_{11}}{\partial \boldsymbol{\varepsilon}}] = \frac{\partial}{\partial \boldsymbol{\varepsilon}}[(n\boldsymbol{\varepsilon}n)\ \mathring{\boldsymbol{\sigma}}] = \mathring{\boldsymbol{\sigma}}\otimes(n\otimes n) \quad (5.46m)$$

$$\frac{\partial}{\partial \boldsymbol{\varepsilon}}[J_{11}\frac{\partial J_4}{\partial \boldsymbol{\varepsilon}}] = \frac{\partial}{\partial \boldsymbol{\varepsilon}}[tr(\boldsymbol{\varepsilon}\ \mathring{\boldsymbol{\sigma}})(n\otimes n)] = \frac{\partial}{\partial \boldsymbol{\varepsilon}}[(\boldsymbol{\varepsilon}\cdot\ \mathring{\boldsymbol{\sigma}})(n\otimes n)] = (n\otimes n)\otimes\mathring{\boldsymbol{\sigma}} \quad (5.46n)$$

$$\frac{\partial}{\partial \boldsymbol{\varepsilon}}[J_4 \frac{\partial J_{15}}{\partial \boldsymbol{\varepsilon}}] = \frac{\partial}{\partial \boldsymbol{\varepsilon}}[(n\boldsymbol{\varepsilon}n)\ \mathring{\boldsymbol{\sigma}}^*] = \mathring{\boldsymbol{\sigma}}^*\otimes(n\otimes n) \quad (5.46o)$$

$$\frac{\partial}{\partial \boldsymbol{\varepsilon}}[J_{15}\frac{\partial J_4}{\partial \boldsymbol{\varepsilon}}] = \frac{\partial}{\partial \boldsymbol{\varepsilon}}[tr(\boldsymbol{\varepsilon})(n\boldsymbol{\varepsilon}\ \mathring{\boldsymbol{\sigma}}\ n + n\ \mathring{\boldsymbol{\sigma}}\ \boldsymbol{\varepsilon}n)(n\otimes n)] = (n\otimes n)\otimes n\otimes n\ \mathring{\boldsymbol{\sigma}} + (n\otimes n)\otimes\mathring{\boldsymbol{\sigma}}\ n\otimes n = (n\otimes n)\otimes[(n\otimes n)\ \mathring{\boldsymbol{\sigma}} + \mathring{\boldsymbol{\sigma}}\ (n\otimes n)] = (n\otimes n)\otimes\mathring{\boldsymbol{\sigma}}^* \quad (5.46p)$$

$$\frac{\partial}{\partial \boldsymbol{\varepsilon}}[J_6\frac{\partial J_2}{\partial \boldsymbol{\varepsilon}}] = \frac{\partial}{\partial \boldsymbol{\varepsilon}}[tr(\mathring{\boldsymbol{\sigma}})\boldsymbol{\varepsilon}] = tr(\mathring{\boldsymbol{\sigma}})\frac{\partial \boldsymbol{\varepsilon}}{\partial \boldsymbol{\varepsilon}} = tr(\mathring{\boldsymbol{\sigma}})\mathbb{I} \quad (5.46q)$$

where $\mathbb{I}$ is the fourth-order identity tensor, defined by $\mathbb{I}_{ijhk} = \delta_{ijhk}$.

$$\frac{\partial}{\partial \boldsymbol{\varepsilon}}[J_9\frac{\partial J_2}{\partial \boldsymbol{\varepsilon}}] = \frac{\partial}{\partial \boldsymbol{\varepsilon}}[(n\ \mathring{\boldsymbol{\sigma}}\ n)\boldsymbol{\varepsilon}] = (n\ \mathring{\boldsymbol{\sigma}}\ n)\frac{\partial \boldsymbol{\varepsilon}}{\partial \boldsymbol{\varepsilon}} = (n\ \mathring{\boldsymbol{\sigma}}\ n)\mathbb{I} \quad (5.46r)$$

$$\frac{\partial}{\partial \boldsymbol{\varepsilon}}[J_6\frac{\partial J_5}{\partial \boldsymbol{\varepsilon}}] = \frac{\partial}{\partial \boldsymbol{\varepsilon}}[tr(\mathring{\boldsymbol{\sigma}})\boldsymbol{\varepsilon}^*] = tr(\mathring{\boldsymbol{\sigma}})\frac{\partial}{\partial \boldsymbol{\varepsilon}}[\boldsymbol{\varepsilon}(n\otimes n) + (n\otimes n)\boldsymbol{\varepsilon}] = tr(\mathring{\boldsymbol{\sigma}})(n\otimes e_i\otimes n\otimes e_i + e_i\otimes n\otimes e_i\otimes n) \quad (5.46s)$$

$$\frac{\partial}{\partial \boldsymbol{\varepsilon}}[J_9\frac{\partial J_5}{\partial \boldsymbol{\varepsilon}}] = \frac{\partial}{\partial \boldsymbol{\varepsilon}}[(n\ \mathring{\boldsymbol{\sigma}}\ n)\boldsymbol{\varepsilon}^*] = (n\ \mathring{\boldsymbol{\sigma}}\ n)\frac{\partial}{\partial \boldsymbol{\varepsilon}}[\boldsymbol{\varepsilon}(n\otimes n) + (n\otimes n)\boldsymbol{\varepsilon}] = (n\ \mathring{\boldsymbol{\sigma}}\ n)(n\otimes e_i\otimes n\otimes e_i + e_i\otimes n\otimes e_i\otimes n) \quad (5.46t)$$

$$[\frac{\partial^2 J_{12}}{\partial \boldsymbol{\varepsilon}^2}] = \frac{\partial}{\partial \boldsymbol{\varepsilon}}[\mathring{\boldsymbol{\sigma}}\ \boldsymbol{\varepsilon} + \boldsymbol{\varepsilon}\ \mathring{\boldsymbol{\sigma}}] = e_i\otimes\mathring{\boldsymbol{\sigma}}\otimes e_i + [e_i\otimes\mathring{\boldsymbol{\sigma}}\otimes e_i]^T \quad (5.46u)$$

where, here, the transpose is in the sense of the minor symmetry, i.e. $[\bullet]^T{}_{ijhk} = [\bullet]_{jikh}$.
The last term of the list is the following:

$$[\frac{\partial^2 J_{16}}{\partial \boldsymbol{\varepsilon}^2}] = \frac{\partial}{\partial \boldsymbol{\varepsilon}}[\mathring{\boldsymbol{\sigma}}\ \boldsymbol{\varepsilon}(n\otimes n) + \mathring{\boldsymbol{\sigma}}\ (n\otimes n)\boldsymbol{\varepsilon} + \boldsymbol{\varepsilon}\ \mathring{\boldsymbol{\sigma}}\ (n\otimes n) + \boldsymbol{\varepsilon}(n\otimes n)\ \mathring{\boldsymbol{\sigma}} + (n\otimes n)\ \mathring{\boldsymbol{\sigma}}\ \boldsymbol{\varepsilon} + (n\otimes n)\boldsymbol{\varepsilon}\ \mathring{\boldsymbol{\sigma}}] = e_i\otimes n\otimes e_i\otimes\mathring{\boldsymbol{\sigma}}\ n + e_i\otimes\mathring{\boldsymbol{\sigma}}\ n\otimes e_i\otimes n + \mathring{\boldsymbol{\sigma}}\ n\otimes e_i\otimes n\otimes e_i + n\otimes e_i\otimes\mathring{\boldsymbol{\sigma}}\ n\otimes e_i + n\otimes\mathring{\boldsymbol{\sigma}}\otimes n + [n\otimes\mathring{\boldsymbol{\sigma}}\otimes n]^T \quad (5.46v)$$

The second derivative of U_R, the part of the strain energy due to the residual stress, takes the form:

$$\frac{\partial^2 U_R(\boldsymbol{\varepsilon},\overset{\circ}{\boldsymbol{\sigma}},n)}{\partial \boldsymbol{\varepsilon}^2}=\frac{\partial \boldsymbol{\sigma}_R(\boldsymbol{\varepsilon},\overset{\circ}{\boldsymbol{\sigma}},n)}{\partial \boldsymbol{\varepsilon}}=$$
$$2\beta_1 tr(\overset{\circ}{\boldsymbol{\sigma}})\mathbf{I}\otimes\mathbf{I}+2\beta_2(n\,\overset{\circ}{\boldsymbol{\sigma}}\,n)\mathbf{I}\otimes\mathbf{I}+\beta_3 tr(\overset{\circ}{\boldsymbol{\sigma}})[(n\otimes n)\otimes\mathbf{I}+\mathbf{I}\otimes(n\otimes n)]+$$
$$\beta_4(n\,\overset{\circ}{\boldsymbol{\sigma}}\,n)[(n\otimes n)\otimes\mathbf{I}+\mathbf{I}\otimes(n\otimes n)]+\beta_5[\overset{\circ}{\boldsymbol{\sigma}}\otimes\mathbf{I}+\mathbf{I}\otimes\overset{\circ}{\boldsymbol{\sigma}}]+\beta_6[\overset{\circ}{\boldsymbol{\sigma}}^{*}\otimes\mathbf{I}+\mathbf{I}\otimes\overset{\circ}{\boldsymbol{\sigma}}^{*}]+$$
$$2\beta_7 tr(\overset{\circ}{\boldsymbol{\sigma}})(n\otimes n)\otimes(n\otimes n)+2\beta_8(n\,\overset{\circ}{\boldsymbol{\sigma}}\,n)(n\otimes n)\otimes(n\otimes n)+\beta_9[\overset{\circ}{\boldsymbol{\sigma}}\otimes(n\otimes n)+(n\otimes n)\otimes\overset{\circ}{\boldsymbol{\sigma}}]+$$
$$\beta_{10}[\overset{\circ}{\boldsymbol{\sigma}}^{*}\otimes(n\otimes n)+(n\otimes n)\otimes\overset{\circ}{\boldsymbol{\sigma}}^{*}]+2\beta_{11}tr(\overset{\circ}{\boldsymbol{\sigma}})\mathbb{I}+2\beta_{12}(n\,\overset{\circ}{\boldsymbol{\sigma}}\,n)\mathbb{I}+\beta_{13}tr(\overset{\circ}{\boldsymbol{\sigma}})(n\otimes e_i\otimes n\otimes e_i+$$
$$e_i\otimes n\otimes e_i\otimes n)+\beta_{14}(n\,\overset{\circ}{\boldsymbol{\sigma}}\,n)(n\otimes e_i\otimes n\otimes e_i+e_i\otimes n\otimes e_i\otimes n)+$$
$$\beta_{15}[e_i\otimes\overset{\circ}{\boldsymbol{\sigma}}\otimes e_i+(e_i\otimes\overset{\circ}{\boldsymbol{\sigma}}\otimes e_i)^T]+\beta_{16}[e_i\otimes n\otimes e_i\otimes\overset{\circ}{\boldsymbol{\sigma}}\,n+e_i\otimes\overset{\circ}{\boldsymbol{\sigma}}\,n\otimes e_i\otimes n+$$
$$\overset{\circ}{\boldsymbol{\sigma}}\,n\otimes e_i\otimes n\otimes e_i+n\otimes e_i\otimes\overset{\circ}{\boldsymbol{\sigma}}\,n\otimes e_i+n\otimes\overset{\circ}{\boldsymbol{\sigma}}\otimes n+(n\otimes\overset{\circ}{\boldsymbol{\sigma}}\otimes n)^T] \quad (5.47)$$

Thanks to the minor symmetry (due to $\overset{\circ}{\boldsymbol{\sigma}}\,\epsilon Sym, \boldsymbol{\varepsilon}\epsilon Sym$), we have:

$$\begin{aligned}
&n\otimes e_i\otimes n\otimes e_i=e_i\otimes n\otimes e_i\otimes n,\\
&e_i\otimes n\otimes e_i\otimes\overset{\circ}{\boldsymbol{\sigma}}\,n=n\otimes e_i\otimes\overset{\circ}{\boldsymbol{\sigma}}\,n\otimes e_i,\\
&\overset{\circ}{\boldsymbol{\sigma}}\,n\otimes e_i\otimes n\otimes e_i=e_i\otimes\overset{\circ}{\boldsymbol{\sigma}}\,n\otimes e_i\otimes n,\\
&e_i\otimes\overset{\circ}{\boldsymbol{\sigma}}\otimes e_i=(e_i\otimes\overset{\circ}{\boldsymbol{\sigma}}\otimes e_i)^T,\\
&n\otimes\overset{\circ}{\boldsymbol{\sigma}}\otimes n=(n\otimes\overset{\circ}{\boldsymbol{\sigma}}\otimes n)^T.
\end{aligned} \quad (5.48)$$

Thus, equation (5.47) can be reduced to the form:

$$\frac{\partial^2 U_R(\boldsymbol{\varepsilon},\overset{\circ}{\boldsymbol{\sigma}},n)}{\partial \boldsymbol{\varepsilon}^2}=\frac{\partial \boldsymbol{\sigma}_R(\boldsymbol{\varepsilon},\overset{\circ}{\boldsymbol{\sigma}},n)}{\partial \boldsymbol{\varepsilon}}=$$
$$2\beta_1 tr(\overset{\circ}{\boldsymbol{\sigma}})\mathbf{I}\otimes\mathbf{I}+2\beta_2(n\,\overset{\circ}{\boldsymbol{\sigma}}\,n)\mathbf{I}\otimes\mathbf{I}+\beta_3 tr(\overset{\circ}{\boldsymbol{\sigma}})[(n\otimes n)\otimes\mathbf{I}+\mathbf{I}\otimes(n\otimes n)]+$$
$$\beta_4(n\,\overset{\circ}{\boldsymbol{\sigma}}\,n)[(n\otimes n)\otimes\mathbf{I}+\mathbf{I}\otimes(n\otimes n)]+\beta_5[\overset{\circ}{\boldsymbol{\sigma}}\otimes\mathbf{I}+\mathbf{I}\otimes\overset{\circ}{\boldsymbol{\sigma}}]+\beta_6[\overset{\circ}{\boldsymbol{\sigma}}^{*}\otimes\mathbf{I}+\mathbf{I}\otimes\overset{\circ}{\boldsymbol{\sigma}}^{*}]+$$
$$2\beta_7 tr(\overset{\circ}{\boldsymbol{\sigma}})(n\otimes n)\otimes(n\otimes n)+2\beta_8(n\,\overset{\circ}{\boldsymbol{\sigma}}\,n)(n\otimes n)\otimes(n\otimes n)+\beta_9[\overset{\circ}{\boldsymbol{\sigma}}\otimes(n\otimes n)+(n\otimes n)\otimes\overset{\circ}{\boldsymbol{\sigma}}]+$$
$$\beta_{10}[\overset{\circ}{\boldsymbol{\sigma}}^{*}\otimes(n\otimes n)+(n\otimes n)\otimes\overset{\circ}{\boldsymbol{\sigma}}^{*}]+2\beta_{11}tr(\overset{\circ}{\boldsymbol{\sigma}})\mathbb{I}+2\beta_{12}(n\,\overset{\circ}{\boldsymbol{\sigma}}\,n)\mathbb{I}+$$
$$2\beta_{13}tr(\overset{\circ}{\boldsymbol{\sigma}})(n\otimes e_i\otimes n\otimes e_i)+2\beta_{14}(n\,\overset{\circ}{\boldsymbol{\sigma}}\,n)(n\otimes e_i\otimes n\otimes e_i)+2\beta_{15}e_i\otimes\overset{\circ}{\boldsymbol{\sigma}}\otimes e_i+$$
$$2\beta_{16}[e_i\otimes n\otimes e_i\otimes\overset{\circ}{\boldsymbol{\sigma}}\,n+e_i\otimes\overset{\circ}{\boldsymbol{\sigma}}\,n\otimes e_i\otimes n+n\otimes\overset{\circ}{\boldsymbol{\sigma}}\otimes n] \quad (5.49)$$

Moreover, it is important to note that the forth-order tensor under exam is symmetric in the sense of the major symmetry, i.e. $[\bullet]^T{}_{ijhk}=[\bullet]_{hkij}$, because

$$\Big[\frac{\partial^2 U_R(\boldsymbol{\varepsilon},\overset{\circ}{\boldsymbol{\sigma}},n)}{\partial \boldsymbol{\varepsilon}^2}\Big]_{ijhk}=\frac{\partial^2 U_R(\boldsymbol{\varepsilon},\overset{\circ}{\boldsymbol{\sigma}},n)}{\partial \boldsymbol{\varepsilon}_{ij}\partial \boldsymbol{\varepsilon}_{hk}}=\frac{\partial^2 U_R(\boldsymbol{\varepsilon},\overset{\circ}{\boldsymbol{\sigma}},n)}{\partial \boldsymbol{\varepsilon}_{hk}\partial \boldsymbol{\varepsilon}_{ij}}=\Big[\frac{\partial^2 U_R(\boldsymbol{\varepsilon},\overset{\circ}{\boldsymbol{\sigma}},n)}{\partial \boldsymbol{\varepsilon}^2}\Big]_{hkij} \quad (5.50)$$

In fact, it is immediate to note that:

$$\begin{array}{l}\mathbf{I}\otimes(n\otimes n)=(n\otimes n)\otimes\mathbf{I},\\ \mathbf{I}\otimes\overset{\circ}{\boldsymbol{\sigma}}=\overset{\circ}{\boldsymbol{\sigma}}\otimes\mathbf{I},\\ \mathbf{I}\otimes\overset{\circ}{\boldsymbol{\sigma}}^{*}=\overset{\circ}{\boldsymbol{\sigma}}^{*}\otimes\mathbf{I},\\ \overset{\circ}{\boldsymbol{\sigma}}\otimes(n\otimes n)=(n\otimes n)\otimes\overset{\circ}{\boldsymbol{\sigma}},\\ \overset{\circ}{\boldsymbol{\sigma}}^{*}\otimes(n\otimes n)=(n\otimes n)\otimes\overset{\circ}{\boldsymbol{\sigma}}^{*},\\ e_i\otimes n\otimes e_i\otimes\overset{\circ}{\boldsymbol{\sigma}}n=e_i\otimes\overset{\circ}{\boldsymbol{\sigma}}n\otimes e_i\otimes n\end{array}\tag{5.51}$$

Hence, equation (5.49) can be rewritten as follows:

$$\frac{\partial^2 U_R(\boldsymbol{\varepsilon},\overset{\circ}{\boldsymbol{\sigma}},n)}{\partial\boldsymbol{\varepsilon}^2}=\frac{\partial\boldsymbol{\sigma}_R(\boldsymbol{\varepsilon},\overset{\circ}{\boldsymbol{\sigma}},n)}{\partial\boldsymbol{\varepsilon}}=$$
$$2\beta_1 tr(\overset{\circ}{\boldsymbol{\sigma}})\mathbf{I}\otimes\mathbf{I}+2\beta_2(n\,\overset{\circ}{\boldsymbol{\sigma}}\,n)\mathbf{I}\otimes\mathbf{I}+2\beta_3 tr(\overset{\circ}{\boldsymbol{\sigma}})\mathbf{I}\otimes(n\otimes n)+2\beta_4(n\,\overset{\circ}{\boldsymbol{\sigma}}\,n)(n\otimes n)\otimes\mathbf{I}+$$
$$2\beta_5\,\overset{\circ}{\boldsymbol{\sigma}}\otimes\mathbf{I}+2\beta_6\,\overset{\circ}{\boldsymbol{\sigma}}^{*}\otimes\mathbf{I}+2\beta_7 tr(\overset{\circ}{\boldsymbol{\sigma}})(n\otimes n)\otimes(n\otimes n)+2\beta_8(n\,\overset{\circ}{\boldsymbol{\sigma}}\,n)(n\otimes n)\otimes(n\otimes n)+$$
$$2\beta_9\,\overset{\circ}{\boldsymbol{\sigma}}\otimes(n\otimes n)+2\beta_{10}\,\overset{\circ}{\boldsymbol{\sigma}}^{*}\otimes(n\otimes n)+2\beta_{11}tr(\overset{\circ}{\boldsymbol{\sigma}})\mathbb{I}+2\beta_{12}(n\,\overset{\circ}{\boldsymbol{\sigma}}\,n)\mathbb{I}+$$
$$2\beta_{13}tr(\overset{\circ}{\boldsymbol{\sigma}})(n\otimes e_i\otimes n\otimes e_i)+2\beta_{14}(n\,\overset{\circ}{\boldsymbol{\sigma}}\,n)(n\otimes e_i\otimes n\otimes e_i)+$$
$$2\beta_{15}e_i\otimes\overset{\circ}{\boldsymbol{\sigma}}\otimes e_i+2\beta_{16}[2e_i\otimes n\otimes e_i\otimes\overset{\circ}{\boldsymbol{\sigma}}n+n\otimes\overset{\circ}{\boldsymbol{\sigma}}\otimes n]\tag{5.52}$$

This fourth-order tensor gives the tangential elastic modulus, at a given (tensor) value of the residual stress $\overset{\circ}{\boldsymbol{\sigma}}$.
In order to obtain the final expression for $\mathfrak{D}(\boldsymbol{\varepsilon},\overset{\circ}{\boldsymbol{\sigma}},n)$, the third derivative of the strain energy has to be calculated. The derivatives of the different terms of (5.52) with respect to $\overset{\circ}{\boldsymbol{\sigma}}$ can be evaluated following the definition of derivative of forth-order tensor valued functions with respect to a second-order tensor.

By denoting $\mathbb{D}$ a forth-order tensor valued function of $\overset{\circ}{\boldsymbol{\sigma}}$, the derivative of $\mathbb{D}$ with respect to $\overset{\circ}{\boldsymbol{\sigma}}$ is the sixth-order tensor $\mathfrak{F}$ defined as follows:

$$\mathfrak{F}:\mathbf{V}=\frac{\partial\mathbb{D}(\overset{\circ}{\boldsymbol{\sigma}})}{\partial\,\overset{\circ}{\boldsymbol{\sigma}}}:\mathbf{V}:=\lim_{\tau\to0}\frac{d\mathbb{D}(\overset{\circ}{\boldsymbol{\sigma}}+\tau\mathbf{V})}{d\tau}\tag{5.53}$$

where $[\mathfrak{F}:\mathbf{V}]_{ijhk}=\mathfrak{F}_{ijhklm}\mathbf{V}_{lm}$. In the case under exam, $\overset{\circ}{\boldsymbol{\sigma}}\,\epsilon Sym$, and hence $\mathbf{V}\epsilon Sym$.

For example, the forth and sixth terms of (5.52) generates $\mathfrak{F}_5$ and $\mathfrak{F}_9$, derived as follows:

$$\mathfrak{F}_5:\mathbf{V}=\frac{\partial}{\partial\,\overset{\circ}{\boldsymbol{\sigma}}}[(n\,\overset{\circ}{\boldsymbol{\sigma}}\,n)(n\otimes n)\otimes\mathbf{I}]=\lim_{\tau\to0}\frac{d}{d\tau}[(n(\overset{\circ}{\boldsymbol{\sigma}}+\tau\mathbf{V})n)(n\otimes n)\otimes\mathbf{I}]=$$
$$\lim_{\tau\to0}\frac{d}{d\tau}[(n\,\overset{\circ}{\boldsymbol{\sigma}}\,n+\tau n\mathbf{V}n)(n\otimes n)\otimes\mathbf{I}]=\lim_{\tau\to0}[(n\mathbf{V}n)(n\otimes n)\otimes\mathbf{I}]=(n\mathbf{V}n)(n\otimes n)\otimes\mathbf{I}=\tag{5.54}$$

where

$$\begin{cases} [\mathfrak{F}_5\mathbf{V}]_{hklm} = \mathfrak{F}_{5hklmst}\mathbf{V}_{st}, \\ (n\mathbf{V}n)[(n\otimes n)\otimes\mathbf{I}]_{hklm} = n_i\mathbf{V}_{ij}n_jn_hn_k\delta_{lm}. \end{cases} \tag{5.55}$$

Hence,

$$\begin{aligned} \mathfrak{F}_{5hklmst}\mathbf{V}_{st} = n_i\mathbf{V}_{ij}n_jn_hn_k\delta_{lm}\delta_{si}\delta_{tj} = n_sn_tn_hn_k\delta_{lm}\mathbf{V}_{st} \\ \Rightarrow \mathfrak{F}_{5hklmst} = n_sn_tn_hn_k\delta_{lm} \quad \Rightarrow \mathfrak{F}_5 = n\otimes n\otimes\mathbf{I}\otimes n\otimes n \end{aligned} \tag{5.56}$$

$$\begin{aligned} &\mathfrak{F}_9 : \mathbf{V} = \frac{\partial}{\partial\,\overset{\circ}{\boldsymbol{\sigma}}}[\overset{\circ}{\boldsymbol{\sigma}}{}^{*}\otimes\mathbf{I}] = \lim_{\tau\to0}\frac{d}{d\tau}[(\overset{\circ}{\boldsymbol{\sigma}}+\tau\mathbf{V})^{*}\otimes\mathbf{I}] = \\ &\qquad \lim_{\tau\to0}\frac{d}{d\tau}[(n\otimes n)(\overset{\circ}{\boldsymbol{\sigma}}+\tau\mathbf{V})\otimes\mathbf{I} + (\overset{\circ}{\boldsymbol{\sigma}}+\tau\mathbf{V})(n\otimes n)\otimes\mathbf{I}] = \\ &\lim_{\tau\to0}\frac{d}{d\tau}[(n\otimes n)\,\overset{\circ}{\boldsymbol{\sigma}}\otimes\mathbf{I} + \tau(n\otimes n)\mathbf{V}\otimes\mathbf{I} + \overset{\circ}{\boldsymbol{\sigma}}\,(n\otimes n)\otimes\mathbf{I} + \tau\mathbf{V}(n\otimes n)\otimes\mathbf{I}] = \\ &\qquad \lim_{\tau\to0}[(n\otimes n)\mathbf{V}\otimes\mathbf{I} + \mathbf{V}(n\otimes n)\otimes\mathbf{I}] = (n\otimes n)\mathbf{V}\otimes\mathbf{I} + \mathbf{V}(n\otimes n)\otimes\mathbf{I} \end{aligned} \tag{5.57}$$

where

$$\begin{cases} [(n\otimes n)\mathbf{V}\otimes\mathbf{I} + \mathbf{V}(n\otimes n)\otimes\mathbf{I}]_{ihkl} = n_in_j\mathbf{V}_{jh}\delta_{kl} + \mathbf{V}_{ij}n_jn_h\delta_{kl} \\ \left[\mathfrak{F}_9\mathbf{V}\right]_{ihkl} = \mathfrak{F}_{9ihklst}\mathbf{V}_{st} \end{cases} \tag{5.58}$$

Hence,

$$\begin{aligned} \mathfrak{F}_{9ihklst}\mathbf{V}_{st} = n_in_j\mathbf{V}_{jh}\delta_{kl}\delta_{sj}\delta_{th} + \mathbf{V}_{ij}n_jn_h\delta_{kl}\delta_{si}\delta_{tj} = n_in_s\delta_{kl}\delta_{th}\mathbf{V}_{st} + n_tn_h\delta_{kl}\delta_{si}\mathbf{V}_{st} \\ \Rightarrow \mathfrak{F}_{9ihklst} = n_in_s\delta_{kl}\delta_{th} + n_tn_h\delta_{kl}\delta_{si} \\ \Rightarrow \mathfrak{F}_9 = n\otimes e_i\otimes\ \mathbf{I}\otimes n\otimes e_i + e_i\otimes n\otimes\ \mathbf{I}\otimes e_i\otimes n \end{aligned} \tag{5.59}$$

The derivatives of the different terms of (5.49) with respect to $\overset{\circ}{\boldsymbol{\sigma}}$ turn out to be as follows:

$$\frac{\partial^2}{\partial\varepsilon\partial\,\overset{\circ}{\boldsymbol{\sigma}}}[J_1J_6\frac{\partial J_1}{\partial\boldsymbol{\varepsilon}}] = \frac{\partial}{\partial\,\overset{\circ}{\boldsymbol{\sigma}}}[tr(\overset{\circ}{\boldsymbol{\sigma}})\mathbf{I}\otimes\mathbf{I}] = \mathbf{I}\otimes\mathbf{I}\otimes\mathbf{I} \tag{5.60a}$$

$$\frac{\partial^2}{\partial\varepsilon\partial\,\overset{\circ}{\boldsymbol{\sigma}}}[J_1J_9\frac{\partial J_1}{\partial\boldsymbol{\varepsilon}}] = \frac{\partial}{\partial\,\overset{\circ}{\boldsymbol{\sigma}}}[(n\,\overset{\circ}{\boldsymbol{\sigma}}\,n)\mathbf{I}\otimes\mathbf{I}] = \mathbf{I}\otimes\mathbf{I}\otimes(n\otimes n) \tag{5.60b}$$

$$\frac{\partial^2}{\partial\varepsilon\partial\,\overset{\circ}{\boldsymbol{\sigma}}}[J_1J_6\frac{\partial J_4}{\partial\boldsymbol{\varepsilon}}] = \frac{\partial}{\partial\,\overset{\circ}{\boldsymbol{\sigma}}}[tr(\overset{\circ}{\boldsymbol{\sigma}})(n\otimes n)\otimes\mathbf{I}] = (n\otimes n)\otimes\mathbf{I}\otimes\mathbf{I} \tag{5.60c}$$

$$\frac{\partial^2}{\partial\varepsilon\partial\,\overset{\circ}{\boldsymbol{\sigma}}}[J_4J_6\frac{\partial J_1}{\partial\boldsymbol{\varepsilon}}] = \frac{\partial}{\partial\,\overset{\circ}{\boldsymbol{\sigma}}}[tr(\overset{\circ}{\boldsymbol{\sigma}})\mathbf{I}\otimes(n\otimes n)] = \mathbf{I}\otimes(n\otimes n)\otimes\mathbf{I} \tag{5.60d}$$

$$\frac{\partial^2}{\partial\varepsilon\partial\,\overset{\circ}{\boldsymbol{\sigma}}}[J_1J_9\frac{\partial J_4}{\partial\boldsymbol{\varepsilon}}] = \frac{\partial}{\partial\,\overset{\circ}{\boldsymbol{\sigma}}}[(n\,\overset{\circ}{\boldsymbol{\sigma}}\,n)(n\otimes n)\otimes\mathbf{I}] = (n\otimes n)\otimes\mathbf{I}\otimes(n\otimes n) \tag{5.60e}$$

$$\frac{\partial^2}{\partial\boldsymbol{\varepsilon}\partial\overset{\circ}{\boldsymbol{\sigma}}}[J_4J_9\frac{\partial J_1}{\partial\boldsymbol{\varepsilon}}]=\frac{\partial}{\partial\overset{\circ}{\boldsymbol{\sigma}}}[(n\overset{\circ}{\boldsymbol{\sigma}}n)\mathbf{I}\otimes(n\otimes n)]=\mathbf{I}\otimes(n\otimes n)\otimes(n\otimes n) \quad (5.60f)$$

$$\frac{\partial^2}{\partial\boldsymbol{\varepsilon}\partial\overset{\circ}{\boldsymbol{\sigma}}}[J_1\frac{\partial J_{11}}{\partial\boldsymbol{\varepsilon}}]=\frac{\partial}{\partial\overset{\circ}{\boldsymbol{\sigma}}}[\overset{\circ}{\boldsymbol{\sigma}}\otimes\mathbf{I}]=e_i\otimes e_j\otimes\mathbf{I}\otimes e_i\otimes e_j \quad (5.60g)$$

$$\frac{\partial^2}{\partial\boldsymbol{\varepsilon}\partial\overset{\circ}{\boldsymbol{\sigma}}}[J_{11}\frac{\partial J_1}{\partial\boldsymbol{\varepsilon}}]=\frac{\partial}{\partial\overset{\circ}{\boldsymbol{\sigma}}}[\mathbf{I}\otimes\overset{\circ}{\boldsymbol{\sigma}}]=\mathbf{I}\otimes e_i\otimes e_j\otimes e_i\otimes e_j \quad (5.60h)$$

$$\frac{\partial^2}{\partial\boldsymbol{\varepsilon}\partial\overset{\circ}{\boldsymbol{\sigma}}}[J_1\frac{\partial J_{15}}{\partial\boldsymbol{\varepsilon}}]=\frac{\partial}{\partial\overset{\circ}{\boldsymbol{\sigma}}}[\overset{\circ}{\boldsymbol{\sigma}}{}^*\otimes\mathbf{I}]=\frac{\partial}{\partial\overset{\circ}{\boldsymbol{\sigma}}}[(n\otimes n)\overset{\circ}{\boldsymbol{\sigma}}\otimes\mathbf{I}+\overset{\circ}{\boldsymbol{\sigma}}(n\otimes n)\otimes\mathbf{I}]=$$
$$n\otimes e_i\otimes\mathbf{I}\otimes n\otimes e_i+e_i\otimes n\otimes\mathbf{I}\otimes e_i\otimes n \quad (5.60i)$$

$$\frac{\partial^2}{\partial\boldsymbol{\varepsilon}\partial\overset{\circ}{\boldsymbol{\sigma}}}[J_{15}\frac{\partial J_1}{\partial\boldsymbol{\varepsilon}}]=\frac{\partial}{\partial\overset{\circ}{\boldsymbol{\sigma}}}[\mathbf{I}\otimes\overset{\circ}{\boldsymbol{\sigma}}{}^*]=\frac{\partial}{\partial\overset{\circ}{\boldsymbol{\sigma}}}[\mathbf{I}\otimes(n\otimes n)\overset{\circ}{\boldsymbol{\sigma}}+\mathbf{I}\otimes\overset{\circ}{\boldsymbol{\sigma}}(n\otimes n)]=$$
$$\mathbf{I}\otimes n\otimes e_i\otimes n\otimes e_i+\mathbf{I}\otimes e_i\otimes n\otimes e_i\otimes n \quad (5.60j)$$

$$\frac{\partial^2}{\partial\boldsymbol{\varepsilon}\partial\overset{\circ}{\boldsymbol{\sigma}}}[J_4J_6\frac{\partial J_4}{\partial\boldsymbol{\varepsilon}}]=\frac{\partial}{\partial\overset{\circ}{\boldsymbol{\sigma}}}[tr(\overset{\circ}{\boldsymbol{\sigma}})(n\otimes n)\otimes(n\otimes n)]=(n\otimes n)\otimes(n\otimes n)\otimes\mathbf{I} \quad (5.60k)$$

$$\frac{\partial^2}{\partial\boldsymbol{\varepsilon}\partial\overset{\circ}{\boldsymbol{\sigma}}}[J_4J_9\frac{\partial J_4}{\partial\boldsymbol{\varepsilon}}]=\frac{\partial}{\partial\overset{\circ}{\boldsymbol{\sigma}}}[(n\overset{\circ}{\boldsymbol{\sigma}}n)(n\otimes n)\otimes(n\otimes n)]=(n\otimes n)\otimes(n\otimes n)\otimes(n\otimes n) \quad (5.60l)$$

$$\frac{\partial^2}{\partial\boldsymbol{\varepsilon}\partial\overset{\circ}{\boldsymbol{\sigma}}}[J_4\frac{\partial J_{11}}{\partial\boldsymbol{\varepsilon}}]=\frac{\partial}{\partial\overset{\circ}{\boldsymbol{\sigma}}}[\overset{\circ}{\boldsymbol{\sigma}}\otimes(n\otimes n)]=e_i\otimes e_j\otimes n\otimes n\otimes e_i\otimes e_j \quad (5.60m)$$

$$\frac{\partial^2}{\partial\boldsymbol{\varepsilon}\partial\overset{\circ}{\boldsymbol{\sigma}}}[J_{11}\frac{\partial J_4}{\partial\boldsymbol{\varepsilon}}]=\frac{\partial}{\partial\overset{\circ}{\boldsymbol{\sigma}}}[(n\otimes n)\otimes\overset{\circ}{\boldsymbol{\sigma}}]=n\otimes n\otimes e_i\otimes e_j\otimes e_i\otimes e_j \quad (5.60n)$$

$$\frac{\partial^2}{\partial\boldsymbol{\varepsilon}\partial\overset{\circ}{\boldsymbol{\sigma}}}[J_4\frac{\partial J_{15}}{\partial\boldsymbol{\varepsilon}}]=\frac{\partial}{\partial\overset{\circ}{\boldsymbol{\sigma}}}[\overset{\circ}{\boldsymbol{\sigma}}{}^*\otimes(n\otimes n)]=\frac{\partial}{\partial\overset{\circ}{\boldsymbol{\sigma}}}[\overset{\circ}{\boldsymbol{\sigma}}(n\otimes n)\otimes(n\otimes n)+(n\otimes n)\overset{\circ}{\boldsymbol{\sigma}}\otimes(n\otimes n)]=$$
$$e_i\otimes n\otimes n\otimes n\otimes n\otimes e_i+n\otimes e_i\otimes n\otimes n\otimes e_i\otimes n \quad (5.60o)$$

$$\frac{\partial^2}{\partial\boldsymbol{\varepsilon}\partial\overset{\circ}{\boldsymbol{\sigma}}}[J_{15}\frac{\partial J_4}{\partial\boldsymbol{\varepsilon}}]=\frac{\partial}{\partial\overset{\circ}{\boldsymbol{\sigma}}}[(n\otimes n)\otimes\overset{\circ}{\boldsymbol{\sigma}}{}^*]=\frac{\partial}{\partial\overset{\circ}{\boldsymbol{\sigma}}}[(n\otimes n)\otimes\overset{\circ}{\boldsymbol{\sigma}}(n\otimes n)+(n\otimes n)\otimes(n\otimes n)\overset{\circ}{\boldsymbol{\sigma}}]=$$
$$n\otimes n\otimes n\otimes e_i\otimes n\otimes e_i+n\otimes n\otimes e_i\otimes n\otimes e_i\otimes n \quad (5.60p)$$

$$\frac{\partial}{\partial\boldsymbol{\varepsilon}}[J_6\frac{\partial J_2}{\partial\boldsymbol{\varepsilon}}]=\frac{\partial}{\partial\overset{\circ}{\boldsymbol{\sigma}}}[tr(\overset{\circ}{\boldsymbol{\sigma}})\mathbb{I}]=\mathbb{I}\otimes\mathbf{I} \quad (5.60q)$$

$$\frac{\partial^2}{\partial\boldsymbol{\varepsilon}\partial\overset{\circ}{\boldsymbol{\sigma}}}[J_9\frac{\partial J_2}{\partial\boldsymbol{\varepsilon}}]=\frac{\partial}{\partial\overset{\circ}{\boldsymbol{\sigma}}}[(n\overset{\circ}{\boldsymbol{\sigma}}n)\mathbb{I}]=\mathbb{I}\otimes n\otimes n \quad (5.60r)$$

$$\frac{\partial}{\partial \boldsymbol{\varepsilon}}[J_6\frac{\partial J_5}{\partial \boldsymbol{\varepsilon}}] = \frac{\partial}{\partial \overset{\circ}{\boldsymbol{\sigma}}}[tr(\overset{\circ}{\boldsymbol{\sigma}})(n\otimes e_i\otimes n\otimes e_i+e_i\otimes n\otimes e_i\otimes n)] = (n\otimes e_i\otimes n\otimes e_i+e_i\otimes n\otimes e_i\otimes n)\otimes\mathbf{I} \tag{5.60s}$$

$$\frac{\partial^2}{\partial \boldsymbol{\varepsilon}\partial \overset{\circ}{\boldsymbol{\sigma}}}[J_9\frac{\partial J_5}{\partial \boldsymbol{\varepsilon}}] = \frac{\partial}{\partial \overset{\circ}{\boldsymbol{\sigma}}}[(n\overset{\circ}{\boldsymbol{\sigma}}n)(n\otimes e_i\otimes n\otimes e_i + e_i\otimes n\otimes e_i\otimes n)] = (n\otimes e_i\otimes n\otimes e_i + e_i\otimes n\otimes e_i\otimes n)\otimes n\otimes n \tag{5.60t}$$

$$[\frac{\partial^2 J_{12}}{\partial \boldsymbol{\varepsilon}^2}] = \frac{\partial}{\partial \overset{\circ}{\boldsymbol{\sigma}}}[e_i\otimes\overset{\circ}{\boldsymbol{\sigma}}\otimes e_i+[e_i\otimes\overset{\circ}{\boldsymbol{\sigma}}\otimes e_i]^T] = e_i\otimes e_j\otimes e_k\otimes e_i\otimes e_j\otimes e_k+e_i\otimes e_j\otimes e_k\otimes e_i\otimes e_k\otimes e_j \tag{5.60u}$$

$$[\frac{\partial^2 J_{16}}{\partial \boldsymbol{\varepsilon}^2}] = \frac{\partial}{\partial \overset{\circ}{\boldsymbol{\sigma}}}[e_i\otimes n\otimes e_i\otimes\overset{\circ}{\boldsymbol{\sigma}}n+e_i\otimes\overset{\circ}{\boldsymbol{\sigma}}n\otimes e_i\otimes n+\overset{\circ}{\boldsymbol{\sigma}}n\otimes e_i\otimes n\otimes e_i+n\otimes e_i\otimes\overset{\circ}{\boldsymbol{\sigma}}n\otimes e_i+ + n\otimes\overset{\circ}{\boldsymbol{\sigma}}\otimes n+[n\otimes\overset{\circ}{\boldsymbol{\sigma}}\otimes n]^T] = (e_i\otimes n\otimes e_i\otimes e_j+e_i\otimes e_j\otimes e_i\otimes n+ e_i\otimes e_j\otimes n\otimes e_i+n\otimes e_i\otimes e_j\otimes e_i)\otimes e_j\otimes n+n\otimes e_i\otimes e_j\otimes n\otimes(e_i\otimes e_j+e_j\otimes e_i)) \tag{5.60v}$$

The third derivative of U_R, the part of the strain energy due to the residual stress, turns out to be:

$$\mathfrak{D}(\boldsymbol{\varepsilon},\overset{\circ}{\boldsymbol{\sigma}},n) = \frac{\partial^3 U_R(\boldsymbol{\varepsilon},\overset{\circ}{\boldsymbol{\sigma}},n)}{\partial\boldsymbol{\varepsilon}^2\partial\boldsymbol{\sigma}} = \frac{\partial\boldsymbol{\sigma}_R(\boldsymbol{\varepsilon},\overset{\circ}{\boldsymbol{\sigma}},n)}{\partial\boldsymbol{\varepsilon}\partial\boldsymbol{\varepsilon}\boldsymbol{\sigma}} = 2\beta_1\mathbf{I}\otimes\mathbf{I}\otimes\mathbf{I}+2\beta_2\mathbf{I}\otimes\mathbf{I}\otimes n\otimes n+\beta_3[\mathbf{I}\otimes n\otimes n\otimes\mathbf{I}+n\otimes n\otimes\mathbf{I}\otimes\mathbf{I}]+ \beta_4[\mathbf{I}\otimes n\otimes n\otimes n\otimes n+n\otimes n\otimes\mathbf{I}\otimes n\otimes n]+\beta_5[e_i\otimes e_j\otimes\mathbf{I}\otimes e_i\otimes e_j+\mathbf{I}\otimes e_i\otimes e_j\otimes e_i\otimes e_j]+ \beta_6[n\otimes e_i\otimes\mathbf{I}\otimes n\otimes e_i+e_i\otimes n\otimes\mathbf{I}\otimes e_i\otimes n+\mathbf{I}\otimes n\otimes e_i\otimes n\otimes e_i+\mathbf{I}\otimes e_i\otimes n\otimes e_i\otimes n]+ 2\beta_7(n\otimes n)\otimes(n\otimes n)\otimes\mathbf{I}+2\beta_8(n\otimes n)\otimes(n\otimes n)\otimes(n\otimes n)+\beta_9[e_i\otimes e_j\otimes n\otimes n\otimes e_i\otimes e_j+ n\otimes n\otimes e_i\otimes e_j\otimes e_i\otimes e_j]+\beta_{10}[e_i\otimes n\otimes n\otimes n\otimes n\otimes e_i+n\otimes e_i\otimes n\otimes n\otimes e_i\otimes n+ n\otimes n\otimes n\otimes e_i\otimes n\otimes e_i+n\otimes n\otimes e_i\otimes n\otimes e_i\otimes n]+2\beta_{11}\mathbb{I}\otimes\mathbf{I}+2\beta_{12}\mathbb{I}\otimes n\otimes n+ \beta_{13}[(n\otimes e_i\otimes n\otimes e_i+e_i\otimes n\otimes e_i\otimes n)\otimes\mathbf{I}]+\beta_{14}[(n\otimes e_i\otimes n\otimes e_i+e_i\otimes n\otimes e_i\otimes n)\otimes n\otimes n]+ \beta_{15}[e_i\otimes e_j\otimes e_k\otimes e_i\otimes e_j\otimes e_k+e_i\otimes e_j\otimes e_k\otimes e_i\otimes e_k\otimes e_j]+\beta_{16}[(e_i\otimes n\otimes e_i\otimes e_j+ e_i\otimes e_j\otimes e_i\otimes n+e_i\otimes e_j\otimes n\otimes e_i+n\otimes e_i\otimes e_j\otimes e_i)\otimes e_j\otimes n+n\otimes e_i\otimes e_j\otimes n\otimes(e_i\otimes e_j+e_j\otimes e_i)] \tag{5.61}$$

Thanks to the minor symmetry (due to $\overset{\circ}{\boldsymbol{\sigma}}\ \epsilon Sym, \boldsymbol{\varepsilon}\epsilon Sym$), we can write the

following relations:

$$\begin{array}{l} n\otimes e_i\otimes \mathbf{I}\otimes n\otimes e_i = e_i\otimes n\otimes \mathbf{I}\otimes e_i\otimes n,\\ \mathbf{I}\otimes n\otimes e_i\otimes n\otimes e_i = \mathbf{I}\otimes e_i\otimes n\otimes e_i\otimes n,\\ e_i\otimes n\otimes n\otimes n\otimes n\otimes e_i = n\otimes e_i\otimes n\otimes n\otimes e_i\otimes n,\\ n\otimes n\otimes n\otimes e_i\otimes n\otimes e_i = n\otimes n\otimes e_i\otimes n\otimes e_i\otimes n,\\ n\otimes e_i\otimes n\otimes e_i\otimes \mathbf{I} = e_i\otimes n\otimes e_i\otimes n\otimes \mathbf{I},\\ n\otimes e_i\otimes n\otimes e_i\otimes n\otimes n = e_i\otimes n\otimes e_i\otimes n)\otimes n\otimes n,\\ e_i\otimes e_j\otimes e_k\otimes e_i\otimes e_j\otimes e_k = e_i\otimes e_j\otimes e_k\otimes e_i\otimes e_k\otimes e_j,\\ e_i\otimes n\otimes e_i\otimes e_j\otimes e_j\otimes n = n\otimes e_i\otimes e_j\otimes e_i\otimes e_j\otimes n,\\ e_i\otimes e_j\otimes e_i\otimes n\otimes e_j\otimes n = e_i\otimes e_j\otimes n\otimes e_i\otimes e_j\otimes n,\\ n\otimes e_i\otimes e_j\otimes n\otimes e_i\otimes e_j = n\otimes e_i\otimes e_j\otimes n\otimes e_j\otimes e_i. \end{array} \tag{5.62}$$

By using equations (5.62), the expression of the sixth order tensor (5.61) can be reduced to:

$$\begin{aligned} \mathfrak{D}(\boldsymbol{\varepsilon},\overset{\circ}{\boldsymbol{\sigma}},n) = \frac{\partial^3 U_R(\boldsymbol{\varepsilon},\overset{\circ}{\boldsymbol{\sigma}},n)}{\partial\boldsymbol{\varepsilon}^2\partial\boldsymbol{\varepsilon}\boldsymbol{\sigma}} = \frac{\partial\boldsymbol{\sigma}_R(\boldsymbol{\varepsilon},\overset{\circ}{\boldsymbol{\sigma}},n)}{\partial\boldsymbol{\varepsilon}\partial\boldsymbol{\varepsilon}\boldsymbol{\sigma}} = \\ 2\beta_1\mathbf{I}\otimes\mathbf{I}\otimes\mathbf{I}+2\beta_2\mathbf{I}\otimes\mathbf{I}\otimes n\otimes n+\beta_3[\mathbf{I}\otimes n\otimes n\otimes\mathbf{I}+n\otimes n\otimes\mathbf{I}\otimes\mathbf{I}]+ \\ \beta_4[\mathbf{I}\otimes n\otimes n\otimes n\otimes n+n\otimes n\otimes\mathbf{I}\otimes n\otimes n]+\beta_5[e_i\otimes e_j\otimes\mathbf{I}\otimes e_i\otimes e_j+\mathbf{I}\otimes e_i\otimes e_j\otimes e_i\otimes e_j]+ \\ 2\beta_6[n\otimes e_i\otimes\ \mathbf{I}\otimes n\otimes e_i+\ \mathbf{I}\otimes n\otimes e_i\otimes n\otimes e_i]+2\beta_7(n\otimes n)\otimes(n\otimes n)\otimes\mathbf{I}+ \\ 2\beta_8(n\otimes n)\otimes(n\otimes n)\otimes(n\otimes n)+\beta_9[e_i\otimes e_j\otimes n\otimes n\otimes e_i\otimes e_j+n\otimes n\otimes e_i\otimes e_j\otimes e_i\otimes e_j]+ \\ 2\beta_{10}[e_i\otimes n\otimes n\otimes n\otimes n\otimes e_i+n\otimes n\otimes n\otimes e_i\otimes n\otimes e_i]+2\beta_{11}\mathbb{I}\otimes\mathbf{I}+2\beta_{12}\mathbb{I}\otimes n\otimes n+ \\ 2\beta_{13}n\otimes e_i\otimes n\otimes e_i\otimes\mathbf{I}+2\beta_{14}n\otimes e_i\otimes n\otimes e_i\otimes n\otimes n+2\beta_{15}e_i\otimes e_j\otimes e_k\otimes e_i\otimes e_j\otimes e_k+ \\ \beta_{16}[2(e_i\otimes n\otimes e_i\otimes e_j+e_i\otimes e_j\otimes e_i\otimes n)\otimes e_j\otimes n+2n\otimes e_i\otimes e_j\otimes n\otimes e_i\otimes e_j]. \end{aligned} \tag{5.63}$$

Moreover, we can note that the sixth-order tensor $\mathfrak{D}(\boldsymbol{\varepsilon},\overset{\circ}{\boldsymbol{\sigma}},n)$ has the following property,

$$\Big[\frac{\partial^3 U_R(\boldsymbol{\varepsilon},\overset{\circ}{\boldsymbol{\sigma}},n)}{\partial\boldsymbol{\varepsilon}^2\partial\ \overset{\circ}{\boldsymbol{\sigma}}}\Big]_{ijhklm} = \frac{\partial^3 U_R(\boldsymbol{\varepsilon},\overset{\circ}{\boldsymbol{\sigma}},n)}{\partial\boldsymbol{\varepsilon}_{ij}\partial\boldsymbol{\varepsilon}_{hk}\partial\ \overset{\circ}{\boldsymbol{\sigma}}_{lm}} = \frac{\partial^3 U_R(\boldsymbol{\varepsilon},\overset{\circ}{\boldsymbol{\sigma}},n)}{\partial\boldsymbol{\varepsilon}_{hk}\partial\boldsymbol{\varepsilon}_{ij}\partial\ \overset{\circ}{\boldsymbol{\sigma}}_{lm}} = \Big[\frac{\partial^3 U_R(\boldsymbol{\varepsilon},\overset{\circ}{\boldsymbol{\sigma}},n)}{\partial\boldsymbol{\varepsilon}^2\partial\ \overset{\circ}{\boldsymbol{\sigma}}}\Big]_{hkijlm} \tag{5.64}$$

which can be regarded as a major symmetry property.
Thanks to this, we can verify that:

$$\begin{array}{l} \mathbf{I}\otimes n\otimes n\otimes\mathbf{I} = n\otimes n\otimes\mathbf{I}\otimes\mathbf{I},\\ \mathbf{I}\otimes n\otimes n\otimes n\otimes n = n\otimes n\otimes\mathbf{I}\otimes n\otimes n,\\ e_i\otimes e_j\otimes\mathbf{I}\otimes e_i\otimes e_j = \mathbf{I}\otimes e_i\otimes e_j\otimes e_i\otimes e_j,\\ n\otimes e_i\otimes\ \mathbf{I}\otimes n\otimes e_i =\ \mathbf{I}\otimes n\otimes e_i\otimes n\otimes e_i,\\ e_i\otimes e_j\otimes n\otimes n\otimes e_i\otimes e_j = n\otimes n\otimes e_i\otimes e_j\otimes e_i\otimes e_j,\\ e_i\otimes n\otimes n\otimes n\otimes n\otimes e_i = n\otimes n\otimes n\otimes e_i\otimes n\otimes e_i,\\ e_i\otimes n\otimes e_i\otimes e_j\otimes e_j\otimes n = e_i\otimes e_j\otimes e_i\otimes n\otimes e_j\otimes n. \end{array} \tag{5.65}$$

Note that the last term, $e_i\otimes n\otimes e_i\otimes e_j\otimes e_j\otimes n$, can be written as $n\otimes e_i\otimes e_i\otimes e_j\otimes e_j\otimes n = n\otimes\mathbf{I}\otimes\mathbf{I}\otimes n$.

Thus, the expression of the sixth order tensor (5.63) can be reduced to:

$$\mathfrak{D}(\boldsymbol{\varepsilon},\overset{\circ}{\boldsymbol{\sigma}},n)=\frac{\partial^3 U_R(\boldsymbol{\varepsilon},\overset{\circ}{\boldsymbol{\sigma}},n)}{\partial\boldsymbol{\varepsilon}^2\partial\,\overset{\circ}{\boldsymbol{\sigma}}}=\frac{\partial\boldsymbol{\sigma}_R(\boldsymbol{\varepsilon},\overset{\circ}{\boldsymbol{\sigma}},n)}{\partial\boldsymbol{\varepsilon}\partial\,\overset{\circ}{\boldsymbol{\sigma}}}=$$
$$2\beta_1\mathbf{I}\otimes\mathbf{I}\otimes\mathbf{I}+2\beta_2\mathbf{I}\otimes\mathbf{I}\otimes n\otimes n+2\beta_3\mathbf{I}\otimes n\otimes n\otimes\mathbf{I}+2\beta_4\mathbf{I}\otimes n\otimes n\otimes n\otimes n+2\beta_5\mathbf{I}\otimes e_i\otimes e_j\otimes e_i\otimes e_j+$$
$$4\beta_6\ \mathbf{I}\otimes n\otimes e_i\otimes n\otimes e_i+2\beta_7(n\otimes n)\otimes(n\otimes n)\otimes\mathbf{I}+2\beta_8(n\otimes n)\otimes(n\otimes n)\otimes(n\otimes n)+$$
$$\beta_9[e_i\otimes e_j\otimes n\otimes n\otimes e_i\otimes e_j+n\otimes n\otimes e_i\otimes e_j\otimes e_i\otimes e_j]+4\beta_{10}n\otimes n\otimes n\otimes e_i\otimes n\otimes e_i+2\beta_{11}\mathbb{I}\otimes\mathbf{I}+$$
$$2\beta_{12}\mathbb{I}\otimes n\otimes n+2\beta_{13}n\otimes e_i\otimes n\otimes e_i\otimes\mathbf{I}+2\beta_{14}n\otimes e_i\otimes n\otimes e_i\otimes n\otimes n+2\beta_{15}e_i\otimes e_j\otimes e_k\otimes e_i\otimes e_j\otimes e_k+$$
$$2\beta_{16}[2(n\otimes\mathbf{I}\otimes\mathbf{I}\otimes n+n\otimes e_i\otimes e_j\otimes n\otimes e_i\otimes e_j]\quad(5.66)$$

5.6 Incremental elasticity tensor for incompressible material

By imposing the incompressibility condition, $tr(\boldsymbol{\varepsilon})=0$, the expression of the stress tensor $\boldsymbol{\sigma}$ (5.33) can be simplified as:

$$\boldsymbol{\sigma}_R(\boldsymbol{\varepsilon},\overset{\circ}{\boldsymbol{\sigma}},n)=\frac{\partial\hat{U}_R(J_i)}{\partial\boldsymbol{\varepsilon}}=$$
$$=\{\beta_3 tr(\overset{\circ}{\boldsymbol{\sigma}})(n\boldsymbol{\varepsilon}n)+\beta_4(n\,\overset{\circ}{\boldsymbol{\sigma}}\,n)(n\boldsymbol{\varepsilon}n)+\beta_5 tr(\boldsymbol{\varepsilon}\,\overset{\circ}{\boldsymbol{\sigma}})+\beta_6(n\boldsymbol{\varepsilon}\,\overset{\circ}{\boldsymbol{\sigma}}\,n+n\,\overset{\circ}{\boldsymbol{\sigma}}\,\boldsymbol{\varepsilon}n)\}\mathbf{I}+$$
$$\{2\beta_7(n\boldsymbol{\varepsilon}n)tr(\overset{\circ}{\boldsymbol{\sigma}})+2\beta_8(n\boldsymbol{\varepsilon}n)(n\,\overset{\circ}{\boldsymbol{\sigma}}\,n)+\beta_9 tr(\boldsymbol{\varepsilon}\,\overset{\circ}{\boldsymbol{\sigma}})+\beta_{10}(n\boldsymbol{\varepsilon}\,\overset{\circ}{\boldsymbol{\sigma}}\,n+n\,\overset{\circ}{\boldsymbol{\sigma}}\,\boldsymbol{\varepsilon}n)\}(n\otimes n)+$$
$$\beta_9(n\boldsymbol{\varepsilon}n)\,\overset{\circ}{\boldsymbol{\sigma}}+\{2\beta_{11}tr(\overset{\circ}{\boldsymbol{\sigma}})\boldsymbol{\varepsilon}+2\beta_{12}(n\,\overset{\circ}{\boldsymbol{\sigma}}\,n)\}\boldsymbol{\varepsilon}+\beta_{10}(n\boldsymbol{\varepsilon}n)\,\overset{\circ}{\boldsymbol{\sigma}}^*+\{\beta_{13}tr(\overset{\circ}{\boldsymbol{\sigma}})+\beta_{14}(n\,\overset{\circ}{\boldsymbol{\sigma}}\,n)\}\boldsymbol{\varepsilon}^*+$$
$$+\beta_{15}(\boldsymbol{\varepsilon}\,\overset{\circ}{\boldsymbol{\sigma}}+\overset{\circ}{\boldsymbol{\sigma}}\,\boldsymbol{\varepsilon})+\beta_{16}[\overset{\circ}{\boldsymbol{\sigma}}\,\boldsymbol{\varepsilon}^*+\boldsymbol{\varepsilon}\,\overset{\circ}{\boldsymbol{\sigma}}^*+(n\otimes n)\,\overset{\circ}{\boldsymbol{\sigma}}\,\boldsymbol{\varepsilon}+(n\otimes n)\boldsymbol{\varepsilon}\,\overset{\circ}{\boldsymbol{\sigma}}]\quad(5.67)$$

Expressions (5.52) and (5.66) reduces, respectively, to:

$$\frac{\partial^2 U_R(\boldsymbol{\varepsilon},\overset{\circ}{\boldsymbol{\sigma}},n)}{\partial\boldsymbol{\varepsilon}^2}=\frac{\partial\boldsymbol{\sigma}_R(\boldsymbol{\varepsilon},\overset{\circ}{\boldsymbol{\sigma}},n)}{\partial\boldsymbol{\varepsilon}}=$$
$$\beta_3 tr(\overset{\circ}{\boldsymbol{\sigma}})\mathbf{I}\otimes(n\otimes n)+\beta_4(n\,\overset{\circ}{\boldsymbol{\sigma}}\,n)\mathbf{I}\otimes(n\otimes n)+\beta_5\mathbf{I}\otimes\overset{\circ}{\boldsymbol{\sigma}}+2\beta_6\,\overset{\circ}{\boldsymbol{\sigma}}^*\otimes\mathbf{I}+$$
$$2\beta_7 tr(\overset{\circ}{\boldsymbol{\sigma}})(n\otimes n)\otimes(n\otimes n)+2\beta_8(n\,\overset{\circ}{\boldsymbol{\sigma}}\,n)(n\otimes n)\otimes(n\otimes n)+2\beta_9\,\overset{\circ}{\boldsymbol{\sigma}}\otimes(n\otimes n)+$$
$$2\beta_{10}\,\overset{\circ}{\boldsymbol{\sigma}}^*\otimes(n\otimes n)+2\beta_{11}tr(\overset{\circ}{\boldsymbol{\sigma}})\mathbb{I}+2\beta_{12}(n\,\overset{\circ}{\boldsymbol{\sigma}}\,n)\mathbb{I}+2\beta_{13}tr(\overset{\circ}{\boldsymbol{\sigma}})(n\otimes e_i\otimes n\otimes e_i)+$$
$$2\beta_{14}(n\,\overset{\circ}{\boldsymbol{\sigma}}\,n)(n\otimes e_i\otimes n\otimes e_i)+2\beta_{15}e_i\otimes\overset{\circ}{\boldsymbol{\sigma}}\otimes e_i+2\beta_{16}[2e_i\otimes n\otimes e_i\otimes\overset{\circ}{\boldsymbol{\sigma}}\,n+n\otimes\overset{\circ}{\boldsymbol{\sigma}}\otimes n]\quad(5.68)$$

$$\mathfrak{D}(\boldsymbol{\varepsilon},\overset{\circ}{\boldsymbol{\sigma}},n)=\frac{\partial^3 U_R(\boldsymbol{\varepsilon},\overset{\circ}{\boldsymbol{\sigma}},n)}{\partial\boldsymbol{\varepsilon}^2\partial\,\overset{\circ}{\boldsymbol{\sigma}}}=\frac{\partial\boldsymbol{\sigma}_R(\boldsymbol{\varepsilon},\overset{\circ}{\boldsymbol{\sigma}},n)}{\partial\boldsymbol{\varepsilon}\partial\,\overset{\circ}{\boldsymbol{\sigma}}}=$$
$$\beta_3\mathbf{I}\otimes n\otimes n\otimes\mathbf{I}+\beta_4\mathbf{I}\otimes n\otimes n\otimes n\otimes n+\beta_5\mathbf{I}\otimes e_i\otimes e_j\otimes e_i\otimes e_j+4\beta_6\ \mathbf{I}\otimes n\otimes e_i\otimes n\otimes e_i+$$
$$2\beta_7(n\otimes n)\otimes(n\otimes n)\otimes\mathbf{I}+2\beta_8(n\otimes n)\otimes(n\otimes n)\otimes(n\otimes n)+\beta_9[e_i\otimes e_j\otimes n\otimes n\otimes e_i\otimes e_j+$$
$$n\otimes n\otimes e_i\otimes e_j\otimes e_i\otimes e_j]+4\beta_{10}n\otimes n\otimes n\otimes e_i\otimes n\otimes e_i+2\beta_{11}\mathbb{I}\otimes\mathbf{I}+2\beta_{12}\mathbb{I}\otimes n\otimes n+$$
$$2\beta_{13}n\otimes e_i\otimes n\otimes e_i\otimes\mathbf{I}+2\beta_{14}n\otimes e_i\otimes n\otimes e_i\otimes n\otimes n+2\beta_{15}e_i\otimes e_j\otimes e_k\otimes e_i\otimes e_j\otimes e_k+$$
$$2\beta_{16}[2(n\otimes\mathbf{I}\otimes\mathbf{I}\otimes n+n\otimes e_i\otimes e_j\otimes n\otimes e_i\otimes e_j]\quad(5.69)$$

5.7 Explicit constitutive law in the case in which $n = e_z$

In order to obtain a useful constitutive law for the axially symmetric sintered specimens, the obtained relation (5.37) can be written in the cylindrical coordinate system (r, ϕ, z). In such a coordinate system, let $n = e_z$, some important simplifications can be performed:

$$
\begin{aligned}
&n\boldsymbol{\varepsilon}n = e_z\boldsymbol{\varepsilon}e_z = \boldsymbol{\varepsilon}_z,\\
&n\ \overset{\circ}{\boldsymbol{\sigma}}\ n = e_z\ \overset{\circ}{\boldsymbol{\sigma}}\ e_z = \overset{\circ}{\boldsymbol{\sigma}}_z,\\
&n\boldsymbol{\varepsilon}\ \overset{\circ}{\boldsymbol{\sigma}}\ n = e_z\boldsymbol{\varepsilon}\ \overset{\circ}{\boldsymbol{\sigma}}\ e_z = \boldsymbol{\varepsilon}_{rz}\ \overset{\circ}{\boldsymbol{\sigma}}_{rz} + \boldsymbol{\varepsilon}_{\phi z}\ \overset{\circ}{\boldsymbol{\sigma}}_{\phi z} + \boldsymbol{\varepsilon}_z\ \overset{\circ}{\boldsymbol{\sigma}}_z =: (\boldsymbol{\varepsilon}\ \overset{\circ}{\boldsymbol{\sigma}})_z,\\
&n \otimes n = \begin{bmatrix} 0 & 0 & 0\\ 0 & 0 & 0\\ 0 & 0 & 1 \end{bmatrix} := \mathbf{I}_{zz},\\
&\boldsymbol{\varepsilon}^* = \begin{bmatrix} 0 & 0 & \boldsymbol{\varepsilon}_{rz}\\ 0 & 0 & \boldsymbol{\varepsilon}_{\phi z}\\ \boldsymbol{\varepsilon}_{rz} & \boldsymbol{\varepsilon}_{\phi z} & 2\boldsymbol{\varepsilon}_z \end{bmatrix},\\
&\overset{\circ}{\boldsymbol{\sigma}}{}^* = \begin{bmatrix} 0 & 0 & \overset{\circ}{\boldsymbol{\sigma}}_{rz}\\ 0 & 0 & \overset{\circ}{\boldsymbol{\sigma}}_{\phi z}\\ \overset{\circ}{\boldsymbol{\sigma}}_{rz} & \overset{\circ}{\boldsymbol{\sigma}}_{\phi z} & 2\ \overset{\circ}{\boldsymbol{\sigma}}_z \end{bmatrix}.
\end{aligned}
\tag{5.70}
$$

The constitutive law (5.37) can thus written as

$$
\begin{aligned}
&\boldsymbol{\sigma} - (\mathbf{W}\overset{\circ}{\boldsymbol{\sigma}} + \overset{\circ}{\boldsymbol{\sigma}}\mathbf{W}^{\mathbf{T}} = \overset{\circ}{\boldsymbol{\sigma}} + \boldsymbol{\varepsilon}\ \overset{\circ}{\boldsymbol{\sigma}} + \overset{\circ}{\boldsymbol{\sigma}}\ \boldsymbol{\varepsilon}^T - (tr\boldsymbol{\varepsilon})\ \overset{\circ}{\boldsymbol{\sigma}} + \lambda(tr\boldsymbol{\varepsilon})\mathbf{I} + 2\mu\boldsymbol{\varepsilon} + \alpha_1\boldsymbol{\varepsilon}_z n \otimes n +\\
&+ \alpha_2[\boldsymbol{\varepsilon}_z\mathbf{I} + tr(\boldsymbol{\varepsilon})\mathbf{I}_{zz}] + 2\alpha_3\boldsymbol{\varepsilon} * + \{2\beta_1 tr(\boldsymbol{\varepsilon})tr(\overset{\circ}{\boldsymbol{\sigma}}) + 2\beta_2 tr(\boldsymbol{\varepsilon})\ \overset{\circ}{\boldsymbol{\sigma}}_z + \beta_3 tr(\overset{\circ}{\boldsymbol{\sigma}})\boldsymbol{\varepsilon}_z +\\
&+\beta_4\ \overset{\circ}{\boldsymbol{\sigma}}_z\ \boldsymbol{\varepsilon}_z + \beta_5 tr(\boldsymbol{\varepsilon}\ \overset{\circ}{\boldsymbol{\sigma}}) + 2\beta_6(\boldsymbol{\varepsilon}\ \overset{\circ}{\boldsymbol{\sigma}})_z\}\mathbf{I} + \{\beta_3 tr(\overset{\circ}{\boldsymbol{\sigma}})tr(\boldsymbol{\varepsilon}) + \beta_4\ \overset{\circ}{\boldsymbol{\sigma}}_z\ tr(\boldsymbol{\varepsilon}) + 2\beta_7\boldsymbol{\varepsilon}_z tr(\overset{\circ}{\boldsymbol{\sigma}}) +\\
&+ 2\beta_8\boldsymbol{\varepsilon}_z\ \overset{\circ}{\boldsymbol{\sigma}}_z + \beta_9 tr(\boldsymbol{\varepsilon}\ \overset{\circ}{\boldsymbol{\sigma}}) + \beta_{10}(\boldsymbol{\varepsilon}\ \overset{\circ}{\boldsymbol{\sigma}})_z\}\mathbf{I}_{zz} + \{\beta_5 tr(\boldsymbol{\varepsilon}) + \beta_9\boldsymbol{\varepsilon}_z\}\ \overset{\circ}{\boldsymbol{\sigma}} + \{2\beta_{11} tr(\overset{\circ}{\boldsymbol{\sigma}})\boldsymbol{\varepsilon} +\\
&2\beta_{12}\ \overset{\circ}{\boldsymbol{\sigma}}_z\}\boldsymbol{\varepsilon} + + \{\beta_6 tr(\boldsymbol{\varepsilon}) + \beta_{10}\boldsymbol{\varepsilon}_z\}\ \overset{\circ}{\boldsymbol{\sigma}}{}^* + \{\beta_{13} tr(\overset{\circ}{\boldsymbol{\sigma}}) + \beta_{14}\ \overset{\circ}{\boldsymbol{\sigma}}_z\}\boldsymbol{\varepsilon}^* +\\
&\beta_{15}(\boldsymbol{\varepsilon}\ \overset{\circ}{\boldsymbol{\sigma}} + \overset{\circ}{\boldsymbol{\sigma}}\ \boldsymbol{\varepsilon}) + \beta_{16}[\overset{\circ}{\boldsymbol{\sigma}}\ \boldsymbol{\varepsilon}^* + \boldsymbol{\varepsilon}\ \overset{\circ}{\boldsymbol{\sigma}}{}^* + \mathbf{I}_{zz}(\overset{\circ}{\boldsymbol{\sigma}}\ \boldsymbol{\varepsilon} + \boldsymbol{\varepsilon}\ \overset{\circ}{\boldsymbol{\sigma}})]
\end{aligned}
\tag{5.71}
$$

For linear elastic incompressible, material with residual stress, whit transverse isotropy axes e_z, the constitutive law (5.71) reduces to:

$$
\begin{aligned}
&\boldsymbol{\sigma} - (\mathbf{W}\overset{\circ}{\boldsymbol{\sigma}} + \overset{\circ}{\boldsymbol{\sigma}}\mathbf{W}^{\mathbf{T}} = \overset{\circ}{\boldsymbol{\sigma}} + \boldsymbol{\varepsilon}\ \overset{\circ}{\boldsymbol{\sigma}} + \overset{\circ}{\boldsymbol{\sigma}}\ \boldsymbol{\varepsilon}^T + 2\mu\boldsymbol{\varepsilon} + \alpha_1\boldsymbol{\varepsilon}_z n \otimes n + \alpha_2\boldsymbol{\varepsilon}_z\mathbf{I} + 2\alpha_3\boldsymbol{\varepsilon} * +\\
&+\{\beta_3 tr(\overset{\circ}{\boldsymbol{\sigma}})\boldsymbol{\varepsilon}_z + \beta_4\ \overset{\circ}{\boldsymbol{\sigma}}_z\ \boldsymbol{\varepsilon}_z + \beta_5 tr(\boldsymbol{\varepsilon}\ \overset{\circ}{\boldsymbol{\sigma}}) + 2\beta_6(\boldsymbol{\varepsilon}\ \overset{\circ}{\boldsymbol{\sigma}})_z\}\mathbf{I} + \{2\beta_7\boldsymbol{\varepsilon}_z tr(\overset{\circ}{\boldsymbol{\sigma}}) + 2\beta_8\boldsymbol{\varepsilon}_z\ \overset{\circ}{\boldsymbol{\sigma}}_z + \beta_9 tr(\boldsymbol{\varepsilon}\ \overset{\circ}{\boldsymbol{\sigma}}) +\\
&+ \beta_{10}(\boldsymbol{\varepsilon}\ \overset{\circ}{\boldsymbol{\sigma}})_z\}\mathbf{I}_{zz} + \{\beta_9\boldsymbol{\varepsilon}_z\}\ \overset{\circ}{\boldsymbol{\sigma}} + \{2\beta_{11} tr(\overset{\circ}{\boldsymbol{\sigma}})\boldsymbol{\varepsilon} + 2\beta_{12}\ \overset{\circ}{\boldsymbol{\sigma}}_z\}\boldsymbol{\varepsilon} + \{\beta_{10}\boldsymbol{\varepsilon}_z\}\ \overset{\circ}{\boldsymbol{\sigma}}{}^* +\\
&\{\beta_{13} tr(\overset{\circ}{\boldsymbol{\sigma}}) + \beta_{14}\ \overset{\circ}{\boldsymbol{\sigma}}_z\}\boldsymbol{\varepsilon}^* + \beta_{15}(\boldsymbol{\varepsilon}\ \overset{\circ}{\boldsymbol{\sigma}} + \overset{\circ}{\boldsymbol{\sigma}}\ \boldsymbol{\varepsilon}) + \beta_{16}[\overset{\circ}{\boldsymbol{\sigma}}\ \boldsymbol{\varepsilon}^* + \boldsymbol{\varepsilon}\ \overset{\circ}{\boldsymbol{\sigma}}{}^* + \mathbf{I}_{zz}(\overset{\circ}{\boldsymbol{\sigma}}\ \boldsymbol{\varepsilon} + \boldsymbol{\varepsilon}\ \overset{\circ}{\boldsymbol{\sigma}})]
\end{aligned}
\tag{5.72}
$$

Chapter 6

Residual stress and mechanical behavior of sintered cylindrical specimens.

6.1 Introduction

The consequences of a porous-viscous-elastic-nonlinear constitutive relation, describing the mechanical behavior of a body undergoing sintering is analyzed in the previous chapters. In particular, the case of a axially-symmetric specimen subject to

- (i) isostatic pressing (also covering the case of free sintering),
- (ii) free forging,
- (iii) constrained forging,

are investigated in Chapters $2, 3, 4$ respectively. The focus of this studies is to underline the effects of the pressure in the pores during the processes and on the properties (e.g. the residual porosity) of the sintered materials. The two fundamental cases in which such a pressure is negligible with respect to the applied stresses and in the case of moderate stresses (in comparison with the interstitial gas pressure) are investigated and compared. In the sequel, only cases (i) and (iii) are of interest and yet analyzed.

It is worth emphasizing that mechanical components made by sintered alloys have the advantage to be suitable for applications in the as-sintered state.

Henceforth, sintering is the phase during which such components acquire the mechanical properties required for their utilization. Obviously, such properties are strongly influenced by the stress at the end of the sintering; this is expected to be a function of the material properties, of the Laplace pressure as well as of the loading mode.

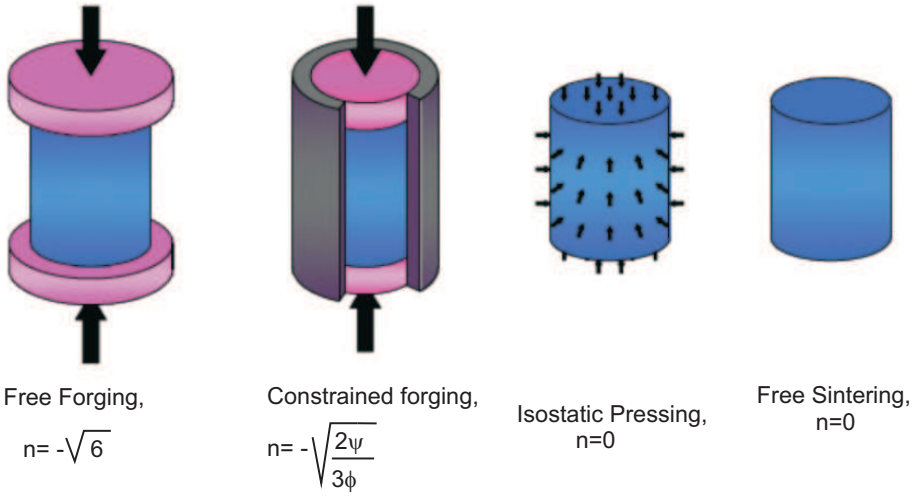

Figure 6.1: Different loading modes: forging, costrained forging, isostatic pressing, free sintering

In particular, as mentioned in Chapter 5, the material behavior, and so the exhibited symmetries, depend upon the adopting loading mode. During their regular utilization, specimens sintered through isostatic pressing may exhibit linear elastic isotropic behavior, whereas those ones sintered through constrained forging present a linear elastic axially transversely isotropic behavior.

The mechanical behavior of a linear elastic prestressed material is given through the following general constitutive law in linear elasticity, clarified in [28], which may be written as:

$$\boldsymbol{\sigma} = \mathring{\boldsymbol{\sigma}} + \mathbf{H}\mathring{\boldsymbol{\sigma}} + \mathring{\boldsymbol{\sigma}}\mathbf{H}^T - (tr\boldsymbol{\varepsilon})\,\mathring{\boldsymbol{\sigma}} + \mathfrak{L}[\mathring{\boldsymbol{\sigma}}, \boldsymbol{\varepsilon}], \tag{6.1}$$

where $\boldsymbol{\sigma}$ is the Cauchy stress, $\mathring{\boldsymbol{\sigma}}$ is the residual stress, $\mathbf{H}$ is the displacement gradient and $\boldsymbol{\varepsilon} = (\mathbf{H} + \mathbf{H}^T)/2$ is the strain tensor. The quantity $\mathfrak{L}$ is the sixth-order incremental elasticity tensor for prestressed materials; its action on both the residual stress $\mathring{\boldsymbol{\sigma}}$ and on the strain $\boldsymbol{\varepsilon}$ results in a second order tensor. Whenever $\mathring{\boldsymbol{\sigma}} = \mathbf{0}$, $\mathfrak{L}[\mathbf{0}, \boldsymbol{\varepsilon}] = \mathbb{C}[\boldsymbol{\varepsilon}]$, namely it reduces to the classical elastic constitutive equation.

The representation formula for $\mathfrak{L}$ in the case of isotropic linear elastic material with residual stress is given by Man [28]. For the case of transverse isotropy the explicit formula for such a tensor is derived in this thesis. The starting point is to enforce hyperelasticity (see e.g. [30], Chapter 5), namely to construct the suitable stored elastic energy whose (partial) second derivative with respect to both strain and residual stress generate the appropriate $\mathfrak{L}$.

6.2 Preliminaries

In Chapters 2, 3, 4 of this thesis, the mechanical response of a material undergoing sintering is described by a porous-viscous-elastic-nonlinear constitutive relation, relating the stress and the (infinitesimal) strain rate tensor $\dot{\boldsymbol{\varepsilon}}$ [29]. The $i^{th} - j^{th}$ component of the stress reads as follows:

$$\sigma_{ij} = \frac{\sigma(w)}{w}[\varphi\dot{\varepsilon}'_{ij} + \psi\dot{e}\delta_{ij}] + p_l\delta_{ij}, \tag{6.2}$$

where $\dot{\boldsymbol{\varepsilon}}'$ denotes the deviatoric strain rate tensor, and w is an effective equivalent strain rate, connected with the current porosity and with the invariants of the strain rate tensor, i.e.:

$$w = \frac{1}{\sqrt{1-\theta}}\sqrt{\varphi\dot{\gamma}^2 + \psi\dot{e}^2}; \tag{6.3}$$

where the quantities $\dot{e}$ and γ are the first and the second invariants of the strain rate tensor (see Chapter 2 for more extended discussion of the constitutive equation). The quantities φ, ψ, p_l and their dependence upon the porosity are treated in [9, 19, 21, 23] and summarized in the first Chapter of this thesis.

The dependence of effective equivalent stress $\sigma(w)$ on the effective equivalent strain rate w determines the constitutive behavior of a porous material. Following Ashby [18], a power-law mechanism of deformation is assumed:

$$\frac{\sigma(w)}{\sigma_0} = A\Big(\frac{w}{\dot{\boldsymbol{\varepsilon}}_0}\Big)^m, \tag{6.4}$$

where A and m are material constants (A is the temperature dependent, $0 < m < 1$), σ_0 and ε_0 are the reference stress and the reference strain rate, respectively. Two limiting cases corresponding respectively to the ideal plasticity and linear viscosity are given by $m = 0$ and $m = 1$.

Equations (6.4) and (6.3) can be used to obtain the ratio between the effective equivalent stress $\sigma(w)$ and the effective equivalent strain rate w:

$$\frac{\sigma(w)}{w} = \frac{\sigma_0 A}{\dot{\varepsilon}_0^m} w^{m-1} = \frac{\sigma_0 A}{\dot{\varepsilon}_0^m}|\dot{e}|^{m-1}\Big[\frac{\psi}{1-\theta}\Big(\frac{\psi}{\varphi}n^2 + 1\Big)\Big]^{\frac{m-1}{2}}. \tag{6.5}$$

In the present thesis, following [43], a cylindrical axially-symmetric specimen, subjected to an external load, is considered. The porosity, θ, is supposed to be constant through the specimen and it is defined as the ratio between the pore volume and the volume of the porous body (see [43]).
Moreover, a volume averages of the stress and strain rate may be considered. In particular, the stress tensor has the diagonal form:

$$[\boldsymbol{\sigma}] = \begin{bmatrix} \sigma_r & 0 & 0 \\ 0 & \sigma_r & 0 \\ 0 & 0 & \sigma_z \end{bmatrix}. \tag{6.6}$$

Following Olevsky [43], a loading mode parameter n, defined in Chapter 1 of the present thesis, can be introduced to describe the different loading modes (shown in figure 6.1). The loading mode parameter assumes the following values for the corresponding loading modes:

1. $n = 0$ for isostatic pressing;
2. $n \to \infty$ for pure shear (p = 0);
3. $n = -\sqrt{6}$ for forging;
4. $n = \sqrt{6}$ for drawing;
5. $n = \sqrt{\frac{2}{3}} sgn(\dot{\varepsilon_z}) \frac{\varphi}{\psi}$ for pressing in a rigid die (constrained forging).

From (6.2), the definition of the loading mode, and the kinetic relation between the porosity, the strain rates and the evolution of the cross-sectional area of the specimen (see Chapter 1), the evolution law can be obtain as follows:

$$\dot{\theta} = sgn(p)\dot{\varepsilon}_0(1-\theta)\Big(\frac{|\sigma_z - p_l|}{A\sigma_0}\Big)^{\frac{1}{m}}\Big[\frac{\psi}{1-\theta}(\frac{\varphi}{\psi}n^2+1)\Big]^{\frac{1-m}{2m}}\Big[\psi\Big|1+\sqrt{\frac{2}{3}}n\ sgn(\dot{\varepsilon}_z-\dot{\varepsilon}_r)\Big|\Big]^{\frac{-1}{m}} \tag{6.7}$$

This relation allows us to determine the time-evolution of the porosity, accounting for the contribution of the Laplace pressure. This is done for each loading mode. The analog of (6.7) by neglecting p_l was obtained by Olewsky and Molinari, [43] eq. 15.

In the sequel, the behavior of materials sintered by using both isostatic pressing and constrained forging are analyzed. The most important assumptions are the following:

- the exhibited behavior of the as-sintered mechanical component depends upon the loading mode during sintering (or hot-pressing): specimens sintered through isostatic pressing present (linearly elastic) isotropic behavior, whereas the ones sintered through constrained forging exhibit transverse isotropy;
- the residual stresses are basically unavoidable at the end of the sintering no matter what the loading mode may be. The corresponding tensor can be evaluated through equation (6.2), in which the values of strain rates, bulk and shear moduli and Laplace pressure are evaluated at time t_f, representing the duration of the process;
- because of the assumed incompressibility of the matrix (the shrinkage is totally due to the reduction of the porosity), the porosity does not change after the end of the process, and hence the sintered material is also incompressible.

6.3 Residual stress and material behavior after isostatic pressing

For the case of isostatic pressing, treated in [54], the stress tensor is hydrostatic, i.e. $\sigma_z = \sigma_r = \sigma$, and the loading mode parameter n is zero; the constitutive law (6.2) reduces to the following relation:

$$\sigma_{ij} = [\frac{\sigma(w)}{w}\psi\dot{e} + p_l]\delta_{ij}; \tag{6.8}$$

and the evolution law of the porosity (6.7) may be evaluated by integrating the resulting ordinary differential equation:

$$\dot{\theta} = -\dot{\varepsilon}_0(1-\theta)^{\frac{3m-1}{2m}}\Big(\frac{|\sigma - p_l|}{A\sigma_0}\Big)^{\frac{1}{m}}\psi^{\frac{-(1+m)}{2m}}. \tag{6.9}$$

This relationship allows us to determine the time-evolution of the porosity and to calculate the residual porosity at a given time, depending on the adopted model owing the bulk and shear moduli (as functions of the porosity), on the "driving forces" of sintering (the external load and the Laplace pressure), on the material constants and on process parameters like pressure, temperature, etc.

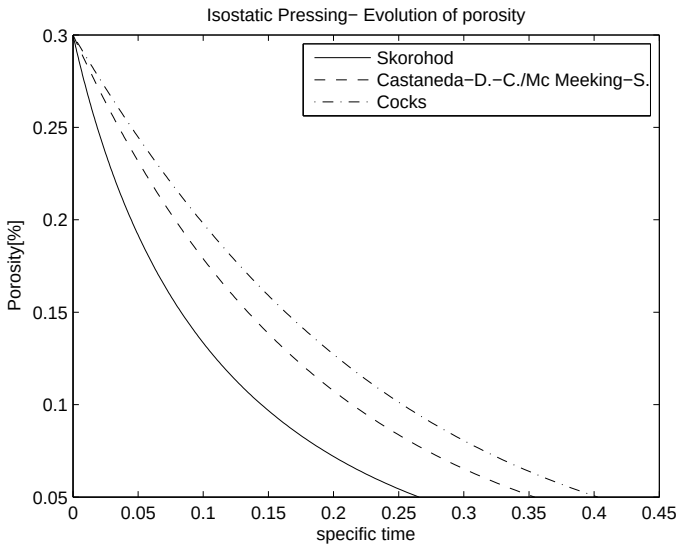

Figure 6.2: Evolution of the porosity

In the sequel, Figure 6.2 shows the evolution of the porosity during isostatic pressing where the porosity is reduced from 30% to 5%, where the shear and bulk moduli are evaluated by the technique developed by Skorohod, Castaneda and Cocks.

Furthermore, Figure 6.3 shows the comparison between the the evolution of the porosity and its residual value evaluated accounting for the effect of the

Laplace pressure and by neglecting it.

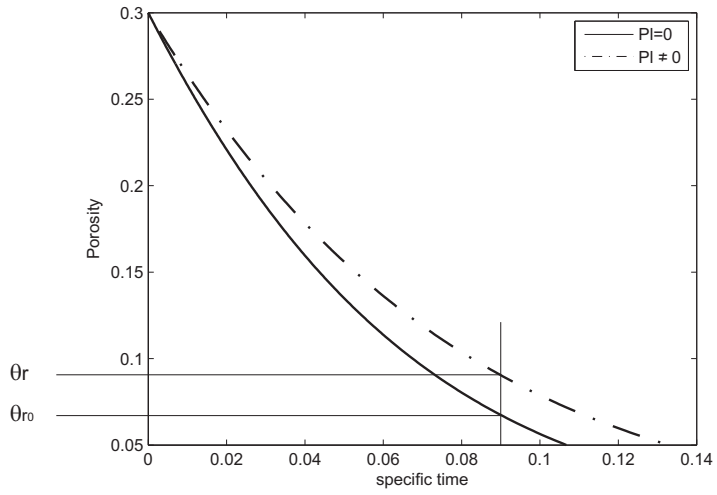

Figure 6.3: Residual porosity evaluated by neglecting and accounting for the effect of the Laplace pressure

6.3.1 Residual stress tensor

Components made by sintered alloys are usually employed in the as-sintered state, with the obvious advantage of avoiding thermal annealing.

The goal of the present study is indeed to evaluate the mechanical behavior of as-sintered specimens. At the end of the sintering process the residual stress $\overset{\circ}{\sigma}$ may depend on the residual porosity $\theta_r = \theta(t_f)$, the final strain the and on the loading mode.

The constitutive law (6.8), particularized for isostatic pressing, yields the following residual stress (averaged on the specimen volume):

$$\overset{\circ}{\sigma}_{ij}\,(t_f) = [\frac{\sigma(w)}{w(t_f)}\psi(t_f)\dot{e}(t_f) + p_l(t_f)]\delta_{ij}; \tag{6.10}$$

In isostatic pressing, the quantity $\frac{\sigma(w(t_f))}{w(t_f)}$, given by (6.3), takes the form (see Chapt. 2)

$$\frac{\sigma(w(t_f))}{w(t_f)} = \frac{\sigma_0 A}{\dot{\varepsilon_0}^m}[w(t_f)]^{m-1} = \frac{\sigma_0 A}{\dot{\varepsilon_0}}\Big[\frac{\varphi(t_f)\dot{\gamma^2}(t_f) + \psi(t_f)\dot{e^2}(t_f)}{1-\theta(t_f)}\Big]^{\frac{m-1}{2}}. \tag{6.11}$$

Hence, equations (6.10) reduces to:

$$\overset{\circ}{\sigma}_{ij}\,(t_f) = \Big[\frac{\sigma(w)}{w(t_f)}\psi(t_f)\dot{e}(t_f) + p_l(t_f)\Big]\delta_{ij} = \\ = \Big[\frac{\sigma_0 A}{\dot{\varepsilon_0}^m}\frac{\psi(t_f)^{\frac{m+1}{2}}\dot{e}(t_f)^m}{[1-\theta(t_f)]^{\frac{m-1}{2}}} + p_l(t_f)\Big]\delta_{ij}; \quad (6.12)$$

i.e. the residual stress tensor the form:

$$\overset{\circ}{\boldsymbol{\sigma}}\,(t_f) = \begin{bmatrix} p_0(t_f) & 0 & 0 \\ 0 & p_0(t_f) & 0 \\ 0 & 0 & p_0(t_f) \end{bmatrix} = p_0(t_f)\mathbf{I}, \quad (6.13)$$

after setting

$$p_0(t_f) = \frac{\sigma_0 A}{\dot{\varepsilon_0}^m}\frac{\psi(t_f)^{\frac{m+1}{2}}\dot{e}(t_f)^m}{[1-\theta(t_f)]^{\frac{m-1}{2}}} + p_l(t_f). \quad (6.14)$$

By substituting the relation between the rate of change of the porosity $\dot{e}$ and the porosity (see Capter 1), we can obtain the following expression for p_0:

$$p_0(t_f) = \frac{\sigma_0 A}{\dot{\varepsilon_0}^m}\Big[\frac{\psi(t_f)}{1-\theta(t_f)}\Big]^{\frac{m+1}{2}}\dot{\theta}(t_f)^m + p_l(t_f). \quad (6.15)$$

The value of the averaged residual stress p_0 depends only upon the residual porosity (both explicitly and implicitly, through the bulk modulus φ) and on the materials properties. It is important to note that, in the case of free sintering, at every instant of the process $p_l = \frac{\sigma(w)}{w}\psi\dot{e}$ (see Chapter 2), thus $p_0 = 0$. Hence, at the end of the free sintering process, the specimen has no residual stress on average.

6.3.2 The constitutive law after isostatic pressing

In order to evaluate the behavior of the sintered material, we may suppose that the material presents a linear elastic isotropic behavior. We consider the general constitutive law in linear elasticity:

$$\boldsymbol{\sigma} - (\mathbf{W}\,\overset{\circ}{\boldsymbol{\sigma}} - \overset{\circ}{\boldsymbol{\sigma}}\,\mathbf{W}) = \overset{\circ}{\boldsymbol{\sigma}} + \boldsymbol{\varepsilon}\,\overset{\circ}{\boldsymbol{\sigma}} + \overset{\circ}{\boldsymbol{\sigma}}\,\boldsymbol{\varepsilon} + (tr\boldsymbol{\varepsilon})\,\overset{\circ}{\boldsymbol{\sigma}} + \mathfrak{L}[\overset{\circ}{\boldsymbol{\sigma}}, \boldsymbol{\varepsilon}], \quad (6.16)$$

where $\mathfrak{L}[\overset{\circ}{\boldsymbol{\sigma}}, \boldsymbol{\varepsilon}]$ is the incremental elasticity tensor, reducing to the classical elasticity tensor $\mathbb{C}[\boldsymbol{\varepsilon}]$ when $\overset{\circ}{\boldsymbol{\sigma}} = 0$. For isotropic materials, $\mathbb{C}[\boldsymbol{\varepsilon}]$ takes the form:

$$\mathbb{C}[\boldsymbol{\varepsilon}] = \lambda(tr\boldsymbol{\varepsilon})\mathbf{I} + 2\mu\boldsymbol{\varepsilon}, \quad (6.17)$$

where λ and μ are the Lame's moduli.

Following Man (see [28]), we can write the following relation:

$$\mathfrak{L}[\overset{\circ}{\boldsymbol{\sigma}}, \boldsymbol{\varepsilon}] = \mathbb{C}[\boldsymbol{\varepsilon}] + \mathfrak{D}[\overset{\circ}{\boldsymbol{\sigma}}, \boldsymbol{\varepsilon}], \quad (6.18)$$

where, for isotropic materials,

$$\mathfrak{D}[\overset{\circ}{\boldsymbol{\sigma}}, \boldsymbol{\varepsilon}] = \beta_1(tr\boldsymbol{\varepsilon})(tr\ \overset{\circ}{\boldsymbol{\sigma}})\mathbf{I} + \beta_2(tr\ \overset{\circ}{\boldsymbol{\sigma}})\boldsymbol{\varepsilon} + \beta_3[(tr\boldsymbol{\varepsilon})\ \overset{\circ}{\boldsymbol{\sigma}} + (tr\boldsymbol{\varepsilon}\ \overset{\circ}{\boldsymbol{\sigma}})\mathbf{I}] + \beta_4[\boldsymbol{\varepsilon}\ \overset{\circ}{\boldsymbol{\sigma}} + \overset{\circ}{\boldsymbol{\sigma}}\ \boldsymbol{\varepsilon}]. \tag{6.19}$$

Since the residual stress is hydrostatic the term $\mathbf{W}\ \overset{\circ}{\boldsymbol{\sigma}} - \overset{\circ}{\boldsymbol{\sigma}}\ \mathbf{W}$ vanishes and hence by combining equations (6.16), (6.17), (6.18) and (6.19), we can write the constitutive equation for linear elastic isotropic materials with residual stresses:

$$\begin{aligned}\boldsymbol{\sigma} =& \overset{\circ}{\boldsymbol{\sigma}} + \boldsymbol{\varepsilon}\ \overset{\circ}{\boldsymbol{\sigma}} + \overset{\circ}{\boldsymbol{\sigma}}\ \boldsymbol{\varepsilon} + (tr\boldsymbol{\varepsilon})\ \overset{\circ}{\boldsymbol{\sigma}} + \lambda(tr\boldsymbol{\varepsilon})\mathbf{I} + 2\mu\boldsymbol{\varepsilon} + \\ &+ \beta_1(tr\boldsymbol{\varepsilon})(tr\ \overset{\circ}{\boldsymbol{\sigma}})\mathbf{I} + \beta_2(tr\ \overset{\circ}{\boldsymbol{\sigma}})\boldsymbol{\varepsilon} + \beta_3[(tr\boldsymbol{\varepsilon})\ \overset{\circ}{\boldsymbol{\sigma}} + (tr\boldsymbol{\varepsilon}\ \overset{\circ}{\boldsymbol{\sigma}})] + \beta_4[\boldsymbol{\varepsilon}\ \overset{\circ}{\boldsymbol{\sigma}} + \overset{\circ}{\boldsymbol{\sigma}}\ \boldsymbol{\varepsilon}].\end{aligned} \tag{6.20}$$

By substituting the value of the residual stress (6.13) into equation (6.19), (6.17) and (6.18), the following relation can be obtained:

$$\mathfrak{L}[\overset{\circ}{\boldsymbol{\sigma}}, \boldsymbol{\varepsilon}] = [\lambda + 3p_0\beta_1 + 2p_0\beta_3]tr(\boldsymbol{\varepsilon})\mathbf{I} + [2\mu + 3p_0\beta_2 + 2p_0\beta_4]\boldsymbol{\varepsilon} \tag{6.21}$$

By substitutin this relation and equation (6.13) into the explicit relation for the stress response (6.20), one can obtain:

$$\boldsymbol{\sigma} = p_0\mathbf{I} + 2p_0\boldsymbol{\varepsilon} + p_0(tr\boldsymbol{\varepsilon})\mathbf{I} + [\lambda + 3p_0\beta_1 + 2p_0\beta_3]tr(\boldsymbol{\varepsilon})\mathbf{I} + [2\mu + 3p_0\beta_2 + 2p_0\beta_4]\boldsymbol{\varepsilon} \tag{6.22}$$

Equation (6.22) states that the behavior of a linear isotropic elastic material with isotropic residual stress is defined by the value of the residual stress p_0, by the two elastic moduli μ (elastic shear modulus) and λ (elastic bulk modulus) and by a linear combinations of the material constants.

By comparing equation (6.21) for the incremental elasticity tensor, reducing to the classical elasticity tensor $\mathbb{C}[\boldsymbol{\varepsilon}]$ when $\overset{\circ}{\boldsymbol{\sigma}} = 0$, and (6.17), we may conveniently define the *equivalent shear and bulk moduli* μ^* and λ^* as follows:

$$\begin{cases} \lambda^* = \lambda + 3p_0\beta_1 + 2p_0\beta_3, \\ \mu^* = \frac{1}{2}[2\mu + 3p_0\beta_2 + 2p_0\beta_4]. \end{cases} \tag{6.23}$$

It is evident that, when the material has no residual stress ($p_0 = 0$), equation (6.23) reduces to

$$\begin{cases} \lambda^* = \lambda, \\ \mu^* = \mu. \end{cases} \tag{6.24}$$

Moreover, because of the matrix is incompressible and the porosity does not change after the end of the sintering process, we can assume that the sintered material is incompressible (i.e. $tr\boldsymbol{\varepsilon} = tr\boldsymbol{\varepsilon} = 0$). Hence, equations (6.20) and (6.22) reduces to:

$$\begin{aligned}\boldsymbol{\sigma} =& \overset{\circ}{\boldsymbol{\sigma}} + \boldsymbol{\varepsilon}\ \overset{\circ}{\boldsymbol{\sigma}} + \overset{\circ}{\boldsymbol{\sigma}}\ \boldsymbol{\varepsilon} + 2\mu\boldsymbol{\varepsilon} + \beta_2(tr\ \overset{\circ}{\boldsymbol{\sigma}})\boldsymbol{\varepsilon} + \beta_3(tr\boldsymbol{\varepsilon}\ \overset{\circ}{\boldsymbol{\sigma}}) + \beta_4[\boldsymbol{\varepsilon}\ \overset{\circ}{\boldsymbol{\sigma}} + \overset{\circ}{\boldsymbol{\sigma}}\ \boldsymbol{\varepsilon}] \\ &= p_0\mathbf{I} + 2p_0\boldsymbol{\varepsilon} + [2\mu + 3p_0\beta_2 + 2p_0\beta_4]\boldsymbol{\varepsilon}.\end{aligned} \tag{6.25}$$

Equation (6.25) states that the behavior of a linear isotropic elastic incompressible material with isotropic residual stress is defined by the value of the

residual stress, the elastic shear modulus μ and by a linear combination of β_2 and β_4. We may conveniently define the following material constant:

$$\beta := \frac{3\beta_2 + 2\beta_4}{2}. \tag{6.26}$$

Hence, the equivalent shear modulus μ^* (defined in (6.23) can be rewritten as follows:

$$\mu^* := \mu + \beta p_0. \tag{6.27}$$

Hence, in order to determine the material constant μ and β, it is sufficient to perform two experimental tests (see figure 6.4):

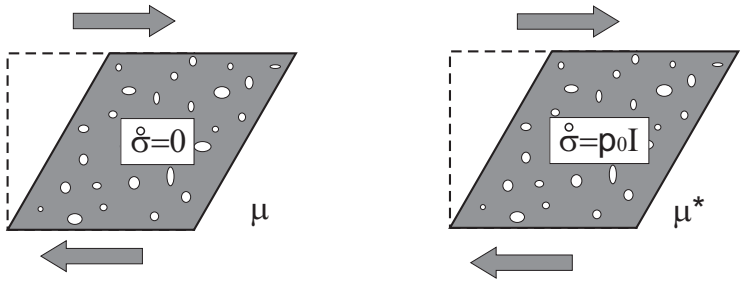

Figure 6.4: Experimenatl procedure to determine the material constants μ and β

- A shear test on thermally annealed free-sintered specimens would allow one to determine the value of the shear modulus μ for the virgin material;
- A shear test on sintered specimens, generally affected by residual stresses, would allow for determining the value of the effective shear modulus μ^*.

6.4 Residual stress and material behavior after constrained forging

Here we may consider the effects of external pressures p_b applied on the top and bottom bases of a given axially symmetric sample. For the sake of illustration, we may consider specimens with constant cross-sections (although this assumptions could be relaxed); this leads to having no radial strains, i.e. $\dot{\boldsymbol{\varepsilon}}_r = 0$.

By imposing this condition, relationship (6.7) reduces to:

$$\dot{\theta} = -\dot{\varepsilon}_0 \Big(\frac{|\sigma_z - p_l|}{A\sigma_0} \Big)^{\frac{1}{m}} (1-\theta)^{\frac{3m-1}{2m}} \Big(\frac{2\varphi}{3} + \psi \Big)^{\frac{-(1+m)}{2m}}. \tag{6.28}$$

6.4.1 Residual stress tensor

It order to evaluate the mechanical behavior of the considered sintered specimen. Similarly to what was done for isostatic pressing, the residual stress $\overset{\circ}{\boldsymbol{\sigma}}$ depending on the residual porosity obeys to equation (6.6) and has the form:

$$\overset{\circ}{\boldsymbol{\sigma}}(t_f) = \begin{bmatrix} \sigma_{r0}(t_f) & 0 & 0 \\ 0 & \sigma_{r0}(t_f) & 0 \\ 0 & 0 & \sigma_{z0}(t_f) \end{bmatrix}. \tag{6.29}$$

The components $\sigma_{r0}(t_f)$ and $\sigma_{z0}(t_f)$ can be evaluated through equations (6.10) and (6.32); furthermore, for forging in a rigid die, $\varepsilon(t_f) = 0$. This leads to:

$$\begin{cases} \dot{e}(t_f) = \dot{\varepsilon}_z(t_f), \\ \dot{\gamma} = \sqrt{\frac{2}{3}}|\dot{\varepsilon}_z(t_f)|. \end{cases} \tag{6.30}$$

The constitutive law (6.2) allows to determine the radial and axial components of the stress tensor:

$$\begin{cases} \sigma_{r0}(t_f) = \frac{\sigma(w)}{w(t_f)}\Big[-\frac{\varphi(t_f)}{3} + \psi(t_f)\Big]\dot{\varepsilon}_z(t_f) + p_l(t_f), \\ \sigma_{z0}(t_f) = \frac{\sigma(w)}{w(t_f)}\Big[\frac{2\varphi(t_f)}{3} + \psi(t_f)\Big]\dot{\varepsilon}_z(t_f) + p_l(t_f). \end{cases} \tag{6.31}$$

Here the quantity $\frac{\sigma(w)}{w(t_f)}$, given by equation (6.32), reduces to the following expression:

$$\frac{\sigma(w)}{w(t_f)} = \frac{\sigma_0 A}{\dot{\varepsilon_0}^m}[w(t_f)]^{m-1} = \frac{\sigma_0 A}{\dot{\varepsilon}_0}\dot{\boldsymbol{\varepsilon}}_z(t_f)^{(m-1)}\Big[\frac{\psi + 2/3\varphi}{1-\theta}\Big]^{\frac{m-1}{2}}. \tag{6.32}$$

In analogy to (6.13), the residual stresses take the form

$$\begin{cases} \sigma_{z0}(t_f) = \frac{\sigma(w)}{w(t_f)}\Big[\frac{2\varphi}{3} + \psi + \frac{p_l}{\dot{\varepsilon}_z}\frac{w(t_f)}{\sigma(w)}\Big]\dot{\varepsilon}_z = (1+x)p_0, \\ \\ \qquad\qquad where \\ \\ p_0 := \sigma_{r0}(t_f) = \frac{\sigma(w)}{w(t_f)}\Big[-\frac{\varphi}{3} + \psi + \frac{p_l}{\dot{\varepsilon}_z}\frac{w(t_f)}{\sigma(w)}\Big]\dot{\varepsilon}_z, \end{cases} \tag{6.33}$$

and x is an non-dimensional parameter defined as follows:

$$x = \frac{\frac{2\varphi}{3} + \psi + \frac{p_l}{\dot{\varepsilon}_z}\frac{w(t_f)}{\sigma(w)}}{-\frac{\varphi}{3} + \psi + \frac{p_l}{\dot{\varepsilon}_z}\frac{w(t_f)}{\sigma(w)}} - 1. \tag{6.34}$$

Finally, we may write the residual stress tensor as

$$\overset{\circ}{\boldsymbol{\sigma}}(t_f) = \begin{bmatrix} p_0 & 0 & 0 \\ 0 & p_0 & 0 \\ 0 & 0 & (1+x)p_0 \end{bmatrix} = p_0\mathbf{I} + xp_0\mathbf{I}_{zz}, \tag{6.35}$$

where $\mathbf{I}$ is the second order identity tensor and

$$\mathbf{I}_{zz} := e_z \otimes e_z = \begin{bmatrix} 0 & 0 & 0 \\ 0 & 0 & 0 \\ 0 & 0 & 1 \end{bmatrix}. \tag{6.36}$$

In the sequel the quantity $\mathbf{W}\,\overset{\circ}{\boldsymbol{\sigma}} - \overset{\circ}{\boldsymbol{\sigma}}\,\mathbf{W}$ where, for the sake of brevity, here $\overset{\circ}{\boldsymbol{\sigma}}$ is identified with $\overset{\circ}{\boldsymbol{\sigma}}\,(t_f)$, needs to be evaluated. Equation 6.35 implies that the following relation holds:

$$\mathbf{W}\,\overset{\circ}{\boldsymbol{\sigma}} - \overset{\circ}{\boldsymbol{\sigma}}\,\mathbf{W} = xp_0(\mathbf{W}\,\mathbf{I}_{zz} - \mathbf{I}_{zz}\mathbf{W}) = -xp_0 \begin{bmatrix} 0 & 0 & w_{31} \\ 0 & 0 & w_{32} \\ w_{31} & w_{32} & 0 \end{bmatrix}. \tag{6.37}$$

6.4.2 Incremental elasticity tensor for transversely isotropic material

Further loading on samples sintered through constrained forging may result on a linear elastic transverse isotropic stress response of the material. The elasticity tensor $\mathbb{C}$ is then given by (see e.g. Weiyi, [30]):

$$\begin{aligned}\mathbb{C} = \lambda\mathbf{I}\otimes\mathbf{I} + 2\mu\mathbb{I} + \alpha_1 n\otimes n\otimes n\otimes n + \alpha_2[\mathbf{I}\otimes n\otimes n + n\otimes n\otimes\mathbf{I}] + \\ \alpha_3[n\otimes e_i\otimes n\otimes e_i + e_i\otimes n\otimes e_i\otimes n + e_i\otimes n\otimes n\otimes e_i + n\otimes e_i\otimes e_i\otimes n]\end{aligned} \tag{6.38}$$

and by applying such a tensor to the strain $\boldsymbol{\varepsilon}$, we obtain the following expression:

$$\mathbb{C}[\boldsymbol{\varepsilon}] = \lambda(tr\boldsymbol{\varepsilon})\mathbf{I} + 2\mu\boldsymbol{\varepsilon} + \alpha_1(n\boldsymbol{\varepsilon}n)n\otimes n + \alpha_2[\mathbf{I}(n\boldsymbol{\varepsilon}n) + tr(\boldsymbol{\varepsilon})n\otimes n] + 2\alpha_3[n\cdot\boldsymbol{\varepsilon}\otimes n + n\otimes\boldsymbol{\varepsilon}\cdot n]. \tag{6.39}$$

The corresponding incremental elasticity tensor has been obtained in Chapter 5 of the present thesis and it may be recalled as follows:

$$\begin{aligned}\mathfrak{D}(\boldsymbol{\varepsilon}, \overset{\circ}{\boldsymbol{\sigma}}, n) = \frac{\partial^3 U_R(\boldsymbol{\varepsilon}, \overset{\circ}{\boldsymbol{\sigma}}, n)}{\partial\boldsymbol{\varepsilon}^2\partial\,\overset{\circ}{\boldsymbol{\sigma}}} = \frac{\partial\boldsymbol{\sigma}_R(\boldsymbol{\varepsilon}, \overset{\circ}{\boldsymbol{\sigma}}, n)}{\partial\boldsymbol{\varepsilon}\partial\,\overset{\circ}{\boldsymbol{\sigma}}} = \\ 2\beta_1\mathbf{I}\otimes\mathbf{I}\otimes\mathbf{I} + 2\beta_2\mathbf{I}\otimes\mathbf{I}\otimes n\otimes n + 2\beta_3\mathbf{I}\otimes n\otimes n\otimes\mathbf{I} + 2\beta_4\mathbf{I}\otimes n\otimes n\otimes n\otimes n + 2\beta_5\mathbf{I}\otimes e_i\otimes e_j\otimes e_i\otimes e_j + \\ 4\beta_6\ \mathbf{I}\otimes n\otimes e_i\otimes n\otimes e_i + 2\beta_7(n\otimes n)\otimes(n\otimes n)\otimes\mathbf{I} + 2\beta_8(n\otimes n)\otimes(n\otimes n)\otimes(n\otimes n) + \\ \beta_9[e_i\otimes e_j\otimes n\otimes n\otimes e_i\otimes e_j + n\otimes n\otimes e_i\otimes e_j\otimes e_i\otimes e_j] + 4\beta_{10}n\otimes n\otimes n\otimes e_i\otimes n\otimes e_i + 2\beta_{11}\mathbb{I}\otimes\mathbf{I} + \\ 2\beta_{12}\mathbb{I}\otimes n\otimes n + 2\beta_{13}n\otimes e_i\otimes n\otimes e_i\otimes\mathbf{I} + 2\beta_{14}n\otimes e_i\otimes n\otimes e_i\otimes n\otimes n + 2\beta_{15}e_i\otimes e_j\otimes e_k\otimes e_i\otimes e_j\otimes e_k + \\ 2\beta_{16}[2(n\otimes\mathbf{I}\otimes\mathbf{I}\otimes n + n\otimes e_i\otimes e_j\otimes n\otimes e_i\otimes e_j].\end{aligned} \tag{6.40}$$

The action of such a tensor on the strain $\boldsymbol{\varepsilon}$ and on the residual stress $\overset{\circ}{\boldsymbol{\sigma}}$ is the following:

$$\begin{aligned}\mathfrak{D}[\overset{\circ}{\boldsymbol{\sigma}}, \varepsilon] = 2\beta_1 tr(\boldsymbol{\varepsilon})tr(\overset{\circ}{\boldsymbol{\sigma}})\mathbf{I} + 2\beta_2 tr(\boldsymbol{\varepsilon})(n\ \overset{\circ}{\boldsymbol{\sigma}}\ n)\mathbf{I} + \\ \beta_3 tr(\overset{\circ}{\boldsymbol{\sigma}})[tr(\boldsymbol{\varepsilon})n\otimes n + (n\boldsymbol{\varepsilon}n)\mathbf{I}] + \beta_4(n\ \overset{\circ}{\boldsymbol{\sigma}}\ n)[tr(\boldsymbol{\varepsilon})n\otimes n + (n\boldsymbol{\varepsilon}n)\mathbf{I}] + \beta_5[tr(\boldsymbol{\varepsilon})\ \overset{\circ}{\boldsymbol{\sigma}} + tr(\boldsymbol{\varepsilon}\ \overset{\circ}{\boldsymbol{\sigma}})\mathbf{I}] + \\ \beta_6\{tr(\boldsymbol{\varepsilon})\ \overset{\circ}{\boldsymbol{\sigma}}^* + (n\boldsymbol{\varepsilon}\ \overset{\circ}{\boldsymbol{\sigma}}\ n + n\ \overset{\circ}{\boldsymbol{\sigma}}\ \boldsymbol{\varepsilon}n)\mathbf{I}\} + 2\beta_7(n\boldsymbol{\varepsilon}n)tr(\overset{\circ}{\boldsymbol{\sigma}}\ (n\otimes n) + 2\beta_8(n\boldsymbol{\varepsilon}n)(n\ \overset{\circ}{\boldsymbol{\sigma}}\ n)(n\otimes n) + \\ \beta_9[(n\boldsymbol{\varepsilon}n)\ \overset{\circ}{\boldsymbol{\sigma}} + tr(\boldsymbol{\varepsilon}\ \overset{\circ}{\boldsymbol{\sigma}})(n\otimes n)] + \beta_{10}[(n\boldsymbol{\varepsilon}n)\ \overset{\circ}{\boldsymbol{\sigma}}^* + (n\boldsymbol{\varepsilon}\ \overset{\circ}{\boldsymbol{\sigma}}\ n + n\ \overset{\circ}{\boldsymbol{\sigma}}\ \boldsymbol{\varepsilon}n)(n\otimes n)] + \\ 2\beta_{11}tr(\overset{\circ}{\boldsymbol{\sigma}})\boldsymbol{\varepsilon} + 2\beta_{12}(n\ \overset{\circ}{\boldsymbol{\sigma}}\ n)\boldsymbol{\varepsilon} + \beta_{13}tr(\overset{\circ}{\boldsymbol{\sigma}})\boldsymbol{\varepsilon}^* + \beta_{14}(n\ \overset{\circ}{\boldsymbol{\sigma}}\ n)\boldsymbol{\varepsilon}^* + \beta_{15}(\boldsymbol{\varepsilon}\ \overset{\circ}{\boldsymbol{\sigma}} + \overset{\circ}{\boldsymbol{\sigma}}\ \boldsymbol{\varepsilon}) + \\ \beta_{16}[\overset{\circ}{\boldsymbol{\sigma}}\ \boldsymbol{\varepsilon}(n\otimes n) + \overset{\circ}{\boldsymbol{\sigma}}\ (n\otimes n)\boldsymbol{\varepsilon} + \boldsymbol{\varepsilon}\ \overset{\circ}{\boldsymbol{\sigma}}\ (n\otimes n) + \boldsymbol{\varepsilon}(n\otimes n)\ \overset{\circ}{\boldsymbol{\sigma}} + (n\otimes n)\ \overset{\circ}{\boldsymbol{\sigma}}\ \boldsymbol{\varepsilon} + (n\otimes n)\boldsymbol{\varepsilon}\ \overset{\circ}{\boldsymbol{\sigma}}]\end{aligned} \tag{6.41}$$

where $\boldsymbol{\varepsilon}^*$ and $\overset{\circ}{\boldsymbol{\sigma}}{}^*$ are symmetric tensors defined as follows:

$$\begin{cases} \boldsymbol{\varepsilon}^* := \boldsymbol{\varepsilon}(n \otimes n) + (n \otimes n)\boldsymbol{\varepsilon}, \\ \overset{\circ}{\boldsymbol{\sigma}}{}^* := \overset{\circ}{\boldsymbol{\sigma}}\,(n \otimes n) + (n \otimes n)\,\overset{\circ}{\boldsymbol{\sigma}}\,. \end{cases} \tag{6.42}$$

By substituting equations (6.39) and (6.41) into the constitutive law (6.1), the general constitutive law for linear elastic prestressed material, with transverse isotropy, can be written as follows:

$$\begin{aligned} &\boldsymbol{\sigma} - (\mathbf{W}\overset{\circ}{\boldsymbol{\sigma}} - \overset{\circ}{\boldsymbol{\sigma}}\mathbf{W}) = \overset{\circ}{\boldsymbol{\sigma}} + \boldsymbol{\varepsilon}\overset{\circ}{\boldsymbol{\sigma}} + \overset{\circ}{\boldsymbol{\sigma}}\boldsymbol{\varepsilon} - (tr\boldsymbol{\varepsilon})\,\overset{\circ}{\boldsymbol{\sigma}} + \lambda(tr\boldsymbol{\varepsilon})\mathbf{I} + 2\mu\boldsymbol{\varepsilon} + \alpha_1(n\boldsymbol{\varepsilon}n)n \otimes n + \\ &\alpha_2[\mathbf{I}(n\boldsymbol{\varepsilon}n) + tr(\boldsymbol{\varepsilon})n \otimes n] + 2\alpha_3[n \cdot \boldsymbol{\varepsilon} \otimes n + n \otimes \boldsymbol{\varepsilon} \cdot n] + 2\beta_1 tr(\boldsymbol{\varepsilon})tr(\overset{\circ}{\boldsymbol{\sigma}})\mathbf{I} + 2\beta_2 tr(\boldsymbol{\varepsilon})(n\,\overset{\circ}{\boldsymbol{\sigma}}\,n)\mathbf{I} + \\ &\beta_3 tr(\overset{\circ}{\boldsymbol{\sigma}})[tr(\boldsymbol{\varepsilon})n \otimes n + (n\boldsymbol{\varepsilon}n)\mathbf{I}] + \beta_4(n\,\overset{\circ}{\boldsymbol{\sigma}}\,n)[tr(\boldsymbol{\varepsilon})n \otimes n + (n\boldsymbol{\varepsilon}n)\mathbf{I}] + \beta_5[tr(\boldsymbol{\varepsilon})\,\overset{\circ}{\boldsymbol{\sigma}} + tr(\boldsymbol{\varepsilon}\,\overset{\circ}{\boldsymbol{\sigma}})\mathbf{I}] + \\ &\beta_6\{tr(\boldsymbol{\varepsilon})\,\overset{\circ}{\boldsymbol{\sigma}}{}^* + (n\boldsymbol{\varepsilon}\,\overset{\circ}{\boldsymbol{\sigma}}\,n + n\,\overset{\circ}{\boldsymbol{\sigma}}\,\boldsymbol{\varepsilon}n)\mathbf{I}\} + 2\beta_7(n\boldsymbol{\varepsilon}n)tr(\overset{\circ}{\boldsymbol{\sigma}}\,(n \otimes n) + 2\beta_8(n\boldsymbol{\varepsilon}n)(n\,\overset{\circ}{\boldsymbol{\sigma}}\,n)(n \otimes n) + \\ &\beta_9[(n\boldsymbol{\varepsilon}n)\,\overset{\circ}{\boldsymbol{\sigma}} + tr(\boldsymbol{\varepsilon}\,\overset{\circ}{\boldsymbol{\sigma}})(n \otimes n)] + \beta_{10}[(n\boldsymbol{\varepsilon}n)\,\overset{\circ}{\boldsymbol{\sigma}}{}^* + (n\boldsymbol{\varepsilon}\,\overset{\circ}{\boldsymbol{\sigma}}\,n + n\,\overset{\circ}{\boldsymbol{\sigma}}\,\boldsymbol{\varepsilon}n)(n \otimes n)] + 2\beta_{11}tr(\overset{\circ}{\boldsymbol{\sigma}})\boldsymbol{\varepsilon} + \\ &2\beta_{12}(n\,\overset{\circ}{\boldsymbol{\sigma}}\,n)\boldsymbol{\varepsilon} + \beta_{13}tr(\overset{\circ}{\boldsymbol{\sigma}})\boldsymbol{\varepsilon}^* + \beta_{14}(n\,\overset{\circ}{\boldsymbol{\sigma}}\,n)\boldsymbol{\varepsilon}^* + \beta_{15}(\boldsymbol{\varepsilon}\,\overset{\circ}{\boldsymbol{\sigma}} + \overset{\circ}{\boldsymbol{\sigma}}\,\boldsymbol{\varepsilon}) + \\ &\beta_{16}[\overset{\circ}{\boldsymbol{\sigma}}\,\boldsymbol{\varepsilon}(n \otimes n) + \overset{\circ}{\boldsymbol{\sigma}}\,(n \otimes n)\boldsymbol{\varepsilon} + \boldsymbol{\varepsilon}\,\overset{\circ}{\boldsymbol{\sigma}}\,(n \otimes n) + \boldsymbol{\varepsilon}(n \otimes n)\,\overset{\circ}{\boldsymbol{\sigma}} + (n \otimes n)\,\overset{\circ}{\boldsymbol{\sigma}}\,\boldsymbol{\varepsilon} + (n \otimes n)\boldsymbol{\varepsilon}\,\overset{\circ}{\boldsymbol{\sigma}}] \end{aligned} \tag{6.43}$$

When $n = e_3$, this constitutive law becomes (see Chapter 5):

$$\begin{aligned} &\boldsymbol{\sigma} - (\mathbf{W}\overset{\circ}{\boldsymbol{\sigma}} - \overset{\circ}{\boldsymbol{\sigma}}\mathbf{W}) = \overset{\circ}{\boldsymbol{\sigma}} + \boldsymbol{\varepsilon}\,\overset{\circ}{\boldsymbol{\sigma}} + \overset{\circ}{\boldsymbol{\sigma}}\,\boldsymbol{\varepsilon} - (tr\boldsymbol{\varepsilon})\,\overset{\circ}{\boldsymbol{\sigma}} + \lambda(tr\boldsymbol{\varepsilon})\mathbf{I} + 2\mu\boldsymbol{\varepsilon} + \alpha_1\boldsymbol{\varepsilon}_z n \otimes n + \\ &\alpha_2[\boldsymbol{\varepsilon}_z\mathbf{I} + tr(\boldsymbol{\varepsilon})\mathbf{I}_{zz}] + 2\alpha_3\boldsymbol{\varepsilon}* + \{2\beta_1 tr(\boldsymbol{\varepsilon})tr(\overset{\circ}{\boldsymbol{\sigma}}) + 2\beta_2 tr(\boldsymbol{\varepsilon})\,\overset{\circ}{\sigma}_z + \beta_3 tr(\overset{\circ}{\boldsymbol{\sigma}})\boldsymbol{\varepsilon}_z + \beta_4\,\overset{\circ}{\sigma}_z\,\boldsymbol{\varepsilon}_z + \\ &\beta_5 tr(\boldsymbol{\varepsilon}\,\overset{\circ}{\boldsymbol{\sigma}}) + 2\beta_6(\boldsymbol{\varepsilon}\,\overset{\circ}{\boldsymbol{\sigma}})_z\}\mathbf{I} + \{\beta_3 tr(\overset{\circ}{\boldsymbol{\sigma}})tr(\boldsymbol{\varepsilon}) + \beta_4\,\overset{\circ}{\sigma}_z\,tr(\boldsymbol{\varepsilon}) + 2\beta_7\boldsymbol{\varepsilon}_z tr(\overset{\circ}{\boldsymbol{\sigma}}) + \\ &2\beta_8\boldsymbol{\varepsilon}_z\,\overset{\circ}{\sigma}_z + \beta_9 tr(\boldsymbol{\varepsilon}\,\overset{\circ}{\boldsymbol{\sigma}}) + \beta_{10}(\boldsymbol{\varepsilon}\,\overset{\circ}{\boldsymbol{\sigma}})_z\}\mathbf{I}_{zz} + \{\beta_5 tr(\boldsymbol{\varepsilon}) + \beta_9\boldsymbol{\varepsilon}_z\}\,\overset{\circ}{\boldsymbol{\sigma}} + \\ &\{2\beta_{11}tr(\overset{\circ}{\boldsymbol{\sigma}})\boldsymbol{\varepsilon} + 2\beta_{12}\,\overset{\circ}{\sigma}_z\}\boldsymbol{\varepsilon} + \{\beta_6 tr(\boldsymbol{\varepsilon}) + \beta_{10}\boldsymbol{\varepsilon}_z\}\,\overset{\circ}{\boldsymbol{\sigma}}{}^* + \{\beta_{13}tr(\overset{\circ}{\boldsymbol{\sigma}}) + \beta_{14}\,\overset{\circ}{\sigma}_z\}\boldsymbol{\varepsilon}^* + \\ &\beta_{15}(\boldsymbol{\varepsilon}\,\overset{\circ}{\boldsymbol{\sigma}} + \overset{\circ}{\boldsymbol{\sigma}}\,\boldsymbol{\varepsilon}) + \beta_{16}[\overset{\circ}{\boldsymbol{\sigma}}\,\boldsymbol{\varepsilon}^* + \boldsymbol{\varepsilon}\,\overset{\circ}{\boldsymbol{\sigma}}{}^* + \mathbf{I}_{zz}(\overset{\circ}{\boldsymbol{\sigma}}\,\boldsymbol{\varepsilon} + \boldsymbol{\varepsilon}\,\overset{\circ}{\boldsymbol{\sigma}})] \end{aligned} \tag{6.44}$$

where

$$\begin{aligned} &(\boldsymbol{\varepsilon}\,\overset{\circ}{\boldsymbol{\sigma}})_z := n\boldsymbol{\varepsilon}\,\overset{\circ}{\boldsymbol{\sigma}}\,n = e_z\boldsymbol{\varepsilon}\,\overset{\circ}{\boldsymbol{\sigma}}\,e_z = \varepsilon_{rz}\,\overset{\circ}{\sigma}_{rz} + \varepsilon_{\theta z}\,\overset{\circ}{\sigma}_{\theta z} + \varepsilon_z\,\overset{\circ}{\sigma}_z \\ &\boldsymbol{\varepsilon}^* = \begin{bmatrix} 0 & 0 & \varepsilon_{rz} \\ 0 & 0 & \varepsilon_{\theta z} \\ \varepsilon_{rz} & \varepsilon_{\theta z} & 2\varepsilon_z \end{bmatrix}, \\ &\overset{\circ}{\boldsymbol{\sigma}}{}^* = \begin{bmatrix} 0 & 0 & \overset{\circ}{\sigma}_{rz} \\ 0 & 0 & \overset{\circ}{\sigma}_{\theta z} \\ \overset{\circ}{\sigma}_{rz} & \overset{\circ}{\sigma}_{\theta z} & 2\,\overset{\circ}{\sigma}_z \end{bmatrix}. \end{aligned} \tag{6.45}$$

In the particular case in which the residual stress tensor has the diagonal

form(6.35), some terms can be reduced, using the following relations:

$$
\begin{aligned}
&(\boldsymbol{\varepsilon}\ \mathring{\boldsymbol{\sigma}})_z = \varepsilon_z\ \mathring{\sigma}_z = \varepsilon_z(1+x)p_0,\\
&\mathring{\boldsymbol{\sigma}}^* = \begin{bmatrix} 0 & 0 & 0\\ 0 & 0 & 0\\ 0 & 0 & 2\,\mathring{\sigma}_z \end{bmatrix} = 2\,\mathring{\sigma}_z\ \mathbf{I}_{zz} = 2(1+x)p_0\mathbf{I}_{zz},\\
&tr(\mathring{\boldsymbol{\sigma}}) = (3+x)p_0,\\
&tr(\boldsymbol{\varepsilon}\ \mathring{\boldsymbol{\sigma}}) = tr(p_0\boldsymbol{\varepsilon}\mathbf{I} + xp_0\boldsymbol{\varepsilon}\mathbf{I}_{zz}) = p_0(tr\boldsymbol{\varepsilon} + x\varepsilon_z),\\
&\boldsymbol{\varepsilon}\ \mathring{\boldsymbol{\sigma}} + \mathring{\boldsymbol{\sigma}}\ \boldsymbol{\varepsilon} = p_0\boldsymbol{\varepsilon} + xp_o\boldsymbol{\varepsilon}\mathbf{I}_{zz} + p_0\boldsymbol{\varepsilon} + xp_o\mathbf{I}_{zz}\boldsymbol{\varepsilon} = p_0(2\boldsymbol{\varepsilon} + x\boldsymbol{\varepsilon}^*),\\
&\mathring{\boldsymbol{\sigma}}\ \mathbf{I}_{zz} = p_0\mathbf{I}\mathbf{I}_{zz} + xp_0\mathbf{I}_{zz}\mathbf{I}_{zz} = p_0(x+1)\mathbf{I}_{zz} = \mathbf{I}_{zz}\ \mathring{\boldsymbol{\sigma}},
\end{aligned}
\tag{6.46}
$$

The last equation allow to simplify some members of the last term of (6.44) as follows:

$$
\begin{aligned}
&\mathring{\boldsymbol{\sigma}}\ \mathbf{I}_{zz}\boldsymbol{\varepsilon} + \mathbf{I}_{zz}\ \mathring{\boldsymbol{\sigma}}\ \boldsymbol{\varepsilon} = 2p_0(x+1)\mathbf{I}_{zz}\boldsymbol{\varepsilon},\\
&\boldsymbol{\varepsilon}\ \mathring{\boldsymbol{\sigma}}\ \mathbf{I}_{zz} + \boldsymbol{\varepsilon}\mathbf{I}_{zz}\ \mathring{\boldsymbol{\sigma}} = 2p_0(x+1)\boldsymbol{\varepsilon}\mathbf{I}_{zz},\\
&\Rightarrow \mathring{\boldsymbol{\sigma}}\ \mathbf{I}_{zz}\boldsymbol{\varepsilon} + \mathbf{I}_{zz}\ \mathring{\boldsymbol{\sigma}}\ \boldsymbol{\varepsilon} + \boldsymbol{\varepsilon}\ \mathring{\boldsymbol{\sigma}}\ \mathbf{I}_{zz} + \boldsymbol{\varepsilon}\mathbf{I}_{zz}\ \mathring{\boldsymbol{\sigma}} = 2p_0(x+1)[\mathbf{I}_{zz}\boldsymbol{\varepsilon} + \boldsymbol{\varepsilon}\mathbf{I}_{zz}] = 2p_0(x+1)\boldsymbol{\varepsilon}^*
\end{aligned}
\tag{6.47}
$$

The remaining terms are

$$
\begin{aligned}
&\mathring{\boldsymbol{\sigma}}\ \boldsymbol{\varepsilon}\mathbf{I}_{zz} = \begin{bmatrix} 0 & 0 & p_0\varepsilon_{rz}\\ 0 & 0 & p_0\varepsilon_{\theta z}\\ 0 & 0 & (1+x)p_0\varepsilon_z \end{bmatrix},\\
&\mathbf{I}_{zz}\boldsymbol{\varepsilon}\ \mathring{\boldsymbol{\sigma}} = \begin{bmatrix} 0 & 0 & 0\\ 0 & 0 & 0\\ p_0\varepsilon_{rz} & p_0\varepsilon_{\theta z} & (1+x)p_0\varepsilon_z \end{bmatrix} = [\mathring{\boldsymbol{\sigma}}\ \boldsymbol{\varepsilon}\mathbf{I}_{zz}]^T,
\end{aligned}
\tag{6.48}
$$

thus we may define the following symmetric tensor

$$
(\mathring{\boldsymbol{\sigma}}\ \boldsymbol{\varepsilon})^* = \mathring{\boldsymbol{\sigma}}\ \boldsymbol{\varepsilon}\mathbf{I}_{zz} + \mathbf{I}_{zz}\boldsymbol{\varepsilon}\ \mathring{\boldsymbol{\sigma}} = \begin{bmatrix} 0 & 0 & p_0\varepsilon_{rz}\\ 0 & 0 & p_0\varepsilon_{\theta z}\\ p_0\varepsilon_{rz} & p_0\varepsilon_{\theta z} & 2(1+x)p_0\varepsilon_z \end{bmatrix} = p_0\varepsilon^* + 2xp_0\varepsilon_z\mathbf{I}_{zz},
\tag{6.49}
$$

By substituting (6.37), (6.46), (6.47) and (6.49) into the constitutive law (6.44), we obtain:

$$
\begin{aligned}
&\boldsymbol{\sigma} + xp_0w_{3\alpha}(e_3\otimes e_\alpha + e_\alpha\otimes e_3) =\\
&p_0(\mathbf{I} + x\mathbf{I}_{zz}) + p_0(2\boldsymbol{\varepsilon} + x\boldsymbol{\varepsilon}^*) - [p_0(tr\boldsymbol{\varepsilon})\mathbf{I} + xp_0(tr\boldsymbol{\varepsilon})\mathbf{I}_{zz}] + \lambda(tr\boldsymbol{\varepsilon})\mathbf{I} + 2\mu\boldsymbol{\varepsilon} +\\
&\alpha_1\boldsymbol{\varepsilon}_z\mathbf{I}_{zz} + \alpha_2[\boldsymbol{\varepsilon}_z\mathbf{I} + tr(\boldsymbol{\varepsilon})\mathbf{I}_{zz}] + 2\alpha_3\boldsymbol{\varepsilon}* + \{2\beta_1tr(\boldsymbol{\varepsilon})(3+x)p_0 + 2\beta_2tr(\boldsymbol{\varepsilon})(1+x)p_0 +\\
&\beta_3(3+x)p_0\varepsilon_z + \beta_4(1+x)p_0\varepsilon_z + \beta_5p_0(tr(\boldsymbol{\varepsilon}) + x\varepsilon_z) + 2\beta_6\varepsilon_z(1+x)p_0\}\mathbf{I} +\\
&\{\beta_3(3+x)p_0tr(\boldsymbol{\varepsilon}) + \beta_4(1+x)p_0tr(\boldsymbol{\varepsilon}) + 2\beta_7\varepsilon_z(3+x)p_0 + 2\beta_8\varepsilon_z(1+x)p_0 +\\
&\beta_9p_0(tr\boldsymbol{\varepsilon} + x\varepsilon_z) + 2\beta_{10}\varepsilon_z(1+x)p_0\}\mathbf{I}_{zz} + \{\beta_5tr(\boldsymbol{\varepsilon}) + \beta_9\varepsilon_z\}p_0(\mathbf{I} + x\mathbf{I}_{zz}) +\\
&\{2\beta_{11}(3+x)p_0 + 2\beta_{12}(1+x)p_0\}\boldsymbol{\varepsilon} + \{\beta_6tr(\boldsymbol{\varepsilon}) + \beta_{10}\varepsilon_z\}2(1+x)p_0\mathbf{I}_{zz} +\\
&\{\beta_{13}(3+x)p_0 + \beta_{14}(1+x)p_0\}\boldsymbol{\varepsilon}^* + \beta_{15}p_0(2\boldsymbol{\varepsilon} + x\boldsymbol{\varepsilon}^*) + \beta_{16}p_0[(2x+3)\boldsymbol{\varepsilon}^* + 2x\varepsilon_z\mathbf{I}_{zz}]
\end{aligned}
\tag{6.50}
$$

Equation (6.50) can be rearranged, by collect p_0, as follows:

$$\begin{gathered}\boldsymbol{\sigma} + xp_0w_{3\alpha}(e_3 \otimes e_\alpha + e_\alpha \otimes e_3) = \\ p_0(\mathbf{I} + x\mathbf{I}_{zz}) + p_0(2\boldsymbol{\varepsilon} + x\boldsymbol{\varepsilon}^*) - [p_0(tr\boldsymbol{\varepsilon})\mathbf{I} + xp_0(tr\boldsymbol{\varepsilon})\mathbf{I}_{zz}] + \\ p_0\{\lambda/p_0 + 2\beta_1(3+x) + 2\beta_2(1+x) + 2\beta_5\}tr(\boldsymbol{\varepsilon})\mathbf{I} + \\ p_0\{\alpha_2/p_0\beta_3(3+x) + \beta_4(1+x) + \beta_5 x + 2\beta_6(1+x) + \beta_9\}\varepsilon_z\mathbf{I} + \\ p_0\{\alpha_2/p_0\beta_3(3+x) + \beta_4(1+x) + \beta_5 x + 2\beta_6(1+x) + \beta_9\}tr(\boldsymbol{\varepsilon})\mathbf{I}_{zz} + \\ p_0\{\alpha_1/p_0 + 2\beta_7(3+x) + 2\beta_8(1+x) + 2\beta_9 x + 4\beta_{10}(1+x) + 2\beta_{16}x\}\varepsilon_z\mathbf{I}_{zz} + \\ p_0\{2\mu/p_0 + 2\beta_{11}(3+x) + 2\beta_{12}(1+x) + 2\beta_{15}\}\boldsymbol{\varepsilon} + \\ p_0\{2\alpha_3/p_0 + \beta_{13}(3+x) + \beta_{14}(1+x) + \beta_{15}x + \beta_{16}(2x+3)\}\boldsymbol{\varepsilon}^*\end{gathered} \tag{6.51}$$

In analogy to the case of isotropic material (isostatic pressing), the incremental elasticity tensor

$$\begin{gathered}\mathfrak{L}[\overset{\circ}{\boldsymbol{\sigma}}, \boldsymbol{\varepsilon}] = \mathfrak{D}[\overset{\circ}{\boldsymbol{\sigma}}, \boldsymbol{\varepsilon}] + \mathbb{C}[\boldsymbol{\varepsilon}] = \\ p_0\{\lambda/p_0 + 2\beta_1(3+x) + 2\beta_2(1+x) + 2\beta_5\}tr(\boldsymbol{\varepsilon})\mathbf{I} + \\ p_0\{\alpha_2/p_0 + \beta_3(3+x) + \beta_4(1+x) + \beta_5 x + 2\beta_6(1+x) + \beta_9\}\varepsilon_z\mathbf{I} + \\ p_0\{\alpha_2/p_0 + \beta_3(3+x) + \beta_4(1+x) + \beta_5 x + 2\beta_6(1+x) + \beta_9\}tr(\boldsymbol{\varepsilon})\mathbf{I}_{zz} + \\ p_0\{\alpha_1/p_0 + 2\beta_7(3+x) + 2\beta_8(1+x) + 2\beta_9 x + 4\beta_{10}(1+x) + 2\beta_{16}x\}\varepsilon_z\mathbf{I}_{zz} + \\ p_0\{2\mu/p_0 + 2\beta_{11}(3+x) + 2\beta_{12}(1+x) + 2\beta_{15}\}\boldsymbol{\varepsilon} + \\ p_0\{2\alpha_3/p_0 + \beta_{13}(3+x) + \beta_{14}(1+x) + \beta_{15}x + \beta_{16}(2x+3)\}\boldsymbol{\varepsilon}^*\end{gathered} \tag{6.52}$$

reduces to classical elasticity tensor $\mathbb{C}[\boldsymbol{\varepsilon}]$ when there is no residual stress (i.e. $\overset{\circ}{\boldsymbol{\sigma}} = 0$). For transversal isotropic material, $\mathbb{C}[\boldsymbol{\varepsilon}]$ takes the form (6.38), depending on the the Lame's constants λ and μ, and the material constants $\alpha_1, \alpha_3, \alpha_3$. In the case in which $n = e_z$,

$$\mathbb{C}[\boldsymbol{\varepsilon}] = \lambda(tr\boldsymbol{\varepsilon})\mathbf{I} + 2\mu\boldsymbol{\varepsilon} + \alpha_1(\boldsymbol{\varepsilon}_z)\mathbf{I}_{zz} + \alpha_2[\boldsymbol{\varepsilon}_z\mathbf{I} + tr(\boldsymbol{\varepsilon})\mathbf{I}_{zz}] + 2\alpha_3\boldsymbol{\varepsilon}^*. \tag{6.53}$$

We can thus define, in analogy to the isotropic case, the equivalent material constants $\lambda^*, \mu^*, \alpha_1^*, \alpha_2^*, \alpha_3^*$. These constants "take the place" of the material constants $\lambda, \mu, \alpha_1, \alpha_2, \alpha_3$ (that characterize the material with no residual stress) in the case of prestressed linear elastic transversely isotropic material. These equivalent material constants can be evaluated by comparing equations (6.52) and (6.53), and have the following form:

$$\begin{aligned}&\lambda^* = p_0\{\lambda/p_0 + 2\beta_1(3+x) + 2\beta_2(1+x) + 2\beta_5\},\\ &\mu^* = p_0\{2\mu/p_0 + 2\beta_{11}(3+x) + 2\beta_{12}(1+x) + 2\beta_{15}\},\\ &\alpha_1^* = p_0\{\alpha_1/p_0 + 2\beta_7(3+x) + 2\beta_8(1+x) + 2\beta_9 x + 4\beta_{10}(1+x) + 2\beta_{16}x\},\\ &\alpha_2^* = p_0\{\alpha_2/p_0 + \beta_3(3+x) + \beta_4(1+x) + \beta_5 x + 2\beta_6(1+x) + \beta_9\},\\ &\alpha_3^* = \tfrac{p_0}{2}\{2\alpha_3/p_0 + \beta_{13}(3+x) + \beta_{14}(1+x) + \beta_{15}x + \beta_{16}(2x+3)\}.\end{aligned} \tag{6.54}$$

Note that, in the case of incompressible material, the expression of $\mathfrak{L}[\overset{\circ}{\boldsymbol{\sigma}}, \boldsymbol{\varepsilon}]$ and of $\mathbb{C}[\boldsymbol{\varepsilon}]$ reduce to:

$$\begin{gathered}\mathfrak{L}[\overset{\circ}{\boldsymbol{\sigma}}, \boldsymbol{\varepsilon}] = \mathfrak{D}[\overset{\circ}{\boldsymbol{\sigma}}, \boldsymbol{\varepsilon}] + \mathbb{C}[\boldsymbol{\varepsilon}] = \\ p_0\{\alpha_2/p_0 + \beta_3(3+x) + \beta_4(1+x) + \beta_5 x + 2\beta_6(1+x) + \beta_9\}\varepsilon_z \mathbf{I} + \\ p_0\{\alpha_1/p_0 + 2\beta_7(3+x) + 2\beta_8(1+x) + 2\beta_9 x + 4\beta_{10}(1+x) + 2\beta_{16}x\}\varepsilon_z \mathbf{I}_{zz} + \\ p_0\{2\mu/p_0 + 2\beta_{11}(3+x) + 2\beta_{12}(1+x) + 2\beta_{15}\}\boldsymbol{\varepsilon} + \\ p_0\{2\alpha_3/p_0 + \beta_{13}(3+x) + \beta_{14}(1+x) + \beta_{15}x + \beta_{16}(2x+3)\}\boldsymbol{\varepsilon}^*\end{gathered} \tag{6.55}$$

$$\mathbb{C}[\boldsymbol{\varepsilon}] = 2\mu\boldsymbol{\varepsilon} + \alpha_1(\boldsymbol{\varepsilon}_z)\mathbf{I}_{zz} + \alpha_2\boldsymbol{\varepsilon}_z\mathbf{I} + 2\alpha_3\boldsymbol{\varepsilon}^*. \tag{6.56}$$

Hence, in order to completely characterize the mechanical behavior f a (linear elastic) transversely isotropic incompressible prestresses material, it is sufficient to determine the values of the four classical moduli $\mu, \alpha_1, \alpha_2, \alpha_3$ and of the four equivalent moduli $\mu^*, \alpha_1^*, \alpha_2^*, \alpha_3^*$ defined by equation (6.54) .

6.4.3 Experimental procedure to determine the mechanical behavior of a transversely isotropic sintered material

In order to experimentally determine the mechanical behavior of a transversely isotropic material, with e_z = axes of transverse isotropy, it is necessary to perform five experimental tests (shown in figure 6.5:

1. an isotropic compression test (that allows to determine the bulk modulus λ
2. an elongation test in e_z direction
3. an elongation test in a direction perpendicular to e_z, i.e. a direction in the plane (e_x, e_y)
4. a shear test in a plane containing e_z
5. a shear test in the plane perpendicular to e_z, i.e. the plane (e_x, e_y)

Obviously, if the material is incompressible (as the the treated case), the test (1) it is not necessary.
By perform the experimental tests on the as-sintered materials, it is possible to evaluate the five equivalent moduli $\lambda^*, \mu^*, \alpha_1^*, \alpha_2^*, \alpha_3^*$. Because of it is well known that thermal treatments eliminate the residual stress, the values of $\lambda, \mu, \alpha_1, \alpha_2, \alpha_3$ can be obtain through the results of the five test on a annealed sintered material. This values can be compared to $\lambda^*, \mu^*, \alpha_1^*, \alpha_2^*, \alpha_3^*$ in order to calculate the variation of the mechanical behavior due to the presence of the residual sintering stresses. In the case of incompressible material, only four tests are required.

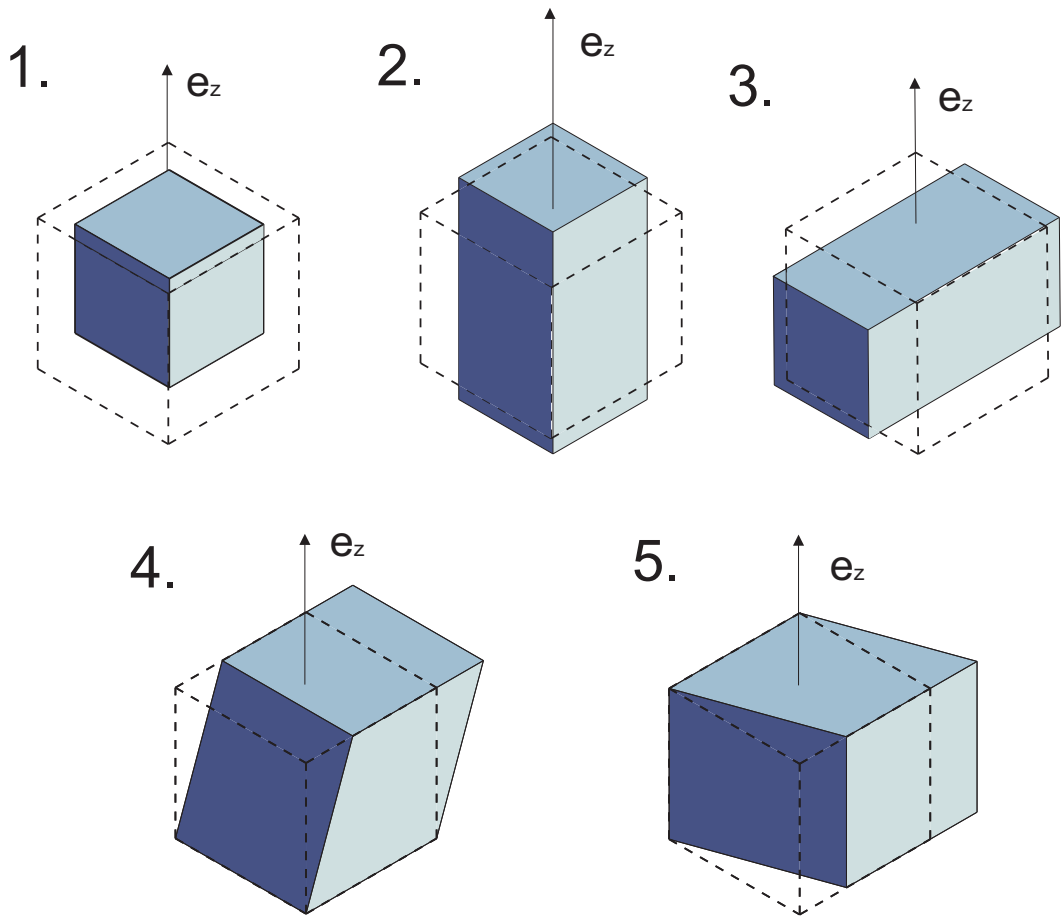

Figure 6.5:

Nomenclature

θ : porosity

σ_{ij} : components of the stress tensor

$\dot{\varepsilon}_{ij}$: components of the deviatoric strain rate tensor

$\dot{\varepsilon}'_{ij}$: components of the deviatoric strain rate tensor

$\dot{e}$: first invariant of the strain rate tensor

$\dot{\gamma}$: second invariant of the deviatoric strain rate tensor

p : first invariant of the stress tensor

τ : second invariant of the stress tensor

w : effective equivalent strain rate

S : cross-sectional area of the cylindrical specimen

S_0 : initial cross-sectional area of the cylindrical specimen

F_z : axial load

$\sigma(w)$: effective equivalent stress

A : time-dependent material constant

σ_0 : reference stress

$\dot{\varepsilon}_0$: reference strain rate

w : strain rate sensitivity

ψ : normalized bulk modulus

φ : normalized shear modulus

p_l : Laplace pressure (interstitial stress)

n : loading mode parameter

τ_E : dimensionless specific time (forging case)

τ_L : dimensionless specific time (isostatic pressing case)

$S.E.P.$: specific external pressure

θ^* : critical porosity

θ_r : residual porosity

α : surface tension

r_0 : characteristic radius of particles

D : dissipation potential

d : dissipation per unit volume mass

$\mathbf{I}$: second-order identity tensor

$\mathbb{I}$: forth-order identity tensor

U : strain energy

$\overset{\circ}{\boldsymbol{\sigma}}$: residual stress tensor

n : transverse isotropy direction

$J_1, ..., J_{18}$: invariants of the strain rate tensor, the residual stress tensor and the transverse isotropy direction

$\mathfrak{L}(\overset{\circ}{\boldsymbol{\sigma}}, \boldsymbol{\varepsilon}, n)$: ixth-order incremental elasticity tensor

$\mathfrak{D}(\overset{\circ}{\boldsymbol{\sigma}}, \boldsymbol{\varepsilon}, n)$: sixth-order tensor, which accounts for the residual stress

$\mathbb{C}(\boldsymbol{\varepsilon}, n)$: forth-order elasticity tensor

$\boldsymbol{\sigma}_R$: part of the stress tensor due to the residual stress

U_R : part of the strain energy due to the residual stress

λ, μ : Lame's constants

$\alpha_1, ..., \alpha_5$: material constants

$\beta_1, ..., \beta_{16}$: material constants

$\boldsymbol{\varepsilon}^*$: second order tensor, accounting for the the strain components and for the direction of transverse isotropy

$\overset{\circ}{\boldsymbol{\sigma}}{}^*$: second order tensor, accounting for the the residual stress components and for the direction of transverse isotropy

$\boldsymbol{\xi}$: structural tensor

$\mathbf{D}$: mechanical agency

$\mathbf{Q}, \mathbf{R}$: arbitrary rotations

Bibliography

[1] J. Frenkel, Viscous flow of crystalline bodies under the action of surface tension, *Journal of Physics USSR* **9 (5)** (1945) 385 – 391.

[2] B.Ya. Pines, Mechanism of sintering, *Journal of Technological Physics* **16** (1946) 737.

[3] G.C. Kuczynski, Self-diffusion in sintering of metallic particles, *Transaction AIME* **185** (1949) 169178.

[4] K. Mackenzie, R. Shuttleworth, A phenomenological theory of sintering, *Proceedings of the Physical Society* **62 (12-B)** (1949) 833852.

[5] W.D. Kingery, M. Berg, Study of the initial stages of sintering, solids by viscous flow, evaporationcondensation, and self-diffusion, *Journal of Applied Physics* **26** (1955) 12051212.

[6] R.S. Rivlin, J.L. ericksen, Sress-deformation relations for isotropic materials, *Journal of Rational Mechanics and Analysis* **4**(1955) 323 – 425.

[7] A.J.M. Spencer, Theory of invariants, *Continuum Physics 1, Academic Press* (1971).

[8] R.G. Green, A plasticity theory for porous solids, *International Journal of Mechanic Science* **4** (1972) 215 – 224.

[9] Skorohod, V.V., Rheological Basis of the Theory of Sintering. *Naukova Dumka, Kiev.* (1972).

[10] W. Beere, The second stage sintering kinetics of powder compacts, *Acta Metall.* **23 (1)** (1975) 139 – 145.

[11] D.S. Wilkinson, M.F.Ashby, Pressure sintering by power law creep, *Acta Metall.* **23** (1975) 1277 – 1285.

[12] S. Shima, M. Oyane, Plasticity theory for porous metals, *International Journal of Mechanic Science* **6** (1976) 285 – 291.

[13] J.W.Hutchinson, K. Neale, A. Needleman, Sheet necking I- validity of plane stress assumptions on the long-wavelenght approximation, in: Koistinen, D.P., Wong, N.M. (Eds.), *Mechanics of Sheet Metal Forming, vol.1* Plenum, NY (1978) 111 – 126.

[14] F.V. Lenel, Powder Metallurgy (Principles and Applications), *Metal Powder Industries Federation, Princeton, NJ* (1980).

[15] V.K.Kumikov, Kh.B. Khokonov, On the measurement of surface free energy and surface tension of solid metals, *Journal of Applied Phisics* **54(3)** (1983) 1346 – 1350.

[16] H. Kehchih, X. Mingde, L. Mingwan, Tensor Analysis, *Tsingua University Press*, 74 – 78 (1986) 172 – 193 (in Chinese).

[17] J.P. Boehler, Applications of tensor functions in solid mechanics, *Springer-Verlag*, Berlin (1987).

[18] Ashby, M.F., Background Reading, HIP 6.0. *University of Cambridge, Cambridge, UK.* (1990).

[19] Ponte Castaneda, P., The effective mechanical properties of nonlinear isotropic composites, *J. Mech. Phys. Solids* **39** (1991) 45 – 71.

[20] Duva, J.M., Crow, P.D.. The densification of powders by power-law creep during hot isostatic pressing. *Acta Metall* **40(1)**(1992) 31 – 35.

[21] Sofronis, P., McMeeking, R.M., Creep of power-law material containing spherical voids. *Trans. ASME* **59** (1992) 88 – 95.

[22] M. Muhlberg, P. Paschen, Liquid phase sintering of AlZnMgCu alloys, *Zeitschrift fr Metallkunde* **84 (5)** (1993) 346 – 350.

[23] Cocks, A.C.F., The structure of constitutive laws for the sintering of fine grained materials. *Overview No. 117, Acta Metall.* **42(7)** (1994) 2191.

[24] G. Strafellini, A. Molinari, Microstructure and mechanical reliability of powder metallurgy (P/M) ferrous alloys, *Journal of Materials Engineering and Performance* , 5(1) (1996) 27 – 33

[25] Olevsky, E., Dudek, H.J., Kaysser, W.A., HIPing conditions for processing of metal matrix composites by using continuum theory for sintering, *Acta Met. Mater.* **44** (1996) 707724.

[26] R.M. German, Sintering Theory and Practice, *Wiley, New York* (1996)

[27] W. Schatt, K. Wieters, Powder Metallurgy-Process and Materials, *European Powder Metallurgy Association, Shrews-bury, UK* (1997)

[28] C.-S. Man, Hartig's law and linear elasticity with initial stress, *Inverse Problem* **14** (1998) 313 – 319.

[29] E.A. Olevsky, Theory of sintering: from discrete to continuum. *Invited Review. Mater. Sci. Eng. Rep. Rev.* **23** (1998) 41 – 100.

[30] Weiyi,C., Derivation of the general form of elasticity tensor of the transverse isotropic material by tensor derivate, *Applied Mathematics and Mechanics* **20 n.3** (1999) 309 – 314.

[31] A. S. Khan, H. Zhang, L. Takacs, Mechanical response and modeling of fully compacted nanocrystalline iron and copper, *Int. Journal of Plasticity* **16** (2000) 1459 – 1476.

[32] E.A. Olevsky, A. Molinari, Instability of sintering of porous bodies. *Int. J. Plast* **16** (2000) 1-37.

[33] C. Gu, M. Kim, L. Anand, Constitutive equations for metal powders: application to powder forming processes, *Int. Journal of Plasticity* **17** (2001) 147 – 209.

[34] R.W. Lewis, A.R. Khoei, A plasticity model for metal powder forming processes,. *Int. Journal of Plasticity* **17** (2001) 1659 – 1692.

[35] G.Schaffer, The effect of trace elements on the sintering of an Al-Zn-Mg-Cu ALLOY, *Acta Materialia*, **49 (14)** (2001) 2671 – 2678.

[36] T.Aizawa, Y. Prawotoa, F. Tsumorib, Coupled, macromicro modeling for hot deformation and sintering, *Journal of Computational and Applied Mathematics* **149** (2002) 307324.

[37] P. Haupt, Continuum mechanics and theory of materials, *Technology and Engineering* (2002) 643.

[38] A.L. Maximenko, E.A. Olevsky, Effective diffusion coefficients in solid-state sintering, *Acta Materialia* **52** (2004) 29532963.

[39] J. Pan, Solid-state diffusion under a large driving force and the sintering of nanosized particles, *Philosophical Magazine Letters* **84(5)**(2004) 303 – 310.

[40] J. Pan, H.N. Ch'ng, A.C.F. Cocks, Sintering kinetics of large pores, *Mechanics of Material* **37** (2005) 705 – 721.

[41] R. M. German, Powder Metallurgy and particulate material processing, *Princeton, NJ* (2005).

[42] A.S. Khan, Y.S. Suh, X. Chen, L. Takacs, H. Zhang, Nanocrystalline aluminum and iron: Mechanical behavior at quasi-static and high strain rates, and constitutive modeling, *Int. Journal of Plasticity* **22** (2006) 195 – 209.

[43] Olevsky, E.A., Molinari, A., Kinetics and stability in compressive and tensile loading of porous bodies. *Mechanics of Materials* **38** (2006) 340 – 366.

[44] A. Piccolroaz, D. Bigoni and A. Gajo, An elastoplastic framework for granular materials becoming cohesive through mechanical densification. Part I - small strain formulation,*European Journal of Mechanics A: Solids* **25** (2006) 334 – 357.

[45] A. Piccolroaz, D. Bigoni and A. Gajo, An elastoplastic framework for granular materials becoming cohesive through mechanical densification. Part II - the formulation of elastoplastic coupling at large strain,*European Journal of Mechanics A: Solids* **25** (2006) 358 – 369.

[46] A.C.F. Cocks, I.C. Sinka, Constitutive modelling of powder compaction I. Theoretical concepts, *Mechanics of Materials* **39** (2007) 392403.

[47] A.C.F. Cocks, I.C. Sinka, Constitutive modelling of powder compaction II. Evaluation of material data, *Mechanics of Materials* **39** (2007) 404416.

[48] I.C. Sinka, Modelling Powder Compaction, *KONA* **25** (2007).

[49] P. Barai, G.J. Weng, The competition of grain size and porosity in the viscoplastic response of nanocrystalline solids, *Int. Journal of Plasticity* **24** (2008) 1380 – 1410.

[50] A. Gokce, F. Findik, A. Gokce, F. Findik, Mechanical and physical properties of sintered aluminum powders, *Journal of Achievements in Materials and Manufacturing Engineering* **30(2)** (2008) 157 – 164.

[51] T.-W. Kim, Determination of densification behavior of AlSiC metal matrix composites during consolidation processes, *Materials Science and Engineering: A* **483-484** (2008) 648 – 651.

[52] I. Apachitei, B. Lonyuk, L. Fratila-Apachitei, J. Zhou, J. Duszczyk, Fatigue response of porous coated titanium biomedical alloys, *Scripta Materialia* **61(2)** (2009) 113 – 116.

[53] M. Frewer, More clarity on the concept of material frame-indifference in classical continuum mechanics, *Acta Mechanica* **202** (2009) 213 – 246.

[54] L.Galuppi, L.Deseri, Effects of the interstitial stress on isostatic pressing and free sintering of cylindrical specimens. *Submitted*

[55] L.Galuppi, L.Deseri, Sintering of cylindrical specimens:
Part I - Effects of the Laplace pressure during "free" forging. Submitted.

[56] L.Galuppi, L.Deseri, Sintering of cylindrical specimens:
Part II - Effects of the lateral confinement and of the Laplace pressure during constrained forging. Submitted.